# Group-13 Catalysed Protocols for Utilisation of $CO_2$ as a Sustainable C1 Source

**Maria Distressa Genita Billacura**

A thesis submitted in partial fulfilment of the requirements of
Sheffield Hallam University
for the degree of Doctor of Philosophy

December 2022

## Candidate Declaration

I hereby declare that:

1. I have not been enrolled for another award of the University, or other academic or professional organisation, whilst undertaking my research degree.
2. None of the material contained in the thesis has been used in any other submission for an academic award.
3. I am aware of and understand the University's policy on plagiarism and certify that this thesis is my own work. The use of all published or other sources of material consulted have been properly and fully acknowledged.
4. The work undertaken towards the thesis has been conducted in accordance with the SHU Principles of Integrity in Research and the SHU Research Ethics Policy.
5. The word count of the thesis is 36,533.

| | |
|---|---|
| Name | *Maria Distressa G. Billacura* |
| Date | *March 2023* |
| Award | *Doctor of Philosophy (PhD)* |
| Faculty | *Health and Wellbeing* |
| Director(s) of Studies | *Prof. Neil Bricklebank,*<br>*Dr. Christopher J. Whiteoak,*<br>*Dr. Sarah Forbes* |

## Abstract

The research described in this thesis focuses on the preparation of group 13-containing compounds and their application as Lewis acid catalysts. This research is in the context of utilizing $CO_2$ as a renewable C1 feedstock, through the atom-efficient conversion with epoxides/aziridines to form useful cyclic carbonates and cyclic oxazolidinones. Significant progress in the search for efficient catalysts for these conversions has been made over the years, with some highly active aluminium compounds being developed. However, potential gaps in this exploration exist, including the study of other metals from group 13 beyond aluminium that have been investigated in many other fields of chemistry. Notably, there are few reports of boron, indium and gallium-based compounds used as a catalyst for the cycloaddition of $CO_2$ to epoxides. With aluminium being thoroughly explored this presents motivation for exploring the potential for use of these other group 13 elements.

In this work, a series of trimethyl borate compounds with different *para*-substitutions on the phenoxy moieties have been prepared. Further to this, boron, gallium and indium complexes containing aminotrisphenolate ligands have been prepared. All these complexes have been tested as potential catalysts for the synthesis of cyclic carbonates, and their reactivity investigated. Boron aminotrisphenolate complexes operate by hydrogen-bonding catalysis rather than the expected Lewis acid catalysis due to the incomplete coordination of the aminotrisphenol ligand to the boron. The resulting free phenol acts as a catalyst for the production of cyclic carbonates at relatively elevated catalyst loading. Meanwhile, the trimethyl borate compounds, with a trigonal planar geometry, provide Lewis acid-driven catalysis rather than via a hydrogen bonding interaction.

The gallium aminotrisphenolate complex was used as a catalyst for oxazolidinone synthesis, demonstrating the gallium complex's versatile efficiency as a more powerful catalyst than the aluminium congener. The results show that the Ga complex converts aziridines into the corresponding oxazolidinones in high yields at relatively low catalyst loading. Indium complexes bearing aminotrisphenolate and halide ligands are competent catalyst for the cycloaddition of $CO_2$ and epoxides to form cyclic carbonates, with evidence that

a coordinated halide can also act as the nucleophile required for the ring-opening step of the mechanism, thus adding more future possibilities to this family of compounds.

Finally, modified cellulose fibres, prepared through anchoring of an epoxide to the surface by the Fenton reaction, followed by cycloaddition of $CO_2$ using gallium catalyst have been prepared. These fibres have shown a positive outcome in the search for materials with antibacterial properties. As a final note, the potential cycloaddition of $CO_2$ to episulfide has been briefly studied. This reaction produces an intractable solid product for which it has been unable to fully confirm its structure.

## Acknowledgement

I would like to thank my supervisory team Prof. Neil Bricklebank, Dr Sarah Forbes, and most of all, Dr Christopher J. Whiteoak, for all your undying support during my PhD journey in the UK. My sincere gratitude for all the knowledge and skills you have provided.

To my sponsor, the Department of Science and Technology-Science Education Institute (DOST-SEI) and the Philippine Government, thank you for this excellent opportunity to study and experience life in the UK.

I would like to thank all the people in BMRC and MERI for making my stay in SHU a memorable experience. Also, to the technical team who always helped me with dry ice and NMR issues, thank you to all of you.

I would like to thank Dr Francis Clegg and Hassan Majiya for helping me analyse my samples in MERI. To Kelly Parkin for assisting me with antimicrobial analysis, I have learned another skill through you.

I would like to thank my Station House Bulwell family for the waves of laughter and tears we shared during my stay in the UK, particularly Andy and Ate Juvy, who has been like parents to us. To all friends and families, we met during our stay, my sincere thank you to all of you.

To my Genita family, Papa Jun, Mama Tina, and Ate Jane, thank you for your undying support and for taking care of our business, I love you all. Thank you so much to my growing family, Billacura Family-Mama Ofelia, Ates and Kuyas, for the support and love.

I would like to thank My Precious Husband, Merell Pabilona Billacura, who always supports me and always there when I need him. Thank you for all the encouragement and love you gave to me. I love you most, Hon.

To my amazing and most gracious God, thank you for all the blessings and challenges I received that give me more reason to continue each day. Thank you, Lord!

Lastly, to all the people I forgot to mention, thank you for making my PhD journey enjoyable.

# List of Abbreviations

| | |
|---|---|
| AN | Acceptor Number |
| BCF | Tris(pentafluorophenyl)borane |
| BSAC | British Society for Antimicrobial Chemotherapy |
| $Bu_4NBr$ | Tetrabutylammonium bromide |
| $Bu_4NI$ | Tetrabutylammonium iodide |
| C1 | Carbon 1 |
| CCDC | Cambridge Crystallographic Data Centre |
| CCS | Carbon Capture and Storage |
| CDU | Carbon dioxide utilization |
| $CO_2$ | Carbon dioxide |
| COCs | Cyclic organic carbonates |
| COSY | COrrelated SpectroscopY |
| cSSSI | Complicated skin and skin structure infections |
| DCM | Dichloromethane |
| DFT | Density Functional Theory |
| DMAP | 4-Dimethylaminopyridine |
| DNA | Deoxyribonucleic acid |
| *E. coli* | Escherichia coli |
| EB | Electron-beam radiation |
| $Et_3N$ | Triethylamine |
| $Et_3PO$ | Triethylphosphine oxide |
| FT-IR | Fourier Transform-Infrared Spectrometer |
| GMA | Glycidyl methacrylate |
| $H_3L$ | Aminotrisphenol ligand |
| HDB | Hydrogen bond |
| HMTA | Hexamethylenetetramine |
| HRMS | High-Resolution Mass Spectra |
| LA | Lewis acid catalyst |
| MDR | Multi-drug resistant bacteria |
| MEK | Methyl ethyl ketone |
| MPa | Megapascal |
| $^{n}Bu_4N^{+}X^{-}$ | Tetra-butylammonium halides |

| | |
|---|---|
| NMIz | 1-methylimidazole |
| NMR | Nuclear Magnetic Resonance |
| $Nu^-$ | Nucleophile |
| $OD_{600}$ | Optical density 600 |
| PO | Propylene oxide |
| ppm | Parts per million |
| PPNCl | Bis(triphenylphosphine)iminium chloride |
| PS | Polystyrene |
| PTFE | Polytetrafluoroethylene |
| RNA | Ribonucleic acid |
| *S. aureus* | Staphylococcus aureus |
| salen | *N*,*N*′-ethylenebis(salicylimine) |
| $scCO_2$ | Supercritical carbon dioxide |
| SN | Nucleophilic substitution |
| TGA | Thermogravimetric analysis |
| THF | Tetrahydrofuran |
| TOF | Turnover frequency |
| TON | Turnover number |
| TPB | Triphenylborane |
| TPBO | Triphenylborate |
| TsOH | *p*-toluenesulfonic acid |
| uSSSI | Uncomplicated skin and skin structure infections |
| UV-vis | Ultraviolet–visible |
| VRE | Vancomycin-resistant enterococci |

# List of Figures

# List of Schemes

# List of Tables

# Table of Contents

# Chapter 1

Introduction, Aims and Objectives

## 1.1 Introduction

The principal subject of this thesis is the synthesis of group 13 complexes bearing an aminotrisphenolate/phenol ligand and the subsequent study of their ability to act as catalysts for the conversion of carbon dioxide ($CO_2$) and epoxides or aziridines, forming the corresponding cycloaddition products. This chapter introduces the challenges of utilising $CO_2$ as a C1 source, the approach to selection of substrates to react with $CO_2$, the reaction mechanism for the cycloaddition of $CO_2$ with epoxides, the surrounding ligand and how it affects the Lewis acidity of the metal centre. Also included is an introduction to an advanced application of one of the developed catalyst systems. The group 13 metals considered during this discussion are boron, gallium, and indium, and the corresponding aminotrisphenolate catalysts of these elements (Figure 1.1, right). These are directly compared with the catalytic activity of the well-established aluminium catalyst congener (Figure 1.1, left).[1]

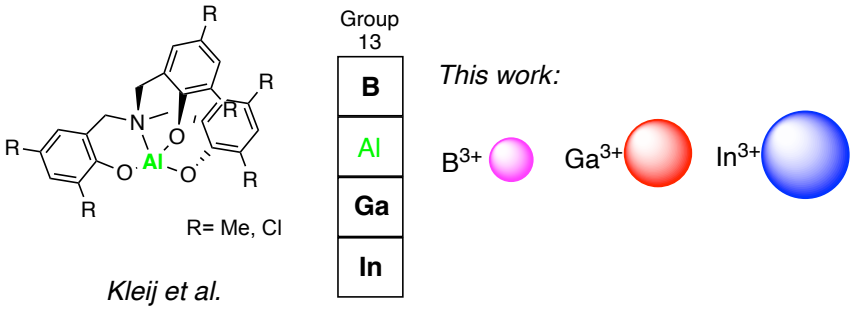


**Figure 1.1** Overview of a metal complex activating substrates to convert $CO_2$ compound.

### 1.1.1 Carbon dioxide as an important component of greenhouse gases

$CO_2$ has been identified as a large contributor to global warming, and the majority of this comes from industrial processes that emit billions of tons to the earth's atmosphere annually.[2,3] The concentration of $CO_2$ in the earth's atmosphere has been increasing over the past 200 years and it has already surpassed an

alarming 400-ppm threshold, as shown in Figure 1.2. Alongside $CO_2$ both methane ($CH_4$) and nitrous oxide ($N_2O$) are increasing in the atmosphere, but $CO_2$ is considered as the biggest contributor to the greenhouse gas problem.[4] $CO_2$ gas can be eliminated from the atmosphere within a specific period, commonly known as "residence time", and this has occurred throughout the earth's history through natural processes. However, with the enormous and increasing atmospheric concentration, eliminating the gas will take hundreds of years based on the natural carbon cycle.[5] This means that the most significant way to prevent this phenomenon is to reduce the emission of $CO_2$ globally or find useful applications of the gas meaning that it becomes economically favourable to capture the gas before it is released into the atmosphere.

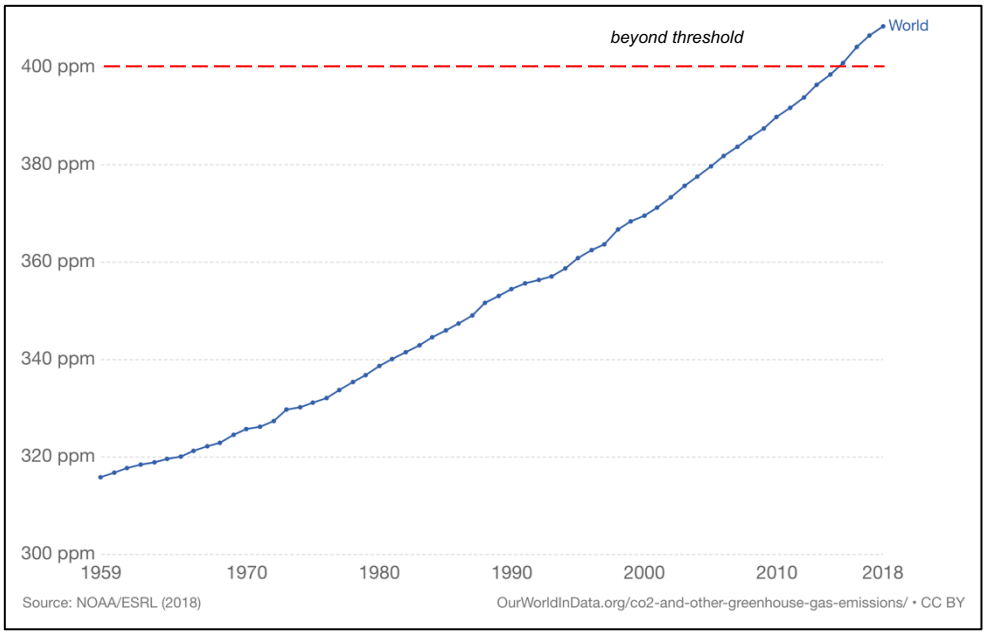


**Figure 1.2** Global mean annual concentration of carbon dioxide ($CO_2$) measured in parts per million in 2018.[4]

Various government institutions from many countries have supported the campaign on decarbonisation by using renewable sources of energy; however, many countries still rely on coal as a source of energy, which generates large quantities of $CO_2$.[6] The overall usage of fossil fuel sources for the demands of

the consumer is one of the reasons why there has been an increase in $CO_2$ concentration each year in the atmosphere.[7,8] With this, researchers are eager to find methods to utilise and synthesise commodity and fine chemicals from $CO_2$.

### 1.1.2 $CO_2$ as a renewable feedstock

Carbon dioxide as a renewable feedstock has been widely introduced and is becoming a very important research topic in both academia and industry. The $CO_2$ molecule is a very appealing carbon source since it is a non-toxic, low-cost, and widely abundant gas. These advantages have motivated many researchers to utilise it as a sustainable and renewable C1 source for organic synthesis, however, $CO_2$ has low free energy.[9-11] In addition, activation and utilisation of $CO_2$ are challenging since it is the most oxidised form of carbon which is thermodynamically stable and kinetically inert in specific desired conversions. To overcome these challenges, routes to its utilisation often rely on reactions combining $CO_2$ with high free-energy substrates.

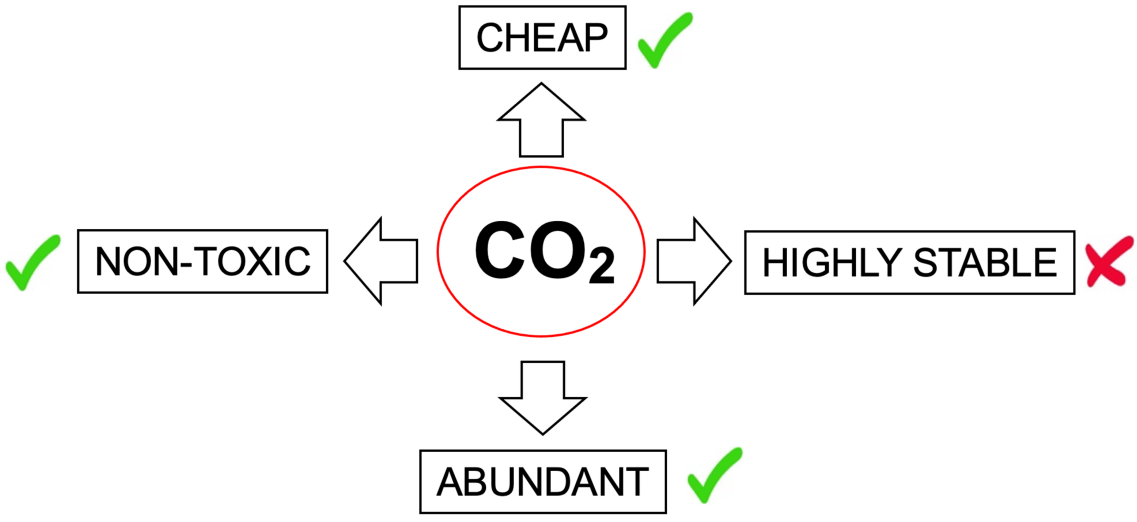


**Figure 1.3** Challenges/advantages to consider when converting $CO_2$ into valuable products.[9-11]

Several existing methods have been developed to decrease the $CO_2$ concentration in the atmosphere. One of these methods is to capture $CO_2$ from the atmosphere.[12] Carbon capture and storage (CCS) can be considered an effective way to reduce the $CO_2$ emission into the atmosphere by collecting $CO_2$ before or after it is released into the atmosphere. Meanwhile transforming $CO_2$ into valuable compounds is also a field of study, known as carbon dioxide utilization (CDU) and not focused on the sourcing of the gas and should work hand in hand with CCS. These approaches support sustainable chemistry that has the potential to reduce $CO_2$ emissions globally, which cause the aforementioned global warming.[4,12,13]

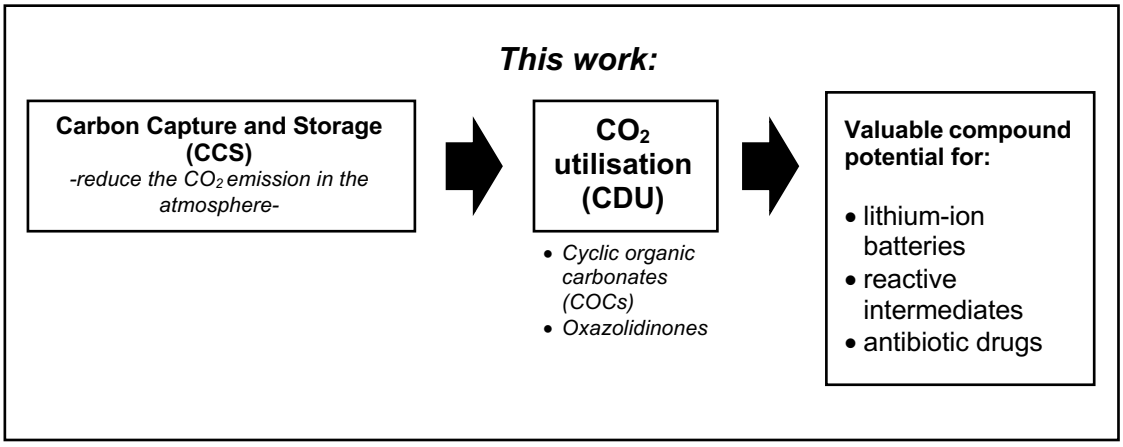


**Figure 1.4** Overview of the process to exploit $CO_2$ compounds and their potential uses.

Apart from being a pollutant, the scientific community has developed ways to use $CO_2$ and finds applications in many industrial procedures. For example, it can be converted into methanol or formic acid from the reduction of $CO_2$ with $H_2$, reaction with heterocyclic molecules like epoxides to yield cyclic or polymeric carbonates, or aziridines to produce oxazolidinones.[2,14-17] Several chemical reactions listed in Figure 1.5 show the conversion of $CO_2$ into a high-value product, although it remains a challenge in synthetic chemistry to find a suitable catalyst to aid its reaction. Many of the products that come from $CO_2$ have been produced on multi-

ton scale annually. Five-membered cyclic carbonates have a diverse range of applications, such as polar aprotic solvents, electrolytes in Li-ion batteries, the monomers for polycarbonate and non-isocyanate polyurethane synthesis, intermediates for the manufacturing of pharmaceuticals and many other fine chemicals.[18,19] The formation of cyclic carbonates from epoxides and $CO_2$ involves fewer hazardous species, as it incorporates $CO_2$ as a C1 feedstock source rather than the conventional highly toxic and corrosive phosgene-based route. In addition, cyclic carbonates can also be used as a monomer in the synthesis of non-isocyanate polyurethanes, polycarbonates, and polyglycerol.[20-22] These carbonate compounds are being used as a commodity chemical whilst oxazolidinones have found use as fragments of antibiotic compounds.[23]

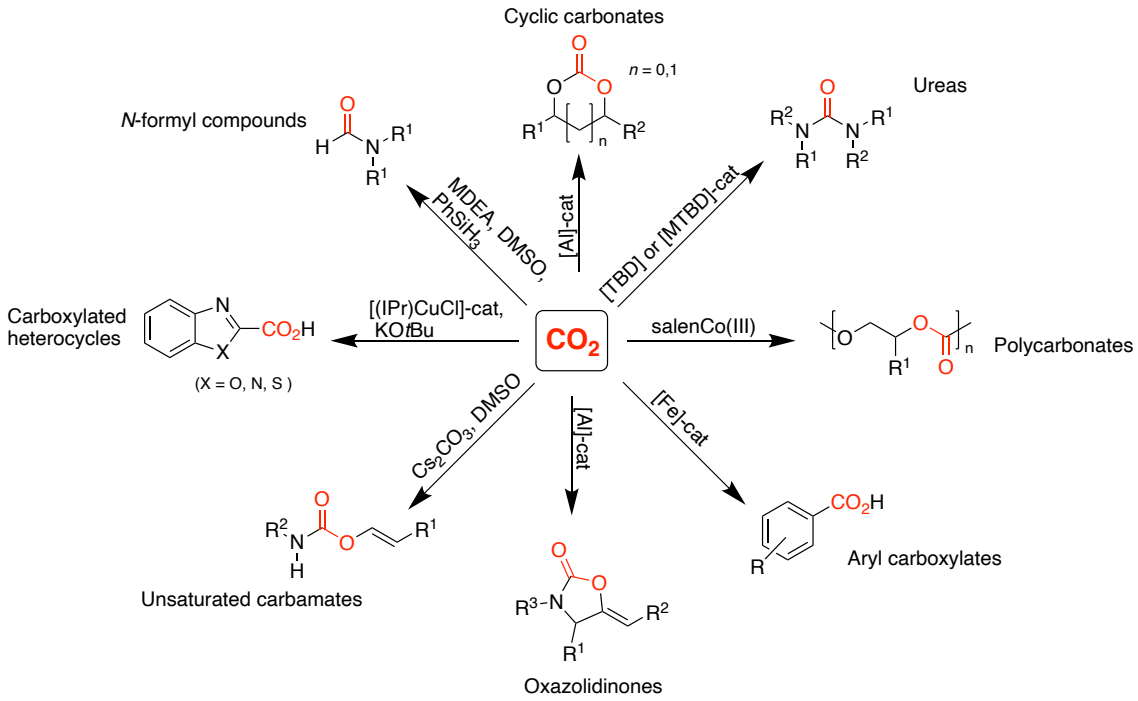


**Figure 1.5** $CO_2$ as a renewable feedstock in synthetic chemistry, with examples of catalysts included.[24-33]

The cycloaddition of epoxide and $CO_2$ is now attracting a lot of interest as a result of its possible further uses. The ring structure allows for making other commodity materials from the cyclic carbonate products. The conversion of aziridines and $CO_2$ to oxazolidinones also presents a new challenge with additional

complications owing to the presence of a substituent on the nitrogen atom of aziridine and the possibility of forming regioisomeric products. The production of oxazolidinones is of importance as this is a crucial heterocyclic fragment found in many commercial pharmaceuticals and also has a range of other further synthetic applications.[34,35]

The production of cyclic carbonates and oxazolidinones from $CO_2$ requires an effective catalyst to overcome the stability of $CO_2$ and allow reactions to be carried out under mild reaction conditions. Due to its thermodynamically stable structure, which provides a significant challenge in synthetic chemistry, various catalysts have been studied, both metal and organic type catalyst, to reduce this high energy requirement.[36,37]

### 1.1.3 Chemo-catalytic activation of $CO_2$

Activation of $CO_2$ is of great interest. However, due to the high kinetic and thermodynamic stability of $CO_2$, the effective utilisation as a C1 building block is challenging, with high free energy substrates. With a catalyst, $CO_2$ can be activated under mild conditions; nonetheless, synthesising an effective and cheap catalyst is also challenging. This section considers the use of different products from specific substrates, in particular, oxazolidinones from epoxide/$CO_2$ and aziridine/$CO_2$ couplings, respectively.

#### 1.1.3.1 Overview of the reaction of epoxides and $CO_2$ to form cyclic carbonates

Oxiranes, also known as epoxides, are a type of cyclic ether that is more reactive than a non-cyclic ether due to the significant ring strain. The structure has a unique three-membered ring structure close to an equilateral triangle with a bond

angle of approximately 60° in contrast to an ideal 109.5° of a tetrahedral carbon, and therefore they readily open under mild conditions by a range of nucleophiles.[38] Apart from having a spring-loaded structure, epoxides have a significant property of displaying Lewis basicity due to non-bonding electron pairs on the oxygen atom.[39] These compounds are commonly used in industry due to their readiness to form other important compounds, which have encouraged the scientific community to develop numerous methods for synthesising epoxides from alkenes.[40] There are several methods used for the epoxidation of alkenes shown in Scheme 1.1. These epoxides can then react with other coupling partners to give different products.[41]

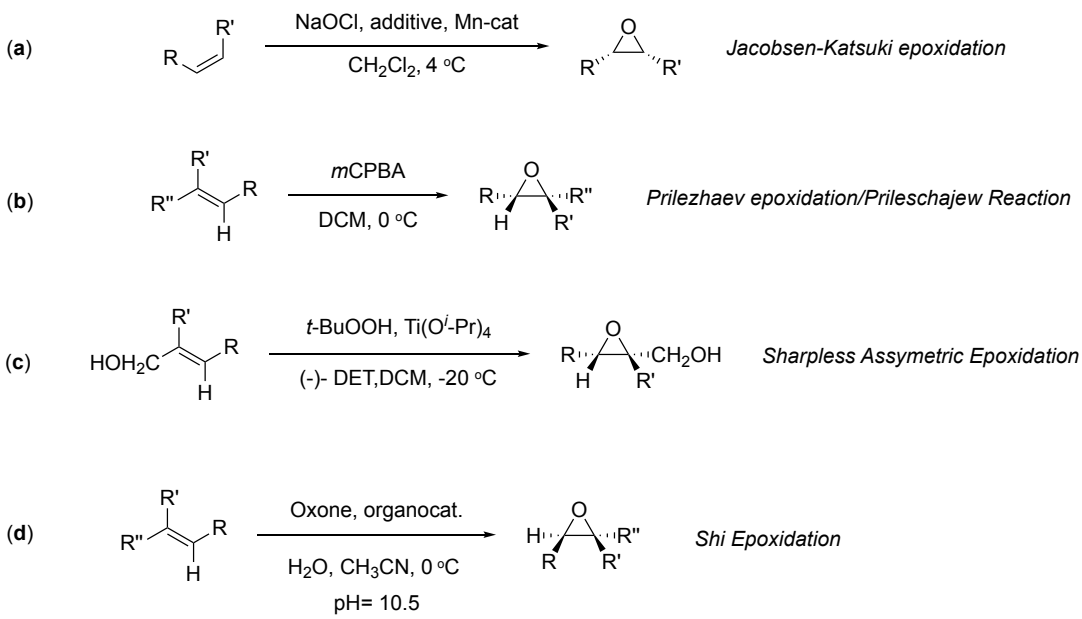


**Scheme 1.1** Different syntheses of epoxides from alkenes.[42-44]

Epoxides have been widely used, mainly in producing plastics by reacting them with Bisphenol-A, a compound known for its carcinogenic properties and coming under increasing legislative scrutiny.[45] Common applications of epoxides include epoxy resins,[46] plasticizers,[47] and precursors to coatings.[48] Furthermore, epoxides are used to sterilise medical equipment and materials in which the DNA

and RNA of microbes will act as a nucleophile and react with epoxides, which forms an alkylated group that interferes with cell function and results in apoptosis.[49] Nonetheless, to ensure the successful conversion of epoxides into cyclic carbonates, an effective catalyst must be used to liberate the ring-strain energy in epoxides and successively activate $CO_2$. There are two possible catalytic pathways according to the applied starting material that promotes the formation of the desired product: hydrogen bonding catalysis and Lewis acid catalysis.

### a. Hydrogen bonding mechanism

Hydrogen bond (HBD) catalysis has emerged over decades where the presence of functional groups such as -*OH* and *COOH* in a compound can also activate the substrate and synthesise a cyclic carbonate (Scheme 1.2) either with a suitable solvent or in a solvent-free reaction.[50] Unfortunately, synthesising polycarbonates using this type of catalysis is quite challenging. This is due to the formation of water during the propagation stage that prevents the formation of a longer polymer chain resulting in unappealing lower molecular weight products.[22,51] There are existing works on a metal-free catalysts for $CO_2$-derived cyclic carbonate synthesis but these are very rare for polymer production.[52,53]

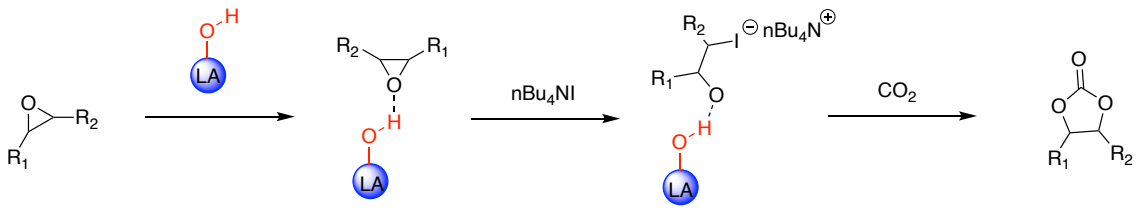


**Scheme 1.2** Catalytic interaction for the synthesis of cyclic carbonates through hydrogen-bond interaction.

Several papers have reported the synthesis of cyclic carbonates in a metal-free catalyst system. For example, Kleij and co-workers reported a binary catalytic system composed of pyrogallol/$Bu_4NI$ with which was efficient for the production of cyclic carbonates.[54] This catalytic system could be applied under very mild conditions (25-45 °C, $P_{CO2}$ = 1.0 MPa) with relatively low catalyst loadings of 2.5 mol % without a solvent. The mode of action of this system was studied using Density Functional Theory (DFT), showing the efficient stabilisation of the reaction intermediates through an extended hydrogen-bonding network, making the epoxide ring-opening by the co-catalytic halide nucleophile more favourable as shown in the proposed mechanism (Scheme 1.3).

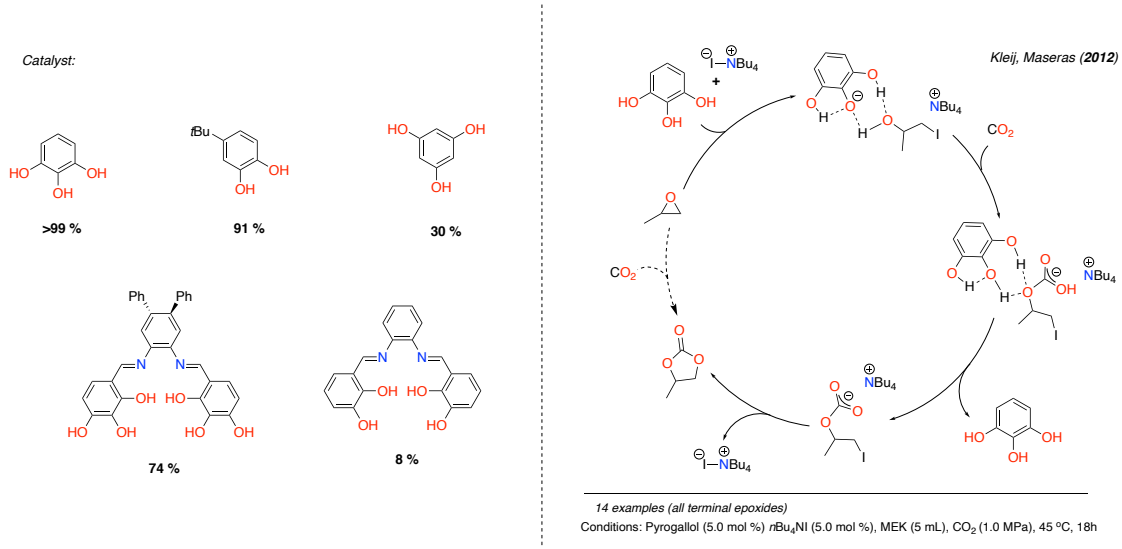


**Scheme 1.3** Polyphenolic catalysts studied for the synthesis of cyclic carbonates (right). Reaction mechanism of pyrogallol/$Bu_4NI$ catalyst with specific parameters (left).[54]

Another report using pyrogallol/$Bu_4NI$ catalyst with polystyrene (PS), as a catalytic support system, by Pericàs and Kleij.[55] They produced a PS-supported catalyst system that does not undergo deactivation problems through formulating a bifunctional resin where the triazolium and pyrogallol units are linked to specific sites along the polymer backbone as shown in Scheme 1.4, showing significant progress from their previous work with pyrogallol regarding the suboptimal

recycling potential. This recyclable catalyst has a single-component binary system composed of a 1,2,3-tris-hydroxybenzene/pyrogallol and polystyrene support that can synthesise cyclic organic carbonates at low temperature (45°C-65°C) and low $CO_2$ pressure of 1.0 MPa from a range of epoxides, both terminal and internal examples. This one-component binary catalyst system retains its activity levels for a more extended period and only requires the addition of methyl iodide to be regenerated once activity starts to deteriorate.

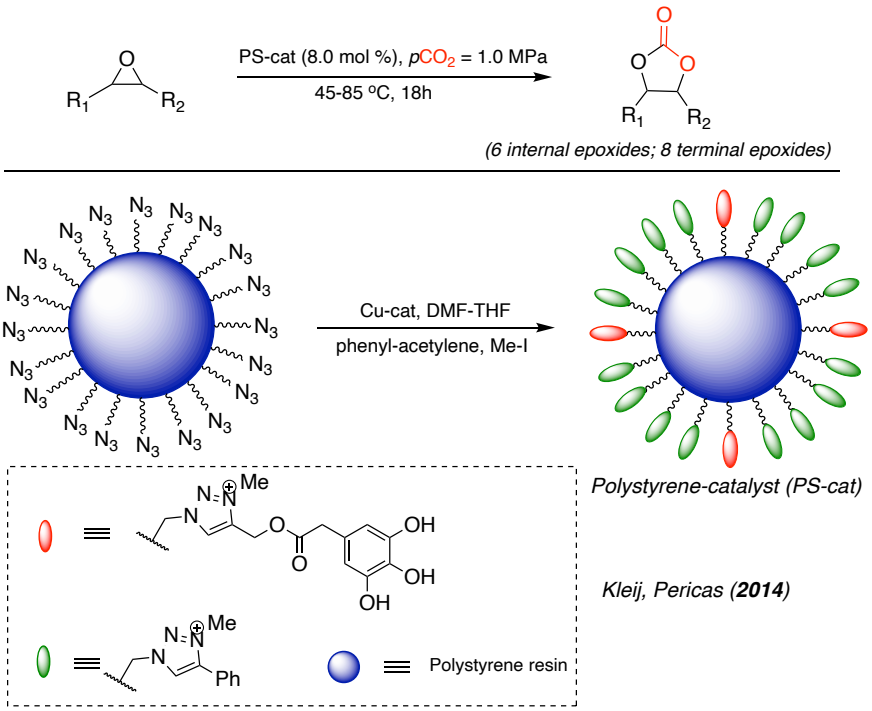


**Scheme 1.4** Catalytic reaction using a heterogeneous PS-supported catalyst.[55]

In 2019, North and co-workers reported a single-component binary catalyst consisting of a metal- and halide-free complex that shows a significant catalytic activity at low $CO_2$ pressure (1.0 MPa) and a temperature of 120 °C.[56] The synthesised compound, *N*,*N*′-Phenylene-bis(5-tert-butylsalicylideneimine), shown in Scheme 1.5 (**1**), belonging to the salophen group and this was used as a catalyst without the presence of a halide nucleophile. This salophen compound

works as a catalyst with one phenol group acting as a Brønsted acid to activate the epoxide, while another phenol group activates the $CO_2$ by forming a carbonic half-ester resulting in an intermediate in Scheme 1.5 (**Int (1)**).

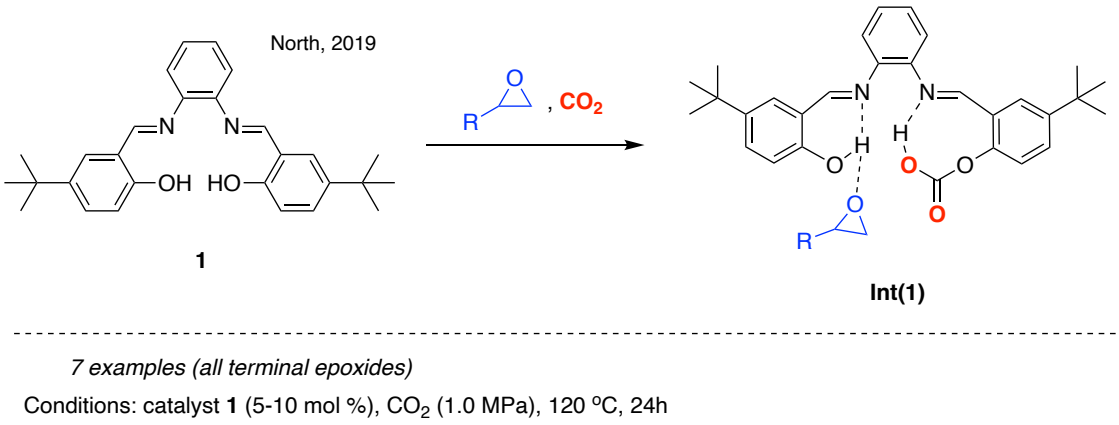


**Scheme 1.5** Formation of intermediate through hydrogen bond interaction, showing a proposed simultaneous activation of epoxide and $CO_2$.[56]

The activity of the catalyst dramatically affects the reaction due to the substituents present in the salophen, as shown in several experiments from various salophen compounds. Kleij has also identified that the position of the hydroxyl group is important in catalysis through experimental and theoretical analysis to provide the required *H*-bond network.[57] In addition, North and co-workers highlighted that those substituents close to the phenol functionality inhibit the activity (Figure 1.6).[56] Simple phenols usually are good nucleophiles, and the observed intramolecular hydrogen bonding increases the nucleophilicity of the phenol oxygen atom in salophen derivatives.[58] This explains the relative para-position of the substituents, which increases the solubility of the catalyst, thus promoting higher catalytic activity. Although the precise mechanism of how the salophen works as a catalyst without a nucleophile is not yet fully understood, it is crucial to see that using uncomplexed salophen ligands can also be used as a catalyst to produce cyclic carbonates.

North, 2019

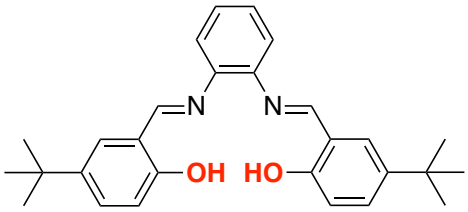


1 mol % catalyst, 120°C,
10 bar $CO_2$, 3.5 h, **93 %**

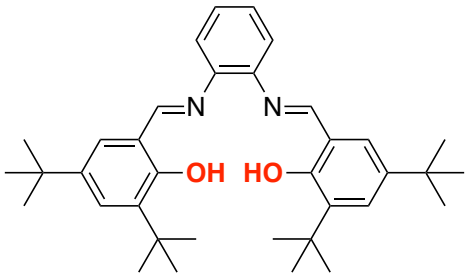


10 mol % catalyst, 120°C,
10 bar $CO_2$, 24 h, **20 %**

---

Kleij & Maseras, 2012

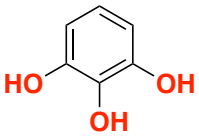


5 mol % catalyst/TBAI co-catalyst,
45°C,10 bar $CO_2$, 18 h, **100 %**

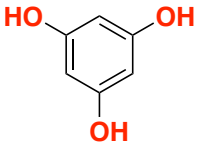


5 mol % catalyst/TBAI co-catalyst,
45°C, 10 bar $CO_2$, 18 h, **30 %**

**Figure 1.6** Salophen and pyrogallol catalyst for cyclic carbonate synthesis with specified reaction conditions.[54,56]

### b. Lewis acid catalysis

A Lewis acid is a chemical species that acts as an electron pair acceptor and can increase the substrate reactivity in a reaction. In the context of cyclic carbonate synthesis most Lewis acids have been used as initiators/catalyst, either directly or indirectly. This includes Group 13 elements which due to their highly vacant p-orbitals, results in robust electron-accepting properties making them strong Lewis acids.[59] For example, complexes with a boron centre can be converted into a tetrahedral $sp^3$-hybridisation from a neutral trigonal planar $sp^2$ hybridised state under suitable conditions resulting in boron compounds with distinctive properties and different chemical structures.[60] Furthermore, three-coordinated boron compounds contain a vacant p-orbital which makes them strong Lewis acids and allows them to form a fourth coordination bond with various nucleophiles.[61]

In previous studies, Lewis acids along with a suitable halide nucleophile, also called co-catalysts, were proven to be an effective catalytic system in the cycloaddition of $CO_2$ and epoxides. A general reaction mechanism is shown in Scheme 1.8.

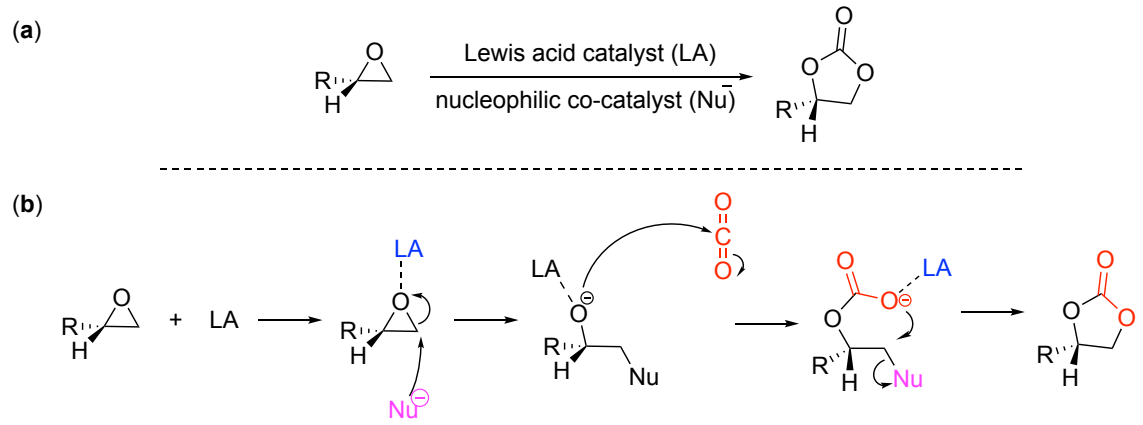


**Scheme 1.6** Reaction mechanism of epoxide and carbon dioxide forms cyclic carbonate in the presence of a Lewis acid catalyst and nucleophile co-catalyst.[62]

Over the past few years, various homogeneous catalytic systems such as phosphonium salts,[63] metal oxides,[64] metal-salen,[65] ionic liquids,[66] and alkali metal salts,[67] have been studied and are particularly effective at coupling $CO_2$ with epoxides under neat conditions without the addition of organic solvent. Moreover, the cycloaddition of $CO_2$ to epoxide does not require solvent addition resulting in an accessible and inexpensive route in forming cyclic carbonate. This commonly requires a binary or bifunctional catalytic system consisting of a Lewis acid or with a hydrogen bond donor alongside a suitable nucleophile, mostly a halide nucleophile, which is an excellent leaving group such as tetrabutylammonium iodide ($Bu_4NI$), *bis*(triphenylphosphine)iminium chloride (PPNCl), and 4-Dimethylaminopyridine (DMAP).[50] In bifunctional homogeneous catalysis, the nucleophile could be a component of a metal complex as an axial ligand or as a sidearm on the ligand scaffold. In contrast, with binary catalytic

systems, the nucleophile is a separate species and is usually referred to as a co-catalyst.[55] The typical mechanism for the catalytic reaction of $CO_2$ is shown in Scheme 1.9, involving the initial coordination of the epoxide to the Lewis acid catalyst, then activates the epoxide towards the nucleophilic attack of the halide nucleophile following the ring-opening of the substrate. This nucleophile assists the ring-opening process of the substrate to form an alkoxide which subsequently interacts with $CO_2$, to form a linear carbonate species and then eliminates the nucleophile after the ring-closure process.[68,69] This could produce a cyclic carbonate or might further propagate by successive insertions of epoxide and $CO_2$ to form the polycarbonate.[70]However, this study does not focus on forming polycarbonates.

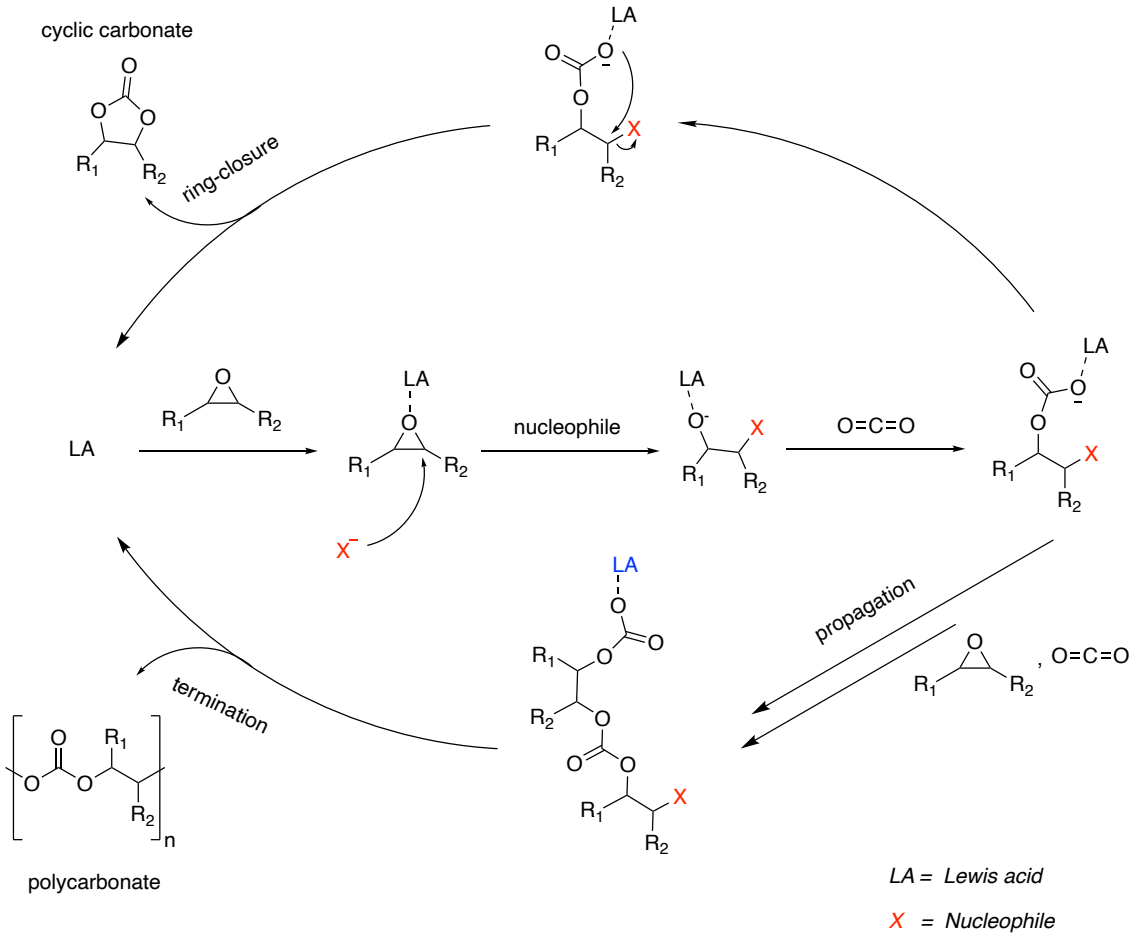


**Scheme 1.7** Established reaction mechanism for the formation of cyclic carbonates and polycarbonates from $CO_2$/epoxide using Lewis acid catalysis.

The order of catalytic activity of halide anions is typically $I^-$ > $Br^-$ > $Cl^-$ > $F^-$ for $CO_2$ cycloaddition to terminal epoxides corresponds with the leaving group ability of halide anions and its nucleophilicity, wherein a small nucleophile is more efficient due to the steric hindrance that plays an essential role towards the catalytic activity with terminal epoxides.[71,72]

The strength of Lewis acid compounds can be measured in several ways, and one of the commonly used methods is the Gutmann-Beckett method.[73] This method is based on NMR spectroscopy data, which uses triethylphosphane oxide ($Et_3PO$), a Lewis base, where the phosphoryl group interacts with the Lewis acid and causes a shift in the $^{31}P\{^1H\}$ NMR of the phosphine oxide. The resulting chemical shift can be used to calculate the Acceptor Number (AN) scale with the equation described below, wherein the higher AN corresponds to the more excellent Lewis acidity of the compounds.

$$\mathbf{AN} = \mathbf{2.21}\ (\boldsymbol{\delta}_{\mathbf{LA{*}Et_3PO}} - \mathbf{41}) \qquad \text{Equation 1}$$

### 1.1.3.2 Overview of aziridines/$CO_2$ reaction to form oxazolidinones

Aziridines are three-membered nitrogen-containing cyclic molecule, commonly used as a building block in many synthetic procedures.[74] The interest in synthetic methodologies for preparing the aziridinyl system has increased in the last decades. The aziridine functional group imparts essential biological activity, mainly as antitumor behaviour, as revealed by some naturally occurring compounds bearing the aziridine ring.[74-76]e resultant tendency toward ring-opening reactions makes aziridine a valuable precursor of more complex molecules. Several functional molecules, such as amines, amino acids, amino alcohols, and other nitrogen-containing compounds could be obtained by ring cleavage.[77] The aziridine structure has a unique three-membered ring structure

close to an equilateral triangle which is similar to epoxides, and therefore they can be readily opened under mild conditions.[21]

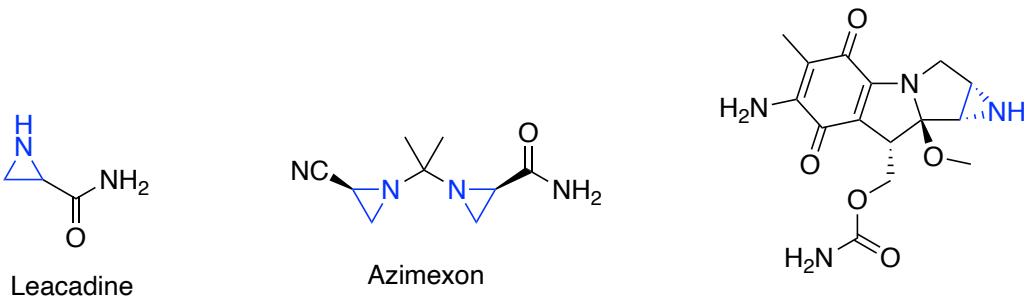


**Figure 1.7** Selected examples of aziridine with crucial biological activity, mainly as anticancer agents.[74-76]

Nowadays, aziridines might be considered the nitrogen equivalents of oxiranes. Despite tremendous progress in aziridine synthesis over the past decade, various *N*-substituted aziridine products remain difficult to access efficiently. This is particularly true for the stereoselective synthesis of aziridines. While general methods for the stereoselective synthesis of oxiranes are available, the same could not be said, until recently, for aziridines. However, in recent years this gap has been filled, and several methodologies were invented or improved and are now available for preparing aziridines in a highly stereo- and enantioselective manner. Many efficient and more general synthetic strategies have been developed to prepare aziridines.

Aziridines can be synthesised in numerous ways, including $SN_2$ displacement, 1-4 addition, the addition of carbenes, electrophiles, nitrenes and reduction. Selected examples of nonactivated aziridines are shown in Figure 1.8.

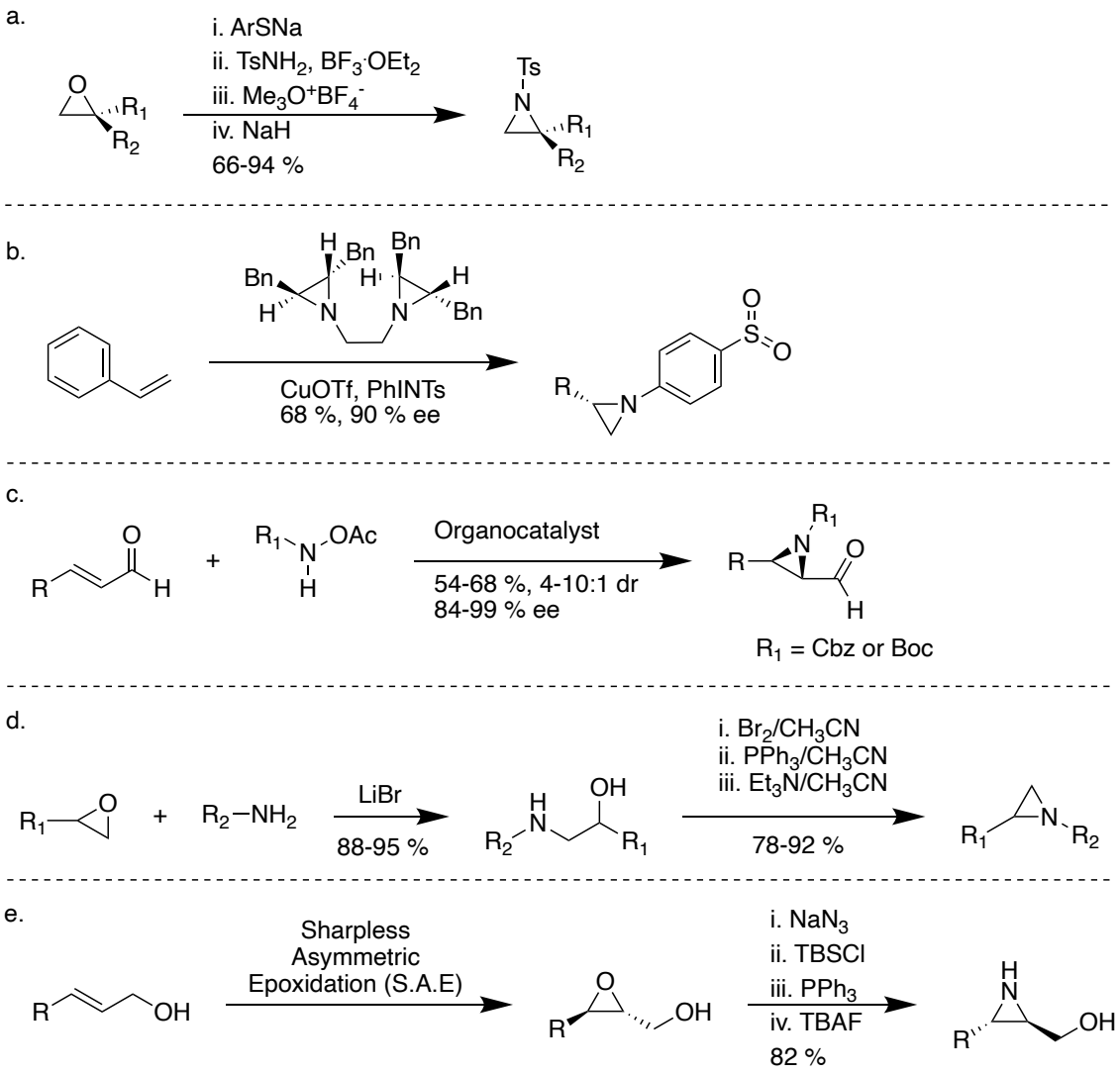


**Figure 1.8** Selected examples of aziridine synthesis.

Aziridines undergo various transformations, and in this thesis almost an entire chapter focuses on converting aziridine and $CO_2$ into oxazolidinone. Oxazolidinones are a widely known group of antibiotics that are active against a large spectrum of Gram-positive bacteria, including methicillin- and vancomycin-resistant staphylococci, vancomycin-resistant enterococci, penicillin-resistant pneumococci, and anaerobes.[78]

The discovery of antibiotics has a profound positive impact on the improvements of human health and life expectancy, although, the emergence of antibiotic resistance has severely limits their clinical efficacy and

applications.[79,804] Drug-resistant bacteria, especially multi-drug resistant (MDR) bacteria, represent the most common causative agents of nosocomial infections that are difficult to deal with using currently existing antibiotics.[81,82] The continuous evolution and spread of antibiotic-resistant bacteria are even more severe, which have caused enormous financial burden worldwide in terms of increased morbidity, mortality and use of medical resources.[83-85] Oxazolidinones exert antibacterial activity by inhibiting protein synthesis, and resistance to other protein synthesis inhibitors does not affect oxazolidinone activity, although there are rare findings on resistance cases during treatment.

The first example of the oxazolidinone-containing antibiotic drug is ZYVOX© (linezolid), an IV and orally available oxazolidinone approved for several indications, including infections caused by vancomycin-resistant enterococci (VRE), nosoco-mialpneumonia, community-acquired pneumonia, uncomplicated skin and skin structure infections (uSSSI), and cSSSI.[86] Since 2011, only three new novel antibacterial structural classes have been approved by the FDA in the last 30 years, and one of them was linezolid. When linezolid was approved in 2000, it became the reference oxazolidinone compound to improve upon going forward, and several studies on oxazolidinone derivatives showed antibacterial activity such as tedizolid and radezolid.[87-89]

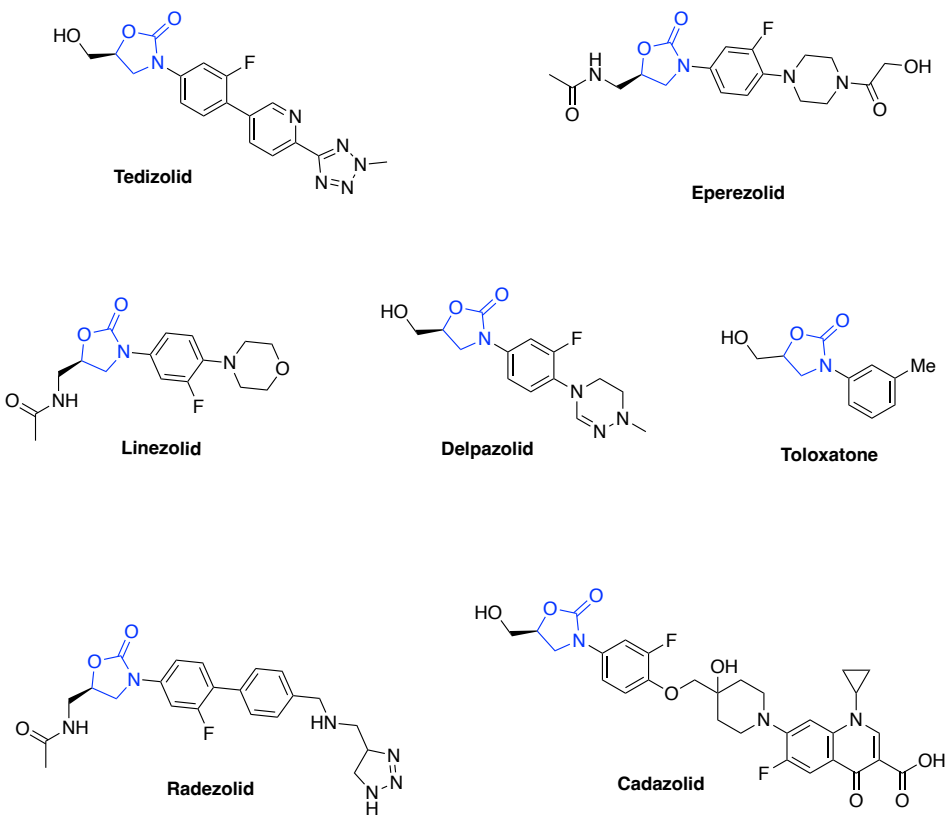


**Figure 1.9** Selected examples of compounds used in the medicinal industry containing oxazolidinone structure.

There are several well-known strategies to synthesise oxazolidinones. The most common reaction is the use of amino alcohol and phosgene substrates. This process has advantages in preserving the regiochemistry and stereochemistry of the starting amino alcohol. However, the toxicity of phosgene and relatively poor atom economy, which losses two equivalents of chlorine during the reaction, are the disadvantages of this reaction.[90] Similarly, the carbonylation reaction of β-amino alcohols with $CO_2$ or dialkyl carbonates represents a more sustainable approach than using amino alcohol substrates.[91] A multicomponent reaction of rare-earth metal amide is another approach to synthesise oxazolidinone.[92] Another method for the formation of oxazolidinones by reaction with a non-aziridine route is the cycloaddition reaction of epoxides with isocyanates.[93] This reaction is analogous to the similar reaction between epoxides and carbon

dioxide and has several advantages, such that epoxides are readily prepared from alkenes, and the reaction with isocyanate substrates is entirely atom economical. The disadvantage of this approach involves the use of isocyanates, which are very toxic with methyl isocyanate, the chemical involved in the 1984 Bhopal disaster, one of the most severe chemical accidents in history.[94] Isocyanates can also react violently with water, increasing the chances of being unintentionally dispersed, as happened at Bhopal. Therefore, the alternative approach from aziridine substrate reacted with carbon dioxide is attractive. Since $CO_2$ is a non-toxic and inexpensive reagent, commonly available as a waste product from several industrial processes, and the reaction with aziridine occurs with 100% atom economy.[95] However, caution is necessary as aziridines are toxic and carcinogenic due to their ability to alkylate biological molecules, including DNA, although the toxicity data is not available for many examples of aziridines.

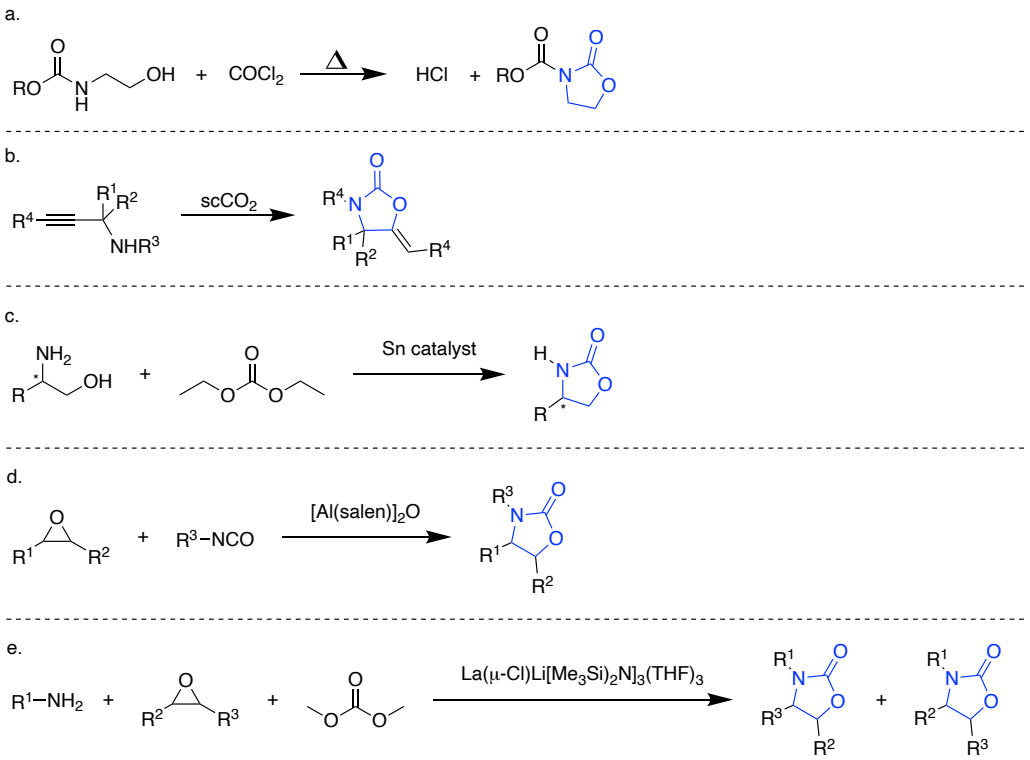


**Scheme 1.8** Selected examples of different ways to synthesise oxazolidinone compound.[91-93,96,97]

In order to successfully convert the substrates, an effective catalyst must be used to liberate the ring-strain energy of aziridine and successively activate $CO_2$. There is considerable variation in the reaction mechanism between aziridine and carbon dioxide substrate, and a broader variety of catalysts have been used, and some reports exist of catalyst-free reactions. However, in general, a Lewis acid catalyst has been used in conjunction with a nucleophile, usually a halide, similarly to the catalyst systems used to react between epoxides and carbon dioxide. With this reaction, however, there are two possible regioisomers, either 4-substituted or 5-substituted oxazolidinone products depending on which side of the parent aziridine the new oxygen-carbon bond is formed. A possible catalytic pathway is proposed that promotes the formation of the desired product through Lewis acid catalysis, as shown in Scheme 1.11. The process is, as mentioned, similar to the proposed mechanism displayed in Scheme 1.9 with the cyclic carbonate synthesis, however, with the existence of a regioisomeric products. The selectivity of regioisomer produced is determined by a combination of the electrophilicity of two sites in the catalyst-aziridine complex and steric influence upon nucleophilic attack of the same species.

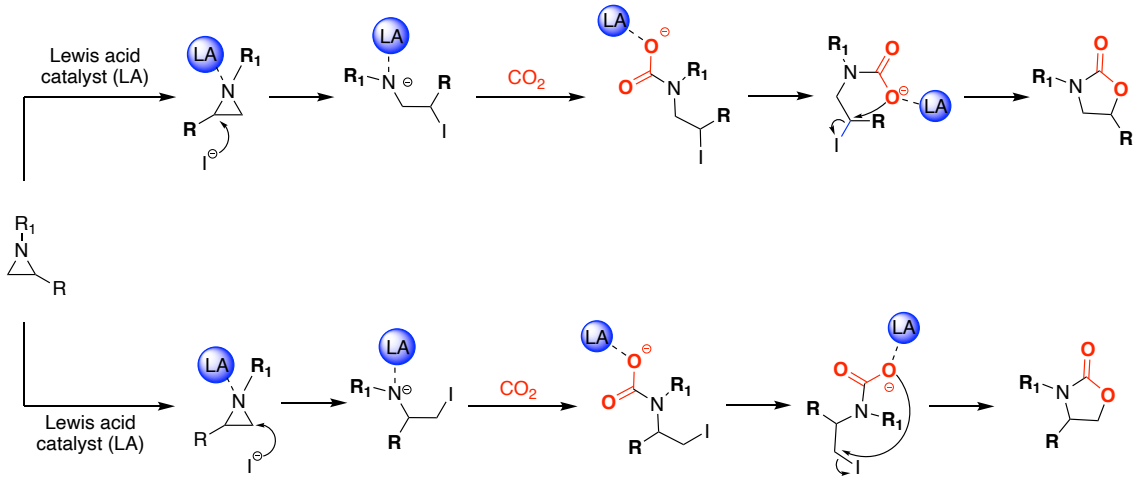


**Scheme 1.9** Proposed mechanism for the formation of oxazolidinones from the reaction of $CO_2$ and aziridine.

The mechanism generally leads to retention of stereochemistry at the carbon atom bonded to oxygen due to double inversion; however, in some specialised cases, multiple inversions due to excess nucleophile or $SN_1$ character may lead to racemisation.

### 1.1.4 Group 13-based Lewis acid catalysts for cycloaddition reaction

Lewis acidity of the catalysts enhances the ring-opening process of epoxides during the mechanistic cycle of the coupling of $CO_2$ and epoxides.[98] Nevertheless, the cycloaddition reaction of epoxide and $CO_2$ involves using an additive with a strong nucleophilicity, such as tetrabutylammonium halides, which play an important role.[99]

In recent years, a halide nucleophile combined with a Lewis acid has been recognised as a powerful catalytic system for the cycloaddition of $CO_2$ to epoxides by promoting the ring-opening step of the mechanism (Figure 1.10). Several metal-based coordination complexes containing Lewis acidic metal centres have been developed as catalysts for this reaction. Metal complexes that have been reported to mediate the coupling of epoxides and $CO_2$ successfully, however, only a few reports detail the reaction of aziridines with $CO_2$, for example, Al, Zn, Mg, Fe, Mn and Yb catalysts.[54,100-101]

For example, Kleij and co-workers reported Ytterbium(salen)-based complexes for the cycloaddition of $CO_2$ and cyclohexene oxide, promoting copolymerization of the cyclic carbonates.[3102] In addition, Kleij developed a highly active aluminium catalyst for the formation of cyclic carbonates consisting of a meta-substituted aluminium-based complex that displays a high turnover frequency (TOF) of up to 36,000 $h^{-1}$ at 90 °C and with $CO_2$ pressure of 1.0 MPa.[103] Several studies were performed to enhance the catalytic activity of this complex

by connecting electron-withdrawing groups to the ligand framework, which theoretically increased the Lewis acidity of the metal centre in the catalyst. Ghosh and co-workers discovered a highly active Co(II)(bisamido-bisamine)-based catalyst which contains a bis-chlorinated substituted ligand that is considered as a Lewis acidic catalyst and converted the propylene oxide to a corresponding cyclic carbonate having an average TOF of 662 $h^{-1}$ at 130 °C in 3 h.[104]

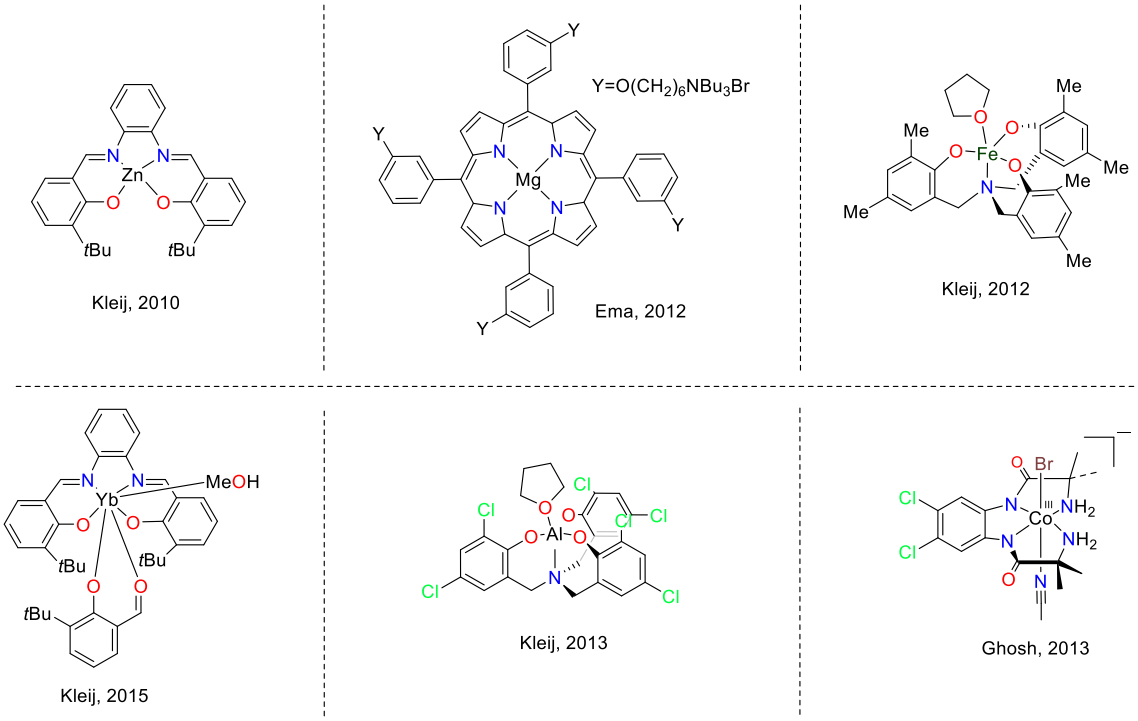


**Figure 1.10** Selected examples of catalysts based on a variety of metals for the conversion of $CO_2$ and epoxides to cyclic carbonates.[1,100-102,104]

Furthermore, the presence of a nucleophile additive such as tetrabutylammonium halides with strong nucleophilicity are usually required in all these examples mentioned above. It should be noted that the use of a small nucleophile is more effective wherein the steric hindrance plays an important role.[105]

Whilst Lewis acidity of the catalyst plays an essential role in activating the substrate that acts as a Lewis base. An attempt to establish an efficient approach

for the cycloaddition reaction in utilising $CO_2$ is the focus of this study. A review of a selected variety of group 13-containing catalysts is reported in this chapter.

### 1.1.4.1 Boron-based catalysts

Boron contains three valence electrons representing a strong electron-withdrawing element and is considered as highly Lewis acidic within its group.[106] Boron is the only non-metal element in group 13 of the periodic table and has slowly been developed for its unique properties in catalysis. Generally, boron reagents are employed as Lewis acids and have shown high Lewis acidity between other elements from group 13.[107] Borates and boranes, are being investigated by researchers interested in exploiting their catalytic potential. [108]

A metal-free catalytic system with metal-like performance containing high Lewis acid properties is also evolving up to now, together with the wider application of boron complexes (Figure 1.11).

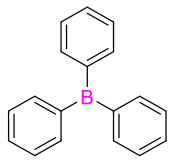


Kerton, 2019

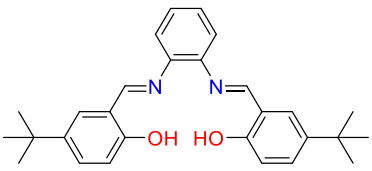


North, 2019

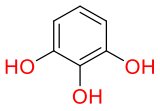


Kleij & Maseras, 2012

**Figure 1.11** Example of successful metal/non-metal catalyst for the synthesis of cyclic carbonates.[54,56]

For example, Mu/Xue and co-workers have reported a molecule comprising of both Lewis acidic and Brønsted acidic sites that individually act as catalyst sites to activate the epoxides simultaneously through interaction with Lewis acidic sites and formation of hydrogen bonds with Brønsted acidic sites, as depicted in Scheme 1.12.[109] This type of catalyst requires more nucleophile to support the coexistence of both acidic sites that activates the substrates simultaneously,

resulting in more than half of the product's yield, thus requiring an extra amount of nucleophile.

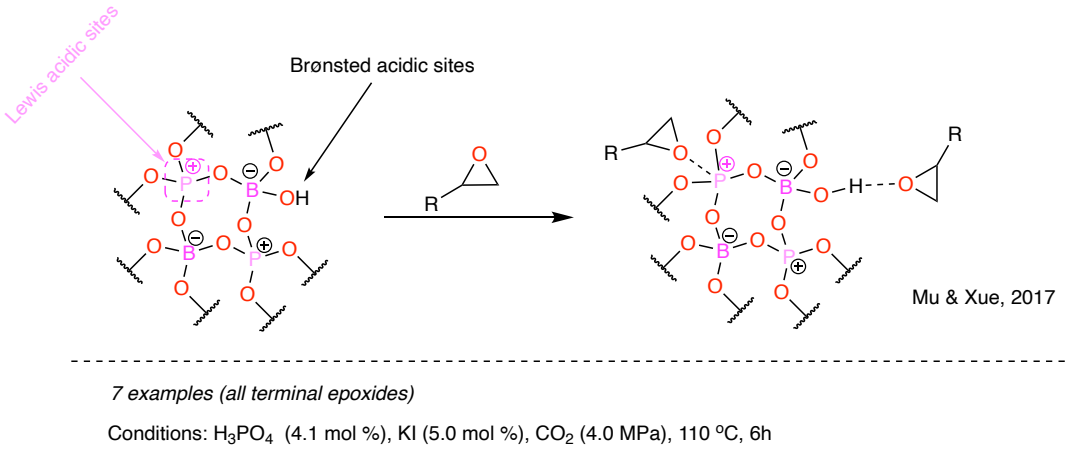


**Scheme 1.10** Simultaneous epoxide activation in a coexistence Lewis and Brønsted acidic site in a solvent-free reaction.[109]

Mu and Xue have reported the synthesis of various cyclic carbonates with an average yield of >90 % using $BPO_4$ as the catalyst and KI as a co-catalyst within a short reaction time. This binary catalyst maintains activity even after five catalytic cycles through precipitation of the dissolved KI in ethyl ether followed by separation along with $BPO_4$ via centrifugation process, making it cheap and easy to recycle. The reactivity of this nucleophile has also been tested and was found to exhibit a consistent nucleophilicity of halide ion (Cl < Br < I) present in potassium which may not be suitable with other binary catalysts, hence, the preparation of an effective catalyst is continuing.

Several catalysts work differently when applied to other substrates, including epichlorohydrin, which has an intriguing form of activation from several catalysts.[110] Mu and Xue have used $BPO_4$/KI binary catalytic system to convert epichlorohydrin into its corresponding carbonate.[109] However, due to the presence of the electron-withdrawing (-$CH_2Cl$) group as a result of the reduced electron density of the oxygen atom within the epoxide ring, the yield is not as

high as other substrates. This is in contrast with the obtained results of Kilic and co-workers in 2019 using boron complexes. They have synthesised neutral and charged boron complexes, and the cationic boron complex displays a higher activity towards five different epoxides, and epichlorohydrin displays the highest yield (Scheme 1.13).[111]

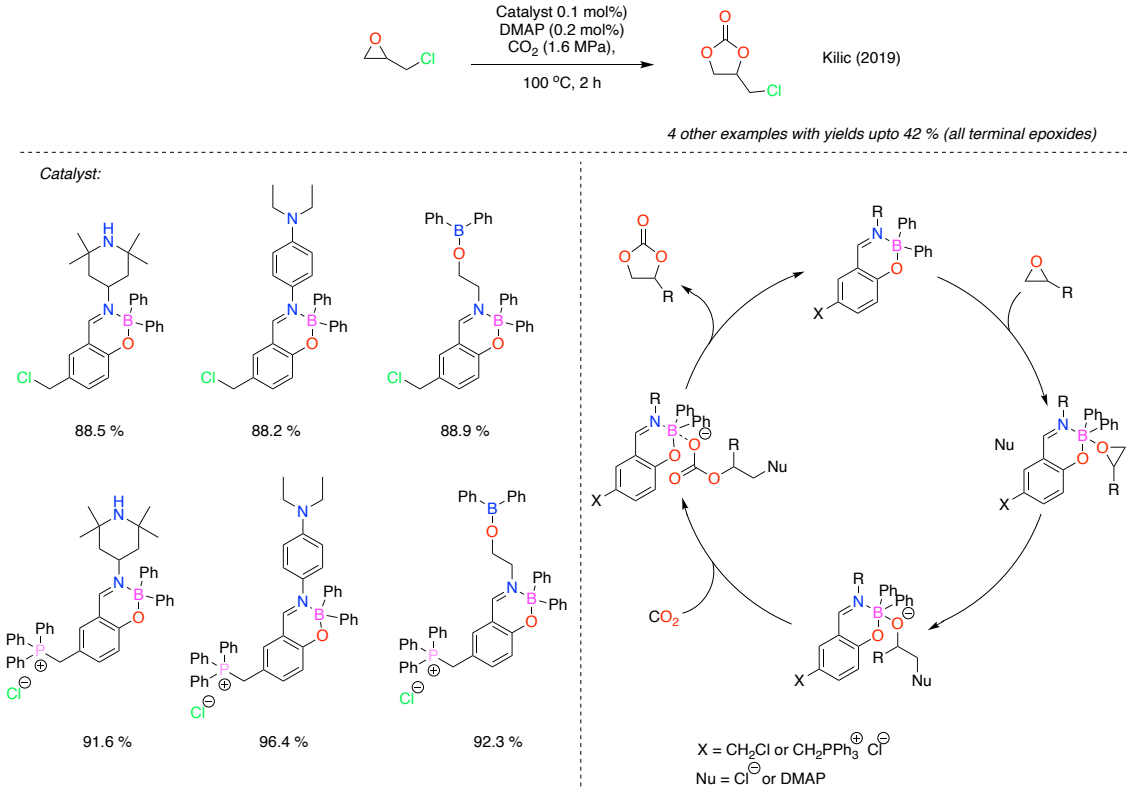


**Scheme 1.11** General mechanism of neutral and charged boron complexes for cyclic carbonate synthesis showing the structure and conversion in percent of epichlorohydrin of each complex.

Based on the work from Kilic, the presence of chloromethyl (-$CH_2Cl$) group in epichlorohydrin weakens the C-O bond of the epoxide, making it more prone to ring-opening of the substrate, thus resulting in a higher rate of conversion.[112] The fact that these cationic catalysts provide a higher yield for epichlorohydrin in contrast to other terminal epoxides, therefore, limits the wider applicability of this catalyst. In addition, the reactivity of the catalyst did not increase even with the presence of two boron centres, which could lead to doubts about the proposed

mechanism shown in Scheme 1.11. Its overall sustainability is also challenging as most of these catalytic systems require an operating temperature above 100 °C.[113] Despite the drawback, this example provides an early example of Lewis acid catalysts based on boron, whilst it also provides significant scope for future development of ionic catalysts.

The pursuit of developing a metal-free catalyst is inspiring researchers to investigate the catalytic potential of boron complexes. This includes Kerton's study on readily available borane reagents that can act as a catalyst in the production of cyclic carbonate and polycarbonates under mild reaction conditions depending on the nature of the substrate and the strength of Lewis acidity.[114] For example, the *tris*(pentafluorophenyl)borane (BCF) was first synthesised in the 1960s and is considered a strong Lewis acid because of its strong electron-withdrawing effects from the three perfluorinated aryl rings.[115] The strength of Lewis acid compounds can be measured in several ways, and one of the commonly used processes is the Gutmann-Beckett method, as outlined above in section 1.1.3.1b[116] As shown in Figure 1.12, triphenylborane (TPB) has an AN of 55.03, whilst the more Lewis acidic *tris*(perfluorophenyl)borane (BCF) provides an AN of 78.90.[73,116] This explains the more Lewis acidic BCF than $BPh_3$, although weaker than the strong Lewis acid $BF_3$.

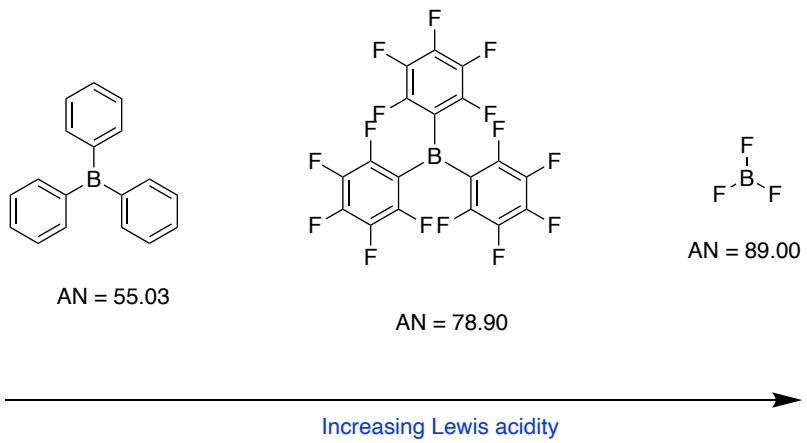


**Figure 1.12**. Comparison of Lewis acidity of boranes. (AN=Acceptor number based on Gutmann-Beckett equation)

The reactivity and selectivity of $BPh_3$ and BCF as a catalyst with the presence of a suitable co-catalyst using 2.0 MPa of $CO_2$ pressure and 100°C of temperature provides an impressive turnover number (TON) of 2,960 and 2,720, respectively. The BCF molecule displays lower activity due to its increased Lewis acidity resulting from the presence of fluorine substituents mentioned above. With reference to higher Lewis acidity, there is a robust affinity between the central atom and ligand to the substrate, and intense interaction may inhibit product release while slowing down the catalysis.[117] Thus, high Lewis acidity and catalytic turnovers are often incompatible, and the choice of either central atom or ligand is crucial to designing a Lewis acid catalyst.[118] This follows the results from using a different substrate wherein using epichlorohydrin as the substrate using 0.1 MPa of $CO_2$ pressure reacted for 24 hours gives a >99 % yield compared to propylene oxide (PO), which only gives 31 % yield under the same conditions by using only $BPh_3$ as a catalyst. Although both of substrates are terminal epoxides, the presence of electron-withdrawing substituents affects the reactivity of the catalyst.[119] This latter report builds on the original work reported in 2016 by Gnanou/Feng and co-workers, who applied triethylborane as a catalyst for the alternating copolymerisation of epoxide and $CO_2$, whereby no cyclic carbonate product was targeted and thus not reported (Scheme 1.12).[120] Later, in 2020, the authors synthesised cyclic carbonates from oxetanes using the same catalyst with some additional co-catalyst. The synthesis of both six-membered and five-membered cyclic carbonates by the metal-free coupling of oxetanes with $CO_2$ or that of epoxides with $CO_2$ was carried out under mild conditions, and this coupling process is co-catalysed by onium iodide salts associated with trialkyl boranes.

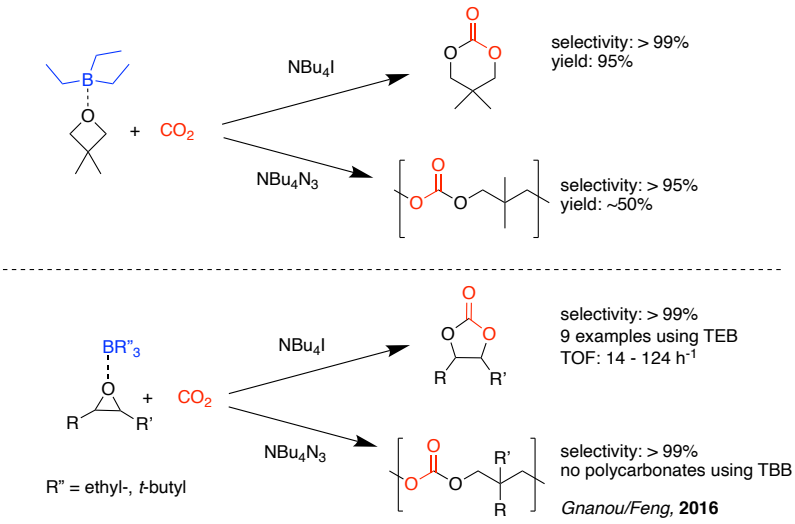


**Scheme 1.12** Reactions involved cyclic ethers and $CO_2$ using trialkyl borane as catalyst and halide co-catalyst.

Lu and co-workers have used the common boron oxide ($B_2O_3$) as a catalyst to investigate its potential for synthesising cyclic carbonates from $CO_2$ and epoxides.[121] The authors pre-treated the catalyst via a ball milling process showing a significant increase in catalytic activity through better substrate adsorption. This enhances the ring-opening process of the epoxide at the surface in the activated boron sites of $B_2O_3$ (Scheme 1.13). This heterogeneous catalyst ($B_2O_3$) has a good optimal recycling potential and can easily be separated through centrifugation and reused for up to five runs.

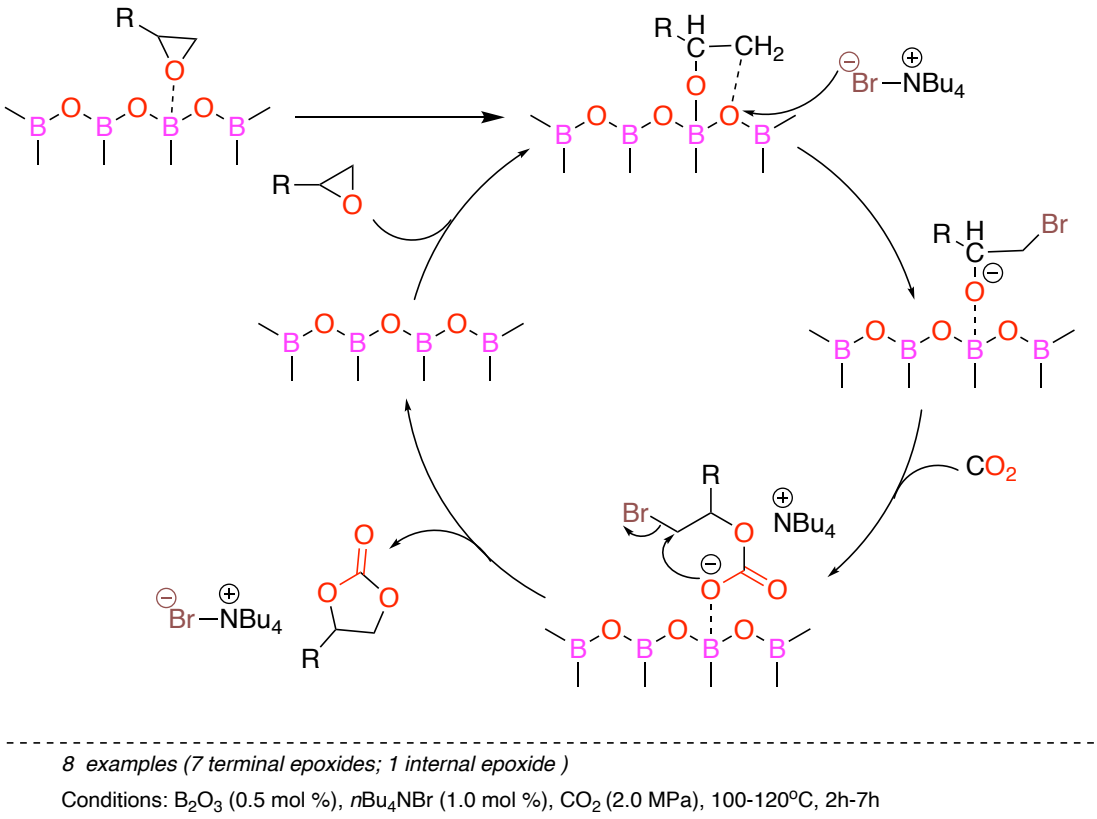


**Scheme 1.13** Reaction mechanism of $B_2O_3$ catalyst showing the conversion of $CO_2$ and epoxide into cyclic carbonate.[121]

Although the catalyst has good stability where there was no observed structural conversion from $B_2O_3$ to $H_3BO_3$ after several runs, this uncertainty cannot be avoided since $B_2O_3$ holds a partial B-OH structure which can form a hydrogen bond with epoxide. This takes into account the hygroscopicity of the compound and may cast doubt on the reaction mechanism if the reaction undergoes Lewis acid catalysis or through hydrogen bond interaction.

Zhang and co-workers investigated a range of boronic acids combined with a Bu$_4$NI co-catalyst using glycidyl phenyl ether as the substrate in water, considering that the catalytic activity was significantly weaker in other solvents compared with water.[122] This reaction mixture was performed at low temperature and $CO_2$ pressure, which provides a more sustainable catalytic system; however, high catalyst and co-catalyst loadings are required for the reaction to reach a

reasonable yield. The reaction mechanism is shown below in Scheme 1.14, where it is proposed that the activation of the substrate occurs through strong hydrogen-bond interaction instead of the Lewis acid catalysis from the boron centre, a finding which was supported through a brief DFT study. The authors have made a readily available non-metallic catalyst that works under mild conditions, but they have not mentioned a potential catalyst (Scheme 1.14-B) with a 4% higher yield than the further optimised catalyst.

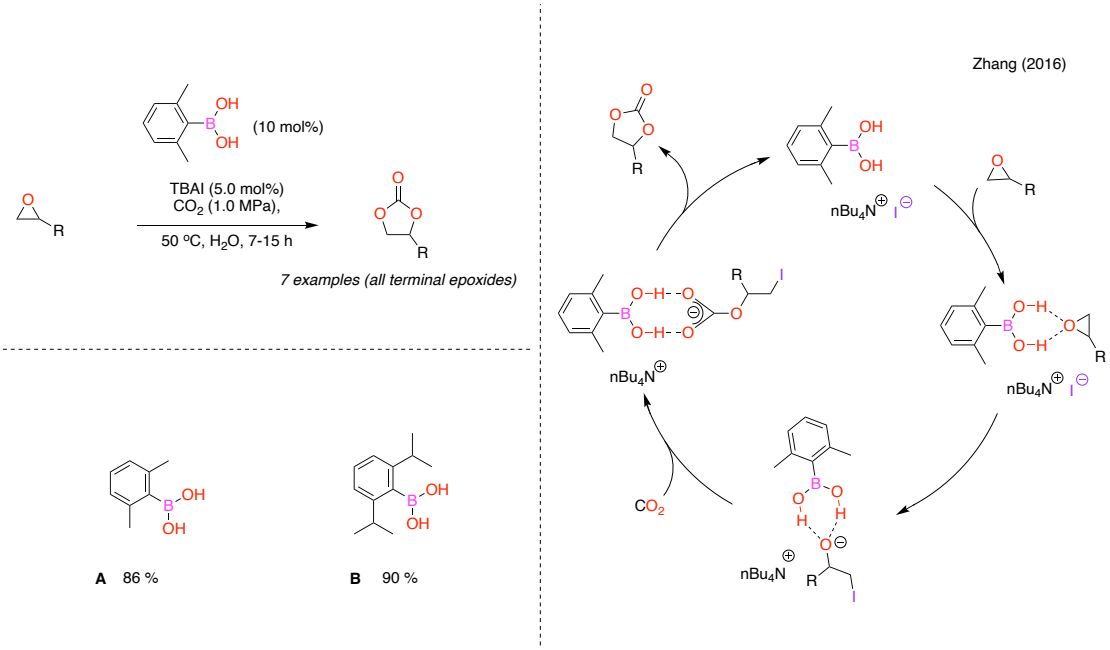


**Scheme 1.14** Overview and mechanism of boronic acid/$Bu_4NI$ catalysed preparation of cyclic carbonates.

Wu and co-workers reported the cycloaddition of epoxides with $CO_2$ in various cyclic carbonates using a bifunctional organoboron catalyst containing an electrophilic site (boron centre) and a nucleophilic site (quaternary ammonium salt).[123] This catalyst was reported as highly active and can withstand a high operating temperature of 150 °C. The proposed reaction mechanism was further investigated based on kinetic studies and its catalytic intermediates (Scheme 1.15). It was found that the synthesis of cyclic carbonate displays a relatively high

activity with a TOF value of 6,950 $h^{-1}$ (exclusive from $Bu_4NI$ nucleophile being used) and was applied to 13 various epoxides with a selectivity of >99 % and a general yield of ~90 %. Applying a metal-free catalyst using boron gradually narrows the gap from the highly efficient metallic catalyst; although this cannot surpass but could shed light on different metal-free catalytic designs.

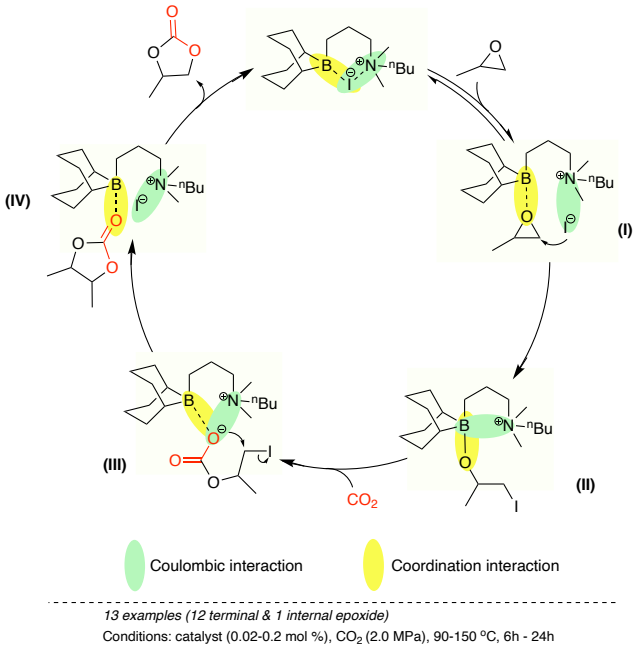


**Scheme 1.15** The proposed mechanism of scalable organoboron catalyst for coupling propylene oxide and $CO_2$.

Moreover, this suggests that a suitable pair of Lewis acid organoborane, co-catalyst and the nature of substrate are essential in reactivity and selectivity. This provides additional data to support the potential advantage of several organoboranes in synthesising cyclic carbonates and polycarbonates.

### 1.1.4.2 Gallium- and Indium-based catalysts

The application of the heavier elements from group 13 in catalysis, such as gallium and indium, still remains relatively rare. Gallium and indium are highly atypical elements due to their large ionic radii, especially indium, which is

challenging to work with as a result of its size.[124] Despite the high prices of gallium and indium compared to aluminium, the precursor of these two elements is typically more stable than the organoaluminium derivatives in polar solvents and contains a biocompatible metal centre. Aluminium complexes have been observed to be highly active catalysts, but this does not apply in all circumstances, based on the work of Beament and co-workers. Indium was seen to have a faster reaction than aluminium when complexed with Jacobsen's ligand.[125]

Indium chloride ($InCl_3$) was already discovered as an active catalyst in 2009.[126] With these examples, the catalytic potential of a large atom is not a problem for catalysis wherein this large atom has already been utilised and shows catalytic activity, and further derivatisation of the surrounding molecule of the metal centre will hopefully provide more potential and properties of a large metal-centre complex.[127] There were a few examples of gallium and indium that display a potential ring-opening initiator of epoxide for synthesising cyclic carbonates and polycarbonates.

Williams and co-workers reported one example of using these metals, the first indium catalyst for epoxide/$CO_2$ copolymerisation in low $CO_2$ pressure and temperature (0.1 MPa, 60°C) reaction.[128] These authors have previously described both bimetallic and bicomponent mechanisms as prevalent pathways of metal salen catalyst; however, this indium catalyst was proven to operate through an unexpected mononuclear copolymerisation mechanism, as shown in Scheme 1.18. They have projected that the reaction mechanism was supposed to form by inserting $CO_2$ into two indium alkoxide groups, the intermediate formed from the catalyst with 1,2-cyclohexanediol. However, it reacted with both alcohol moieties of 1,2-cyclohexanediol with two molecules of indium catalyst to form an

alkoxide bridged dimer. Although a dimeric carbonate intermediate structure was isolated, this does not convey a bimetallic mechanism since $CO_2$ insertion happens individually at both indium centres of the catalyst. Therefore, the chain propagation occurs independently at each indium centre and does not require cooperativity by two indium atoms during insertion; thus, it undergoes a mononuclear copolymerisation reaction mechanism.

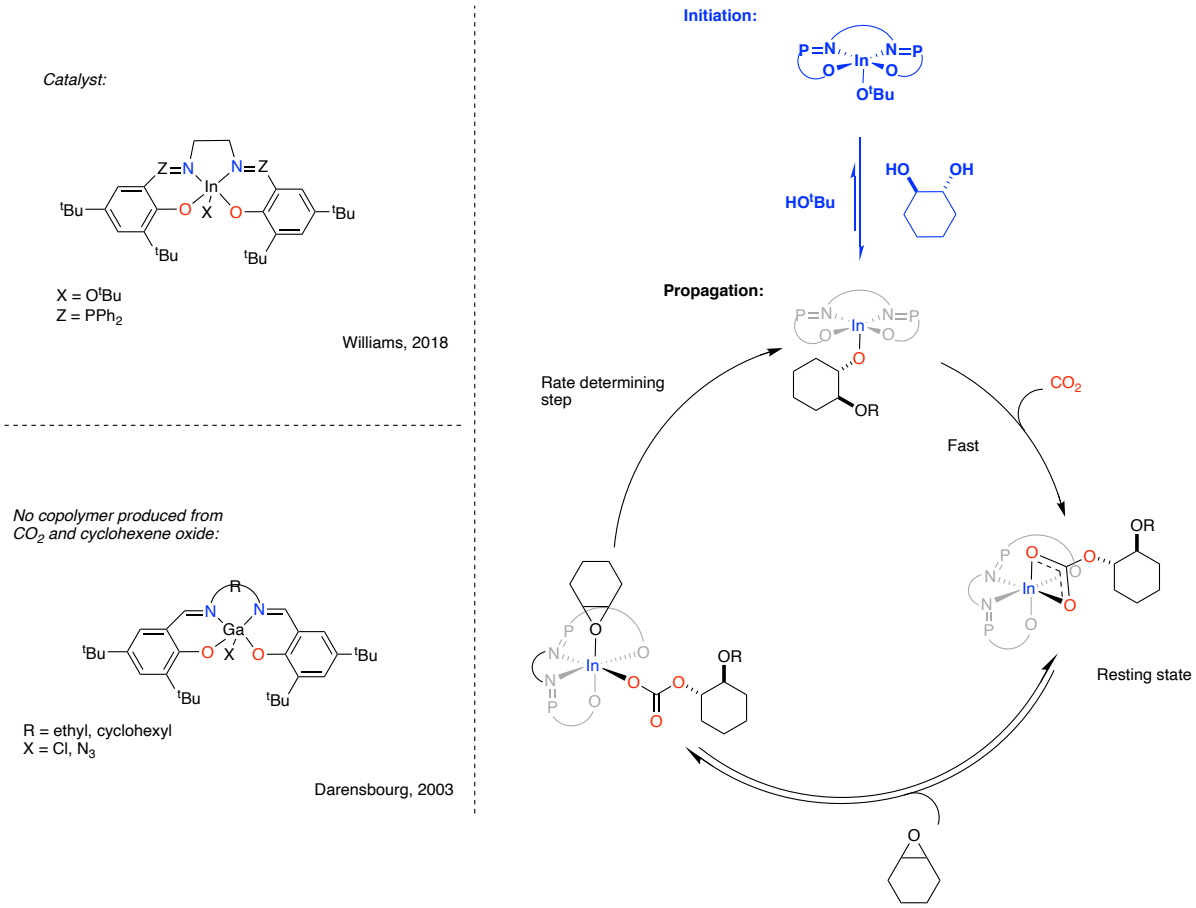


**Scheme 1.16** First Indium catalyst and the proposed mononuclear mechanism for $CO_2$/epoxide copolymerisation.

The catalytic activity of the indium salen catalyst was proven to be more effective with the presence of a phosphasalen ligand without any co-catalyst. By modifying the surrounding ligand, the catalytic activity of the complex may be changed. In contrast, using only the indium salen complex shows poorer performance which needs more ligand design to enhance its activity. This result may also lead to the

idea that gallium could also work as a catalyst since indium works for the $CO_2$/epoxide copolymerisation. However, Darensbourg has synthesised a gallium salen complex (Scheme 1.18), which unfortunately did not produce a copolymer from $CO_2$ and cyclohexene oxide even with a co-catalyst.[129] The authors also synthesised the azide analogues of gallium salen complex, and these show trace amounts of copolymer production, indicating the possibility of copolymerisation, but this system needs more improvement on the structure of the metal complex.

Aluminium catalysts are well established in cyclic carbonate and polycarbonate synthesis, unlike indium and gallium. This finding affords a new opportunity to apply indium and gallium for carbon dioxide utilisation. However, there are many factors to consider in order to understand the structure of the different metal centres of each complex from the same group of atoms. Thus, it is important to study the coordination chemistry of any ligand framework attached to boron, gallium, and indium to compare their properties and capabilities as catalysts in $CO_2$/epoxide coupling.

Overall, this highlights the importance of combining of metal and ligand in catalysis. Which to the best of our knowledge, group 13 metal complexes have not been explored in full detail for the synthesis of five-membered cyclic carbonates beyond aluminium.

### 1.1.5 Synthesis of the aminotrisphenol ligand

The existence of a different type of ligand attached to the metal centre significantly alters the catalytic behaviour of the complex. One ligand being used is the aminotrisphenol ligand which is considered of major importance due to its flexible coordination behaviour around the metal centre and facile synthesis.[130] A

salen ligand containing a phenolate base has also been used due to its structural rigidity. This type of ligand has also been an attractive scaffold for developing bifunctional complexes.[131] Also, synthesis and derivatisation of salen-based ligands are straightforward and cost-effective. Another commonly used ligand is the atrane. This ligand can be a five or six-membered ring tricyclic structure through a transannular coordination bond from N atom that has become popular nowadays in catalysis, specifically in utilising $CO_2$ as C1 feedstock.[132] Several atranes have been utilised, however, synthesising these catalysts involves several stages and is less attractive.

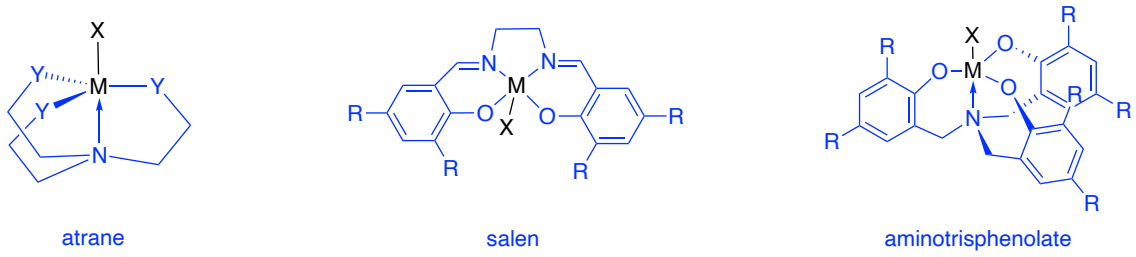


**Figure 1.13** Selected examples of ligand coordinated to a metal centre.

The use of aminotrisphenol ligand has been applied for synthesising boron, gallium and indium compounds and its flexible coordination towards the central atom is highly beneficial. The ortho position of the substituents to the phenol when complexed to a particular metal ion is near the metal centre and can therefore use as the control element. The para-position can modify the electronic properties of the ligand without affecting the steric demand of the system. The stability of the ligand is also advantageous to the metal compounds to avoid degradation when used as a catalyst during the reaction process. Historically, the synthesis of aminotrisphenol ligand started in 1922.[133] Later, several methods arose, and Koch and co-workers managed to reproduce the **$H_3L^{Me}$** more simply through a one-step Mannich reaction.[134-136]

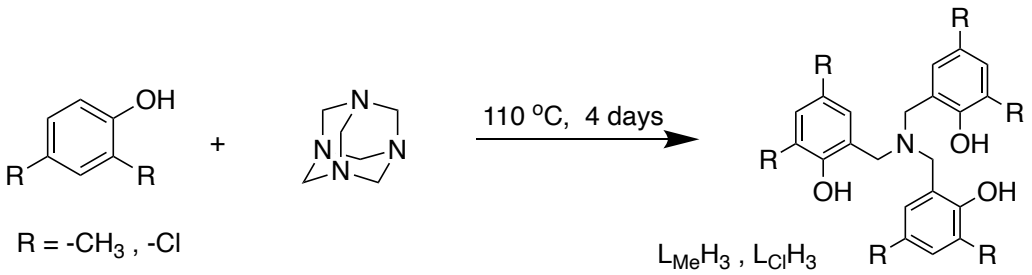


**Scheme 1.17** Synthesis of $\mathbf{H_3L^{Me}}$ and $\mathbf{H_3L^{Cl}}$ via Mannich reaction.

The produced ligand has a high yield product depending on the *R*-substituent present in the phenyl ring of the compound. Synthesis of aminotrisphenol ligand was done in several attempts where the reaction time affects the yield of the product, such as it requires 72 hours to collect a high yield.

In this study, 2,4-dimethylphenol was reacted with HMTA in a 4.5:1 ratio using *p*-toluenesulfonic acid as the catalyst. This reaction proceeds in an acid-catalysed reaction mechanism from the formation of iminium ion of HMTA. The presence of strong electron-donating substituents on the aromatic ring forms a tautomer (enol form) after it attacks the iminium ion. The formation of benzoxazine intermediate was the first compound observed and was validated using $^1$H NMR spectroscopy after heating the mixture for 48 h, and only at a higher concentration of phenol was the ligand formed. This compound could be isolated and an essential intermediate to synthesise an unsymmetrical ligand. The bond between the oxazine ring could react efficiently with different phenol to produce a new substituent on the amino ligand. The addition of excess phenol is the key component to form the aminotrisphenol ligand. The proposed reaction mechanism through a Mannich reaction of 2,4-dimethylphenol and HMTA is shown in Scheme 1.20.

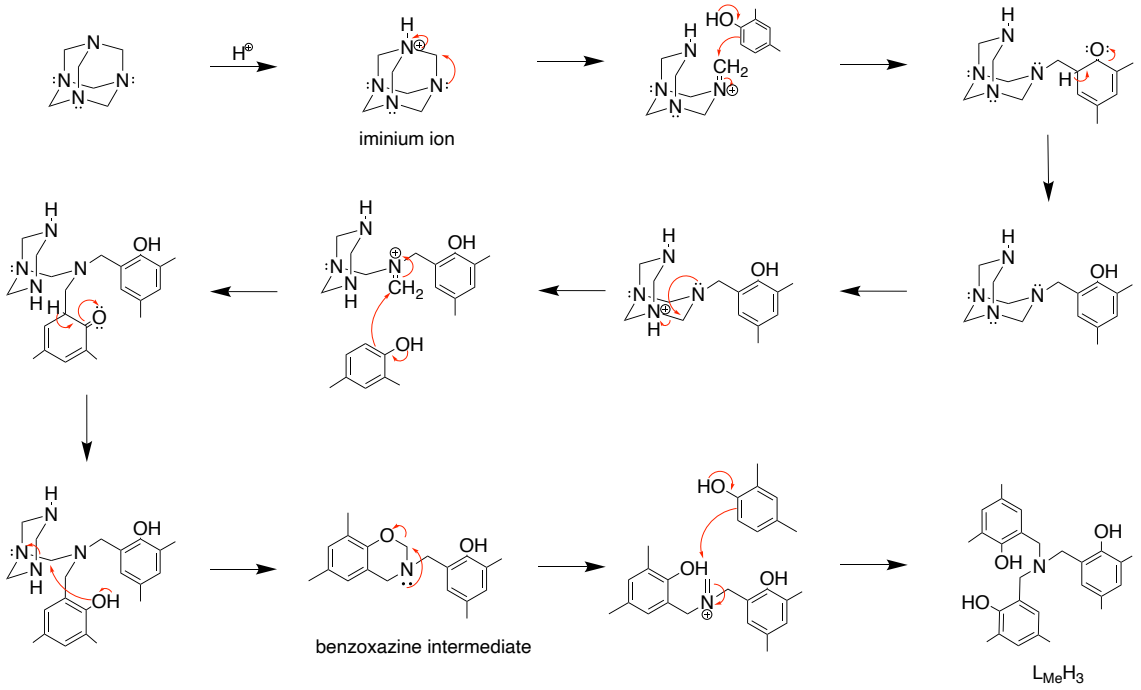


**Scheme 1.18** The proposed mechanism of the $H_3L^{Me}$ ligand.

## 1.2 Summary

In summary, $CO_2$ utilisation is being widely investigated due to the current issue of global warming; wherein $CO_2$ is the main greenhouse gas contributor. The strong covalent bond of the $CO_2$ molecule has led to challenges in the development of efficient approaches to activate $CO_2$ and convert it into a valuable product. In this context, requirement for a catalyst is often implied. One application of $CO_2$ is for the synthesis of cyclic carbonates from epoxides and $CO_2$ coupling. A summary of the main reported mechanisms has been presented and the examples mentioned above clearly highlight diverse routes for this commonly using Lewis acids and hydrogen bond interactions. The reported proposed mechanism using epoxide and $CO_2$ substrate displays a similar approach with aziridine substrate but the aziridines are more complex as regioselectivity must be taken into account as a result of two possible products.

With these recent advances in applying group 13 elements as a catalyst for epoxide/$CO_2$ and aziridine/$CO_2$ coupling, many possibilities can be made to contribute to society. Beyond simple cyclic carbonate synthesis, the preparation of oxazolidinone, an antimicrobial compound and also the grafting of cyclic carbonates onto cellulose provide interesting advances. Also, further investigation on all synthesised products for its advanced application on larger scales. The result in this thesis also provides the basis for potential investigation of group 13-based compounds beyond aluminium to realise efficient approaches for other Lewis acid-catalysed organic transformations.

### 1.3 Aims and objectives

This study aims to develop a novel group 13 catalysts for converting epoxide/aziridine and $CO_2$ into cyclic carbonates/oxazolidinones. The work of Kleij and co-workers on aluminium aminotrisphenolate catalyst as a powerful catalyst for $CO_2$ utilisation in 2013 provides the motivation to study other group 13 elements with the aminotrisphenolate catalyst for this application. The established Lewis acidity of these other elements is likely to be key for their success. With limited work reported, especially with gallium and indium complexes, this sets a high motivation to utilise and develop their potential to provide new catalysts.

This study has the following principal objectives, and the specific objective of each study is stated in each chapter.

1. To prepare boron aminotrisphenolate compounds that can used as a catalyst for the conversion of epoxides and $CO_2$ into cyclic carbonates.
2. To synthesise a range of triarylborate compounds with various *para*-substituents having electron-donating and electron-withdrawing

properties. Thereafter, the study of these compounds as catalysts for the conversion of epoxides and $CO_2$ into cyclic carbonates.

3. To apply a gallium aminotrisphenolate compound as a catalyst for the synthesis of oxazolidinone compounds through the cycloaddition of aziridines and $CO_2$.
4. To convert an epoxide functionalised cellulose into cyclic carbonate functionalised cellulose using a gallium aminotrisphenolate compound. Thereafter, to investigate potential antibacterial applications of the cyclic carbonate functionalised cellulose.
5. To synthesise indium aminotrisphenolate compounds and study there potential as catalysts for the cycloaddition of epoxides and $CO_2$ into cyclic carbonate products.

# Chapter 2

Synthesis of Boron Compounds Bearing an Aminotrisphenolate Ligand and Study of their Application as Catalysts for the Conversion of $CO_2$ and Epoxides into Cyclic Carbonates

## 2.1 Introduction

Over the past decade, the synthesis of cyclic carbonates using non-metal catalysts (organocatalysts) has attracted significant attention.[57,137-140] This is most likely as a result of them being cheap and less toxic than many metal-based catalysts. However, in general, the understanding of such organocatalysts is underdeveloped compared with the more established field of metal-based catalysts. A method of epoxide activation typical for non-metal catalysis is through hydrogen bonds. This approach has been widely applied with various simple molecules that display hydrogen-bonding properties being demonstrated to be catalysts for the synthesis of cyclic carbonates (For selected examples, see Scheme 2.1).[54,56,122] Similar to the traditional metal-catalysed reactions, these catalysts require addition of a Lewis base with strong nucleophilicity, such as *tetra*-butylammonium halides ($^{n}Bu_4N^+X^-$), which play an integral part in the cycloaddition reaction.

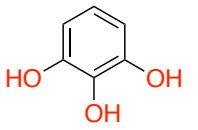


Kleij, Maseras (2012)

14 examples (all terminal epoxides)
Conditions: catalyst (5.0 mol %), $Bu_4NI$ (5.0 mol %), MEK (5 mL), $CO_2$ (1.0 MPa), 45 °C, 18 h

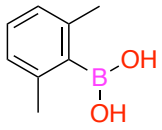


Zhang (2016)

7 examples (all terminal epoxides)
Conditions: catalyst (10 mol %), $Bu_4NI$ (5.0 mol %), $H_2O$, $CO_2$ (1.0 MPa), 50 °C, 7-15 h

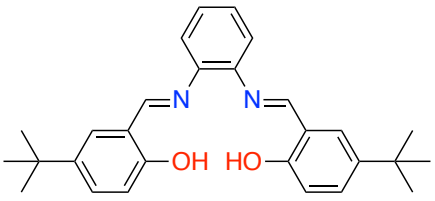


North (2019)

7 examples (all terminal epoxides)
Conditions: catalyst (5-10 mol %), $CO_2$ (1.0 MPa), 120 °C, 24 h

**Scheme 2.1** Selected examples of simple catalysts for cyclic carbonate synthesis which operate through a hydrogen-bonding activation approach.[54,56,122]

In general, metal-based catalysis has been found to be more potent than organocatalysis for the synthesis of cyclic carbonates. In 2013, Kleij and co-workers developed a robust aluminium catalyst (readily prepared from an aminotrisphenol ligand) that showed high turnover frequency (TOF) and turnover number (TON) values of up to 36,000 $h^{-1}$ and >110,000, respectively, for the cycloaddition of $CO_2$ and epoxides to produce a wide range of cyclic carbonates (Scheme 2.2).[103] The work in this chapter was directly inspired by this aforementioned work, intending to study the outcome of changing the metal centre from aluminium to boron, which has well established Lewis acid properties. In 2016 the first boron-based catalyst system for cyclic carbonate synthesis was reported by Zhang and co-workers where the hydrogen-bonding properties of boronic acids were exploited. The mechanism was confirmed through a DFT study (Scheme 2.1).[122] Despite the mode of activation not involving the boron centre, it provided the first example of a boron-based compound applied as a catalyst for the catalytic synthesis of cyclic carbonates.

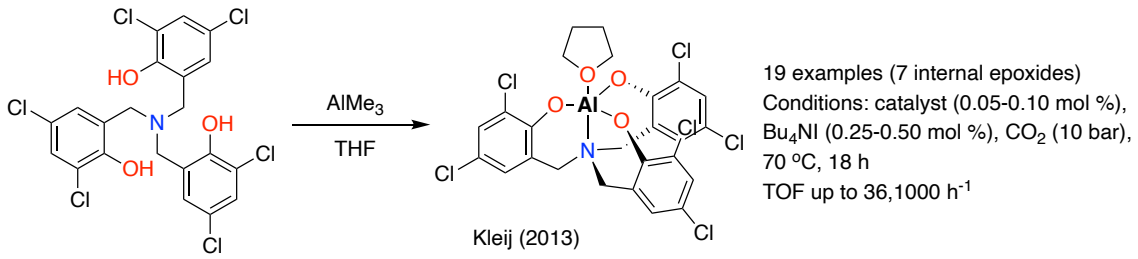


**Scheme 2.2** Preparation of the aluminium aminotrisphenolate used for the catalytic synthesis of cyclic carbonates from $CO_2$ and epoxides.[103]

The aminotrisphenol ligand can be readily prepared and has been used as a ligand scaffold in combination with many metals.[101,141-160] Not surprisingly, it has already been combined with boron, whereby in 2011, Kim and co-workers reported the synthesis and structure of a boron-based aminotrisphenolate compound, however, they did not seek any application of the resulting complex[161]

The lack of further study beyond the synthesis and structure of this compound is likely attributed to the expected inertness of the boron compound resulting from the interaction of the empty p-orbital of the boron atom, the reason for the Lewis acidic properties, with the lone pair of the nitrogen atom of the aminotrisphenolate ligand. In a related study, cage-like trisphenol ligands without the nitrogen atom of the aminotrisphenol have been described and found to be active Lewis acid catalysts by Baba and Yasuda.[108]

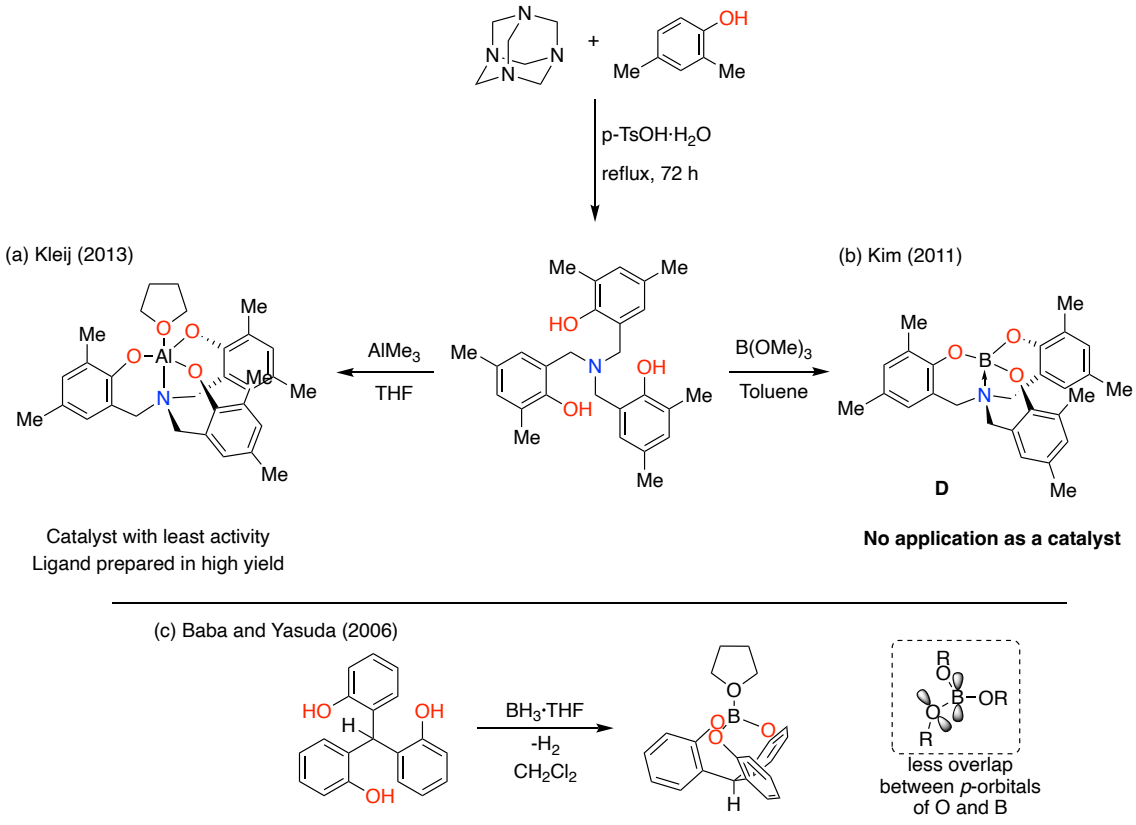


**Scheme 2.3** Synthesis of aluminium and boron-based aminotrisphenolate compounds.[103,108,161]

The relatively limited number of boron-based catalyst systems reported for cyclic carbonate synthesis[37,112] and the lack of reactivity studies with boron aminotrisphenolate compounds directed us to study these compounds as potential catalysts for this conversion. In this chapter, results from this study are presented, including an unexpected coordination behaviour of the ligand and a

mode of catalysis for the cycloaddition reaction that arises from the structure of these unusual compounds.

## 2.2 Results and Discussion

### 2.2.1 Synthesis of Boron compounds

As previously mentioned, a boron compound bearing an aminotrisphenol ligand was first synthesised by Kim and co-workers, however, no further application was sought.[161] The reaction involved refluxing the ligand **$H_3L^{Me}$** with trimethyl borate ($B(OMe)_3$) in toluene for 2 h. After repeated attempts, this synthesis failed in our hands, repeatedly leading to the formation of an unexpected compound, **A**. This unexpected compound has one phenol moiety unreacted with the third methoxide. The synthesised compound **A** contains two phenolates, a nitrogen atom and a methoxide (from the boron precursor), and as mentioned, the third phenol moiety remains unreacted resulting as a "free-phenol" (Scheme 2.4). The incomplete coordination of **$H_3L^{Me}$** may be due to the small radius of the boron resulting in strain-related challenges for the final methoxide of the $BOMe_3$ to be reacted. The same has been reported with central atom nitrogen and three surrounding pyridines of other related tetradentate tripodal ligands,[154,162] however, this is the first example of incomplete coordination with the aminotrisphenolate ligand family to the best of our knowledge.

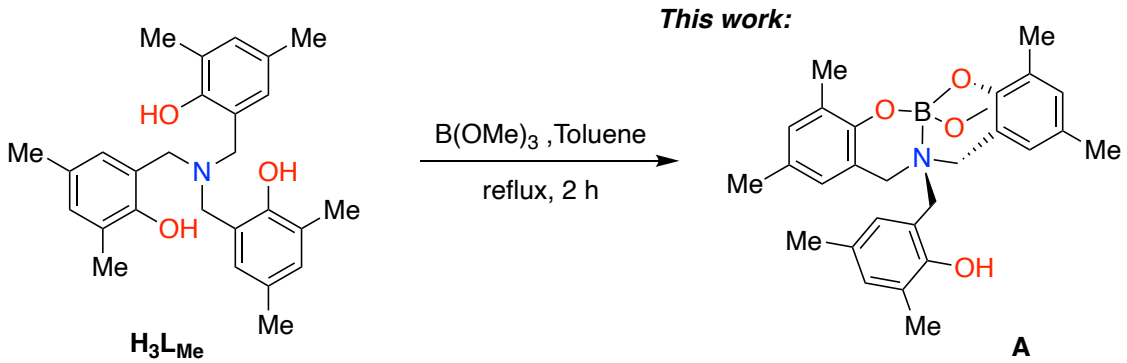


**Scheme 2.4** Synthesis of a boron compound bearing the aminotrisphenol ligand.

The synthesis was further investigated, and the ligand was reacted with different boron precursors to identify the effect of substituents attached to boron *B-X* by changing the B-OMe to *B-H* from $BH_3$.THF. Both $B(OMe)_3$ and $BH_3$.THF were reacted with the ligand under an inert atmosphere for comparison; the reaction mixture with $B(OMe)_3$ was reacted at elevated temperature, whereas ambient temperature was used with $BH_3$.THF. However, the reaction with $BH_3$.THF still resulted in incomplete reaction of the ligand (compound **B**), which as a result furnished an unusual mixed borate-borane compound O-B-H that is surprisingly stable to the atmosphere, even under prolonged storage and in solution. Synthesis of the expectedly more acidic phenol derivative with chloro-substituents $\mathbf{H_3L^{Cl}}$ in place of methyl-substituted ligand, $\mathbf{H_3L^{Me}}$ resulted in the analogous compound **C**. Crystals suitable for single crystal X-ray analysis were obtained by diffusion of pentane into a concentrated solution of boron compounds in chloroform for compounds **A** and **C**. However, no suitable crystals were obtainable for compound **B**.

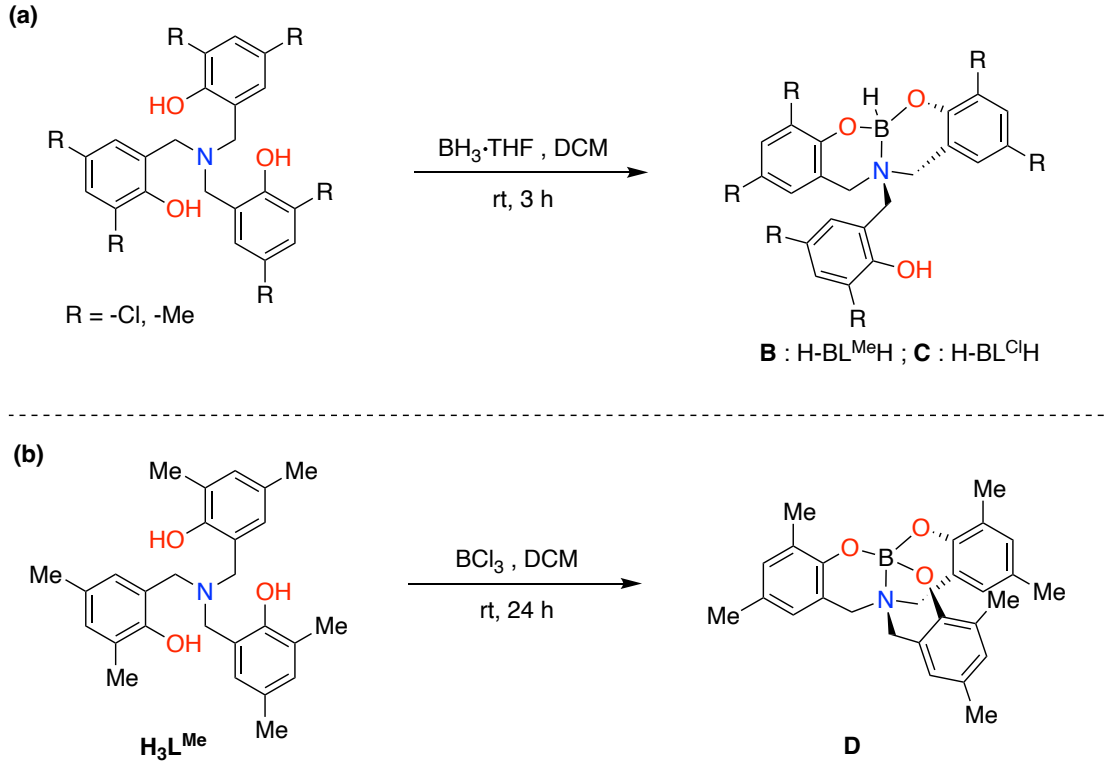


**Scheme 2.5** General reaction synthesis of compounds **B**, **C** and **D**.

Compound **D**, reported by Kim and co-workers, could not be reproduced after several attempts, but could be obtained with minor modification to the reaction; the synthesis of **D** was successful using the boron precursor $BCl_3$, whereby the reaction mixture was left stirring overnight under the same conditions as for the synthesis of compound **B**. Although the yield obtained was satisfactory, the procedure was more reproducible than reported by Kim and co-workers using their $B(OMe)_3$ route.

The free phenol in compounds **A**, **B**, and **C** provides a handle for further reactivity, and as a result, a facile experiment to exemplify this was performed. Synthesis of compound **A'**, a compound with phenoxy ether, was achieved by reacting the free phenol group with methyl iodide (MeI) in the presence of a base (potassium carbonate, $K_2CO_3$). With the masking of the phenoxy group, investigations into the potential for the third unreacted phenol moiety in compounds **A**, **B** and **C** could then be studied.

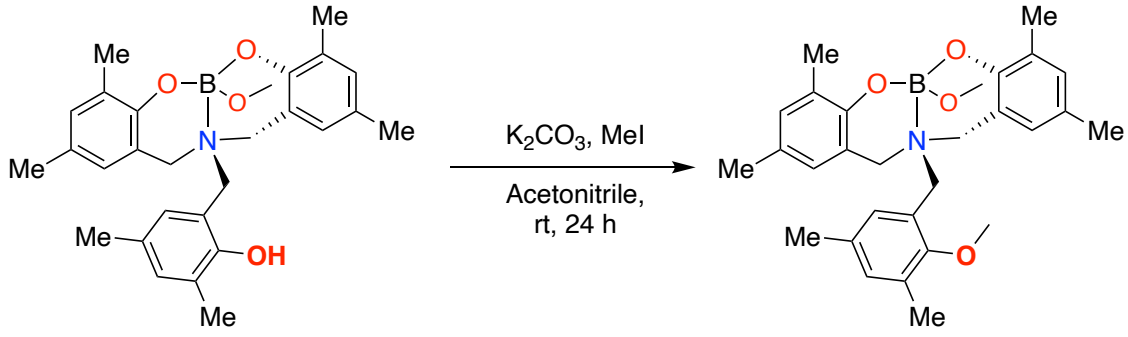


**Scheme 2.6** Synthesis of compound **A'** for study into the reactivity of free phenol in catalysis.

All boron compounds were found to be highly stable under ambient laboratory conditions. The compounds were characterised by $^{1}H$ NMR, $^{13}C\{^{1}H\}$, $^{11}B$, and COSY NMR spectroscopy and the spectra obtained were consistent with the

proposed structures. Complete characterisation data for all compounds can be found in Chapter 6 of this thesis.

### 2.2.2 Characterisation of Boron-based compounds

#### 2.2.2.1 NMR Spectroscopy

All boron-containing compounds were found to be soluble in organic solvents and were characterised by NMR spectroscopy using deuterated chloroform as solvent. The incomplete coordination of compounds **A**, **B** and **C** was confirmed through the appearance of a peak ratio of 2:1 between 6.5-7.6 ppm of the aromatic ring, where one phenol ring of each compound appears to be distinct from the other two phenolates supporting that one phenol ring was not attached to the boron atom as would be expected. The structure was further confirmed with the presence of a hydroxy signal of each boron compound, showing a broad singlet appearing at 6.05 ppm for **C** and singlet peaks at 7.42 ppm and 8.57 ppm for **A** and **B**, respectively (Figure 2.1).

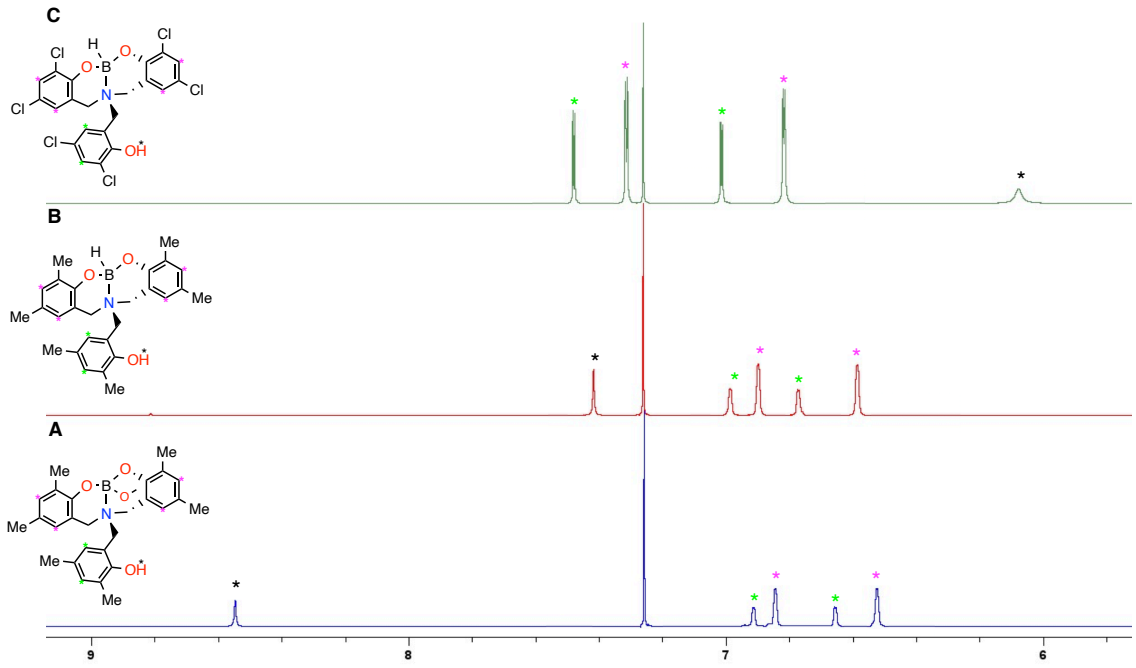


**Figure 2.1** Stacked $^{1}H$ NMR spectra ($CDCl_3$, 298 K) of compounds **A**, **B** and **C**, between 6.00 and 9.00 ppm, highlighting the peaks for distinct phenolate/phenol groups of the complexes.

The -O*H* peaks of compounds **A** and **B** were found to be more de-shielded than the -O*H* peak of compound **C** due to the presence of electron-withdrawing group in the surrounding ligand. The peaks between 3.80-4.30 ppm of the $^{1}$H NMR spectrum arise from the N-C$H_2$- of the compounds. In the case of compounds **B** and **C**, one singlet and two doublets are observed (Figure 2.2). This pattern arises due to the diastereotopic nature of the N-C$H_2$- of the coordinated phenolate moieties. Meanwhile, the freedom of rotation present in the N-C$H_2$- of the unreacted phenol moiety gives rise to a singlet similar to that observed in the starting ligand $\mathbf{H_3L^{Me}}$. In contrast, the N-C$H_2$- peaks in compound **A** are all observed as slightly broadened singlet peaks. Notably, the hydride coordinated to the boron in compounds **B** and **C** is not visible in the spectrum, which is likely a result of the significant broadening of this peak by the strong $^{1}J_{HB}$ coupling to $^{10}B$ (s = 3) and $^{11}B$ (s = 3/2) nuclei. Meanwhile, in compound **A** a singlet peak appears at 3.46 ppm, confirming the coordination of the -O$CH_3$ to the boron centre.

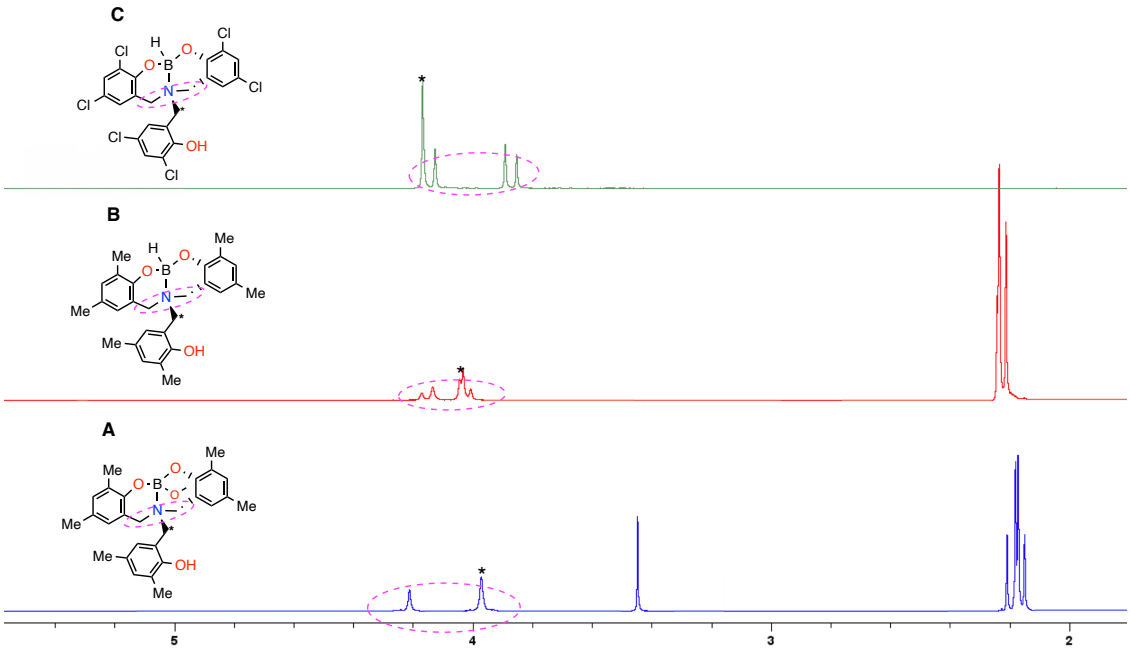


**Figure 2.2** Stacked $^{1}$H NMR spectra ($CDCl_3$, 298 K) of compounds **A**, **B** and **C** between 2.00 and 6.00 ppm showing the peaks for N-$CH_2$ and $OCH_3$.

As mentioned, compound **A'** was synthesised to investigate the significance of the free -OH substituent of the unreacted phenol present in compound **A**. In the $^{1}$H NMR of this compound, the two peaks at 3.47 and 3.55 ppm indicates the presence of two -*OCH*$_3$ groups; one -*OCH*$_3$ coordinated to the boron and the formation of a new -*OCH*$_3$ from the reaction of the free phenol substituent (Figure 2.3) to form the corresponding methylether. The pair of doublets at 3.67 and 4.13 ppm again arise as a result of the diastereotopic nature of the N-*CH*$_2$- of the coordinated phenolate moieties, with a singlet resonance present at 4.20 ppm for the N-*CH*$_2$- of the unreacted phenol. The aromatic peaks between 6.50-7.26 ppm are similar to those of parent compound **A**, presenting an integration of 2:1.

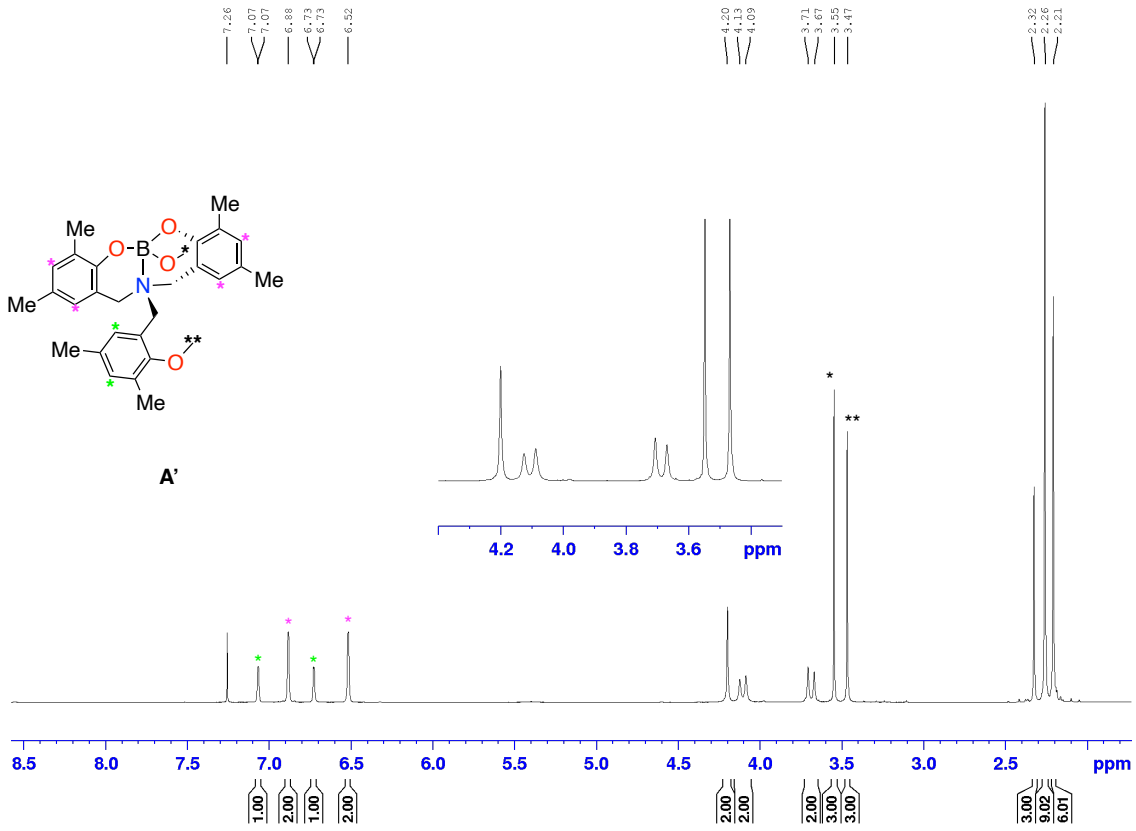


**Figure 2.3** $^{1}$H NMR spectra ($CDCl_3$, 298 K) of compound **A'** highlighting the peaks around N-*CH*$_2$- and the presence of two -*OCH*$_3$ peaks.

Boron-11 NMR analysis was performed using a boron-free probe and a specialised quartz NMR tube to avoid interference in the analysis, and the sample was referenced to $BF_3{\cdot}OEt_2$. Compounds **A**, **A'**, **B**, **C** and **D** were analysed, and the resulting $^{11}B$ NMR spectra are displayed as stacked spectra where each exhibited only a slight difference in its chemical shift. Both related compounds **A** and **A'** only contain *B*-*O* bonds surrounding the boron atom, giving the most pseudo-symmetric environment around the boron centre of the compounds studied and thus these compounds display relatively well resolved peaks at around 2.5 ppm, which provide almost similar result for compound **D** at a slightly lower chemical shift (Figure 2.4).

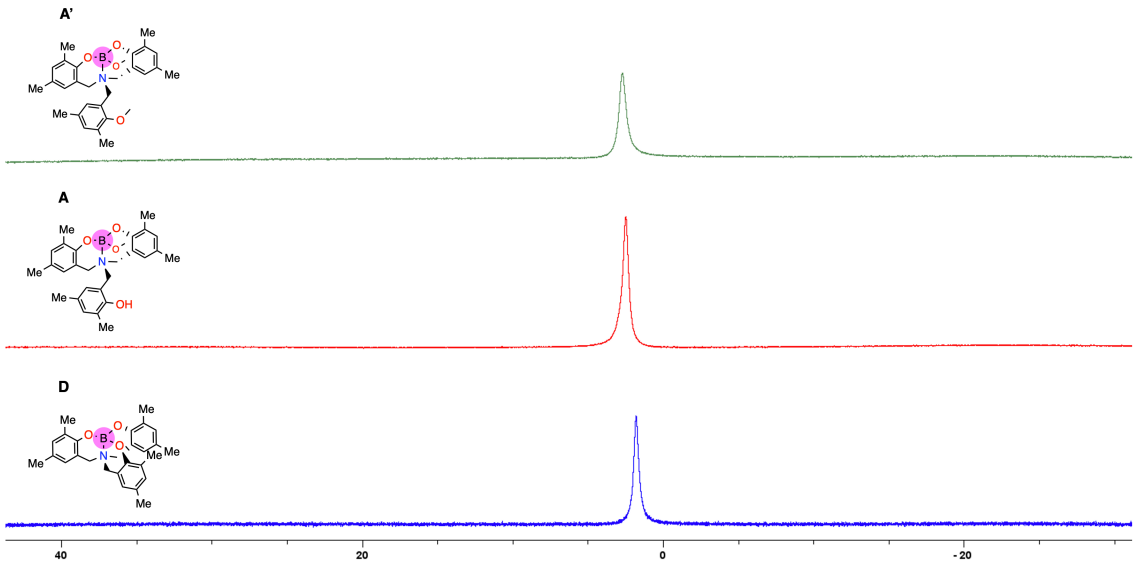


**Figure 2.4** $^{11}B$ NMR spectra ($CDCl_3$, 298 K) of compounds **A'**, **A** and **D**.

The results from compounds **B** and **C** provided spectra with significantly broader signals which likely arise from the strong $^1J$ {$^{11}B$-$^1H$} nucleus coupling (3/2 and 1/2, respectively). Indeed, an overlapped doublet for **B** was observed and appears a broad peak, whereas this has fully broadened out in the case of compound **C** and a single peak was detected. The broadening arises from a reduced symmetry in compounds **B** and **C**.

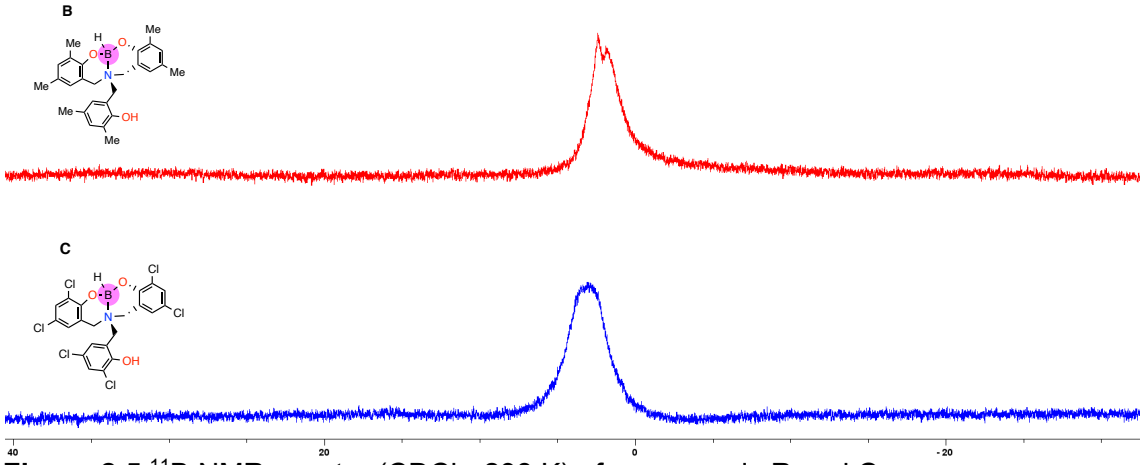


**Figure 2.5** $^{11}$B NMR spectra ($CDCl_3$, 298 K) of compounds **B** and **C**.

### 2.2.2.2 X-ray Crystal Structure Analysis

Crystals suitable for single-crystal X-ray diffraction studies were grown by slow diffusion of pentane into a concentrated chloroform solution of the compound. The obtained molecular structures of **A** and **C** are shown in Figures 2.4 and 2.5, respectively, with their corresponding crystallographic parameters presented in Table 2.1. Both structures confirm that the third phenol group has not reacted with the boron precursor and are in agreement with the solution structures proposed from the obtained $^1$H NMR data. It should be noted that the unreacted B-*OMe* and B-*H* bond is in the correct position for reaction with free phenol. The structure of compound **A** has a hydrogen bonding interaction between the free phenol and the unreacted B-*OMe* moiety. In the solid-state structure of **C**, two interactions are visible; a hydrogen bond formed between the free phenol and the phenolate of another compound and an intramolecular Cl···H hydrogen bond between the chloro and phenol substituents of a free phenol in one of the molecules.

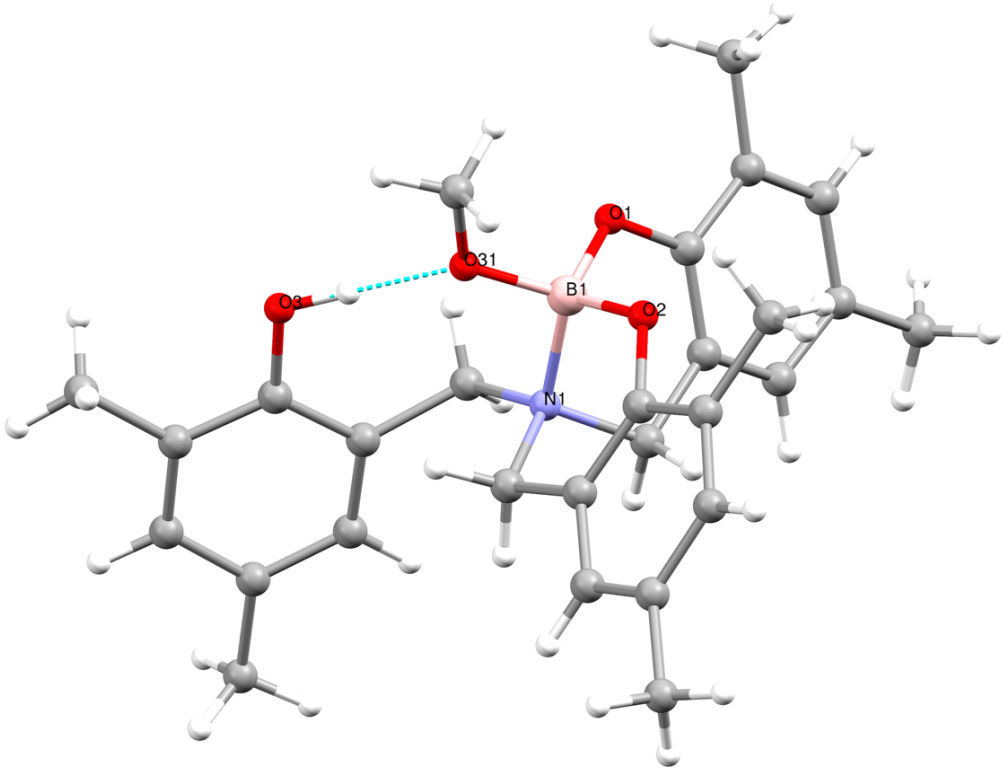


**Figure 2.6** Solid-state molecular structure of **A**. The hydrogen-bonding interactions with a maximum D-D distance of 2.86 Å and a minimum angle of 120 ° are shown: O3–O31 = 2.618 Å. CCDC 2067314 contains supplementary X-ray crystallographic data for compound **A**.

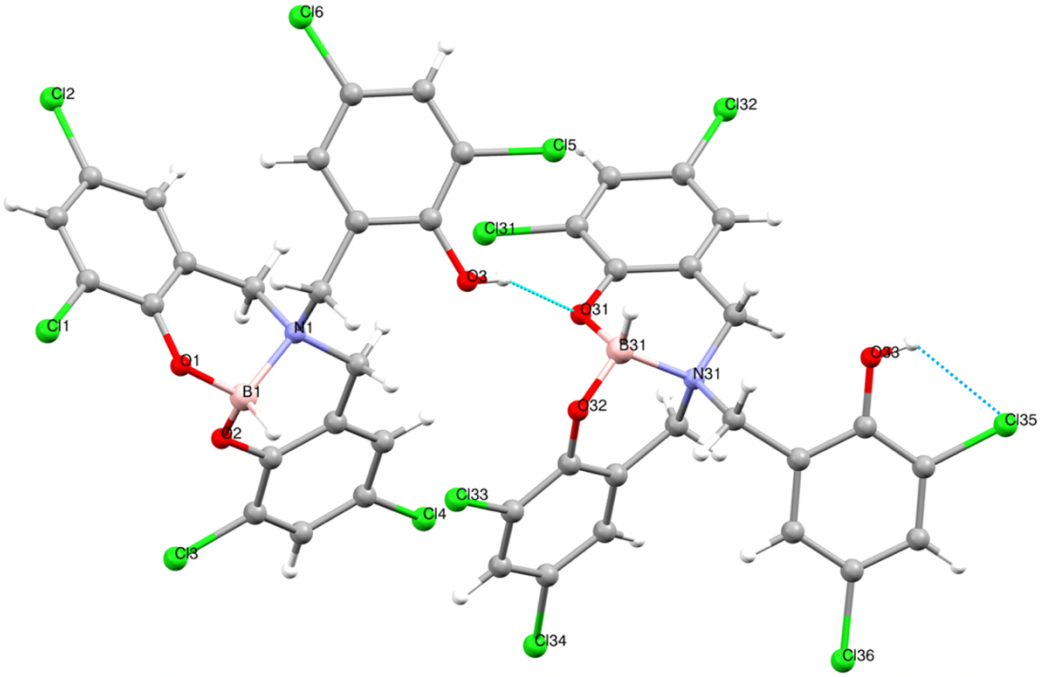


**Figure 2.7** Solid-state molecular structure of **C**. The hydrogen-bonding interactions with a maximum D-D distance of 3.14 Å and a minimum angle of 120 ° are shown: O3–O31 = 2.875 Å and O33–Cl35: 2.963 Å. Note: two molecules were found in the unit cell and displayed. CCDC 2067313 contains supplementary X-ray crystallographic data for compound **C**.

**Table 2.1** X-ray crystallographic parameters for complexes **A** and **C**.

| Compound | **A** | **C** |
|---|---|---|
| Formula | $C_{28}H_{34}BNO_4$ | $C_{21.25}H_{14.25}BCl_{6.75}NO_3$ |
| Crystal system | Triclinic | Triclinic |
| Space group | *P*-1 (No. 2) | *P*-1 (No. 2) |
| Volume (Å$^3$) | 1208.51(3) | 2358.22(7) |
| *a* (Å$^3$) | 8.74510(10) | 13.2908(2) |
| *b* (Å$^3$) | 9.47880(10) | 13.5066(2) |
| *c* (Å$^3$) | 15.8152(2) | 14.8411(2) |
| *a* (º) | 76.3670(10) | 77.1290(10) |
| *b* (º) | 86.9550(10) | 67.725(2) |
| *g* (º) | 71.5910(10) | 75.015(2) |
| *Z* | 2 | 4 |
| *Z'* | 1 | 2 |
| Formula weight (g mol$^{-1}$) | 459.37 | 581.68 |
| Density (g cm$^{-3}$) | 1.262 | 1.638 |
| Absorption coefficient (mm$^{-1}$) | 0.657 | 0.840 |
| Radiation type | Cu $K_a$ | Mo $K_a$ |
| $\theta_{max}$ (º) | 68.237 | 27.483 |
| Temperature (K) | 100(2) | 100(2) |
| Total no. reflections | 37073 | 126284 |
| Unique reflections [*R*(int)] | 4402 [0.0281] | 10815 [0.0464] |
| Final *R* indices [$I > 2(I)$] | $wR_2$ = 0.0890 | $wR_2$ = 0.1292 |
| | $R_1$ = 0.0336 | $R_1$ = 0.0459 |
| GooF | **1.032** | **1.042** |

### 2.2.3 Catalytic screening

The optimisation of the catalyst system for the synthesis of cyclic carbonates involved variation and optimisation of the catalyst and co-catalyst loading, temperature, reaction time at constant pressure. The cycloaddition reaction was conducted using freshly prepared dry ice. Once all the substrates were added to the 50 mL reactor, the dry ice was prepared, weighed, and introduced immediately to the vessel, and then the reactor was sealed. The weight of the dry ice used was 2.68 g which represents a starting pressure of approximately 15 bar.

Compound **B** was selected for the optimisation studies as it has one structural change from both **A** and **C**. The initial conditions used to investigate

the catalytic effectiveness of the compound for the conversion of 1,2-epoxyhexane (benchmark substrate) were 1.0 mol% of **B**, 2.0 mol% *tetra*-butylammonium iodide ($Bu_4NI$) at 40 °C with 15 bar of $CO_2$ pressure, obtained from adding 2.63 g of solid $CO_2$, for 24 h, which provided a yield of 75 % (Table 2.2, Entry 1). This yield was promising at such a low temperature, and upon increasing to 60 °C, quantitative conversion of the substrate was observed, resulting in >99 % yield of the cyclic carbonate product (Table 2.2, Entry 2). It is important to note that the reaction does not require a solvent, which paves the way to a sustainable synthesis of 4-butyl-1,3-dioxolan-2-one (**1b**, cyclic carbonate product obtained from 1,2-epoxyhexane). The use of the related co-catalyst *tetra*-butylammonium bromide ($Bu_4NBr$) in place of $Bu_4NI$ resulted in a decreased yield of cyclic carbonate product (Table 2.2, Entry 3) wherein the reactivity of the iodide nucleophile is higher than that of bromide. Furthermore, in the absence of **B**, a significant decrease in the yield of **1b** occurred under the applied reaction conditions, indicating the importance of **B** and indicating that it promotes the conversion of **1a** (Table 2.2, Entries 4, 8 and 11). Whilst no conversion was observed in the absence of $Bu_4NI$, highlighting the essential nature of the co-catalyst in the reaction (Table 2.2, Entry 5). The percentage yield of each reaction was determined based on the $^1H$ NMR spectrum of the crude product with mesitylene as the internal standard for identifying the relevant peaks that correspond to the literature values of the cyclic carbonate products.

Nevertheless, the loading of 1.0 mol% **B** and 2.0 mol% $Bu_4NI$ remains relatively high from a sustainability point of view; consequently, optimisation of the catalyst was further investigated by lowering the amount of the catalyst and the co-catalyst loading to half of the original (0.5 mol % **B** and 1.0 mol % $Bu_4NI$), whereby this new loading afforded 85 % yield (Table 2.2, Entry 6). Decreasing

the amount of the $Bu_4NI$ co-catalyst to 0.5 mol% from 1.0 mol% whilst retaining the catalyst loading at 0.5 mol% resulted in a 69 % yield, which is significantly higher than only $Bu_4NI$ alone (28 %; Table 2.2, Entries 7 and 8). Upon increasing the temperature to 80 °C, lowering the catalyst and $Bu_4NI$ co-catalyst loading both to 0.25 mol %, an improved yield of 81 % was obtained (Table 2.2, Entry 9). This conversion prompted the increase in temperature to 100 °C. However, a slight increase in yield was obtained (Table 2.2, Entries 9 and 10). With $Bu_4NI$ alone at 100 °C, a 52 % yield of **1a** was attained whilst with the presence of catalyst **B**, 85 % yield was obtained (Table 2.2, Entries 10 and 11). Importantly throughout this optimisation study, the selectivity for cyclic carbonate product was >99 %, with no side products observed. In addition, different times of less than 24 h were also investigated, but there no significant disparity in the conversions was observed.

**Table 2.2** Catalyst optimisation using compound **B**.

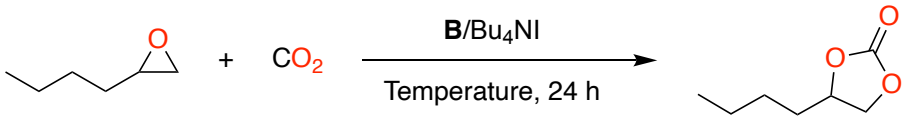


**1a** **1b**

| Entry | **2** (mol%) | $Bu_4NI$ (mol%) | Time (h) | Temp. (°C) | Conv (%)[a] |
|---|---|---|---|---|---|
| 1 | 1.0 | 2.0 | 24 | 40 | 75 |
| **2** | **1.0** | **2.0** | **24** | **60** | **>99** |
| 3[b] | 1.0 | 2.0 | 24 | 60 | 84 |
| 4 | - | 2.0 | 24 | 60 | 45 |
| 5 | 1.0 | - | 24 | 60 | 0 |
| 6 | 0.5 | 1.0 | 24 | 60 | 85 |
| 7 | 0.5 | 0.5 | 24 | 60 | 69 |
| 8 | - | 0.5 | 24 | 60 | 23 |
| 9 | 0.25 | 0.25 | 24 | 80 | 81 |
| **10** | **0.25** | **0.25** | **24** | **100** | **85** |
| 11 | - | 0.25 | 24 | 100 | 52 |

**Conditions**: 1,2-epoxyhexane (**1a**) (1.0 g, 9.98 mmol), catalyst, $Bu_4NI$ co-catalyst, temperature, 24 h, $CO_2$ (2.63 g, 59.8 mmol, 6.0 equiv., approx. 15 bar). [a]Conversion of **1b** was determined by inspection of the $^1H$ NMR spectrum of the crude reaction mixture using mesitylene as the internal standard. [b]$Bu_4NBr$ co-catalyst.

Interestingly, upon inspection of the crude NMR spectra, the signals of the catalyst were still present, confirming the stability of the catalyst during the reaction (Figure 2.6).

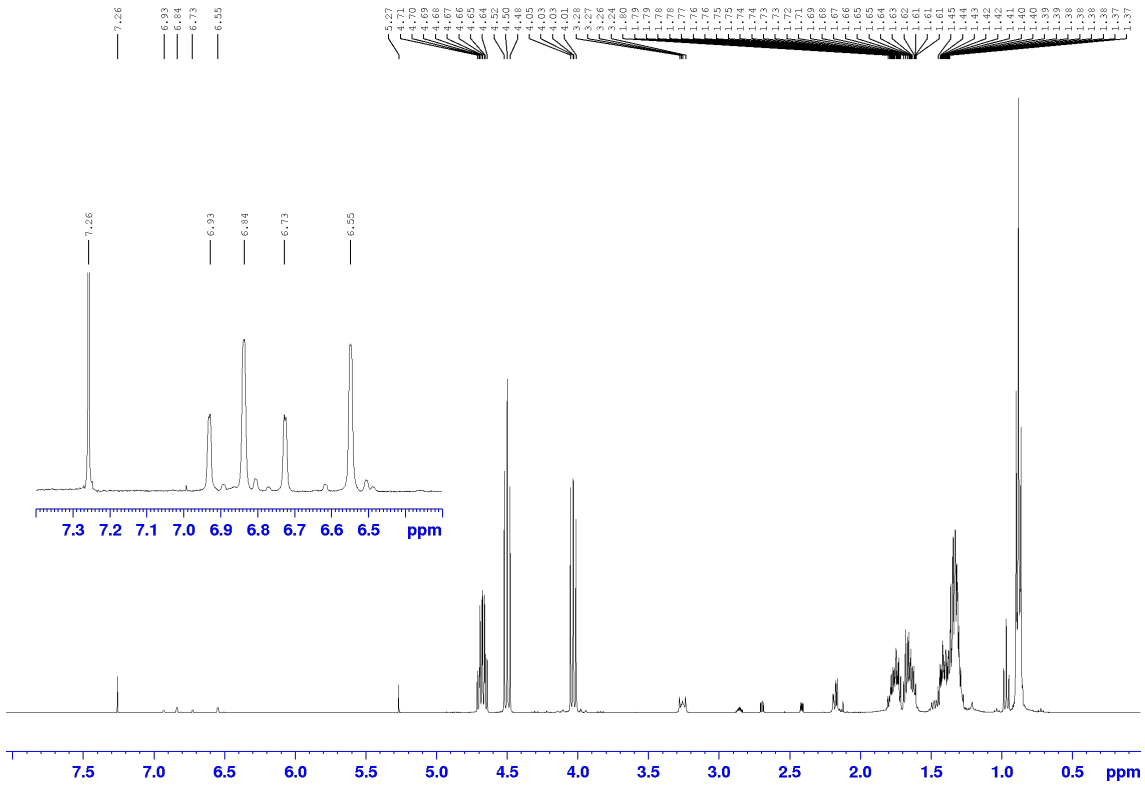


**Figure 2.8** An example of a $^{1}$H NMR spectrum ($CDCl_3$ at 298 K) of a crude reaction mixture using compound **B** after conversion of 1,2-epoxyhexane to **1b** without purification and without the addition of mesitylene. The aromatic peaks of the catalyst are expanded to highlight that it is still intact.

As can be seen and expected, changing the reaction parameters such as reaction time, temperature, and catalyst loading affects the rate of the cycloaddition of $CO_2$. These can also be plotted to provide greater insight into the results. As shown in Figure 2.7, the catalytic activity was affected significantly by an increase of the catalyst loading between 0.5 - 1.0 mol%. After this, no effect is observed as more, or less complete conversion has been achieved. A yield of >99 % could be obtained at 110 °C with 0.25 mol% of **B**, 0.25 mol% of $Bu_4NI$ for 24 h, whilst a

decrease to 92 % when the temperature was increased further to 120 °C was observed. This trend could be due to the degradation of the catalyst at elevated temperatures. Reaction time is another critical parameter that affects the reactivity for cyclic carbonate synthesis. As shown in Figure 2.7 (c), the catalytic activity increased from 4 h - 36 h, and a maximum of 99 % for 36 h at 100 °C was achieved, but a decrease in yield after 48 h resulted in 90 %, which may be a result of product degradation. Indeed, at elevated temperatures, cyclic carbonates might decompose to the corresponding diol.

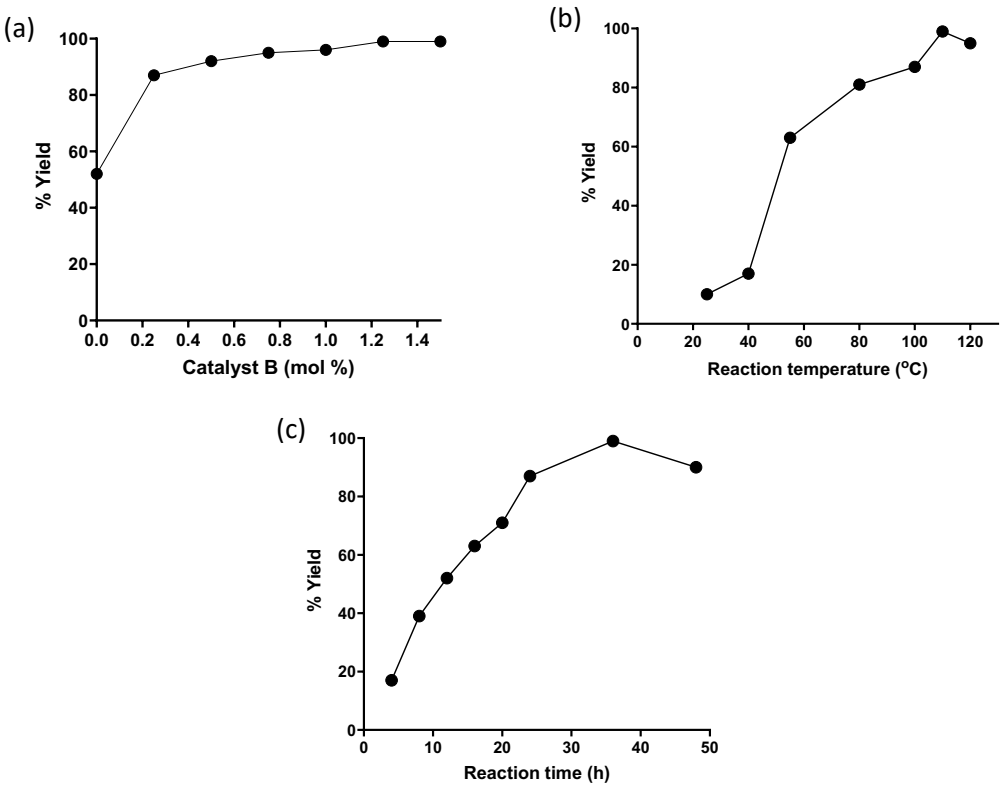


**Figure 2.9** Effect of various reaction parameters on the cycloaddition reaction of $CO_2$ with **1b** using **B**/$Bu_4NI$. (a) mol % of catalyst (**1a** 9.98 mmol, 0.25 mol % $Bu_4NI$, 15 bar $CO_2$, 100 °C, 24 h); (b) reaction temperature (**1a** 9.98 mmol, 0.25 mol % B, 0.25 mol % $Bu_4NI$, 15 bar $CO_2$, 24 h); (c) reaction time (**1a** 9.98 mmol, 0.25 mol % B, 0.25 mol % $Bu_4NI$, 15 bar $CO_2$, 100 °C).

### 2.2.4 Mechanistic considerations

After the optimisation with compound **B**, all boron compounds were tested for their potential to catalyse the conversion of $CO_2$ and epoxides into cyclic

carbonates. All compounds afforded high yields except compound **A'**, which does not contain a free-phenol moiety. The optimised conditions (Table 2.2, Entry 10) were applied to all boron compounds **A**-**D** and **A'**. Interestingly, upon inspection of the crude reaction mixture at the end of the reaction, the peaks of each catalyst used were identifiable, as highlighted in Figure 2.7 for compound **B** during the reaction condition optimisation study. Overall, both **A** and **C** showed a slight increase in conversion over compound **B**, but this is not an overly significant increase (Table 2.3, Entries 1 and 3). The change to chloro substituents can justify that this minor increase of conversion with **C** should affect the acidity of the phenol in this compound which supports catalytic activity promoted by the OH of the free phenol moiety. Meanwhile, compound **D** reported by Kim and co-workers and compound **A'** showed no catalytic activity (Table 2.3, Entries 4 and 5), providing yields comparable to $Bu_4NI$ alone (Table 2.2, Entry 11).

**Table 2.3** Catalyst optimisation using different catalyst.

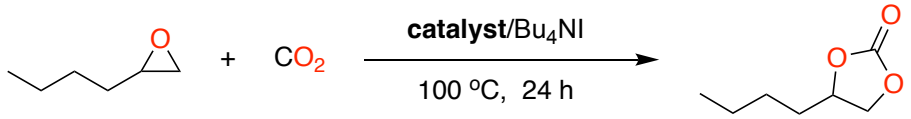


**1a** **1b**

| Entry | Catalyst | Conv (%)[a] |
|---|---|---|
| 1 | **A** | 85 |
| 2 | **B** | 87 |
| 3 | **C** | 90 |
| 4 | **D** | 59 |
| 5 | **A'** | 56 |
| 6[b] | - | 52 |

**General conditions**: **1a** (1.0 g, 9.98 mmol), catalyst (0.25 mol %), $Bu_4NI$ (0.25 mol %), $CO_2$ (59.8 mmol, 6.0 equiv., ~15 bar). [a]Conversion of **1a** was determined by inspection of the $^1H$ NMR spectrum of the crude reaction mixture. [b]$Bu_4NI$ only.

Based on the results discussed above, the proposed reaction mechanism for the cycloaddition of $CO_2$ with epoxide is shown in Scheme 2.7 and is based on a

hydrogen-bonding type of interaction and catalysis. This mode of catalysis explains the slight difference in epoxide conversion using catalysts **A**-**C** which does not significantly affect the reaction even with different surrounding ligands. For this reason, the absence of -*OH* functionality (compound **A'**) provides experimental evidence that the free phenol participates in catalysis and explains the potential hydrogen-bonding type interaction rather than Lewis acid catalysis of the synthesised boron compounds.

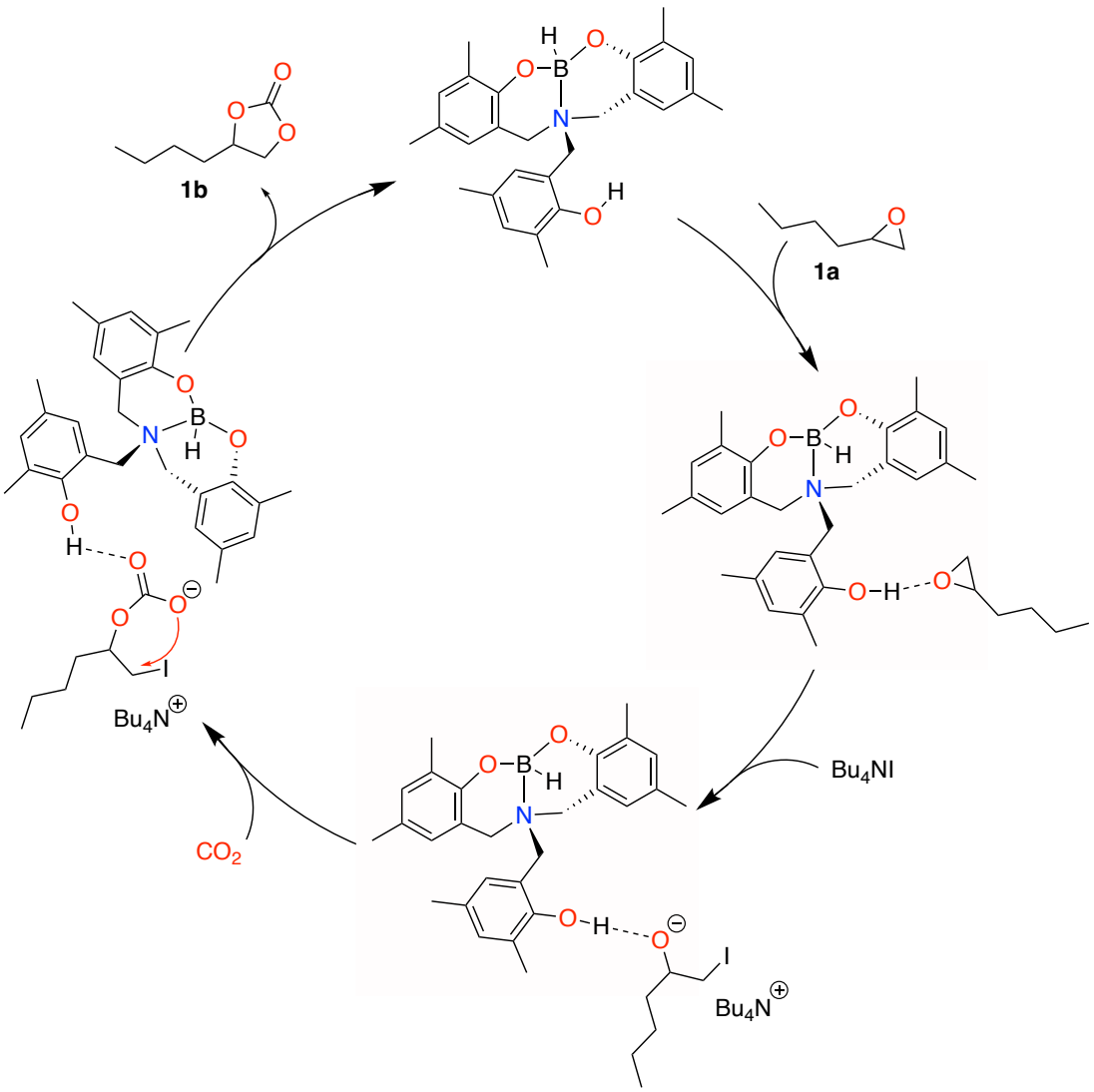


**Scheme 2.7** Proposed reaction mechanism for the cycloaddition of $CO_2$ and 1,2-epoxyhexane to synthesise cyclic carbonate product **1b**.

### 2.2.5 Substrate scope for the $CO_2$ cycloaddition reaction

Delighted with the high activities of the **A/Bu$_4$NI**, **B/Bu$_4$NI**, and **C/Bu$_4$NI** catalyst systems towards the cycloaddition of 1,2-epoxyhexane and $CO_2$, the possibility of $CO_2$ cycloaddition with other epoxides, both terminal and internal epoxide under the optimised reaction conditions was explored. Scheme 2.8 summarises the results obtained with various epoxide substrates. Only a slight difference in yields was observed between using catalysts **A**, **B** and **C**, and was found to be effective for various terminal epoxides (**1b**-**8b**, **10b** and **11b**), except for epoxides with bulky *tert*-butyl substituents (**6b**) and in all cases excellent selectivity towards cyclic carbonate products. Furthermore, epoxides with synthetically useful functional groups could be converted; alkenes (**7b**), alcohols (**8b**), halides (**3b**), alkynes (**10b**), ethers (**4b**, **10b**), aromatics (**5b**, **11b**), alkyl (**1b**, **2b**), all displaying higher yields than the more challenging internal epoxides (**9b**, **12b**-**14b**) owing to steric factors. Epichlorohydrin was the most active substrate with an excellent yield of >99 % of the corresponding carbonate using all three catalysts. This phenomenon was consistent with other reported results[112] wherein the presence of chloromethyl (-*CH$_2$Cl*) group of epichlorohydrin weakens the *C*-*O* bond of the epoxide, making it more susceptible to ring-opening. The yield of compounds **4b** and **8b** showed a closely high conversion with a slight decrease when using catalyst **A**. The internal epoxides could be converted with only a low yield obtained using all three-boron catalysts.

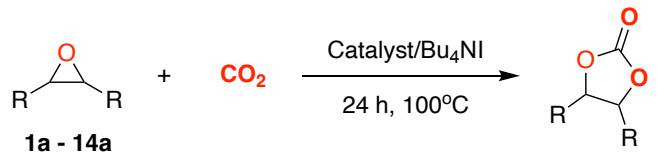


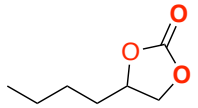

**1b**

A: 85 %, B: 87 %,
C: 90 %

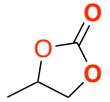

**2b**

A: 90 %, B: 96 %,
C: 96 %

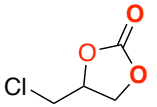


**3b**

A: >99 %, B: >99 %,
C: >99 %

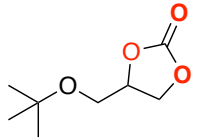

**4b**

A: 84 %, B: >99 %,
C: >99 %

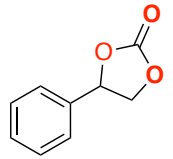

**5b**

A: 95 %, B: 89 %,
C: 97 %

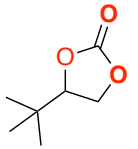

**6b**

A: 38 %, B: 41 %,
C: 54 %

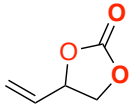

**7b**

A: 90 %, B: 95 %,
C: 88 %

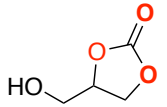


**8b**

A: 93 %, B: >99 %,
C: >99 %

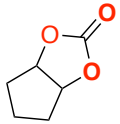

**9b**

A: 49 %, B: 42 %,
C: 40 %

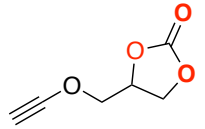

**10b**

A: 95 %, B: 94 %,
C: 98 %

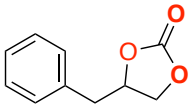

**11b**

A: 89 %, B: 97 %,
C: 98 %

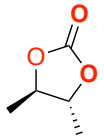

**12b**

A: 16 %, B: 27 %,
C: 28 %

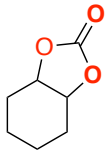

**13b**

A: 41 %, B: 37 %,
C: 38 %

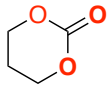

**14b**

A: trace, B: 10 %,
C: 15 %

**Scheme 2.8** Cycloaddition of $CO_2$ with various epoxides using catalyst **A-C** and $Bu_4NI$ co-catalyst. **Conditions**: Epoxides(**1a-14a**) (1.0 g), 0.25 mol % catalyst, 0.25 mol % $Bu_4NI$, $CO_2$ (2.63 g, 59.8 mmol, 6.0 equiv., approx. 15 bar). Conversion of **1b-14b** determined by inspection of the $^1H$ NMR spectrum of the crude reaction mixture.

## 2.3 Conclusions and Outlook

This chapter has presented studies on the first application of boron complexes bearing an aminotrisphenol ligand as catalysts for cyclic carbonate synthesis from epoxides and $CO_2$. Initially, attempted synthesis of the boron complexes repeatedly provided incomplete coordination of the ligand towards the boron centre resulting in a single unreacted phenol, a novel compound which in this work has allowed for the synthesis of unusual mixed borane-borate species. The existence of free phenol was confirmed through both NMR spectroscopy and X-ray crystallography. The proposed reaction mechanism for the cycloaddition of $CO_2$ was driven by hydrogen bonding to the substrate as in the absence of the free phenol, no cyclic carbonate product was obtained beyond the co-catalyst mediated reaction. In particular, the conversion of the free phenol to methyl ether moiety confirmed the importance of the phenol for catalysis. The boron compound displaying the complete coordination of aminotrisphenolate ligand to boron precursor does not produce a cyclic carbonate product, likely because the p-orbital is filled with electrons from the amine and therefore the compound does not display Lewis acid behaviour. In this context, in the future, it would be interesting to prepare a ligand where *C-H* replaces the nitrogen atom, and therefore no electrons are transferred to the p-orbital leaving it vacant and as a result providing the potential for a novel strong Lewis acid catalyst.

# Chapter 3

Triarylborate Compounds as Lewis Acid Catalysts for the Synthesis of Cyclic Carbonates from $CO_2$ and Epoxide

## 3.1 Introduction

Boron-containing compounds have attracted much attention over the last few decades,[163-167] and their reactivity and chemical properties are very well established. The electronic structure of boron and its specific position in the periodic table, adjacent to carbon, results in trivalent boron compounds that behave as electrophilic molecules with trigonal planar structures that are neutral yet isoelectronic to carbocations.[59,61,168] However, the formation of an additional bond to boron generates interesting anionic tetravalent compounds that have tetrahedral structures and behave as nucleophilic molecules (Scheme 3.1). Boron compounds can be stable while retaining significant reactivity that defines their distinctive, versatile, interconvertible, and tuneable chemical behaviour.[107,169,170] Indeed, this broad spectrum of structural, electronic, and reactivity of organoboron compounds has led to several recent discoveries of beneficial chemical reactions.[166,167,171-174]

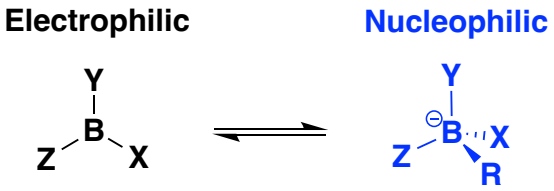


**Scheme 3.1** Transition of neutral to four coordinated bonds boron compounds.[59,61,168]

Almost every common type of boron bonds, such as *B-H*, *B-F*, *B-O*, and *B-C*, have a unique reactivity that can be controlled and exploited. Nearly all chemical species (both organic and inorganic) containing trivalent boron atoms are considered Lewis acids due to their strongly electrophilic nature which is the result from a vacant p-orbital into which electrons can be received and can be

further attenuated through variation of the three substituents bound to boron.[107,175] The strength of Lewis acid compounds can be measured in several ways, and one of the commonly used processes is the Gutmann-Beckett method (Equation 1).[116] This method is based on the NMR chemical shift, and the results are by conventionally presented as an acceptor number (AN) wherein the higher AN value corresponds to greater Lewis acidity of the compounds. For example, triphenylborane (TPB) has AN of 55.03, whilst the more Lewis acidic *tris*(perfluorophenyl)borane (BCF) gives AN of 78.90.[73,116]

$$\mathbf{AN} = \mathbf{2.21}\ (\boldsymbol{\delta}_{\mathbf{LA{*}Et_3PO}} - \mathbf{41}) \qquad \textbf{Equation 1}$$

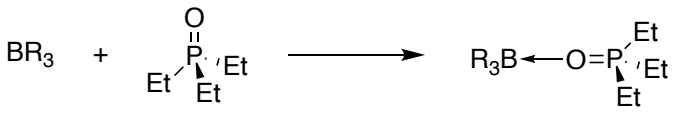


**Scheme 3.2** Interaction of borate compounds with triethylphosphine oxide based on the Gutmann-Beckett method.

Whilst many neutral boron-containing compounds have been synthesised, few have been applied as catalysts for the conversion of $CO_2$ and epoxides to form cyclic carbonates. Examples of boron compounds used as Lewis acid catalysts for this conversion are shown in Scheme 3.3, which aid the pursuit of metal-free catalysts for the utilisation of $CO_2$.[111,114,121,176]

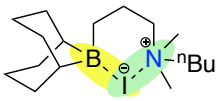

Wu, 2020

13 examples (12 terminal; 1 internal epoxide)
Conditions: catalyst (0.02-0.2 mol %),
$CO_2$ (2.0 MPa), 90-150 °C, 6-24 h

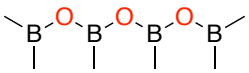

Lu, 2019

8 examples (7 terminal; 1 internal epoxide)
Conditions: catalyst (0.5mol %), $Bu_4NB$ (1.0 mol %),
$CO_2$ (2.0 MPa), 100-120 °C, 2-7 h

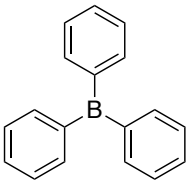

Kerton, 2019

2 examples (terminal epoxides)
Conditions: catalyst (0.025 mol %),
PPNCl (0.1 mol %) $CO_2$ (2.0 MPa),
100 °C, 22 h

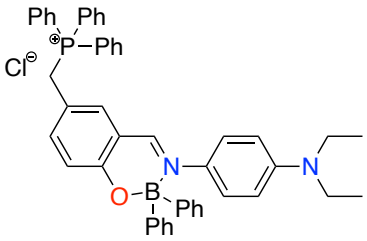

Kilic, 2019

4 examples (terminal epoxides)
Conditions: catalyst (0.1 mol %),
DMAP (0.2 mol %), $CO_2$ (1.6 MPa),
100 °C, 2 h

**Scheme 3.3** Selected examples of boron-containing compounds used as a Lewis acid catalyst for cyclic carbonate synthesis.[111,114,121,176]

In 2019, Kerton and co-workers reported on the use of arylboranes as catalysts to synthesise cyclic carbonates, whereby they have applied commercially available TPB and BCF as catalysts (Scheme 3.4).[114] More recently, Wu and co-workers reported on a highly active one-component catalyst system containing a borane and ammonium salt in the same molecule.[176]

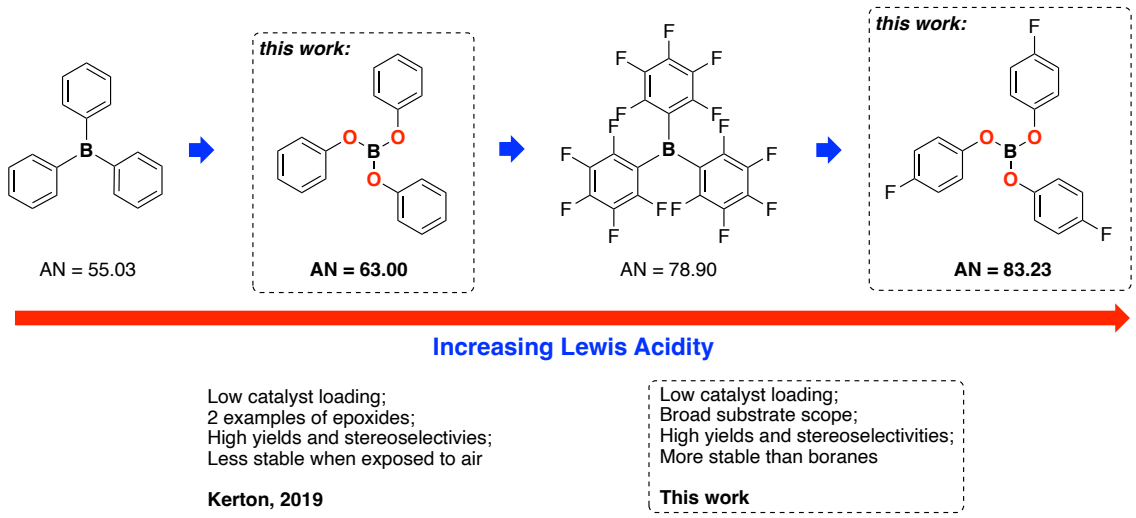


**Scheme 3.4** Comparison of arylboranes and arylborates with their corresponding AN.[114,116]

The Lewis acidity of boron-containing compounds is highly controllable.[116] It is well understood that the reactivity can be varied by modifying the substituents on, for example, an aromatic group of an aryl borane in the para-position or meta-position since ortho-position substituents introduce a steric interaction with the reacting centre not only intramolecularly but also possibly with other reagents during intermolecular interactions with the boron centre. Beyond arylboranes, arylborates provide an opportunity for additional functionality and the ability to modify the electronic properties of the boron atom.

The work described in this chapter applies triphenyl borate (TPBO) as the basis to develop an environmentally benign and attractive catalytic process that uses commercially available and cheap compounds. The proposed key Lewis acid mediated ring-opening steps of the mechanism are shown in Scheme 3.5.

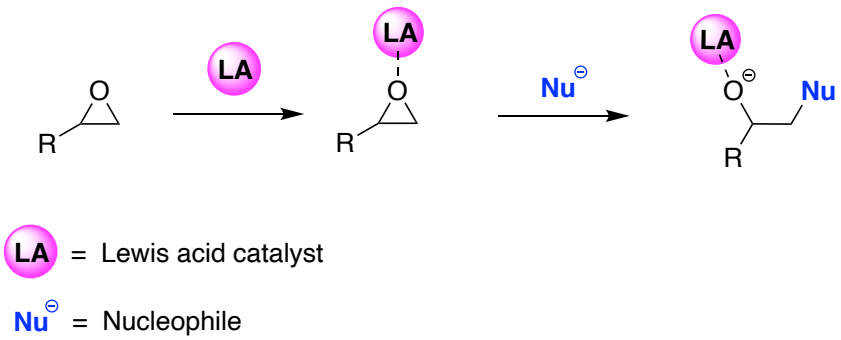


**Scheme 3.5** Coordination of Lewis acid catalyst and the presence of nucleophile for the ring-opening of an epoxide (example of ring-opening at the least hindered carbon atom is demonstrated).

To the best of our knowledge, this is the first study into the cycloaddition reaction of $CO_2$ with epoxides to synthesise cyclic carbonate catalysed by arylborates. This study provides information on the versatility of boron-containing compounds and highlights the potential application of simple boron compounds as a catalyst to utilise $CO_2$, a compound with remarkable thermodynamic stability and limited reactivity.

## 3.2 Results and Discussion

### 3.2.1 Synthesis of Triarylborate Compounds

The synthesis of triarylborate compounds was challenging and highly dependent on the boron precursor used. The same challenges were encountered with the boron-containing compounds reported in Chapter 2 of this thesis. Wherein choice and selection of the boron precursor directly affected the outcome of the reaction. Several approaches were attempted to synthesise triarylborate compounds. The first approach was through the obvious reaction of $BH_3$·THF with *p*-cresol to synthesise compound **F** at room temperature, but unexpectedly the crude reaction mixture only contained *p*-cresol, clearly indicating that the approach was

not suitable. The second method involved the use of Dean-Stark apparatus to collect water produced from the reaction of boric acid and phenol, thus driving the condensation equilibrium towards formation of the desired product.[177,178] In this reaction, boric acid was reacted with three equivalents of *p*-cresol to obtain a tri-substituted arylborate compound and water, as shown in Scheme 3.6 (bottom). However, this reaction produced a very low yield and was unsuccessful with other triarylborate compounds when other phenols were employed.

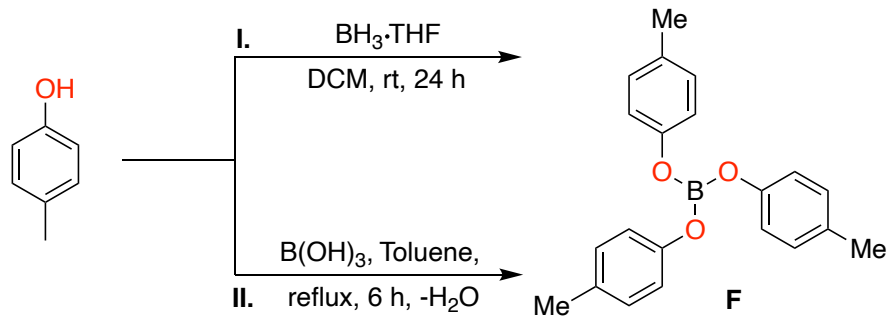


**Scheme 3.6** Attempts to synthesise compound **F**.[177,178]

A range of arylborate compounds were, however, successfully synthesised as shown in Scheme 3.7, where the synthesis was achieved using $BCl_3$ as boron precursor at room temperature, providing good to excellent yields of the target arylborate compounds ranging from 81-91 %. During this synthesis, the reaction was kept cool throughout with a dry ice/acetone bath (-78 °C). After the reaction time was completed, the crude product was recrystallised through slow titration with cold pentane at -35°C, and the product was stored directly in the glovebox. Most of the products collected were oils and slowly turned to solid afterwards whilst inside the glovebox without any visual changes to their $^1$H NMR spectra as a result of this change in state. This observation indicates that the storage of arylborate compounds was possible under inert conditions. TPBO was purchased

commercially and was used directly without further purification as a catalyst for the cycloaddition reactions reported in this chapter.

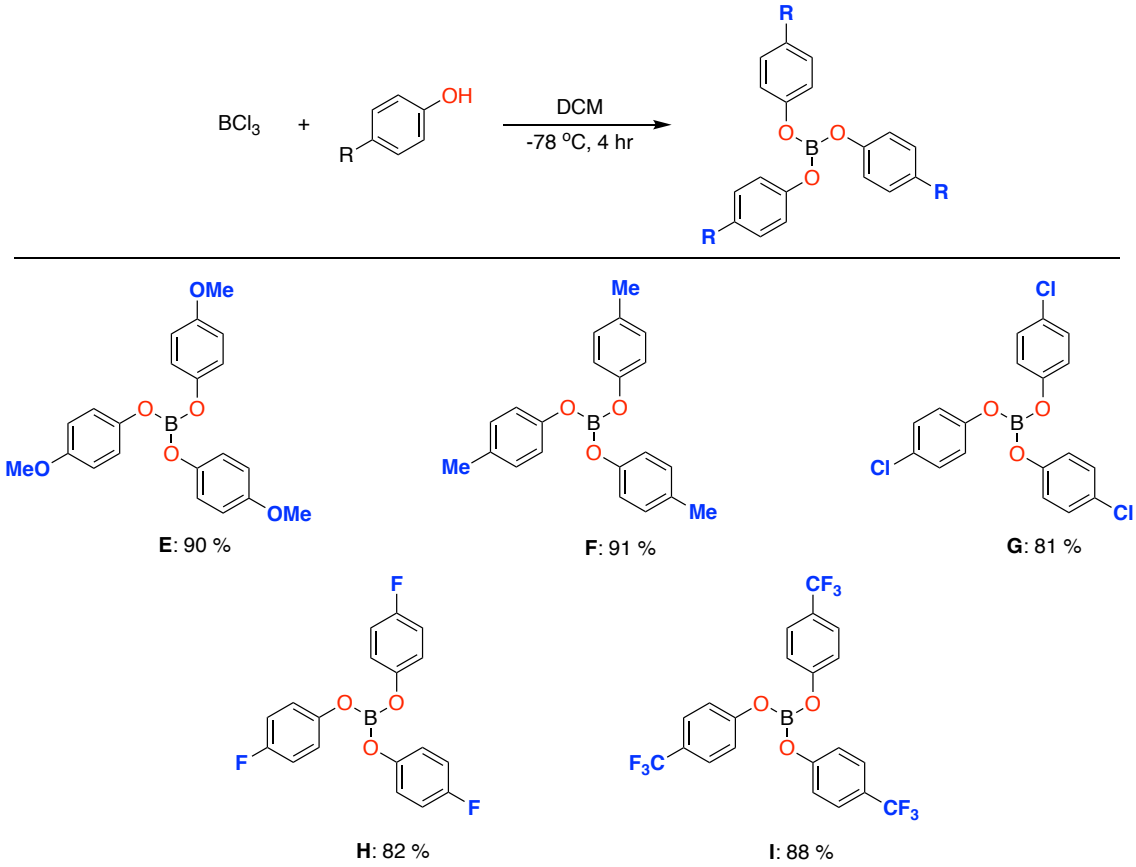


**Scheme 3.7** General procedure for the synthesis of substituted triarylborate compounds **E-I**.

The boron atom contains three valence electrons, representing a strong electron-withdrawing element and is considered highly Lewis acidic within its group.[179,180] The introduction of R-substituents on the phenol is likely to affect the Lewis acidity of the boron centre. Arylborates with the following *para* substituents have been prepared and are arranged according to the most electron-withdrawing substituent.[180-182]

Least Electron Withdrawing **-$OCH_3$ < -$CH_3$ < -H < -Cl < -F < -$CF_3$** Most Electron Withdrawing

The uncollected traces of product left in the Schlenk tube from the reactions were examined after 2 – 5 days of exposure to air. It was therefore discovered that they appeared to be sensitive to moisture and had decomposed to phenol. In all cases, the phenol peak could be observed in the $^{1}H$ NMR spectrum, confirming this hydrolysis reaction.

### 3.2.2 Characterisation of triarylborate compounds

#### 3.2.2.1 NMR Spectroscopy

The solubility of the synthesised triarylborate compounds was excellent in chloroform-*d* ($CDCl_3$). Although the compound was unstable when exposed to air, it was observed that the compounds have more extended stability when dissolved in a solvent rather than stored in a container. A stacked spectrum is shown in Figure 3.1, highlighting the gradual decomposition of compound **E** at room temperature in $CDCl_3$. The phenol peak was not visible after a day in $CDCl_3$ solution whilst exposed to air. Although the aromatic peaks of the phenol were quite visible, the percentage of its presence was <1.5 %. After four days in $CDCl_3$ solution, the phenol peak was clearly visible at 4.66 ppm, and the increasing aromatic peaks at 6.78 ppm of the parent phenol gave an integration of 0.31, which indicates that 76 % of the product was still not decomposed. The methoxy peak of the substrate could also be seen where another peak appeared at 3.78 ppm. A higher concentration, as expected, was observed after eight days in solution, where the aromatic peak at 6.80 ppm of the starting phenol becomes dominant.

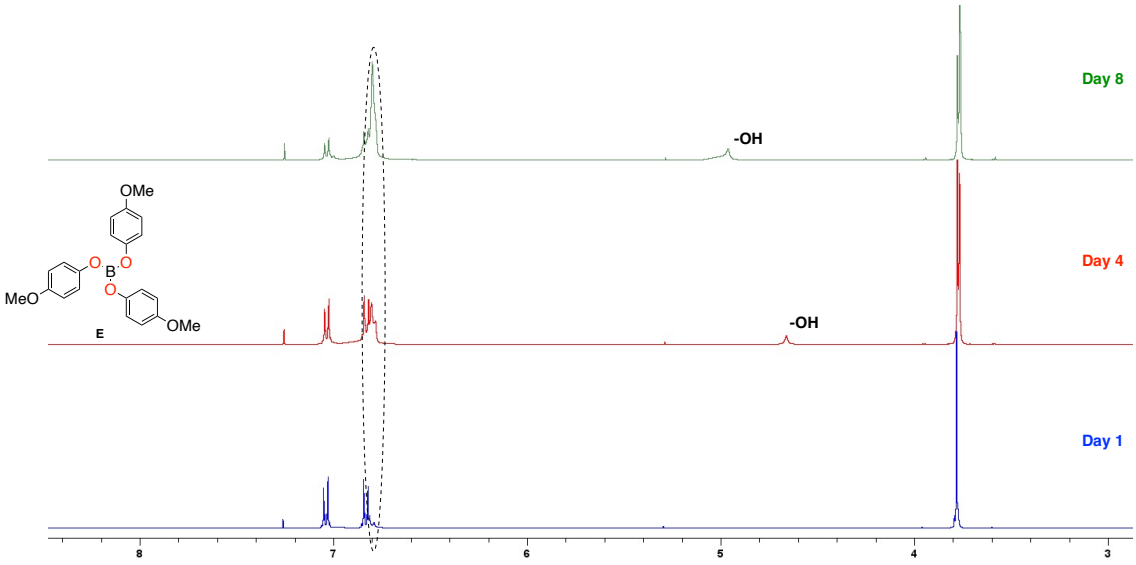


**Figure 3.1** $^{1}$H NMR spectra ($CDCl_3$, 298 K) showed the gradual decomposition of compound **E** over 8 days.

With the potential instability of compound **E** now established, further studies into the other arylborates were performed and the same outcome was observed where the presence of hydroxy peak was visible over time when the compounds were exposed to moisture. The issue of stability of compounds was appropriately addressed by using the glove box to store all the synthesised triarylborate under inert conditions.

As shown in Figure 3.2, the spectrum of compound **E** displays an example of a $^{1}$H NMR spectrum of a pure compound showing two aromatic peaks at 7.04 ppm and 6.83 ppm, with the absence of the hydroxy peaks confirming the formation of *B-O* bonds. This trend in the $^{1}$H NMR spectrum was consistent throughout the synthesis of all the arylborate compounds, where the hydroxy peak was not visible in the $^{1}$H NMR. (See Appendix for $^{1}$H NMR spectra of all the arylborate products).

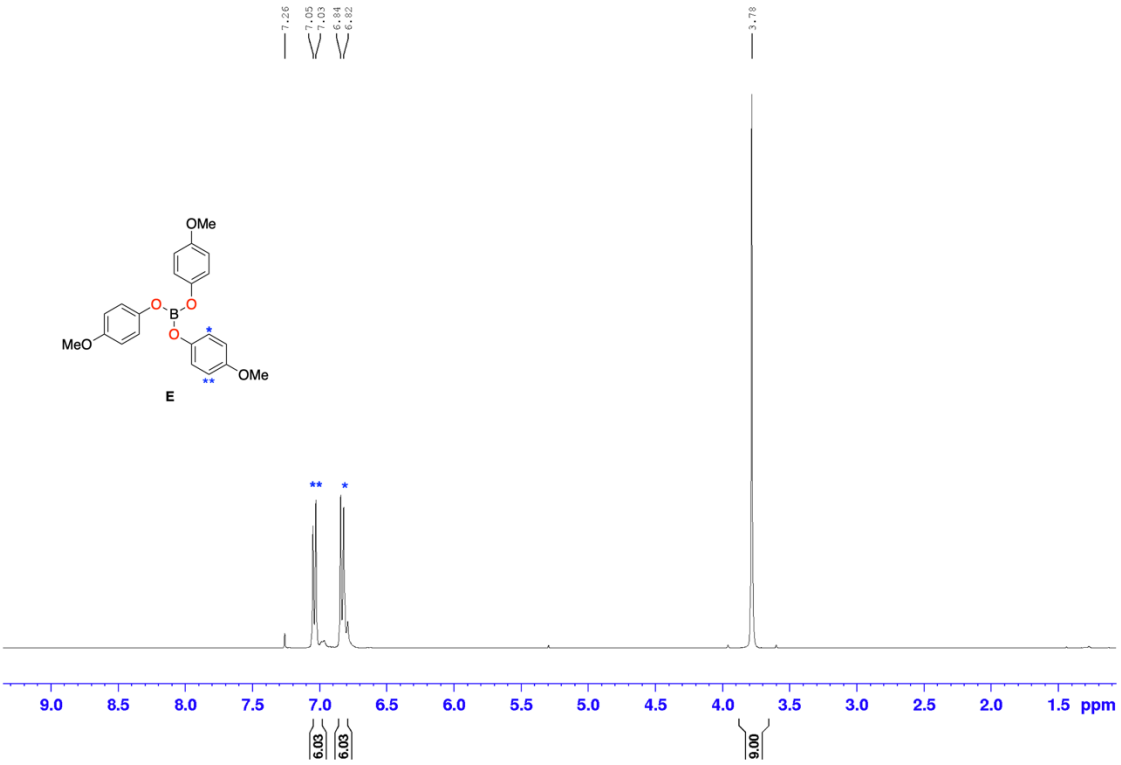


**Figure 3.2** $^{1}$H NMR spectrum ($CDCl_3$, 298 K) of triarylborate E showing the aromatic peaks and methyl peaks of the compound.

### 3.2.3 Catalyst Screening

At the outset, the triarylborate compounds were considered moderately unstable when exposed to moisture. TPBO was available commercially and was used directly without further purification. This compound was used for catalyst system optimisation in a similar manner to that applied in Chapter 2 of this thesis in determining the optimised conditions in terms of catalyst and co-catalyst loading, temperature, and reaction time in the solvent-free reaction. The cycloaddition reaction was conducted using freshly prepared dry ice as in Chapter 2. Once all the reagents (catalyst, co-catalyst and epoxide) were added to the 50 mL reactor, the dry ice was prepared, weighed and introduced, and then the reactor was sealed. The weight of the dry ice used was 2.68 g which achieved a pressure of approximately 15 bar. This is slightly lower than that of the reported work on TPB by Kerton, whereby 20 bar of $CO_2$ pressure was used.[114]

In terms of co-catalyst, the iodide nucleophile from *tetra*-butylammonium iodide ($Bu_4NI$) was used in this study as it showed higher conversions than neutral 4-Dimethylaminopyridine (DMAP) and the chloride nucleophile from *bis*(triphenylphosphine)imidium chloride (PPNCl) (Table 3.1, Entries 27, 28 and 31). As shown in Table 3.1, TPBO was clearly an active catalyst at 1.0 mol %, even at a low temperature of 40 °C, giving an excellent yield of 93 %, whilst 76 % was obtained when the catalyst loading was decreased to 0.5 mol % (Table 3.1, Entries 1 and 2). When the catalyst and co-catalyst loadings were decreased to 0.5 mol % and 0.25 mol %, respectively, with an increased temperature of 80 °C and 100 °C, yields above 90 % were still obtained (Table 3.1, Entries 3 and 4).

**Table 3.1** Catalyst optimisation using TPBO.

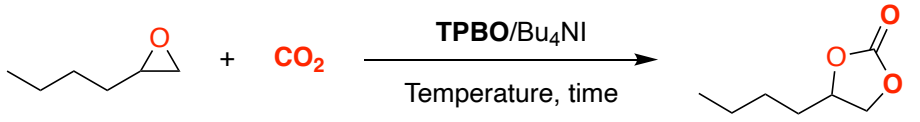


**1a** **1b**

| Entry | TPBO(mol %) | $Bu_4NI$(mol %) | Time(h) | Temp(°C) | Conv (%)[a] |
|---|---|---|---|---|---|
| 1 | 1 | 2 | 24 | 40 | 93 |
| 2 | 0.5 | 2 | 24 | 40 | 76 |
| 3 | 0.5 | 0.25 | 24 | 80 | 93 |
| 4 | 0.5 | 0.25 | 24 | 100 | 96 |
| 5 | 0.25 | 1 | 24 | 100 | >99 |
| 6 | 0.25 | 0.5 | 24 | 100 | >99 |
| 7 | 0.125 | 0.5 | 24 | 100 | 98 |
| 8 | 0.0625 | 0.5 | 24 | 100 | 96 |
| 9 | 0.25 | 0.5 | 24 | 80 | 94 |
| **10** | **0.05** | **0.5** | **24** | **100** | **95** |
| 11 | - | 0.5 | 24 | 100 | 55 |
| 12 | 0.05 | 0.5 | 18h | 100 | 84 |
| 13 | 0.25 | 0.25 | 24 | 100 | 93 |
| 14 | 0.125 | 0.25 | 24 | 100 | 79 |
| 15 | 0.125 | 0.25 | 24 | 80 | 76 |
| 16 | 0.05 | 0.2 | 24 | 100 | 92 |
| 17 | 0.5 | 0.125 | 24 | 100 | 95 |
| 18 | 0.25 | 0.125 | 24 | 80 | 79 |
| 19 | 0.25 | 0.125 | 24 | 100 | 88 |
| 20 | 0.125 | 0.125 | 24 | 100 | 84 |
| 21 | 0.125 | 0.125 | 24 | 80 | 61 |
| 22 | 0.05 | - | 24 | 100 | 0 |
| 23 | 0.1 | 0.1 | 3 | 100 | 42 |
| 24 | 0.1 | 0.1 | 24 | 100 | 81 |
| 25 | 0.025 | 0.1 | 24 | 100 | 72 |
| 26 | 0.025 | 0.1 | 22 | 100 | 83 |
| 27[b,d] | 0.025 | 0.1 | 22 | 100 | 74 |
| 28[c] | 0.025 | 0.1 | 22 | 100 | 34 |
| 29 | 0.025 | 0.1 | 3 | 100 | 41 |
| 30[d] | 0.025 | 0.1 | 3 | 100 | 40 |
| 31[b] | 0.025 | 0.1 | 3 | 100 | 33 |

**Conditions**: 1,2-epoxyhexane (**1a**) (1.0 g, 9.98 mmol), TPBO, $Bu_4NI$ co-catalyst, $CO_2$ (2.63 g, 59.8 mmol, 6.0 equiv., approx. 15 bar). [a]Conversion of **1a** determined by inspection of the $^1H$ NMR spectrum of the crude reaction mixture. [b]PPNCl, [c]DMAP co-catalyst. [d]TPB used as a catalyst.

With the $Bu_4NI$ co-catalyst increased to 1.0 mol % and the catalyst to 0.25 mol %, the conversion was >99 % (Table 3.1, Entry 5). A further decrease of the co-catalyst to 0.5 mol % without changing the catalyst loading still provides complete substrate conversion and a yield of >99 %, whilst a further decrease of the catalyst to 0.125 mol % provides a 98 % yield (Table 3.1, Entries 6 and 7). The loading of TPBO catalyst was further decreased to 0.0625 mol% whilst retaining the co-catalyst loading of 0.5 mol % and provided a yield of up to 96 % (Table 3.1, Entry 8). As mentioned earlier, the presence of a co-catalyst in the reaction was essential for excellent conversions, whereby only 55 % conversion was obtained in the absence of a catalyst and no product was formed when there was an absence of co-catalyst (Table 3.1, Entries 11 and 22). The catalytic performance of the binary catalytic system was further investigated by changing the catalyst system loading and temperature of the reaction whilst retaining the reaction time and pressure, which still provides a good yield (Table 3.1, Entries 13-21).

As the catalyst used was reasonably well structurally related to the arylborane (TPB) reported by Kerton and co-workers, additional experiments were carried out to compare this catalyst system in our hands. The product yield using TPBO (Table 3.1, Entry 23) was low at 42 % compared to the reported 92 % yield using TPB, but when the time was extended to 24 hours, the yield increased to 81 % (Table 3.1, Entry 24); therefore, under these conditions, the TPB is clearly a more active catalyst. However, a decrease of the catalyst loading at a longer reaction time of 22 h provided a higher yield using TPBO than TPB (Table 3.1, Entries 26 and 27). Whilst Table 3.1, Entries 29 and 30 provide an almost exact yield of 41 % and 40 % using TPBO and TPB as a catalyst, respectively, with the same co-catalyst ($Bu_4NI$). This data demonstrates

promising results in using TPBO as a catalyst for the cycloaddition of $CO_2$ and epoxides to form cyclic carbonates.

### 3.2.4 Comparative Investigation

TPBO was then compared to the other arylborates synthesised in this study. The presence of different *para*-substituents in the aromatic ring should affect the catalytic ability of each arylborate compound. Hence, the potential Lewis acid catalysis was expected to be distinct for each compound.

As shown in Table 3.2, all the catalyst provides an excellent yield under identical conditions. Although the use of catalysts TPB and **E** gives the lowest conversion rate, the result may depend on the Lewis acidic nature of each compound (Table 3.2, Entry 1). Catalyst **G** and **H** gave the highest conversion of substrate **1a** (Table 3.2, Entries 3 and 4), indicating that more electron-withdrawing substituents are beneficial to the catalytic activity of the compounds. However, although catalyst **I** contain the most electron-withdrawing substituent, $CF_3$ (Table 3.2, Entry 5), the Lewis acidity of the boron centre could also be affected by other factors.

**Table 3.2** Comparison of catalyst used for the synthesis of compound **1b**.

| Entry | Catalyst | % Conversion[a] |
|---|---|---|
| 1 | **E** (OMe) | 93 |
| 2 | **F** (Me) | 94 |
| 3 | **G** (Cl) | 97 |
| 4 | **H** (F) | 97 |
| 5 | **I** ($CF_3$) | 95 |
| 6 | TPBO | 95 |
| 7 | TPB | 93 |
| 8 | --- | 55 |

**Conditions**: 1,2-epoxyhexane (**1a**) (1.0 g, 9.98 mmol), catalyst (0.05 mol %), $Bu_4NI$ (0.5 mol %), 24 h, 100 °C, $CO_2$ (2.63 g, 59.8 mmol, 6.0 equiv., approx. 15 bar). [a]Conversion of **1a** determined by inspection of the $^1H$ NMR spectrum of the crude reaction mixture.

Although arylborate was initially considered an unstable compound, especially when exposed to moisture. Its application as a catalyst at a higher temperature of 100 °C is clearly possible. Interestingly, upon inspection of the crude $^{1}H$ NMR spectra after the reaction, the catalyst signals were still present, confirming the stability of the catalyst during the period of the reaction (Figure 3.3). Also, the selectivity for cyclic carbonate synthesis was >99 %, with no by-products observed.

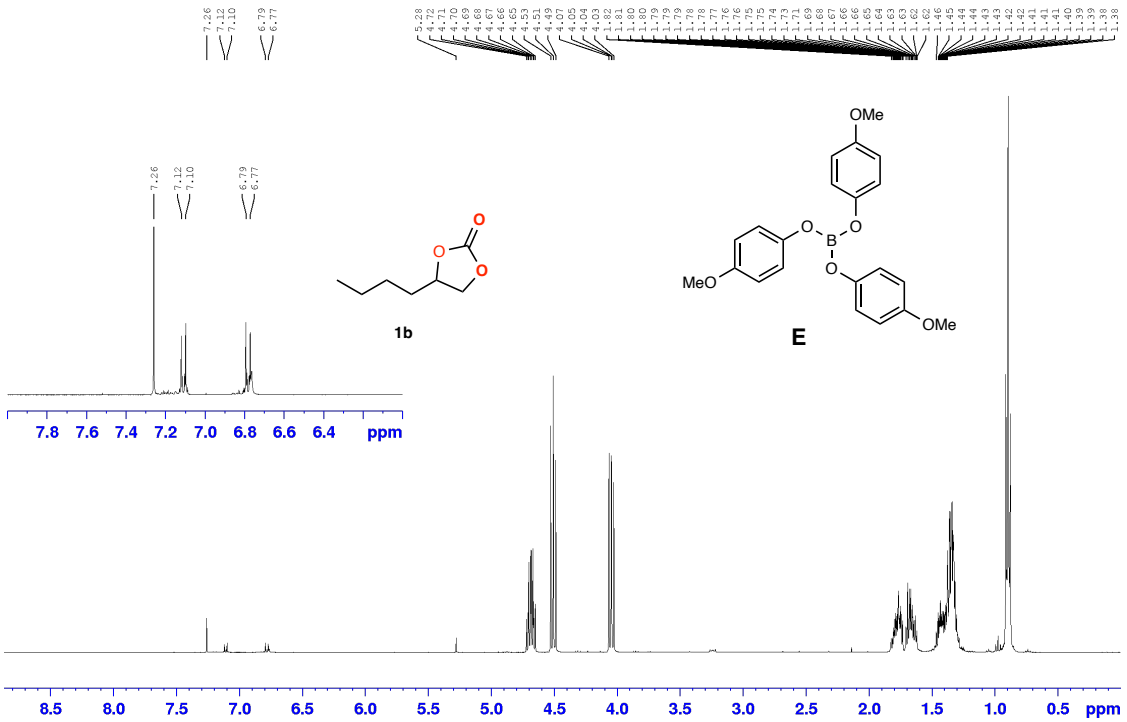


**Figure 3.3** An example of a $^{1}H$ NMR spectrum ($CDCl_3$ at 298 K) of a crude reaction mixture using compound **E** as a catalyst after conversion of 1,2-epoxyhexane to **1b** without purification and without the addition of mesitylene, with the aromatic peaks of the catalyst expanded to highlight that it is on the whole intact.

The Lewis acidity of several boron-containing species has been assessed by determining their AN. The AN value was calculated using the Gutmann-Beckett method to measure the Lewis acidity of each borate compound by acquiring the observed chemical shift from the solution of triethylphosphine oxide ($Et_3PO$) and arylborate in $CDCl_3$ using the $^{31}P\{^{1}H\}$ NMR.

**Table 3.3** Gutmann-Beckett $^{31}P\{^{1}H\}$ NMR and calculated acceptor numbers (AN) of boron-containing compounds.

| Entry | Catalyst | δ / ppm[a] | AN[b] |
|---|---|---|---|
| 1 | **E** (OMe) | 57.78 | 37.1 |
| 2 | **F** (Me) | 59.98 | 42.0 |
| 3 | **G** (Cl) | 71.08 | 66.5 |
| 4 | **H** (F) | 78.66 | 83.2 |
| 5 | **I** ($CF_3$) | 78.15 | 82.1 |
| 6 | TPBO | 69.40 | 63.0 |
| 7 | TPB | 65.90 | 55.0 |

**Conditions:** Solution in $CDCl_3$, [a]Observed chemical shift of the 1:1 $Et_3PO$ ratio with arylborate compounds. [b]$\mathrm{AN} = 2.21\ (\delta_{\mathrm{LA}*\mathrm{Et_3PO}} - 41)$.

The presence of the para-substituents affects the Lewis acidity of the boron centre. Table 3.3 shows all the observed $^{31}P\{^{1}H\}$ NMR chemical shifts and the calculated AN of each boron compound where catalyst **H** presents the highest AN, which means the most Lewis acidic amongst other arylborate compounds (Table 3.3, Entry 4). It is worth noting that the equation used is not valid for *ortho*-substituents as it implies steric interaction with the boron centre.

In Table 3.4, arylborates were compared based on their catalytic activity at a shorter reaction time of 3 h. The results demonstrate a different reactivity at a shorter time than 24 h reaction. These data show that compound **G** has the highest catalytic activity, higher than **H** and **I** (Table 3.4, Entries 3-5). The efficiency of the catalyst was tested at a longer reaction time, whilst a shorter time provided a different result from what was expected. Whilst catalyst **F** has the lowest conversion of 56 % amongst all compounds (Table 3.4, Entry 2).

**Table 3.4** Comparison of catalyst used for the synthesis of compound **1b** at a shorter reaction time.

| Entry | **Catalyst** (substituent) | **% Conversion**[a] |
|---|---|---|
| 1 | **E** (OMe) | 60 |
| 2 | **F** (Me) | 56 |
| 3 | **G** (Cl) | 72 |
| 4 | **H** (F) | 59 |
| 5 | **I** ($CF_3$) | 63 |
| 6 | **TPBO** | 67 |

**Conditions**: 1,2-epoxyhexane (**1a**) (1.0 g, 9.98 mmol), catalyst (0.05 mol %), $Bu_4NI$ (0.5 mol %), 3 h, 100 °C, $CO_2$ (2.63 g, 59.8 mmol, 6.0 equiv., approx. 15 bar). [a]Conversion of **1a** determined by inspection of the $^1H$ NMR spectrum of the crude reaction mixture.

Based on the results discussed above, the proposed reaction mechanism for the cycloaddition of $CO_2$ with 1,2-epoxyhexane is shown in Scheme 3.8, which undergoes a Lewis acid catalysis type of interaction. Initial coordination of the epoxide to the boron centre (Lewis acid), followed by a Lewis base-mediated ring-opening step resulting from the $Bu_4NI$ co-catalyst (Int. 1). The ring-opening of the epoxide occurs at the least hindered carbon atom, as shown in the mechanism. Following the ring-opening by nucleophilic iodide, $CO_2$ insertion then occurs into the B--O bond (Int. 2) and closes the ring, releasing the co-catalyst and catalyst (Int. 3), forming a cyclic carbonate product **1b**.

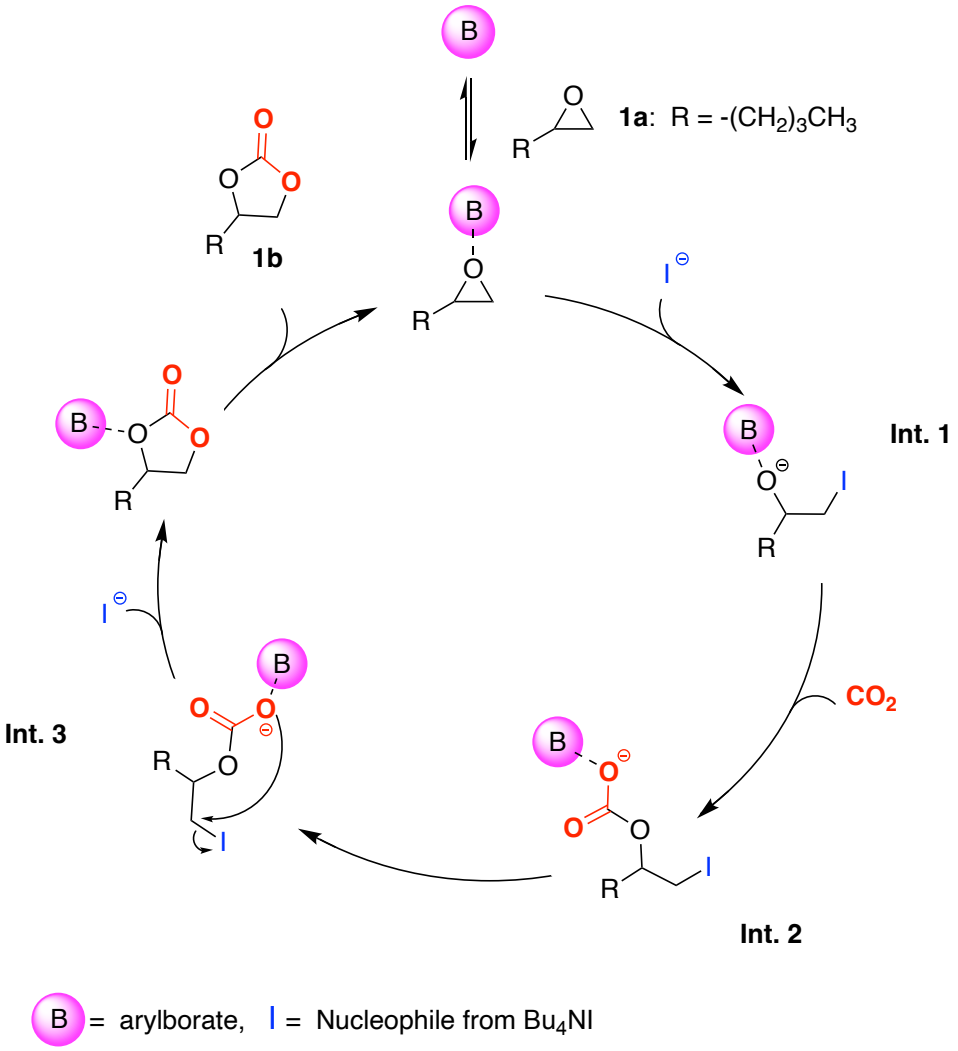


**Scheme 3.8** The proposed general reaction mechanism for the formation of compound **1b** from a coupling reaction between 1,2-epoxyhexane and $CO_2$ catalysed by arylborates where the ring-opening step occurs at the least hindered carbon atom (to form Int. 1).

### 3.2.5 Substrate scope for the $CO_2$ cycloaddition reaction

With optimised reaction conditions in hand (Table 3.1, Entry 10), the substrate scope of epoxides, both terminal and internal, was investigated for the cycloaddition of $CO_2$ and epoxide. Scheme 3.9 summarises the results obtained from this work. Epoxides bearing an alkyl substituent like 1,2-epoxyhexane (**1a**) and propylene oxide (**2a**) were readily converted into the desired products (**1b** and **2b**, respectively) in excellent yield except for epoxides with bulky *tert*-butyl substituents **6a**, where the desired product (**6b**) provides a significantly lower conversion rate of 85 %, likely because of steric effects. The epoxide bearing an

alkyl halide substituent (**3a**) also reacted smoothly with $CO_2$ to give the corresponding cyclic carbonate **3b**. Furthermore, cyclic carbonates functionalised with alkenes (**7b**), alcohols (**8b**), alkynes (**10b**), ethers (**4b**, **10b**), and aromatics (**5b**, **11b**) showed almost quantitative yields.

The challenging internal epoxides were converted into the corresponding cyclic carbonates (**9b**, **12b-13b**) with reduced yields of 39 - 47 % because of their highly hindered nature owing to steric effects, wherein the addition of the catalyst loading to 0.5 mol % was required to achieve a high conversion rate with a rise to 70 %. Whilst only a trace amount of cyclic carbonate product was observed from the four-membered oxirane, oxetane (**14a**)**.**

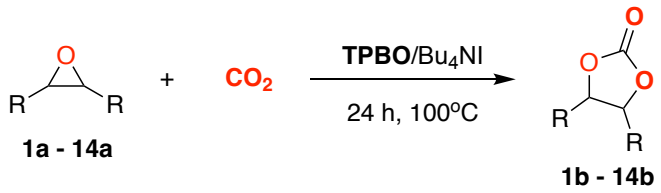


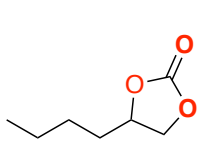

**1b**
95 %

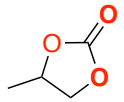

**2b**
99 %

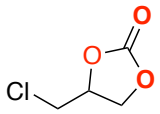


**3b**
>99 %

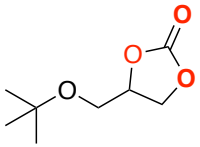

**4b**
>99 %

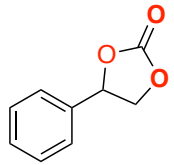

**5b**
99 %

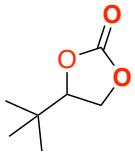

**6b**
85 %

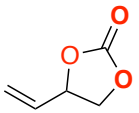

**7b**
98 %

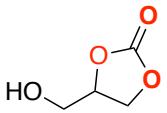


**8b**
99 %

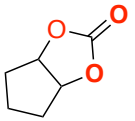

**9b***
40 %

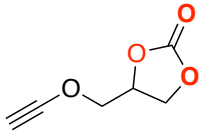

**10b**
99 %

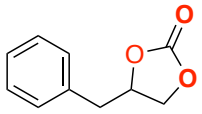

**11b**
99 %

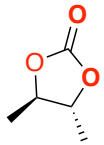

**12b***
39 %

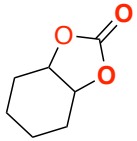

**13b***
47 %

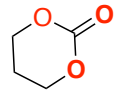

**14b***
trace

**Scheme 3.9** Cycloaddition of $CO_2$ with various epoxides using **TPBO** catalyst and $Bu_4NI$ cocatalyst. **Conditions**: Epoxides(**1a-14a**) (1.0 g), 0.05 mol % catalyst, 0.5 mol % $Bu_4NI$, $CO_2$ (2.63 g, 59.8 mmol, 6.0 equiv., approx. 15 bar). Conversion of **1b-14b** determined by inspection of the $^1H$ NMR spectrum of the crude reaction mixture. Note: *An increase of catalyst loading to 0.5 mol%, increases the yield of product up to 70 % except with **14b**.

## 3.3 Conclusions and Outlook

The results in this chapter clearly demonstrate that arylborate compounds are active catalysts for converting epoxides and $CO_2$ to form cyclic carbonate compounds. The catalytic activity was efficient, and catalyst loadings are lower than with many metal-free systems to date. Since dry ice was used in the entire experiment, another factor to investigate in the future is the optimal amount of $CO_2$ required. The data shows that the synthesised arylborates have more extended stability when stored in the glovebox as they are prone to hydrolysis in the presence of moisture. However, it is clear from inspection of the crude $^1H$ NMR after the cycloaddition reaction that the catalysts remain intact during the reaction. Overall, these results provide proof of concept that bridges the gap between a non-metal and metal-catalysed process and highlight the potential for the application of simple boron compounds as catalysts for the synthesis of cyclic carbonates from epoxides and $CO_2$.

`

# Chapter 4

A Gallium Catalyst for $CO_2$ Utilisation as C1 Source – Synthesis of Oxazolidinones and a Cyclic Carbonate Functionalised Cellulose

## 4.1 Introduction

The commercially viable exploitation of carbon dioxide ($CO_2$) as a feedstock requires both the production of large-volume and low-value chemicals; and the production of lower-volume and high-value products. The latter class includes the cycloaddition reaction of $CO_2$ with aziridines as an efficient, atom-economic route for the preparation of oxazolidinones. Building on experience in developing catalysts for the synthesis of cyclic carbonates from epoxides and $CO_2$, the conversion of aziridines and $CO_2$ to oxazolidinones presented a new challenge with additional complications owing to the presence of a substituent on the nitrogen atom of aziridine and the possibility of forming regioisomeric products.

The oxazolidinone moiety is a crucial heterocyclic structure found in commercial pharmaceuticals and has a range of other synthetic applications.[34,35] For example, antibiotics such as tedizolid, radezolid, linezolid, delpazolid, and toloxatone an antidepressant drug; all contain an oxazolidinone fragment (Figure 4.1).[35,87,183,184]

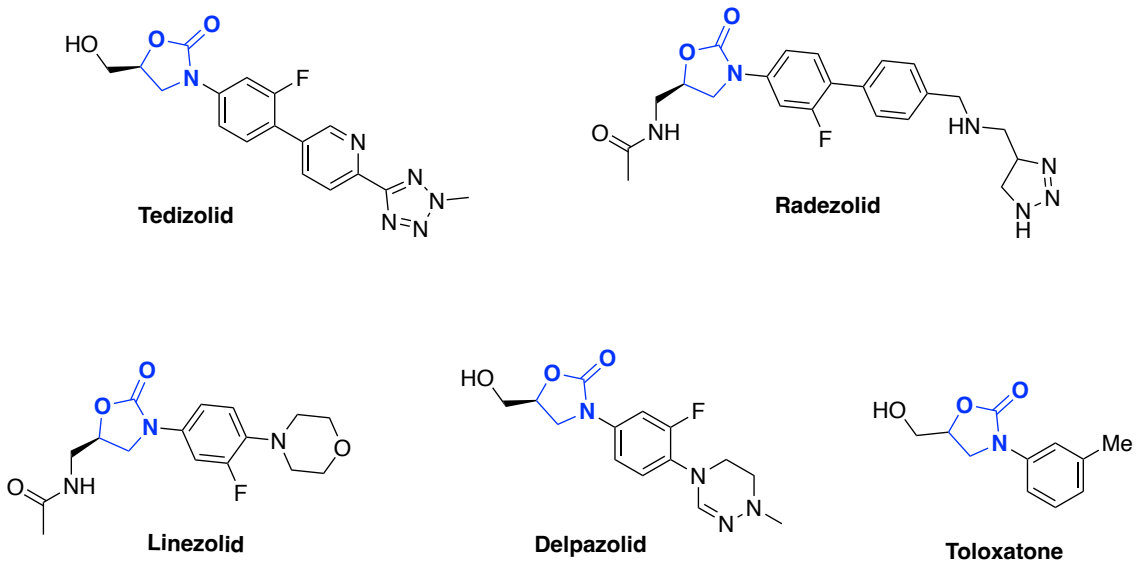


**Figure 4.1** Example of pharmaceutical drugs containing oxazolidinone fragments.[35,87,183,184]

Although oxazolidinones are known for their wide applicability, relatively few preparative reports exist for their synthesis, with those reported including reaction of amino alcohols with highly toxic phosgene[90,185,186] and starting from highly elaborated reagents such as propargylamine or propargylic alcohols and reacting these with supercritical $CO_2$.[187-190]

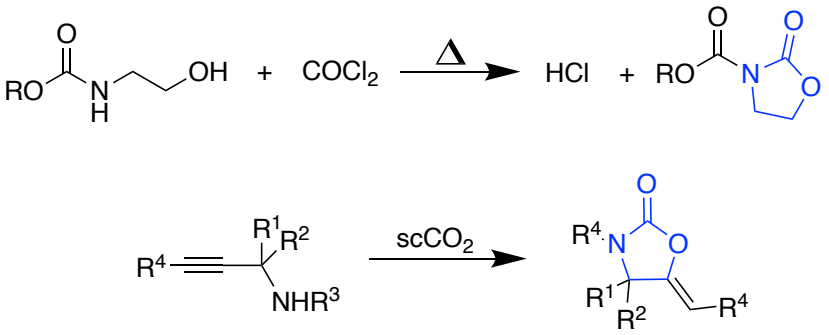

**Scheme 4.1** Different methods for the preparation of oxazolidinone compounds.[90,185-190]

However, both of the mentioned methods are non-eco-friendly routes. The atom-efficient cycloaddition of aziridines and $CO_2$ would be much more attractive approach than the aforementioned processes (Scheme 4.2). As a result, a slowly growing effort has been dedicated to developing efficient methodologies for producing oxazolidinones from the reaction of aziridines and $CO_2$.

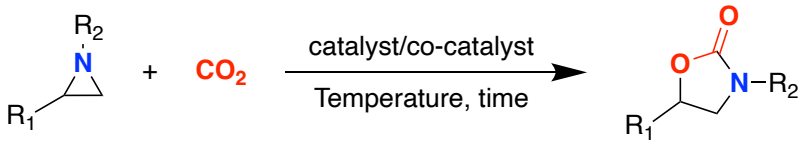

**Scheme 4.2** General reaction for oxazolidinone synthesis from aziridine and $CO_2$.

Several catalysts have been reported for the synthesis of oxazolidinones from $CO_2$ and aziridines, such as iodine, alkali metal halides, quaternary ammonium bromide functionalised polyethylene glycol, naturally occurring amino acids, (salen)-Cr(III)/DMAP, Al(salen), and the combination of 4-methoxyphenol/

DMAP.[10,95,191-195] Although significant advances have been made; still, there are some disadvantages like the requirement of high reaction temperatures, prolonged reaction times, the use of toxic solvents, and co-catalysts to achieve higher yields.

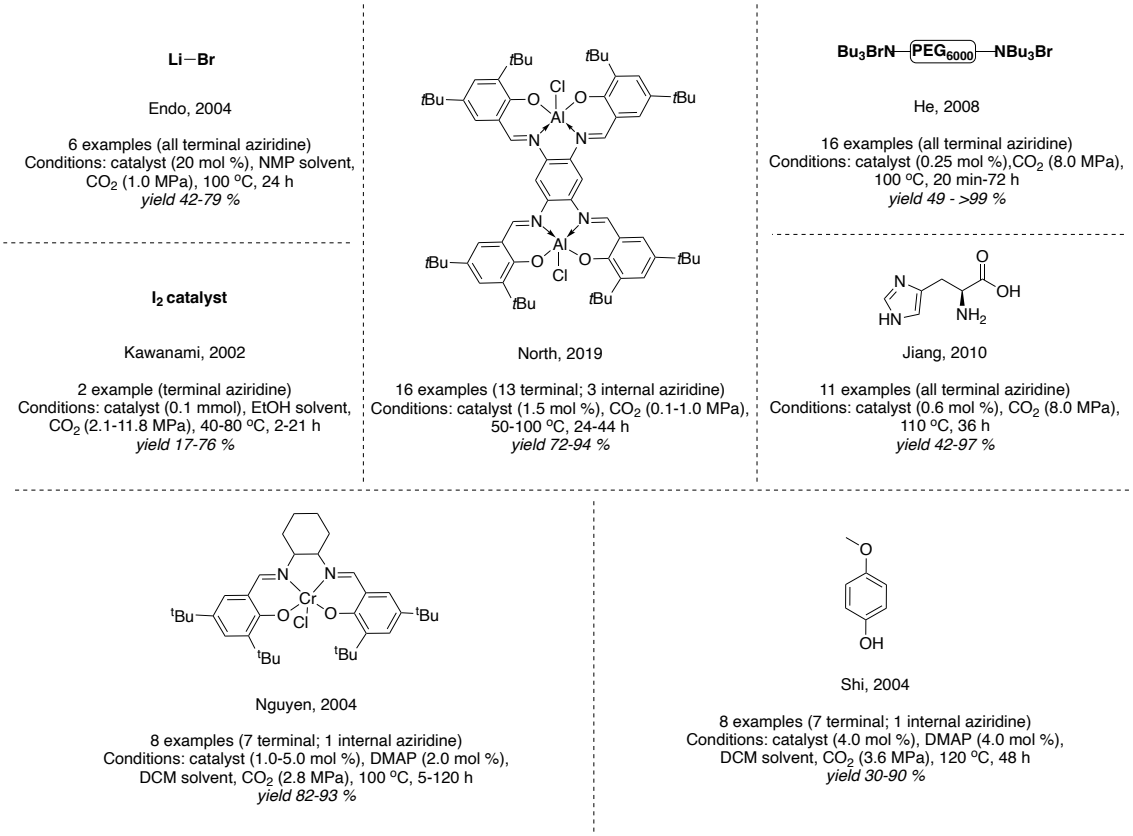


**Figure 4.2** Examples of catalysts used for the synthesis of oxazolidinone from $CO_2$ and aziridine.[10,95,191-195]

Recently, Whiteoak and co-workers have developed a gallium aminotrisphenolate catalyst (**GaL$^{Me}$**) to convert epoxide and $CO_2$ into cyclic carbonates, surpassing aluminium's catalytic ability with the corresponding catalyst containing the aminotrisphenol ligand reported by Kleij in 2013.[1,196] This successful work on gallium-based catalyst for the formation of cyclic carbonates provided the inspiration to use the catalyst to convert aziridine substrate; however, it brings along new challenges due to the possibility of forming

regioisomeric products, either 4-substitued or 5-substituted oxazolidinone, of the target heterocyclic compound.


**Scheme 4.3** A possible regioisomeric product from the reaction of various aziridine with $CO_2$.

The target of this work was therefore the development of an environmentally friendly approach for the synthesis of oxazolidinones under the mildest reaction conditions possible. In addition, the gallium-based catalyst was used in the synthesis of cyclic carbonate functionalised cellulose, which was studied for its antibacterial properties, which could potentially change the concept of antimicrobial surfaces for medical devices.

Many research efforts are devoted towards sustainable and efficient antimicrobial research. Implantable medical devices such as urinary catheters, prosthetic implant and wound dressings are indispensable across the medical field. However, the microbial contamination of these devises is a leading cause of hospital acquired infection. Coatings that leach antimicrobials into the surrounding environment have been criticised due to potential cytotoxicity effects and due to concerns over the selection of resistant bacterial population at sub-lethal antimicrobial concentration, such as may be generated with an eluting coating. However, Vismara and co-workers have managed to synthesise an epoxide functionalised surface of cotton cellulose which was identified as an effective adsorbent.[197] Their study focuses on the preparation of a cheap and effective adsorbent to remove aromatic pollutants from wastewaters. Inspired by their work, an attempt to use the said functionalised compound towards $CO_2$

utilisation was one of the objectives of this study and, to the best of our knowledge, had not been investigated previously.

There are many key challenges and opportunities to deepen our understanding of structure-activity relationships as well as the mechanisms of action as the field of antimicrobial polymers continues to expand. Molecules with new structural features are being introduced to afford both high antibacterial activity and selectivity, a key challenge in this field. Furthermore, the use of cyclic carbonate functionalised cellulose as antibactericidal is one of the target of this study as there are no other reports on this application to the best of our knowledge.

## 4.2 Results and Discussion

### 4.2.1 Synthesis of Gallium-aminotrisphenolate complex (GaL$^{Me}$)

The gallium-aminotrisphenolate catalyst was not thoroughly explored until the work of Whiteoak and co-workers in 2021 when they discovered the more efficient catalytic potential of the **GaL$^{Me}$** complex compared to the analogous well-known aluminium-based complex reported by Kleij.[1,196]

As described in Chapter 2 of this thesis, the synthesis of boron aminotrisphenolate complex[59] was unsuccessful and resulted in a synthesis of incomplete coordination of the ligand towards the centre atom, leaving an unreacted phenol from the ligand. Since the preparation was somehow similar to the gallium complex synthesis, complete coordination of the aminotrisphenolate ligand to gallium was successful with a high isolate yield. The complete coordination of the ligand is likely due to the size of the gallium atom, which can accommodate more ligands than the boron atom. The product of gallium complex resulted in a fine powder, which was purified through successive washing with

hexane. The NMR spectra and HRMS data were consistent with that reported by Whiteoak.[196]

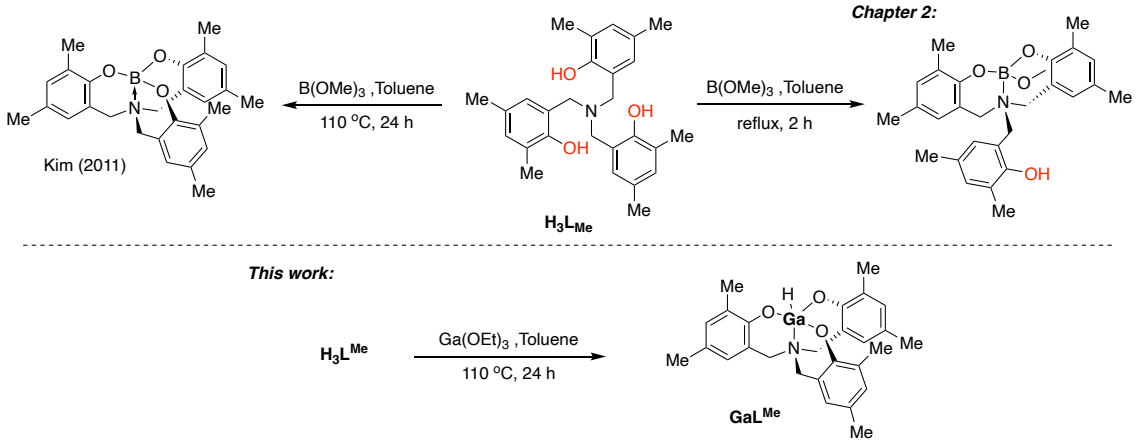


**Scheme 4.4** General procedure on gallium-aminotrisphenolate complex synthesis, **GaL$^{Me}$**.[59,196]

### 4.2.2 Synthesis of aziridines

Commercially available aziridine substrates were favoured in this study, however, the limited range and expensive cost of aziridines encouraged us to investigate the synthesis of a family of aziridines. After several attempts to synthesise the substrate, a two-step reaction was identified as follows: (1) formation of amino alcohol and (2) ring-closure to form aziridine, as shown in Scheme 4.5. This general process provides the potential to access a wide range of aziridines from readily available starting materials.

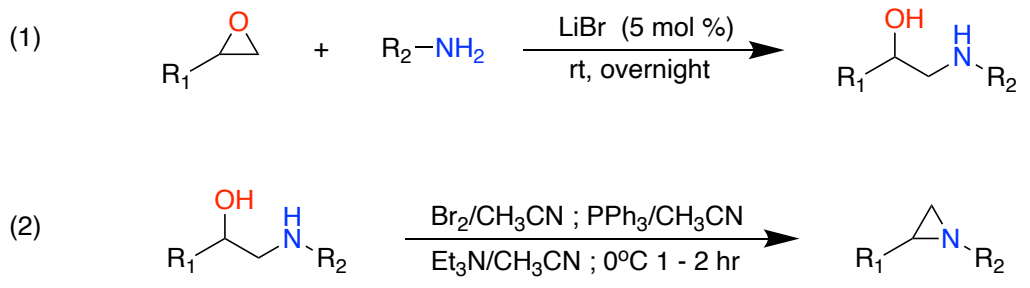


**Scheme 4.5** General reaction for the synthesis of aziridine substrates in this study.

Chakraborti and co-workers reported the use of LiBr as a catalyst to activate the epoxide ring for nucleophilic cleavage, forming amino alcohol at room temperature under solvent-free conditions in only 1-5 hours.[198] With some modifications to the procedure, the reaction was found to be only completed when the mixture was left overnight instead of 1-5 hours reaction time in our hands. In many cases the reaction mixture turns into a solid, whilst in others the reaction mixture turns into viscous oil, both of which indicate the reaction is complete. The efficiency of the LiBr was due to a strong oxophilicity of lithium that activates oxygen-containing electrophiles for nucleophilic attack.

Subsequently, the amino alcohol was then reacted with bromine and triphenylphosphine as hydroxyl activating agents, which converted the -*OH* into an enhanced leaving group and formed halogenamines (Scheme 4.5 (2)). The addition of triethylamine was used as base to promote ring closure forming the aziridine product, where both triethylamine hydrobromide and triphenylphosphine oxide were successively removed through standard filtration procedures. The crude product was then purified using column chromatography, and the structures were confirmed through NMR spectroscopy, FT-IR and HRMS. The crude form of 1,2-diphenylaziridine (**25a**) was unable to be isolated as it appears to decompose when exposed to silica. Even when neutralising the silica, the separation was not successful. Compounds **23a-26a** were not isolated but were directly used without further purification in the reaction to give the corresponding 1,2-diphenyl oxazolidinones and to form other products in this study. Selected purification of the product by column chromatography was due to the decomposition reaction of the aziridine. The synthesis of aziridine described here provides a cost-effective process. The importance of performing the second reaction under an inert atmosphere and with dry solvents should be noted.

Indeed, when an air atmosphere was used, very low yields were obtained compared to the same reactions under nitrogen.

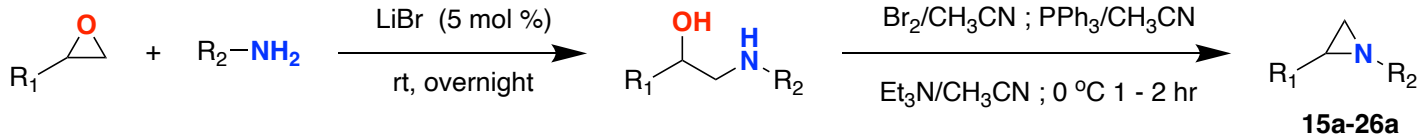


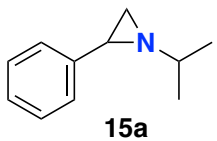

**15a**

[95 %] **90 %**

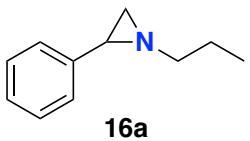

**16a**

[95 %] **91 %**

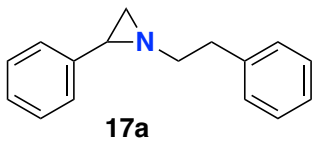

**17a**

[94 %] **89 %**

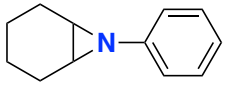

**18a***

[89 %] **78 %**

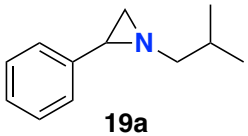

**19a**

[93 %] **90 %**

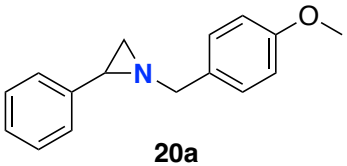

**20a**

[94 %] **88 %**

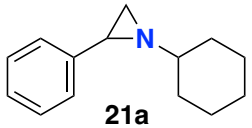

**21a**

[90 %] **87 %**

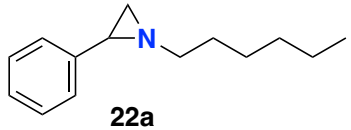

**22a**

[90 %] **92 %**

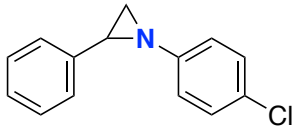

**23a***

[90 %] **88 %**

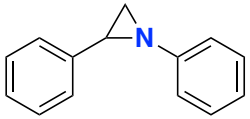

**24a***

[88 %] **85 %**

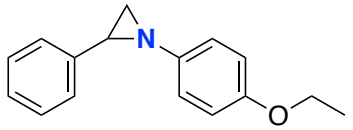

**25a***

[90 %] **82 %**

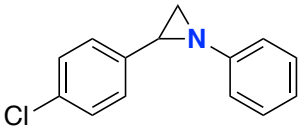

**26a***

[89 %] **85 %**

**Scheme 4.6** General reaction for the synthesis of aziridines in preparation of substrate scoping process.

**General conditions:** epoxide (30 mmol), amines (30 mmol), LiBr (5 mol %), $PPh_3$ (20 mmol), $Br_2$ (20 mmol), $Et_3N$ (60 mmol). Yields were isolated via column chromatography and were immediately used for $CO_2$ reactions. **Note:** Yields shown in [ ] for the aminoalcohol products (Step 1). *crude product directly used for oxazolidinone synthesis.

### 4.2.3 Catalytic screening

Following the study of the cycloaddition using epoxides and $CO_2$ in Chapters 2 and 3, this work focuses on the use of aziridines and $CO_2$ to give a broader application of the **GaL$^{Me}$** catalyst. The synthesis of oxazolidinone compounds in the presence of a co-catalyst tetrabutylammonium iodide ($Bu_4NI$) with some modifications towards the temperature and reaction time was therefore attempted. Initial reactions were performed using the 1-isopropyl-2-phenylaziridine (**15a**) substrate due to its abundance. Methyl ethyl ketone (MEK) was used as a solvent in the cycloaddition reaction to form a homogeneous mixture. The role of the solvent was essential to increase the solvation of the mixture and to improve yield since aziridine substrates used in the reaction were either solids or highly viscous oils. Regioselectivity was also considered with the presence of unsymmetrical aziridine substrates (Scheme 4.7).

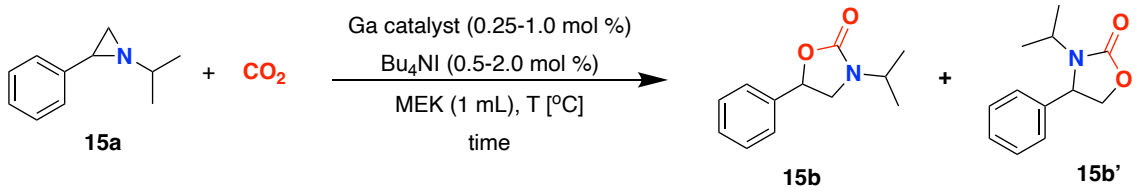


15a 15b 15b'

**Scheme 4.7** Optimisation reaction using **GaL$^{Me}$** catalyst for the synthesis of 3-isopropyl-5-phenyloxazolidin-2-one.

The cycloaddition reaction was conducted using freshly prepared dry ice as $CO_2$ source. Once all the compounds (catalyst, co-catalyst, aziridine and 1 mL of MEK solvent) were added to the 50-mL reactor, the dry ice was prepared, weighed, and introduced immediately to the vessel, and then the reactor was closed. The weight of the dry ice used was 2.68 g which achieved a pressure of approximately 15 bar, identical to previous chapters of this thesis.

In the initial experiments high temperature (70-90 °C) was applied, and this clearly led to the formation of two regioisomeric products, **15b** and **15b'** as shown in the $^1$H NMR spectrum (Figure 4.3). As observed in Table 4.1 Entries 1-4, regioisomer formation only occurs at a higher temperature, 70-90 °C, with the major product 3-isopropyl-5-phenyloxazolidin-2-one (**15b**). It was also identified that the regioselectivity towards product **15b** favours the reaction with an excellent yield at a lower temperature of 60 °C (Table 4.1, Entries 5-13). This indicates that the reaction could be controlled with temperature and gives an excellent selectivity towards the production of **15b**. The same scenario was previously observed with aluminium salen catalysts, wherein employing high temperature resulted in two oxazolidinone products.[199]

**Table 4.1** Optimisation of **GaL$^{Me}$** catalyst with 1-isopropyl-2-phenylaziridine substrate.

| Entry | **GaL$^{Me}$** (mol %) | $Bu_4NI$ (mol %) | Time (h) | Temp (°C) | Regioselectivity [**15b/15b'**][a] | Conv (%)[a] |
|---|---|---|---|---|---|---|
| 1 | 1 | 2 | 48 | 90 | 80:20 | 80 |
| 2 | 1 | 2 | 24 | 90 | 91:9 | 91 |
| 3 | 1 | 2 | 24 | 80 | 92:8 | 92 |
| 4 | 1 | 2 | 24 | 70 | 98:2 | 98 |
| 5 | 1 | 2 | 16 | 60 | >99 % | 96 |
| 6 | 1 | 2 | 24 | 60 | >99 % | >99 |
| **7** | **0.5** | **2** | **24** | **60** | >99 % | **>99** |
| 8 | 0.5 | - | 24 | 60 | >99 % | 20 |
| 9 | - | 2 | 24 | 60 | >99 % | 27 |
| 10 | 0.5 | 1 | 24 | 60 | >99 % | 93 |
| 11 | 0.25 | 1 | 24 | 60 | >99 % | 89 |
| 12 | 0.25 | 1 | 16 | 60 | >99 % | 81 |
| 13 | 0.25 | 2 | 24 | 60 | >99 % | 91 |

**Conditions**: 1-isopropyl-2-phenylaziridine (**15a**) (1.0 g, 6.2 mmol), **GaL$^{Me}$** catalyst, $Bu_4NI$ co-catalyst, $CO_2$ (2.63 g, 59.8 mmol, 6.0 equiv., approx. 15 bar). [a]Conversion of **15a** determined by inspection of the $^1$H NMR spectrum of the crude reaction mixture.

As the temperature was maintained at 60 °C, catalyst loading of 1 mol % and co-catalyst loading of 2 mol % gave an excellent yield of >99 % after 24 h, whereas a reaction time of 16 h also led to a decrease in the yield to 96 % (Table 4.1, Entries 5 and 6). The catalyst loading was lowered to 0.5 mol % while maintaining the co-catalyst loading at 2.0 mol %, which provided an excellent yield of >99 % yield (Table 4.1, Entry 7). The catalyst was very efficient at 0.5 mol %; hence, a decision to lower the co-catalyst loading to half was made (1 mol %), which gave a 93 % yield of the product without any sign of regioisomer **15b'** (Table 4.1, Entry 10). A further decrease of the catalyst loading to one-half, 0.25 mol %, whilst maintaining the co-catalyst at 1.0 mol %, provides a good yield of 89 % and lowering the reaction time to 16 h gave 81 % yield (Table 4.1, Entries 11 and 12, respectively). Maintaining the catalyst loading to 0.25 mol % and increasing the co-catalyst loading to 2 mol % provides a higher yield of 91 % after 24 h (Table 4.1, Entry 13).

The presence of catalyst and co-catalyst were essential in the reaction, as confirmed in Table 4.1, Entries 7-9. When neither **GaL$^{Me}$** nor $Bu_4NI$ was applied in the reaction, it only gave a 20-27 % yield (Table 4.1, Entries 8 and 9), compared to when both catalyst and co-catalyst were present in the reaction, the yields were excellent without the presence of other product. This confirms the binary catalytic system wherein a catalyst and co-catalyst are required to efficiently promote the reaction and provide an excellent conversion of the substrates rather than the catalyst alone.

### 4.2.4 Mechanistic investigation into the regioselectivity

The regioselectivity was determined by $^1H$ NMR spectroscopy of the crude mixture based on the integral values of the proton adjacent to the aromatic ring

of the oxazolidinone compound (Figure 4.3), and compound **15b** can be obtained after separating through column chromatography. The compound was initially detected using 1.0 mol % of **GaL$^{Me}$** and 2.0 mol % of $Bu_4NI$ at 90 °C for 24 h with 80:20 selectivity (Table 4.1, Entry 1) as shown in Figure 4.3 of the crude product. The regioisomer **15b'** has a triplet signal at 5.67 ppm, and the major product **15b** appears at 5.45 ppm with respect to mesitylene as the internal standard

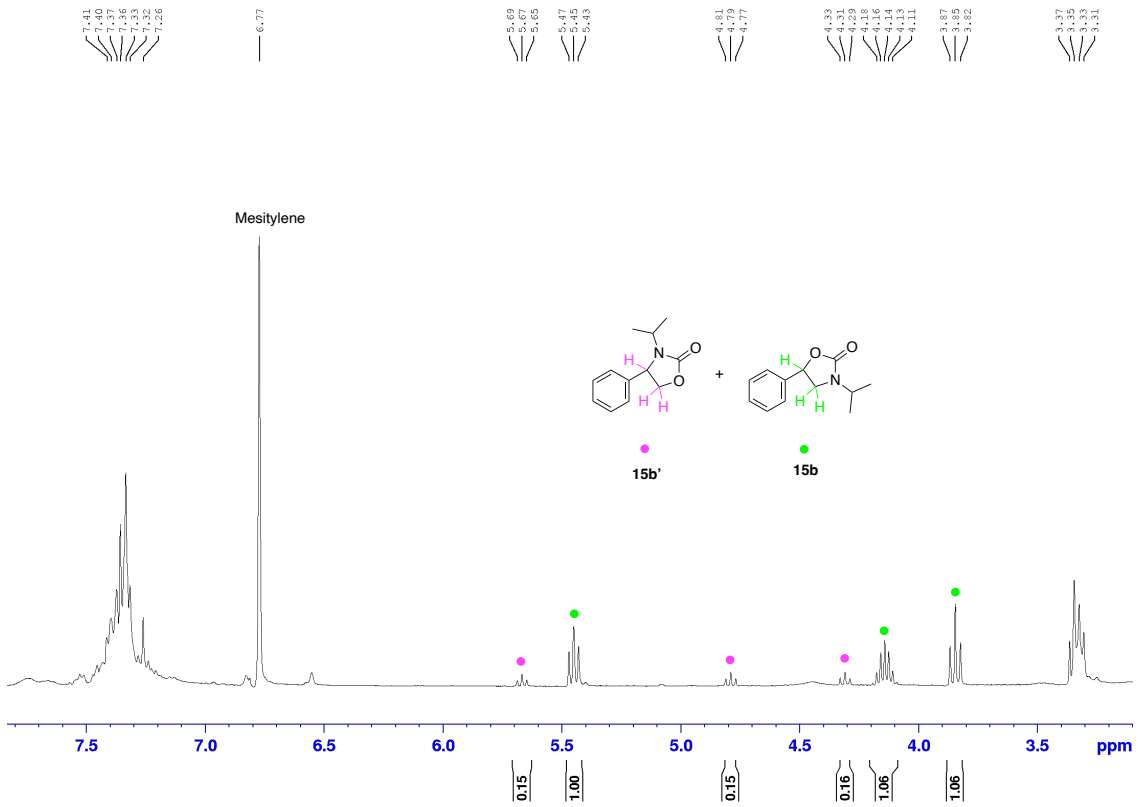


**Figure 4.3** Example of $^1$H NMR spectrum ($CDCl_3$ at 298 K) of a crude reaction mixture for the optimisation reaction data from Table 4.1 Entry 1 with mesitylene as internal standard yielding a regioisomeric product **15b** and **15b'**.

Investigations into the substituent group found that the coupling reaction of isopropyl-substituted aziridines with $CO_2$ afforded the 5-substituted products **15b** exclusively at milder temperature (60 °C) (Table 4.1, Entries 6-7). As the temperature was maintained to 60 °C (Table 4.1, Entries 5-13), the regioselectivity of the reaction was also maintained at >99 %, with no other regioisomer detected even with different catalyst and co-catalyst loading applied

(0.25-1.0 mol % and 1.0-2.0 mol %, respectively) as shown with one of the examples using the $^1$H NMR spectrum of the crude product presented in Figure 4.4.

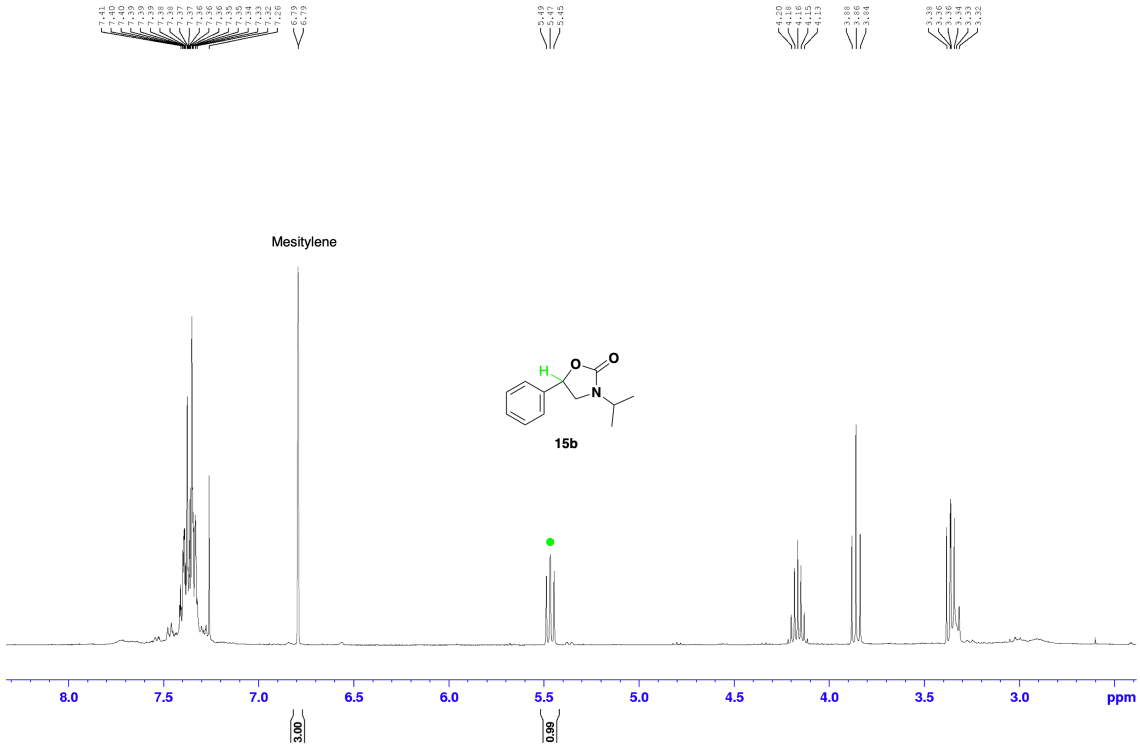


**Figure 4.4** Example of $^1$H NMR spectrum ($CDCl_3$ at 298 K) of a crude reaction mixture for the optimisation reaction data from Table 4.1 Entry 7 with mesitylene as internal standard without the presence of regioisomeric product confirming the >99 % selectivity of forming **15b** product.

These results demonstrate that **GaL$^{Me}$** complex shows high regioselectivity for the ring-opening of *N*-substituted aziridines occurring at the methine *C*−*N* bond, which is distinctly different from the corresponding coupling reaction of $CO_2$ and epoxides.[196]

Furthermore, the coupling reactions of $CO_2$ with 1-isopropyl-2-phenylaziridine (**15a**) afforded 5-substituted oxazolidinones. A possible formation pathway involving nucleophilic attack towards the most hindered carbon atom of the substrate as suggested in Scheme 4.7. The nucleophilic ring-opening of *N*-substituted aziridine at the methine *C*−*N* bond **(I)**. This is followed by backbiting,

forming the carbamate species at the methine carbon after the insertion of $CO_2$ **(ii)**. Then a selective formation of the methine carbon of the 5-substituted oxazolidinone is favoured **(iii)** in the reaction rather than a nucleophilic attack towards less hindered carbon **(II)**. North and co-workers recently reported the synthesis of oxazolidinones from epoxides and aromatic or aliphatic isocyanates mediated by a bimetallic aluminium−salen complex.[195]

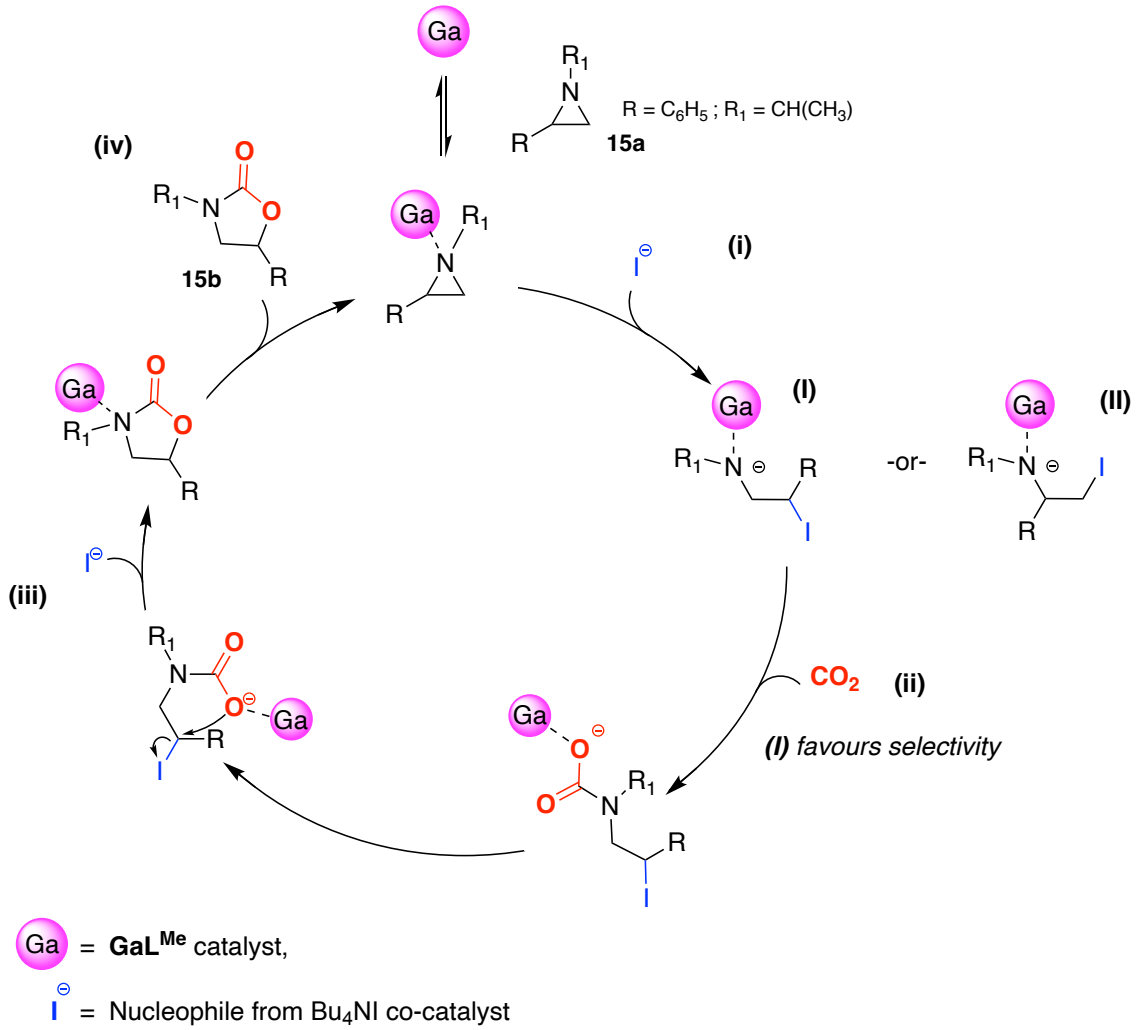


**Scheme 4.8** The proposed general reaction mechanism for the formation of compound **15b** with complete selectivity using unsymmetrical aziridine and $CO_2$ catalysed by **GaL$^{Me}$** and $Bu_4NI$ wherein the ring-opening step occurs at the most hindered carbon atom **(i)**.

### 4.2.5 X-ray Crystal Structure Analysis

Crystals suitable for single-crystal X-ray diffraction study was grown by slow diffusion of pentane into a concentrated chloroform solution of the compound.

The obtained molecular structure of **27b** is shown in Figure 4.5 and is in agreement with the solution structures obtained from the $^1$H NMR data. The crystal structures confirmed the stereoselectivity of the reaction wherein the stereochemistry of the substrate was retained and produces the same stereochemistry of the product. These were supported through the $^1$H NMR data where no presence of regioisomer present in the spectra, and the yield was excellent. With the solid-state molecular structure, the successful cycloaddition of $CO_2$ to aziridine forming 5-substituted oxazolidinone product could be seen.

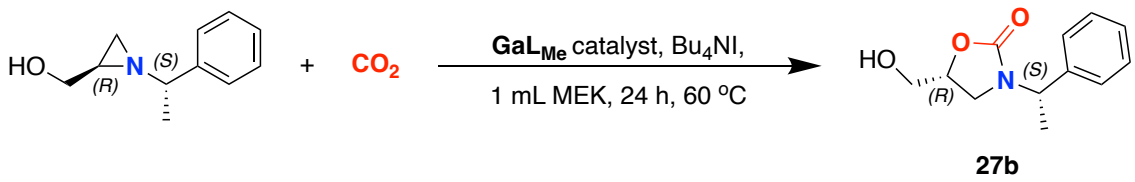


**27b**

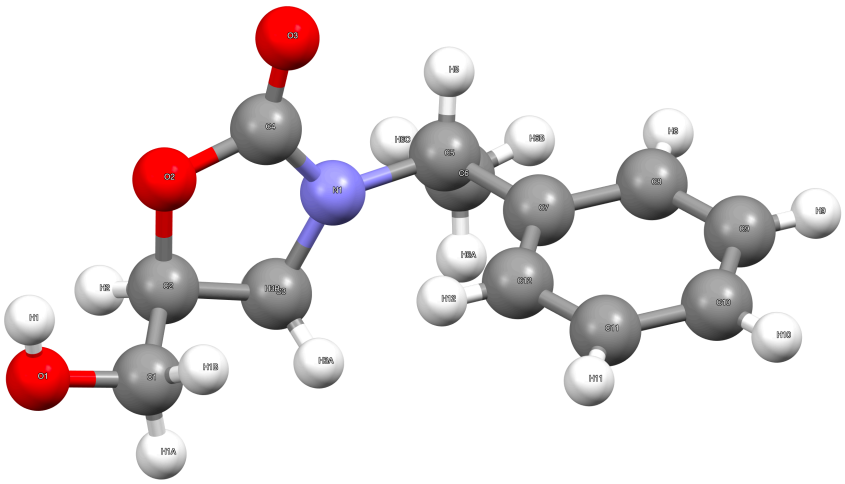

**Figure 4.5** General reaction for synthesising compound **28b** and its solid-state molecular structure of **28b**.

**Table 4.2** X-ray crystallographic parameters for complexes **28b**.

| Compound | **28b** |
|---|---|
| Formula | $C_{12}H_{15}NO_3$ |
| Crystal system | Monoclinic |
| Space group | P-$2_1$ |
| Volume (Å$^3$) | 560.92(6) |
| *a* (Å$^3$) | 8.3156(5) |
| *b* (Å$^3$) | 6.4855(4) |
| *c* (Å$^3$) | 10.8741(6) |
| *a* (°) | 90 |
| *b* (°) | 106.968(3) |
| *g* (°) | 90 |
| *Z* | 2 |
| *Z'* | 1 |
| Formula weight (g mol$^{-1}$) | 221.25 |
| Density (g cm$^{-3}$) | 1.310 |
| Absorption coefficient (mm$^{-1}$) | 0.094 |
| Radiation type | Mo $K_a$ |
| $\theta_{max}$ (°) | 58.956 |
| Temperature (K) | 200 |
| Total no. reflections | 3850 |
| Unique reflections [*R*(int)] | 2341 [0.0399] |
| Final *R* indices [$I > 2(I)$] | $wR_2$ = 0.1162 |
| | $R_1$ = 0.0439 |
| GooF | **0.877** |

### 4.2.6 Substrate scoping

To evaluate the scope and broader application of the developed protocol, various aziridines previously prepared in this chapter were reacted with $CO_2$ to form the oxazolidinone product using **GaL$^{Me}$** catalyst and $Bu_4NI$ co-catalyst. The optimised reaction conditions were selected from Table 4.1 Entry 7 for the cycloaddition of $CO_2$ and aziridine for both terminal and internal substrates. Quantitative formation of the corresponding oxazolidinone demonstrated the efficiency of **GaL$^{Me}$** catalyst as shown in Scheme 4.9.

As stated earlier, the formation of oxazolidinone with an unsymmetrical aziridine substrate may result in two regioisomeric products, which could be controlled by the reaction temperature. This observation was consistent when the mild temperature (60 °C) was applied in the reaction with various aziridines.

Excellent results were obtained when aziridines bearing an alkyl substituent like **15a, 16a, 19a** and **22a** were converted into the desired products **15b**, **16b**, **19b**, and **22b**, respectively, with a >99 % regioselectivity of all compounds. The reaction worked well with aziridine containing aliphatic substituents such as **17a**, **20a**, **21a**, and **28a**, affording excellent yields of 96-99 % with no presence of the regioisomeric product.

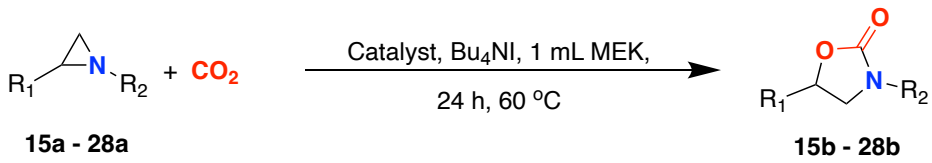


**15a - 28a** **15b - 28b**

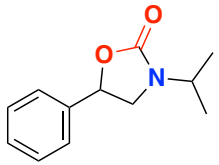

**15b**

>99 %

[>99]

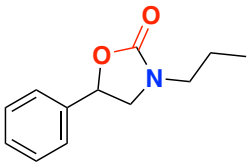

**16b**

>99 %

[>99]

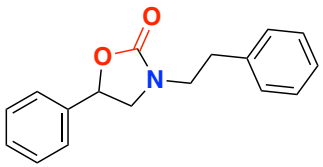

**17b**

98 %

[>99]

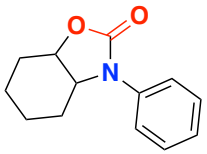

**18b**

[a]65 %

[90:10]

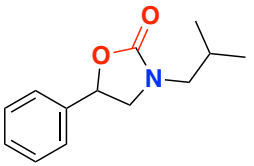

**19b**

>99 %

[>99]

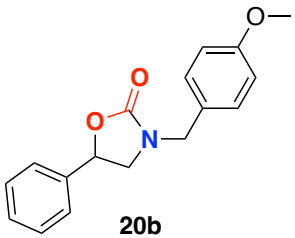

**20b**

96 %

[96:4]

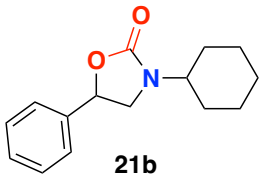

**21b**

99 %

[>99]

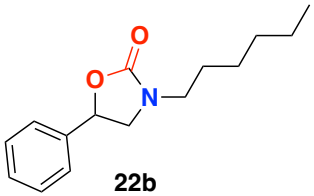

**22b**

98 %

[98:2]

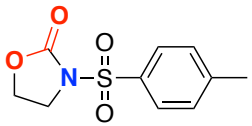

**27b**

>99 %

[>99]

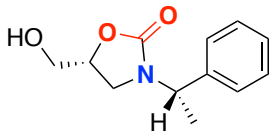

**28b**

96 %

[>99]

**Scheme 4.9** . Cycloaddition of $CO_2$ with various aziridines using **GaL$^{Me}$** catalyst and $Bu_4NI$ co-catalyst.

**General conditions**: Aziridines (**15a-28a**) (1.0 g), 0.5 mol % catalyst, 2.0 mol % $Bu_4NI$, 24 h, 60 °C, $CO_2$ (2.63 g, 59.8 mmol, 6.0 equiv., approx. 15 bar). Conversion of **15b-28b** determined by inspection of the $^1H$ NMR spectrum of the crude reaction mixture. [a]reaction time: 72 h. Regioselectivity ratio shown in [ ] of compound **b/b'**.

Unlike with the other aziridines, **23a**–**26a** required a longer reaction time (72 h) to achieve only 48-61 % yields at 60 °C with the obvious significant presence of another product. In these reactions, all the diphenyl aziridines were reacted, with other product being identified as a 1,4-piperazine (**29**–**32**) which forms from "dimerization" process of aziridine substrates. This unexpected product was previously reported by Suzuki and co-workers in 1984.[200]

**Table 4.3** Conversion of aziridines with diphenyl substituents to oxazolidinones.

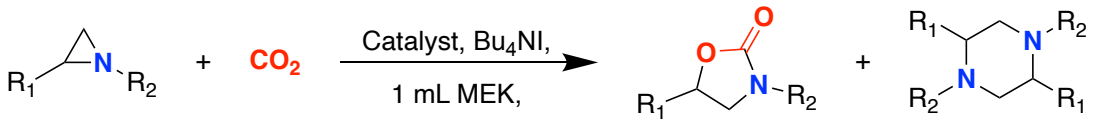


**23a - 25a** **23b - 25b** **29 - 32**

| Entry | -$R_2$ | Temp (°C) | Regioselectivity (b/b')[a] | Oxazolidinone[a] (%) | Piperazine[a] (%) |
|---|---|---|---|---|---|
| 1 | **23a** | 60 | 90:10 | 59 | 31 |
| 2 | **23a** | 100 | 95:5 | 70 | 12 |
| 3[b] | **24a** | 45 | - | - | 74 |
| 4 | **24a** | 60 | 89:11 | 61 | 29 |
| 5 | **24a** | 100 | 96:4 | 75 | 16 |
| 6 | **25a** | 60 | 90:10 | 48 | 31 |
| 7 | **25a** | 100 | 95:5 | 67 | 13 |

**Conditions**: Aziridines (**23a-25a**) (1.0 g, 6.2 mmol), 0.5 mol % **GaL$^{Me}$** catalyst, 2.0 mol % $Bu_4NI$ co-catalyst, $CO_2$ (2.63 g, 59.8 mmol, 6.0 equiv., approx. 15 bar), 72 h. [a]Conversion of aziridines determined by inspection of the $^1H$ NMR spectrum of the crude reaction mixture using mesitylene as internal standard. [b]reaction time: 48 h.

The temperature changes as shown in table 4.3 affects the formation of oxazolidinone with aromatic substituted substrates. The decision to increase the reaction time was due to the absence of the expected product after 24 h. The reaction time was then increased to 72 h at the same temperature of 60 °C and the oxazolidinones was formed at low yield (Table 4.3, Entries 1, 4 and 6). When the temperature was increased to 100 °C, a notable increase of oxazolidinone

yields was obtained ranging from 67-75 % (Table 4.3, Entries 2, 5 and 7). Lowering the temperature to 45 °C after 48 h for substrate **24a** produced an unexpected product, a piperazine, without any presence of oxazolidinone product in a 74 % yield (Table 4.3, Entry 3). The existence of piperazine product was further explored through repeating the same reaction from Scheme 4.9 without the presence of $CO_2$ at 60 °C with reaction time of 24 h. The formation of piperazine was successful and can also be detected selectively (compounds **29**-**32**). This unexpected production of piperazine was achieved with only catalyst, co-catalyst and MEK solvent in the reaction.

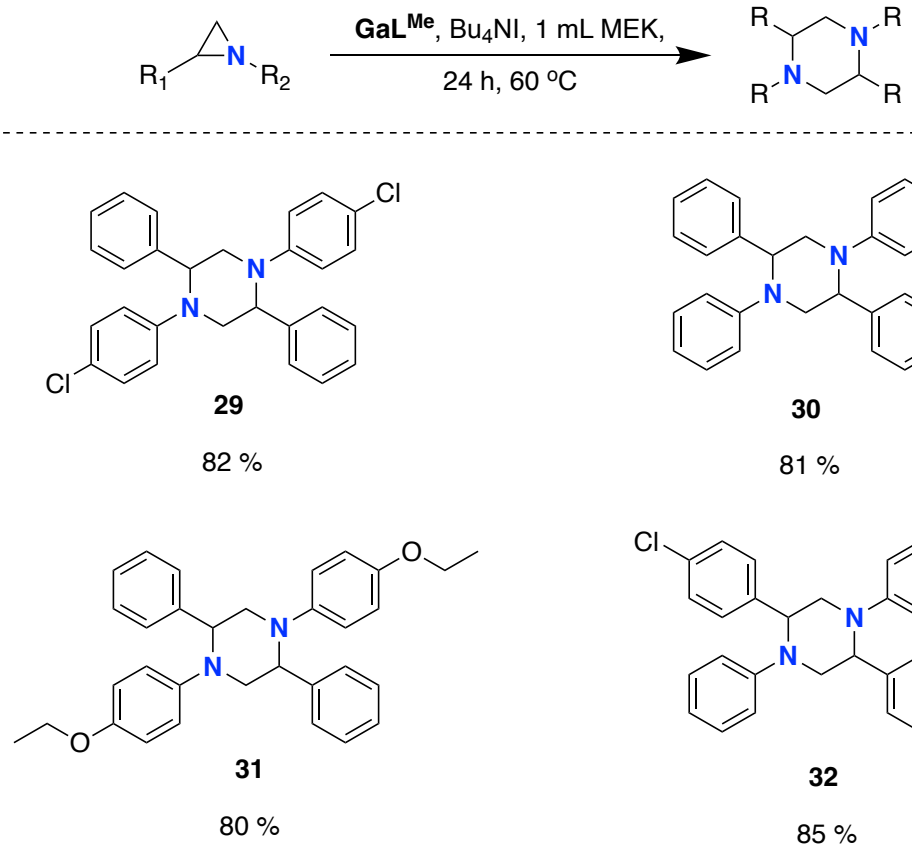


**Scheme 4.10** Various piperazine products obtained from the reaction of aziridine containing diphenyl substituents without $CO_2$ at 60 °C.

A proposed reaction mechanism is reported to understand the formation of piperazine in the reaction using gallium catalyst, as displayed in Scheme 4.10. The reaction mechanism involves the nucleophilic attack toward the most

hindered carbon atom of aziridine. The catalyst is coordinated to the nitrogen atom of the aziridine, followed by the nucleophilic attack of the $Bu_4NI$ co-catalyst, which ring opens the substrate (**I** and **II**). Followed by the attack of an amino nitrogen atom towards another aziridine to form **a**.[201,202] Then followed by the attack of an identical nitrogen atom towards carbon connected to the iodide to give a six-membered ring, piperazine (**V**). Thus, it favours the piperazine synthesis instead of oxazolidinone even with the presence of $CO_2$ at high pressure.

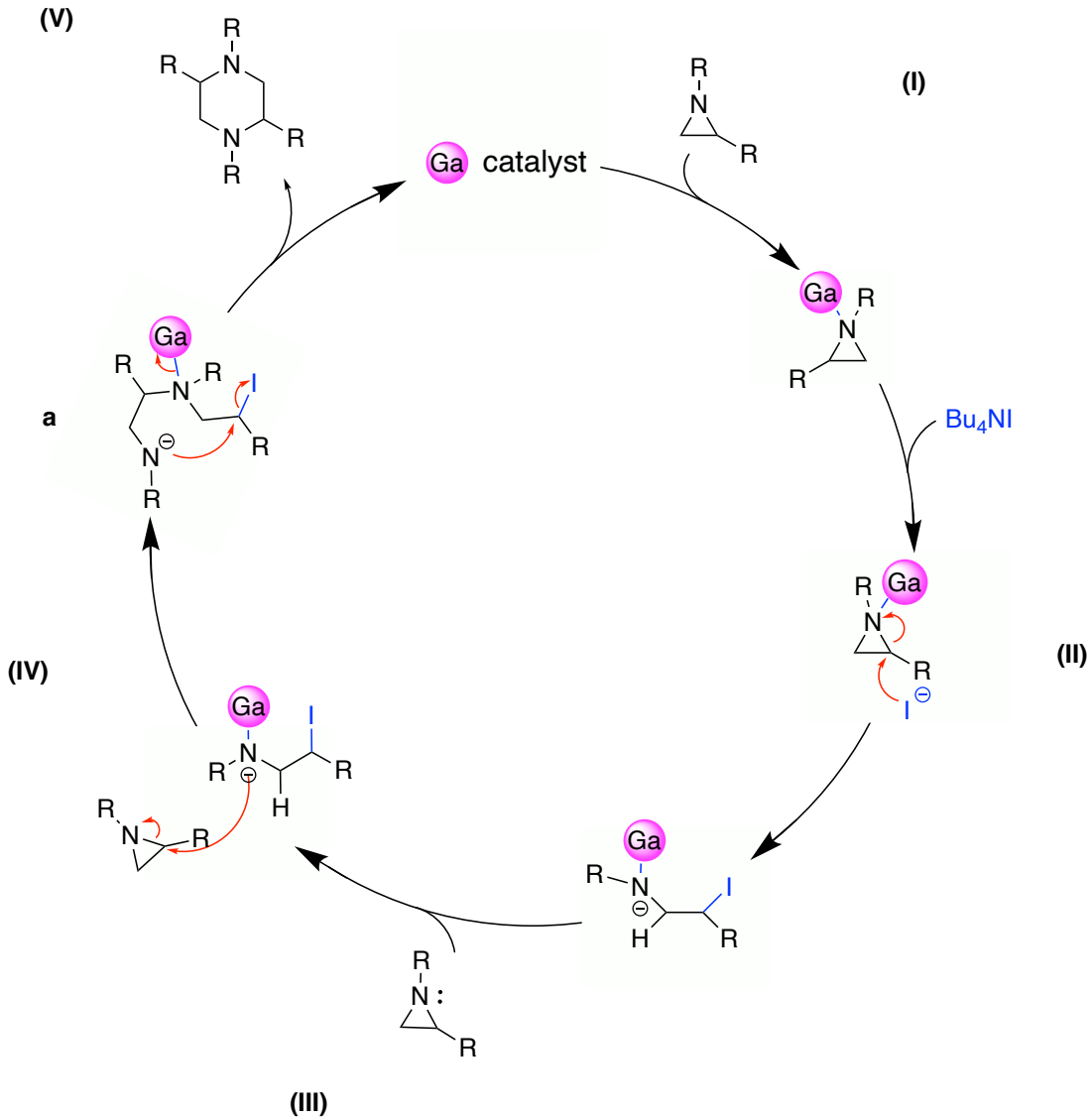


**Scheme 4.11** The proposed mechanism for the formation of the piperazine product.

### 4.2.7 Modification of cellulose fibres and Antibacterial activity test

#### 4.2.7.1 Overview of functionalised cellulose

As an abundant and renewable resource, cellulose possesses many applications in industry and pharmaceutical science; hence, extensive studies have been carried out to transform its structure. Functionalising cellulose allows for its chemical properties to be modified to produce novel characteristics. This inspired us to synthesise cellulose fibres modified with cyclic carbonate functionalities and study their potential for antimicrobial application.

Hirotsu and co-workers reported a method of plasma graft polymerisation of glycidyl methacrylate (GMA) using ultrasonic irradiation and immobilised cyclodextrin substrate.[203,204] GMA has been produced since the early 1990s as a dual functionality monomer for coatings and resins. Whilst cellulose is a renewable, abundant, and cheap natural polymer that can be manufactured in various forms like yarns, woven and non-woven fabrics, and sheets, this provides a broader range of choice for several processes conditions. Potential applications of cellulose-modified materials, such as GMA, include substrates to remove metals from water and as flame retardant cotton fabric.[205,206]This allows an opportunity to functionalise cellulose not only as an adsorbent but also valuable in other purposes identified depending on the characteristics of the synthesised sample.

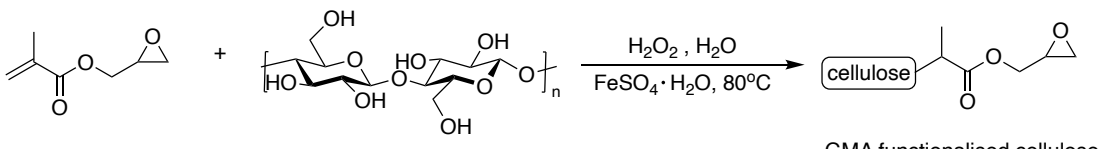


Glycidyl methacrylate

-raw material for polymer coatings, adhesives and plastics.
-monomer for production of epoxy resin

Cellulose

-cheap natural polymer
-as fiber supplement
-raw material for production of paper

GMA functionalised cellulose

**Scheme 4.12** General reaction for the grafting of GMA onto cellulose fibre.

Grafting of GMA onto cotton, flax and viscose was previously performed by the Vismara group using three different cellulose activation strategies; electron-beam (EB) irradiation, plasma activation, and Fenton-type reactions. [207,208] In this study, a Fenton-type reaction was used to functionalised cellulose with glycidyl methacrylate (GMA). The reaction starts with the activation phase which generates a hydroxyl radical on the cellulose surface. This is achieved by the oxidative nature of $H_2O_2$ coupled with $FeSO_4.7H_2O$ to increase the oxidative strength further. The $H_2O_2$ is broken down to produce an electrophilic *HO•* species, which removes a hydrogen atom from a hydroxyl group on the surface of cellulose, producing hydroxyl radical. Then, addition of an epoxide molecule allows it to be grafted onto the surface of the cellulose which opens further functionalisation of the polymer. The epoxide functionalised cellulose is then converted into cyclic carbonate functionalised cellulose by adding a $CO_2$ substrate using a suitable catalyst (Scheme 4.13).

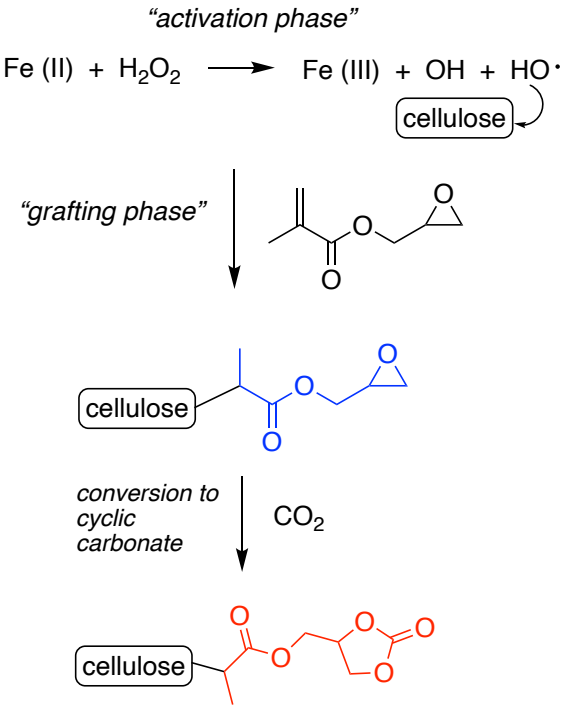


**Scheme 4.13** A simple representation for the grafting of GMA on the cellulose through Fenton type reaction followed by the formation of cyclic carbonate functionalised cellulose through the addition of $CO_2$.

The generation of cyclic carbonate was done using the gallium aminotrisphenolate catalyst, the same catalyst that was used to convert single epoxide and $CO_2$ into cyclic carbonate monomer. The application of the same catalyst demonstrates its effectiveness in converting grafted epoxide without damaging the cellulose. The cyclic carbonate functionalised cellulose was then applied and tested for its antibacterial properties.

Growing concerns over the rising occurrence of antibiotic-resistant bacterial strains has led to an increase in interest in the preparation of antibacterial polymers. The incorporation of the cyclic carbonate on the cellulose repeating units permits easy modification of these polycarbonates, offering potential opportunity for antibacterial activity, as well as other possible applications such as hydrophilic properties, pH-dependent solubility, or gas separation.[209-211] Cellulose is a non-toxic material; hence, with cellulose alone, the compound is not capable of killing bacteria or any microorganisms. In several studies over the past few decades, numerous groups have found the relationships between the structure and activity of antimicrobial polymers. For example, Hauenstein and Greiner successfully showed new antibacterial, mechanical, thermal, self-healing, and new protective coating properties for different poly(limonene carbonate)-derived polymers obtained by thiolene chemistry derivatisation of the double bond of the limonene moiety.[212-214]Palermo and co-workers reported on the antibacterial activity of polymers in relation to their amphiphilic balance wherein cationic and hydrophobic functionalities of synthetic polymers mimics the cationic amphiphilicity of an antimicrobial substance.[209] Collectively, it is known that balancing the hydrophobicity and cationic charge is an essential ingredient for the optimisation of antimicrobial activity combined with low toxicity to human cells.[215]

### 4.2.7.2 Synthesis of epoxide functionalised cellulose

The epoxide functionalised cellulose was obtained using the chemical reaction shown in Scheme 4.14. The cellulose was allowed to swell at 80 °C in the water then $FeSO_4 \cdot 7H_2O$ and $H_2O_2$ was added to generate hydroxyl radical on the cellulose surface. Then GMA was added and was left stirring for successful grafting of the epoxide molecule onto the surface of cellulose.

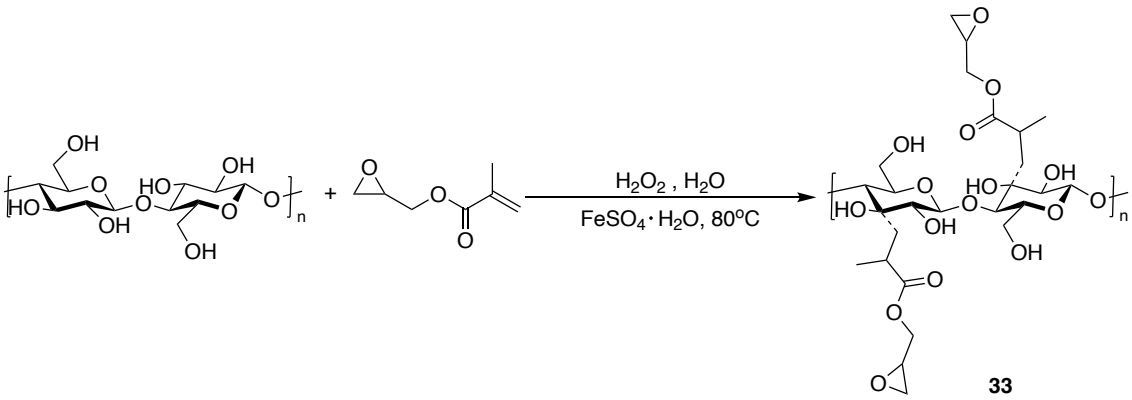


**Scheme 4.14** General reaction for the grafting of glycidyl methacrylate (GMA) to cellulose fibres.

Throughout this reaction, there were several visible colour changes, the first being the addition of $FeSO_4 \cdot 7H_2O$ and $H_2O_2$ to the cellulose and water solution. The addition of these reagents changed the solution from a cloudy-white colour to vivid orange. This colour change was due to the oxidative properties that the Fe(II) ions have on $H_2O_2$. After approximately 20 minutes, the orange colour changed gradually into a bright yellow. The excess reagents were removed through overnight washing (Soxhlet extraction with acetone). The product was found to be very lumpy and almost viscous. After the solvent was removed, the resulting product was a white solid. The resulting product was then analysed using Bruker Alpha FTIR since the solid was insoluble to any common NMR solvents. The result from the IR spectrum (Figure 4.6) showed a strong carbonyl peak (1717 $cm^{-1}$) which suggests that the cellulose had been functionalised by

the glycidyl methacrylate (GMA) successfully to a degree that would be adequate for further modifications.

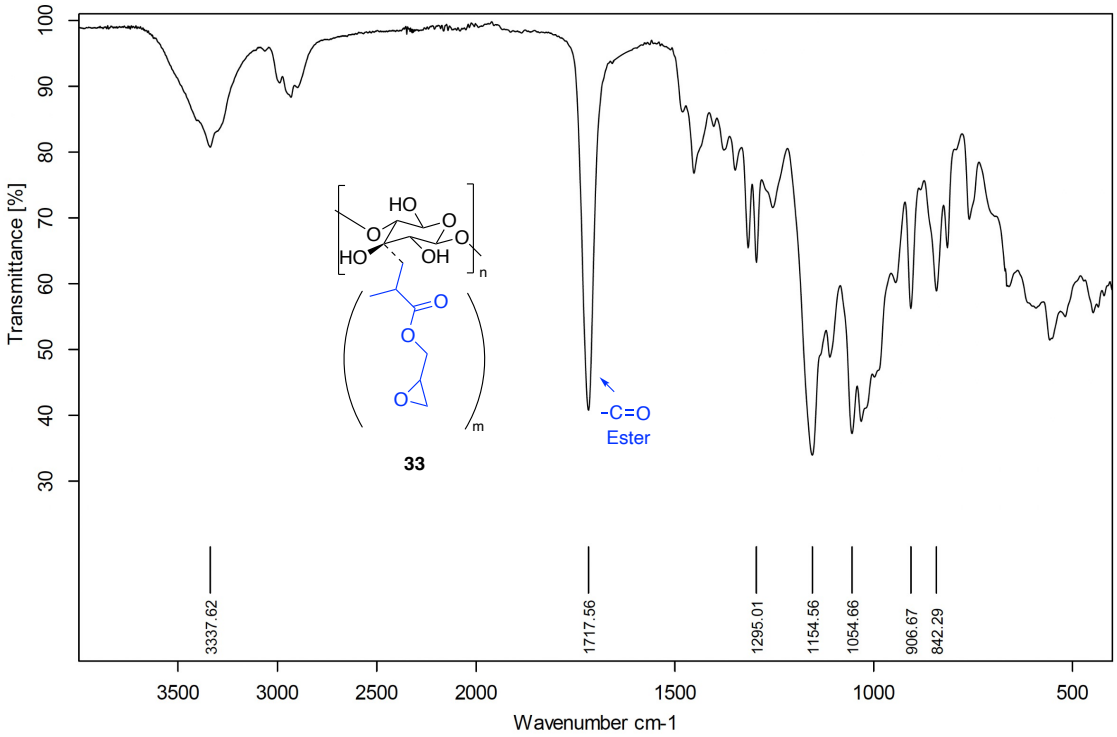


**Figure 4.6** IR spectrum (298 K) of optimised epoxide functionalised cellulose.

#### 4.2.7.3 Preparation of cyclic carbonate functionalised cellulose

Cycloaddition of $CO_2$ towards compound **33** to synthesise cyclic carbonate functionalised cellulose was successful under relatively mild temperature (Scheme 4.15). The reaction mixture contained 0.5 g of epoxide functionalised cellulose, 5.0 mg of **GaL$^{Me}$** catalyst,184 mg of $Bu_4NI$, 5 mL MEK and 3.0 g of $CO_2$ (approximately 12 bar of pressure) at 50 °C and was left stirring overnight.

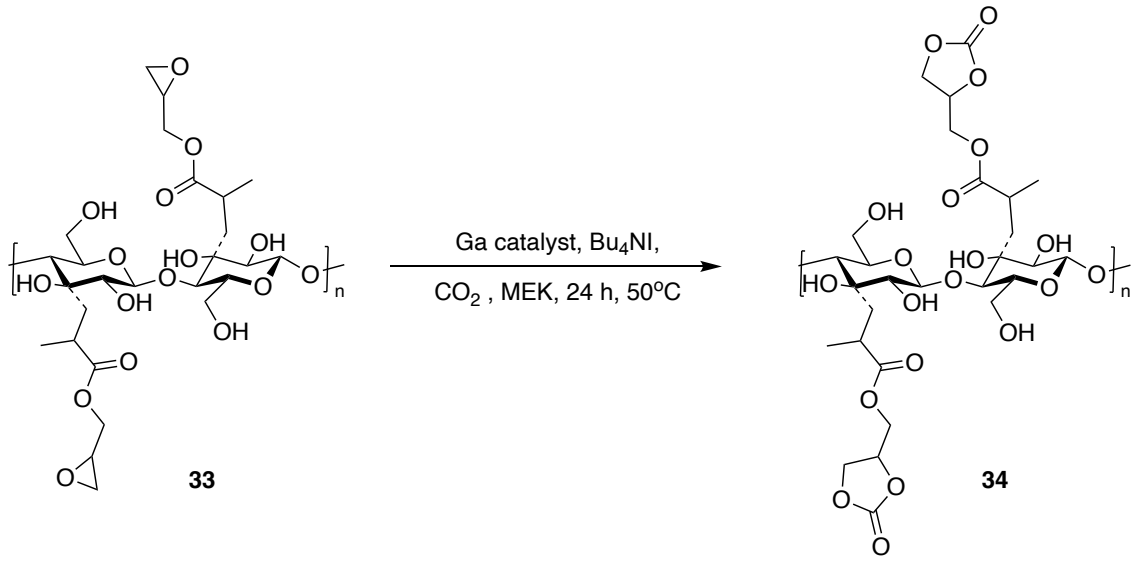


**Scheme 4.15** General reaction for the conversion of **33** into cyclic carbonate functionalised cellulose **34**.

The proposed reaction mechanism is similar to the cyclic carbonate synthesis reported by Whiteoak using **GaL$^{Me}$** catalyst.[196]The typical mechanism for the catalytic reaction of $CO_2$ is shown in Scheme 4.16 involving the initial coordination of the epoxide to the Lewis acid catalyst, then activates the epoxide towards the nucleophilic attack of the iodide nucleophile following the ring-opening of the substrate. The iodide nucleophile from $Bu_4NI$ co-catalyst undergoes nucleophilic attack towards the less hindered carbon of epoxides **(i)**, which aids the ring-opening of the epoxide. This nucleophile assists the ring-opening process of the substrate in forming an alkoxide, then subsequent insertion of $CO_2$ molecule, forming linear carbonate. After the ring-closure process, the negatively charged oxygen eliminates the iodine nucleophile and Ga catalyst.

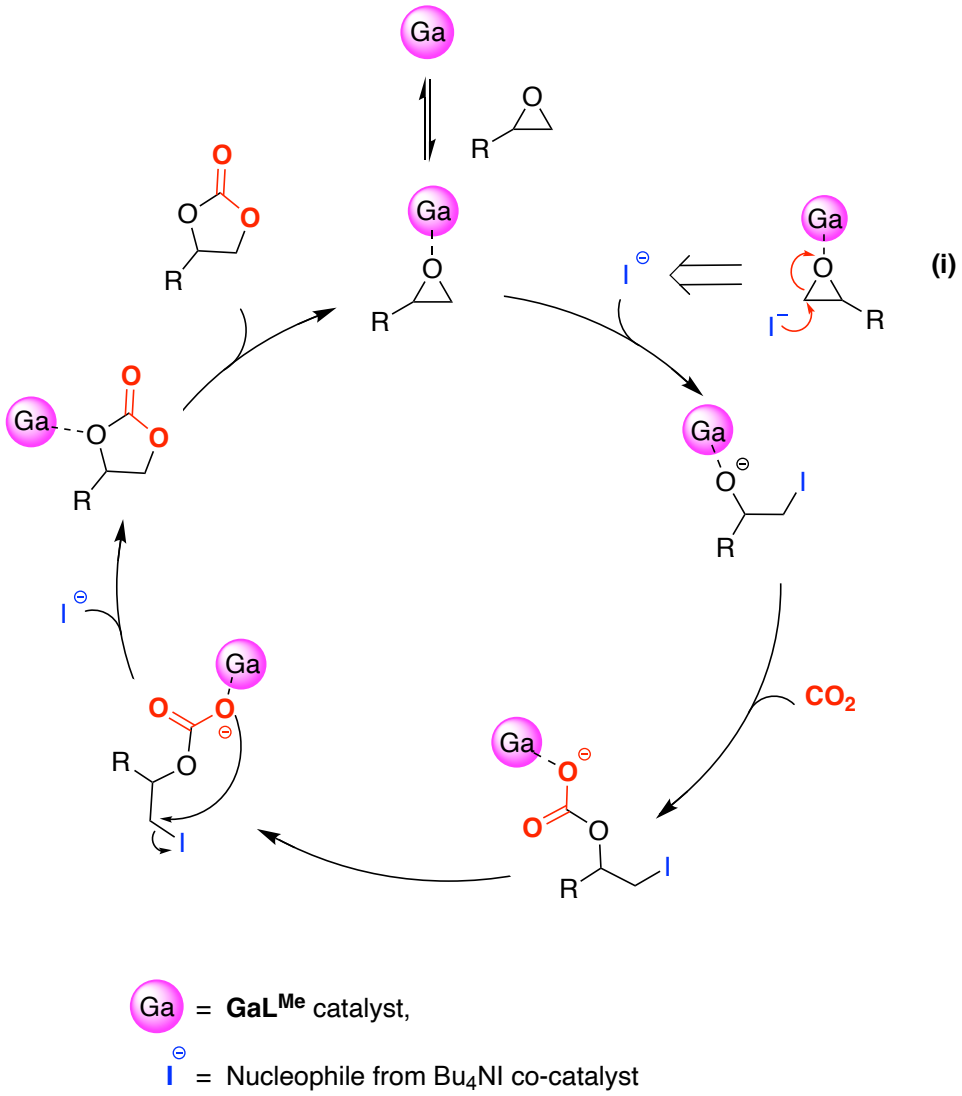


Ga = **GaL$^{Me}$** catalyst,

$I^{\ominus}$ = Nucleophile from $Bu_4NI$ co-catalyst

**Scheme 4.16** The proposed reaction mechanism of cyclic carbonate synthesis using **GaL$^{Me}$** catalyst.

The crude product was thoroughly washed with acetone overnight and then dried under a vacuum. Due to the insoluble nature of the final product, FT-IR analysis was used to characterise the compound. The IR spectrum of compound **34** was compared against the initial poly-GMA **33**, and a second carbonyl stretch from the cyclic carbonate group would be expected. The initial carbonyl peak from poly-GMA **33** located at 1717 $cm^{-1}$ was projected to remain (from the carbonyl of the GMA), whilst another carbonyl peak was expected to appear from the insertion of $CO_2$ and formation of the carbonyl of the carbonate. As shown in Figure 4.7, two carbonyl peaks could be seen from the spectrum where the peak

at 1720 $cm^{-1}$ and 1790 $cm^{-1}$ indicates the presence of two carbonyl stretch and a successful conversion into a cyclic carbonate compound. The two peaks are relatively equivalent in intensity indicating that the reaction had reached >99 % conversion of poly-GMA **33** substrates into cyclic carbonate **34** from the cycloaddition reaction of $CO_2$.

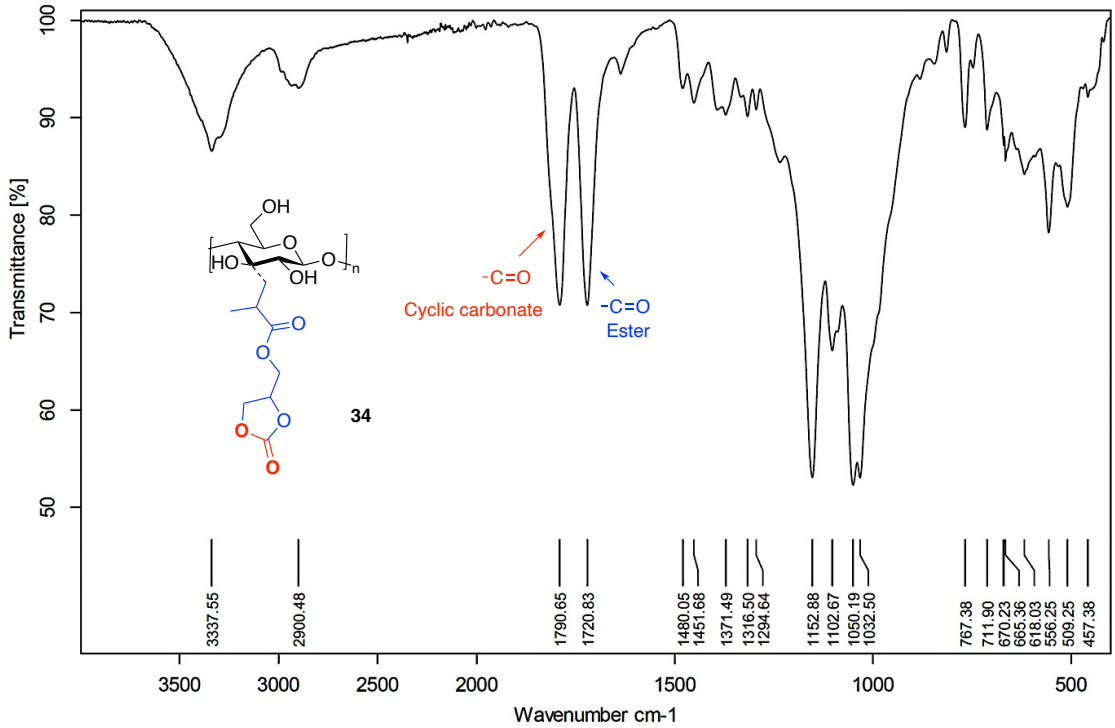


**Figure 4.7** IR spectrum (298 K) of cyclic carbonate functionalised cellulose.

#### 4.2.7.4 Antibacterial analysis of cyclic carbonate functionalised cellulose compound

Antimicrobial compounds were synthesised by grafting GMA to cellulose fibres and subsequently converted into cyclic carbonate through cycloaddition of $CO_2$ with **GaL$^{Me}$** catalyst and $Bu_4NI$ co-catalyst.

Since compounds **33** and **34** contain cellulose fibres, the solubility of the compound was not possible in any common solvents. All samples were pressed to form a disc of approximately 6mm in diameter by using a hydraulic press. The

antimicrobial activity of the compound was assessed via a disc diffusion method, performed according to the standardized BSAC disc diffusion method for antimicrobial susceptibility testing.[216] The antibacterial activity of the modified cellulose fibres **34** were evaluated against *Staphylococcus aureus* SH 1000 (*S. aureus*) and *Escherichia coli* JM 109 (*E. coli*) at $OD_{600}$ 0.008. Three biological replicates with three technical repeats were performed for both bacteria.

The compounds **33** and **34** were used as a test subject for the analysis, with cellulose fibres as a blank sample. The decision to include compound **33** in the analysis was to confirm the ability of either of these polymers to kill microorganisms. After overnight incubation, the result shows a high zone of inhibition with *S. aureus* and appears to have a low inhibition when exposed to *E. coli* bacteria.

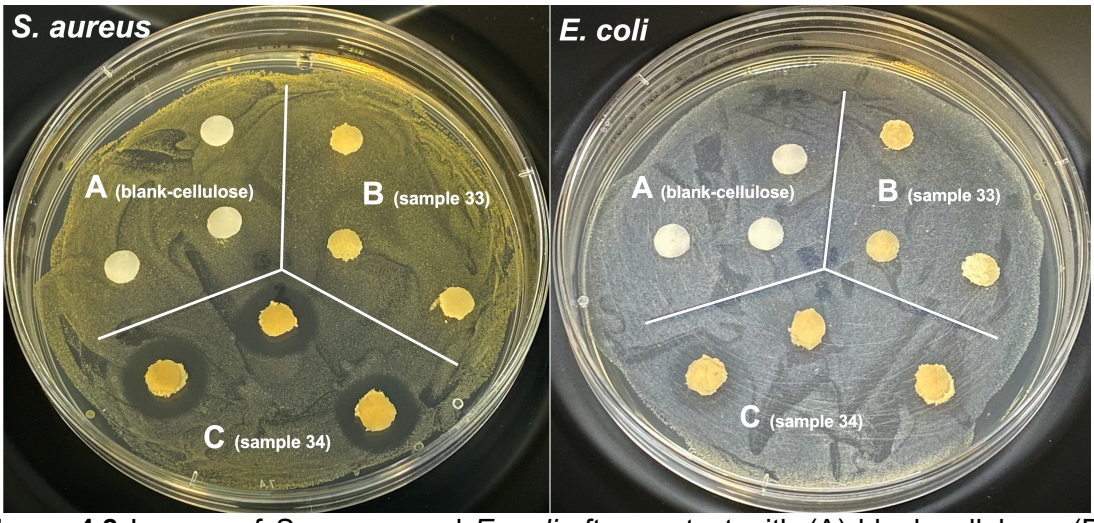


**Figure 4.8** Images of *S. aureus* and *E. coli* after contact with (A) blank-cellulose, (B) epoxy-functionalised cellulose (sample **33**) and (C) cyclic carbonate functionalised cellulose (sample **34**).

Vismara reported an antimicrobial analysis of GMA grafted oxidized nanocellulose together with several modified polymers including GMA grafted hydrolysed nanocellulose resulting to have a presence of inhibition zone demonstrated as antibacterial nanomaterials. This corresponds to the application

of GMA grafted cellulose **33** without further modification resulted to no zone of inhibition.[217]

The results indicated that the modified fibres, **34**, were antibactericidal for *S. aureus* with 12.3 mm inhibition but were very low for *E. coli* with only a 6.4 mm inhibition (Figure 4.9). The zone of inhibition of the modified fibres was not changed even after the disc was incubated for seven days; however, no inhibition was found with *E. coli*. The antibactericidal efficiency of the pure cyclic carbonate was also tested and found to be similar to that of the modified fibres, indicating that it is the cyclic carbonate moiety which is exhibiting antibactericidal activity.

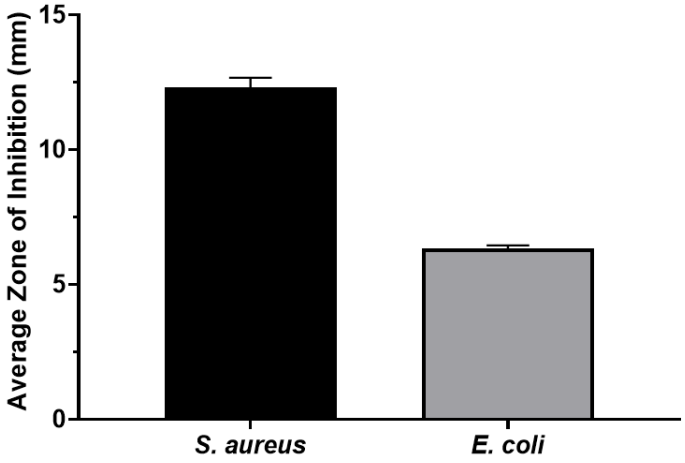


**Figure 4.9** Average zone of inhibition of *S.aureus* and *E.coli* measured in mm using cyclic carbonate functionalised cellulose as a discs. Data represents a sample taken from three biological replicates with three technical repeats performed in each organism. No zone of inhibition was found from blank and compound **33** samples. For data that varied between replicates, SDs are given as error bars.

### 4.2.8 Reaction of $CO_2$ towards episulfide substrates

The catalytic efficiency of using **GaL$^{Me}$** as a catalyst was high and proficient with epoxides and aziridines as substrates even under mild reaction conditions. An attempt to apply the same catalyst for converting of episulfide and $CO_2$ into cyclic monothiocarbonate was performed. There are very few examples of cyclic monothiocarbonate synthesis with the exception of reaction of epoxides and COS

reaction (Scheme 4.17), whilst no reports were found with episulfide and $CO_2$ starting materials.[218-222]

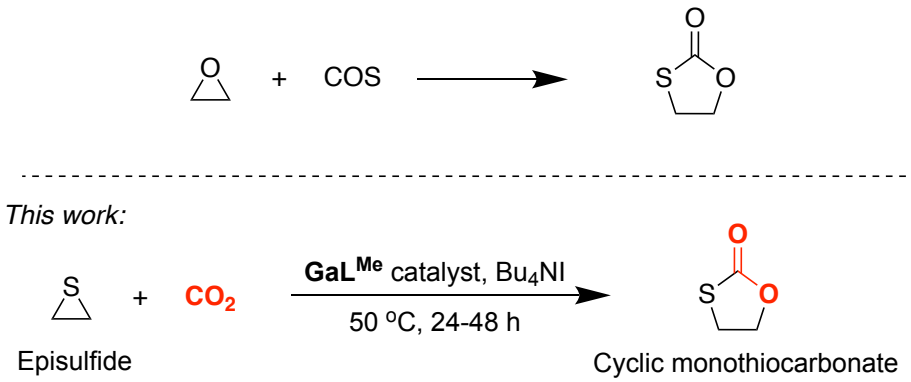


**Scheme 4.17** General reaction towards the formation of cyclic monothiocarbonate compounds.[218-222]

The reaction was attempted in the same manner to synthesise cyclic carbonate/oxazolidinone. Several attempts were made, either with MEK solvent or without solvent. Unfortunately, irrespective of the reaction conditions, the resulting product was always a light-yellow solid which was insoluble in any common organic solvents, and it was challenging to determine the acquired mass. The product was washed several times in organic solvents prior to analysis to remove the catalyst and co-catalyst. Due to the insoluble nature of the product, characterisation using NMR spectroscopy was not possible and was only determined using FT-IR spectroscopy. The data from the IR spectrum displays a weak carbonyl peak at 1794 $cm^{-1}$ after 24 h (Figure 4.10), whilst an intense peak of the carbonyl stretch was observed after 48 h at 1739 $cm^{-1}$ (Figure 4.11).

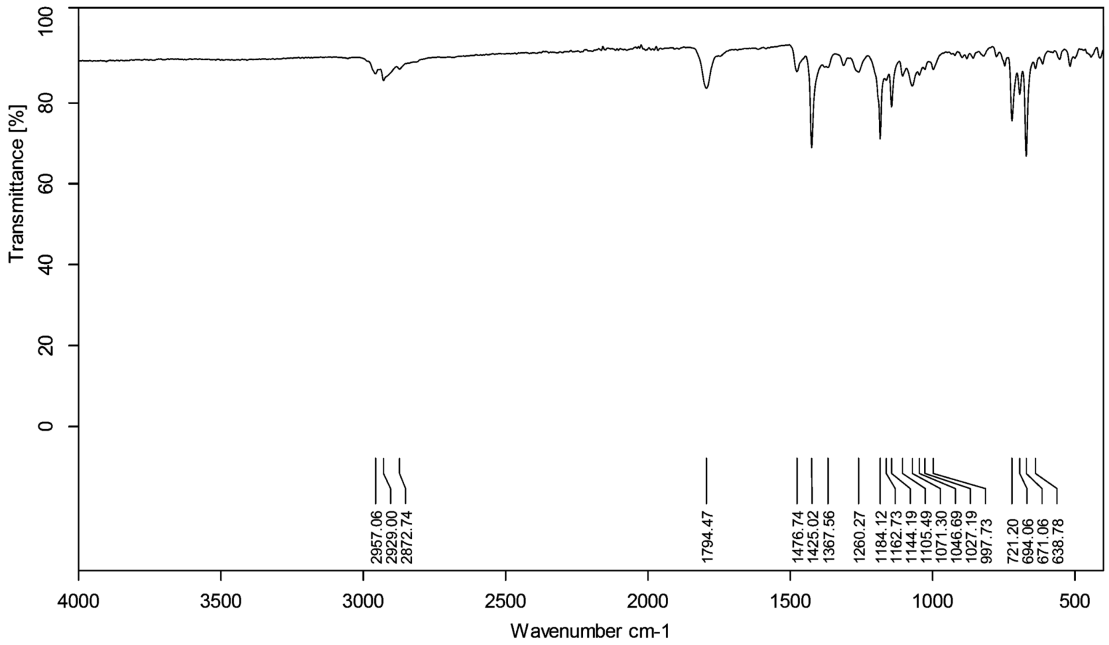


**Figure 4.10** IR spectrum (298 K) of product synthesised from ethylene sulfide and $CO_2$ reaction after 24 h.

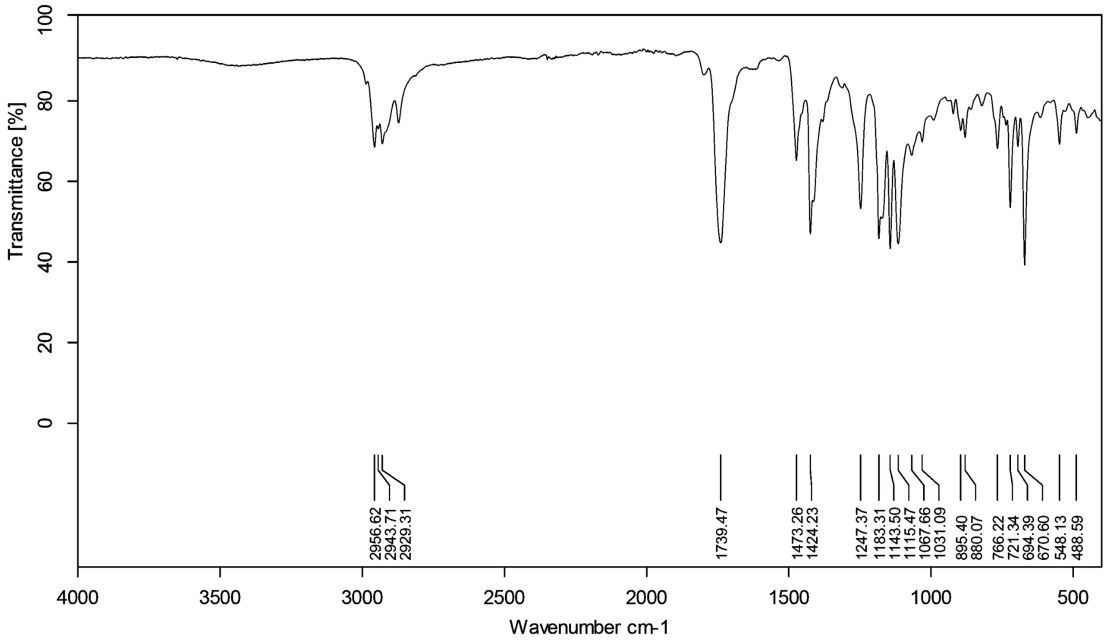


**Figure 4.11** IR spectrum (298 K) of product synthesised from ethylene sulfide and $CO_2$ reaction after 48 h.

The expected monothiocarbonate compound from the cycloaddition of $CO_2$ towards ring-opened ethylene sulfide intermediate was not successful but instead an unknown insoluble compound was synthesised. The unexpected compound was assumed to be polythioester due to the insolubility of the solid product.

Further attempts to investigate the compound were made using Thermogravimetric analysis (TGA). The TGA data shows two significant losses from the sample at 240 °C and 300 °C with a further mass loss at 575 °C. At the present time the origin of the chemical changes that result in these mass losses are unclear. There is also a small initial mass loss at 50 °C which could be a solvent that was not completely removed from the compound (Figure 4.12). In addition, the synthesis of this compound needs to address the presence of sulfide, which could easily damage the reactor as it decomposes the seal inside that prevents the pressure from leaking.

Although there is evidence that the gallium complex converts the ethylene sulfide and $CO_2$ into a new compound, due to the intractable nature of the product it has not been possible to identify its precise composition or chemical structure.

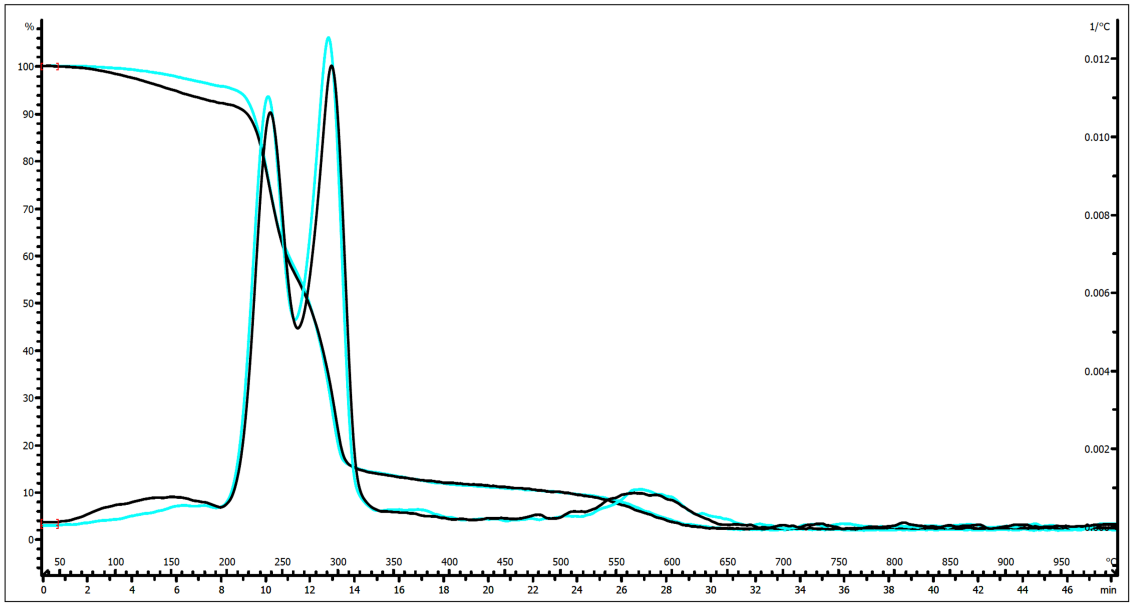


**Figure 4.12** Thermal analysis data of the synthesised compound from ethylene sulfide and $CO_2$ reaction after 48 h under inert condition $N_2$ (blue line) and when exposed to air (black line).

## 4.3 Conclusions and Outlook

The synthesis of aziridines using a simple 2-step approach from epoxides has been exploited which provides high isolated yields. Whilst few aziridines were available commercially and expensive this is therefore an attractive approach, with variation in the *N*-protecting group from *N*-alkyl to *N*-aromatics. The application of **GaL$^{Me}$** catalyst for converting of aziridine and $CO_2$ into 2-oxazolidinone was successful and was the first application of gallium complex to be used for aziridine conversion, to the best of our knowledge. Regioselectivity was observed in the reaction where a 5-substituted compound was highly favoured at mild temperature into complete selectivity of the compound. Whilst formation of a dimer was observed when two phenyl groups were present in the *N*-substituted and R-substituted imines.

When using episulfides as substrates, the expected cyclic monothiocarbonate was not synthesised, but a new compound was formed from the reaction of ethylene sulfide and $CO_2$. Further analysis of this product is required to fully understand its structure.

Moreover, since **GaL$^{Me}$** catalyst was proven to be an efficient catalyst for the synthesis of cyclic carbonate, the epoxide ring of the modified cellulose fibres was successfully converted into cyclic carbonates. The modified cellulose compound was found to be effective antibactericidal against *S.aureus* bacteria. This work has a promising results wherein various epoxides could be grafted to cellulose and then data acquired on whether the modified fibres have the ability to inhibit microorganisms.

# Chapter 5

An Indium-based Catalyst Bearing Aminotrisphenolate Ligand for the Cycloaddition of $CO_2$ and Epoxides to Form Cyclic Carbonates

## 5.1 Introduction

The interest in searching for efficient catalysts for cyclic carbonate synthesis based on other group 13 elements beyond aluminium is attracting increasing attention.[127,155,167] The established efficacy of aluminium aminotrisphenolate catalysts provides impetus to study the ability of neighbouring elements within its group in combination with the aminotrisphenol ligand.[1,125,223] Previously, Mosquera/Hamilton/ Whiteoak and co-workers reported on the first gallium aminotrisphenolate catalyst system for cyclic carbonate synthesis and, encouragingly in the context of this chapter, discovered it to be a more active catalyst than the aluminium congener of the same structure.[1,196] This report on gallium was the inspiration for the work carried out in this chapter.

Indium(III) has similar coordination properties to gallium(III). Surprisingly, few reports have described complexes based on this element as a catalyst for the cycloaddition of epoxides and $CO_2$.[128,224,225] Despite the potential of these previously reported catalysts; in many cases they contain complex ligand scaffolds that require many steps to synthesise and are likely to be challenging to scale up, prompting the need for simpler catalysts that are efficient under milder conditions for the cycloaddition reaction.[16,124,226,227]

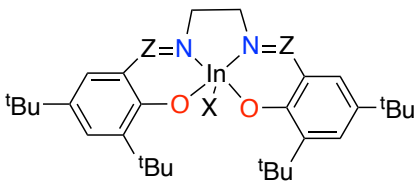


X = O$^t$Bu
Z = $PPh_2$

Williams, 2018

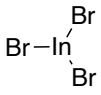


Hein and Mehrkhodavandi, 2021

16 examples (terminal epoxides)
Conditions: catalyst (5 mol %), $Bu_4NB$ (10.0 mol %), $CO_2$ (0.1 MPa), 20-60 $^oC$, 2 h

**Figure 5.1** Selected examples of indium catalyst for the synthesis of cyclic carbonate from epoxide and $CO_2$.[128,228]

Aminotrisphenolate scaffolds are accessible and in comparison not laborious to synthesise as a result of their one step synthesis. Numerous reports are available in the literature on the coordination of the aminotrisphenolate ligand with transition metals and main group elements.[96] This ligand system presents a certain rigidity which arises from the phenolic arms and through the bulkiness caused by *ortho*- and *para*- substituted phenyl rings.

Williams and co-workers reported the first indium salen catalyst (Figure 5.1, left) for $CO_2$/epoxide copolymerisation at low $CO_2$ pressures and mild reaction temperatures (0.1 MPa and 60°C, respectively). However, the report only focused on polymer synthesis, whilst in contrast, Mehrkhodavandi and co-workers have used a simple indium halide ($InX_3$), specifically indium bromide ($InBr_3$), as a catalyst for the synthesis of cyclic carbonate compounds (Figure 5.1, right).[128,228] Meanwhile, Shibata and co-workers reported the combination of $InBr_3$ and $PPh_3$ as an active catalyst, but the substrate scope and reaction mechanism were relatively poorly studied.[225] Despite the higher cost of gallium and indium derivatives compared with aluminium, both metal complexes exhibit attractive features, including their biocompatibility; and the metal precursors are typically more stable than organoaluminium species in polar media.[124,125,224]

The limited reports on indium compounds are perhaps surprising given extensive and successful research on the well-established aluminium catalysts and some reports of highly active boron and gallium compounds. Indeed, in general, it appears that the synthetic potential of organoindium compounds has not been fully appreciated since the importance of indium chemistry is almost entirely related to indium semiconductors and other related materials.[229-231]

Herein, indium aminotrisphenolate compounds are synthesised and used as a catalyst along with tetrabutylammonium iodide ($Bu_4NI$) for coupling a range

of epoxides with $CO_2$, under relatively mild reaction conditions, to synthesise cyclic carbonates with complete selectivity (Scheme 5.1). This work is the first example of an indium aminotrisphenolate complex applied as a catalyst in this reaction.

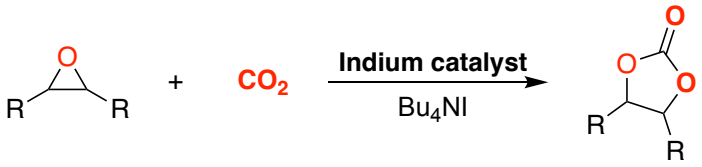


**Scheme 5.1** Synthesis of cyclic carbonate using indium complex/$Bu_4NI$ catalyst.

## 5.2 Results and Discussions

### 5.2.1 Synthesis of Indium-based catalyst

The indium aminotrisphenolate complex was prepared using a slightly modified approach to that reported by Koch.[224] The complexes were prepared as shown in Scheme 5.2. The indium complex contains additional ligands due to the excess of 1-methylimidazole (NMIz) added in the synthesis. The presence of these additional ligands was necessary for the stability of the indium complex. Indeed, attempts to prepare the compound without the extra ligands failed, and no compound could be obtained from the synthesis.

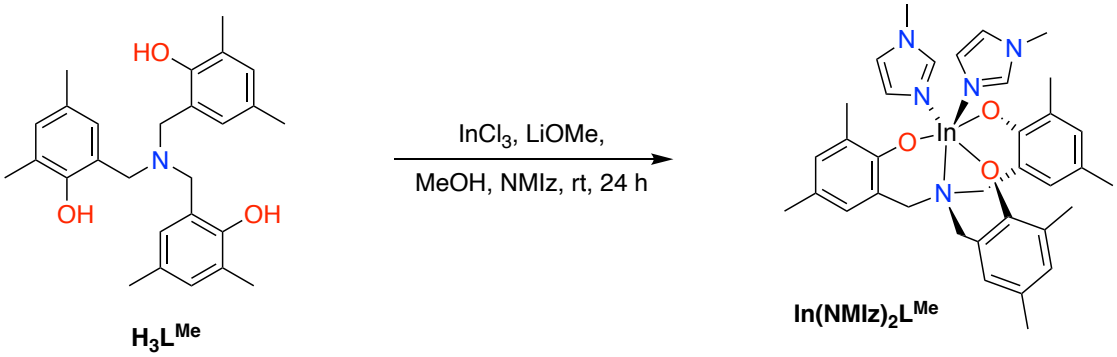


**Scheme 5.2** General reaction for the synthesis of **$In(NMIz)_2L^{Me}$** as a catalyst.

In addition, several attempts were made to synthesise indium complexes using different indium precursors such as $InCl_3$, indium ethoxide, and indium isopropoxide. Unfortunately, these experiments failed, and the ligand was not coordinated to the indium atom. The indium complexes were prepared by reacting the aminotrisphenolate ligand ($H_3L$) and lithium methoxide (LiOMe) to form a lithium salt of the ligand ($Li_3L$) and subsequent reaction with $InCl_3$ in methanol. The reaction was left at room temperature for 24 h. Attempts to completely coordinate the aminotrisphenolate ligand to the indium atom were successful, but with the requirement for two molecules of NMIz as additional ligand. The same result was observed when 4-dimethylaminopyridine (DMAP) was added in excess as the stabilising ligand (Figure 5.2). It may be hypothesised that the halide remains in the coordination sphere of the indium centre as a result of the Lewis acidic nature and size of the indium,[125] producing a charged intermediate, which with the addition of excess NMIz or DMAP, it is then displaced, providing a stable indium complex (Scheme 5.3).

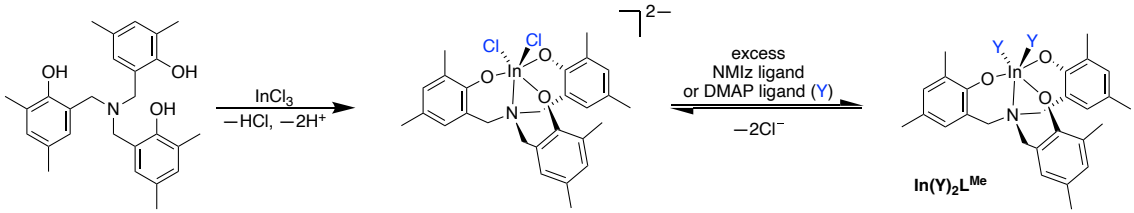


**Scheme 5.3** Proposed reaction towards excess NMIz or DMAP ligand to synthesised indium complexes.

The presence of the additional ligand also accounts for the differences in reactivity. The final product was characterised using NMR spectroscopy; however, when analysed through HRMS, the product forms a dimer, and the NMIz/DMAP ligand appears to have been removed. This might be due to the intense energy exposure during the analysis. Synthetic attempts to remove the

NMIz/DMAP ligands were unsuccessful as the complexes decomposed. This confirms the importance of excess ligands in the complex to give higher stability. The indium complexes were recrystallised from THF/hexane and were soluble in chloroform to enable NMR analysis in this solvent.

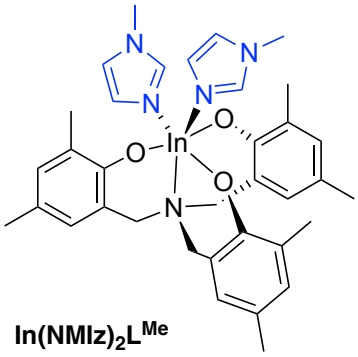


**In(NMIz)$_2$L$^{Me}$**

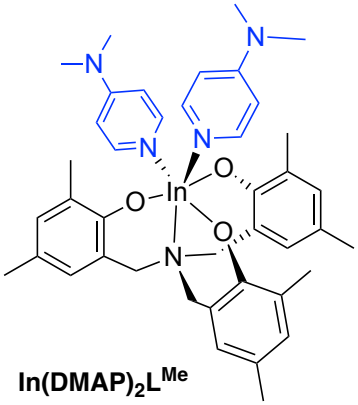


**In(DMAP)$_2$L$^{Me}$**

**Figure 5.2** The indium complexes synthesised after reaction of LiOMe, **H$_3$L$^{Me}$**, and $InCl_3$.

### 5.2.2 Characterisation of Indium-based catalyst

#### 5.2.2.1 NMR Spectroscopy

Both indium complexes were highly stable under ambient laboratory conditions, even under prolonged storage and in solution. All compounds were soluble in organic solvents and were characterised by NMR spectroscopy using deuterated chloroform as solvent. The coordination of NMIz and DMAP ligand was confirmed in the spectrum where peaks of the ligand were visible even after prolonged drying of the sample and recrystallisation. In Figure 5.3, complete coordination of the aminotrisphenolate ligand was observed, and the coordination of two molecules of the NMIz ligand was based on the integrated value shown in the spectrum. The same result was obtained when NMIz was replaced with DMAP as a ligand, where two molecules were found based on the integrated values of the compound (Figure 5.4). The NMIz and DMAP ligands are not visible in the HRMS (even under reduced energies), and the formation of an indium dimer

complex was detected ([InL]$_2$). This supports the potential for liability of these additional ligands.

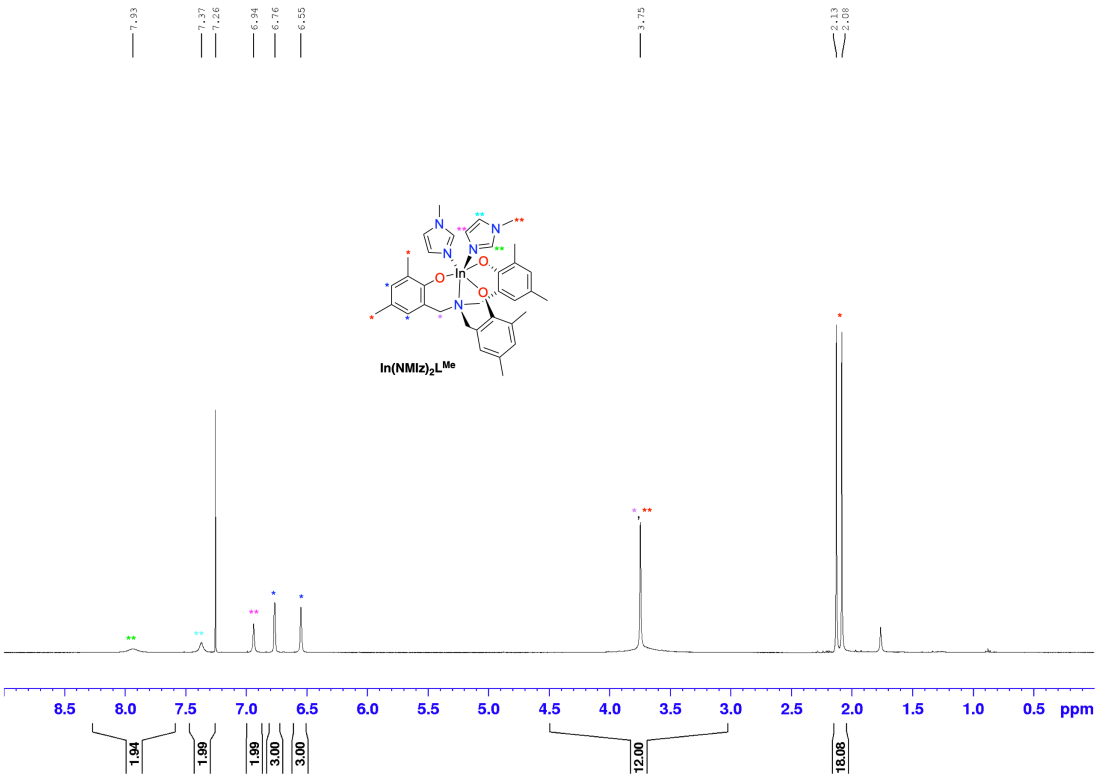


**Figure 5.3** $^1$H NMR spectra ($CDCl_3$, 298 K) of **In(NMIz)$_2$L$^{Me}$**.

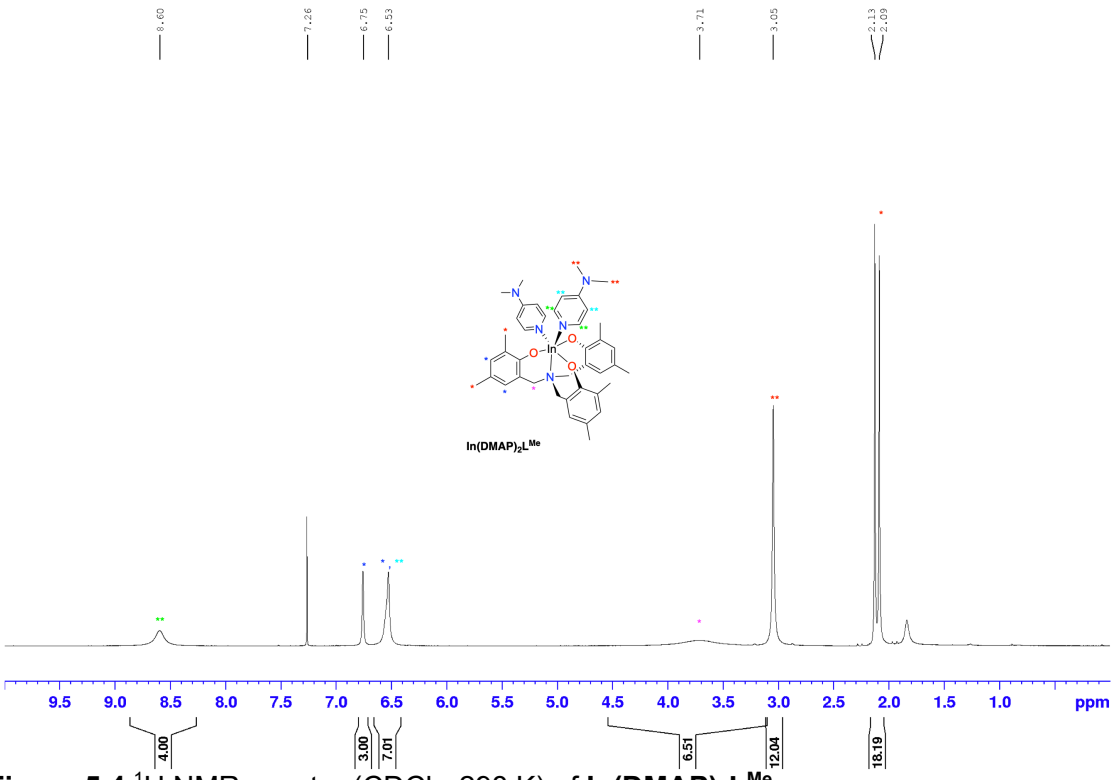


**Figure 5.4** $^1$H NMR spectra ($CDCl_3$, 298 K) of **In(DMAP)$_2$L$^{Me}$**.

### 5.2.3 Catalyst screening

As mentioned, the synthesised indium complexes were highly stable when coordinated to NMIz or DMAP ligand. With these compounds in hand, their potential application as catalysts for the cycloaddition of epoxides and $CO_2$ was studied.

The cycloaddition reaction was performed using freshly prepared dry ice as prepared in other chapters of this thesis. Once all the reagents (catalyst, co-catalyst and epoxide) were added to the 50 mL reactor, the dry ice was prepared, weighed and introduced, and then the reactor was sealed. The weight of the dry ice used was 2.68 g which achieved a pressure of approximately 1.5 MPa.

**Table 5.1** Optimisation of **In(NMIz)$_2$L$^{Me}$/Bu$_4$NI** catalyst with 1,2-epoxyhexane substrate.

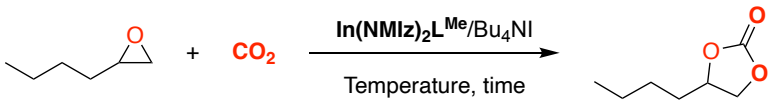


**1a** **1b**

| Entry | **In(NMIz)$_2$L$^{Me}$** (mol %) | Bu$_4$NI (mol %) | Time (h) | Temp (°C) | Conv (%)[a] |
|---|---|---|---|---|---|
| 1 | 1.0 | 2.0 | 24 | 40 | >99 |
| 2 | 1.0 | 2.0 | 24 | rt | 73 |
| 3 | 0.5 | 2.0 | 24 | 40 | >99 |
| 4 | 0.5 | 1.0 | 24 | 40 | 78 |
| 5 | 0.5 | 2.0 | 24 | rt | 71 |
| 6 | 0.5 | 2.5 | 16 | rt | 63 |
| 7 | 0.4 | 2.0 | 16 | rt | 62 |
| 8 | 0.4 | 2.0 | 24 | rt | 83 |
| 9 | 0.4 | 2.0 | 24 | 40 | 98 |
| **10** | **0.4** | **2.0** | **24** | **45** | **>99** |
| 11 | - | 2.0 | 24 | 45 | 26 |
| 12 | 1.0 | - | 24 | 40 | -- |
| 13 | 2.0 | - | 24 | 100 | 72 |
| 14 | 2.0 | - | 24 | 45 | 35 |
| 15 | 3.0 | - | 24 | 100 | 82 |
| 16[b] | 0.4 | 2.0 | 24 | 40 | 97 |

**Conditions**: 1,2-epoxyhexane (**1a**) (1.0 g, 9.98 mmol), **In(NMIz)$_2$L$^{Me}$** catalyst, Bu$_4$NI co-catalyst, $CO_2$ (2.63 g, 59.8 mmol, 6.0 equiv., approx. 1.5 MPa). [a]Conversion of **1a** determined by inspection of the $^1$H NMR spectrum of the crude reaction mixture. [b] **In(DMAP)$_2$L$^{Me}$** as a catalyst.

Initially, complete and selective conversion of the epoxide was found using 1.0 mol % of **In(NMIz)$_2$L$^{Me}$** and 2.0 mol % of $Bu_4NI$ for 24 h at 40 °C (Table 5.1, Entry 1). Since the conversion was excellent, the reaction was repeated at room temperature using the same catalyst and co-catalyst loading, giving a 73 % yield (Table 5.1, Entry 2). Increasing the temperature to 40 °C and reducing the catalyst loading by half (to 0.5 mol %) provided a yield of >99 % (Table 5.1, Entry 3). With an excellent yield under mild reaction conditions of 40 °C, the co-catalyst loading was decreased by half (to 1.0 mol %) whilst maintaining the catalyst loading to 0.5 mol %, which provided a reduced yield of only 78 %. Other experiments were then performed at room temperature with 16-24 h reaction time, giving a range of yields from 62-83 % with <2.5 mol % co-catalyst loading and variation of catalyst concentration (0.4 and 0.5 mol %) (Table 5.1, Entries 5-8). In particular, this includes entry 5, which was conducted at room temperature without changing the catalyst and co-catalyst loading (0.5 mol % and 2.0 mol %, respectively), which gave a 71 % yield. A slight decrease of the catalyst loading to 0.4 mol % gives a 98 % yield, and an increase to 40 °C provided a 98 % yield, which was very similar to that obtained (97 %) when using **In(DMAP)$_2$L$^{Me}$** as catalyst (Table 5.1, Entries 9 and 16). A slight increase in temperature to 45 °C provided a quantitative yield of the cyclic carbonate product (Table 5.1, Entry 10).

The presence and combination of catalyst and co-catalyst were essential in the reaction to achieve the quantitative yield, as seen in Table 5.1, Entries 11 and 12. With only $Bu_4NI$ co-catalyst present in the reaction at 45 °C, the yield was only 26 %, whilst no product was formed with 1.0 mol % of catalyst at 40 °C. The **In(NMIz)$_2$L$^{Me}$** catalyst contains the NMIz ligand that may act as a co-catalyst in the reaction at high temperatures. In this context, 2.0 mol % of the catalyst

(without additional co-catalyst) was trailed at 100 °C, confirming the hypothesis as it provides a yield of 72 % (Table 5.1, Entry 13). As it gives a respectable yield, lowering the temperature to 45 °C was applied, but this led to a significant decrease in the yield (35 %), around half of the yield at 100 °C (Table 5.1, Entry 13-14). Increasing the catalyst loading to 3.0 mol % whilst maintaining the temperature to 100 °C allowed for an 82 % yield (Table 5.1, Entry 15). Interestingly, the experiments with the absence of a co-catalyst produced cyclic carbonate compounds, but the amount of the catalyst loading applied was relatively high compared with the binary catalyst system containing $Bu_4NI$ as a co-catalyst.

### 5.2.4 Mechanistic investigation

The cycloaddition reaction of epoxide and $CO_2$ using indium complex as a catalyst was intriguing since, to the best of our knowledge, there was no report on using indium aminotrisphenolate complex for this conversion. There are few reports on indium compounds, such as Williams and co-workers on indium salen complex but focused on polymer synthesis, whilst Mehrkhodavandi and co-workers have used the indium halide as a catalyst.[128,228] The indium complexes worked as a catalyst and were stable due to the presence of additional NMIz/DMAP ligands. Investigation of the presence of different ligands (NMIz or DMAP) could affect the catalytic efficiency of the catalyst; hence, an experiment was made to compare its yields. As observed in Table 5.2 Entries 1-3, cyclic carbonate formation occurs when a high temperature (100 °C) applied, whilst no product was formed when the temperature was decreased to 40 °C. The result gave a reasonable yield when a 2.0 mol % of catalyst loading was used. This result could indicate that the NMIz and DMAP ligand attached to the indium

complex were separated as it reached high temperature and worked as a potential co-catalyst in the reaction. The presence of NMIz in the complex was proposed to operate as a co-catalyst; hence an experiment using 1-methylimidazole (NMIz) solely as a catalyst with $Bu_4NI$ co-catalyst was performed. However, the result yielded only 62 % of cyclic carbonate products. Compared to reactions with indium complexes, the product yield was lower than when using the catalyst, which yielded >99 % (Table 5.2, Entries 4 and 5). These results show the catalytic efficiency of indium complex for converting **1a** and $CO_2$ into **1b**.

**Table 5.2** Comparison of catalyst used for the synthesis of compound **1b**.

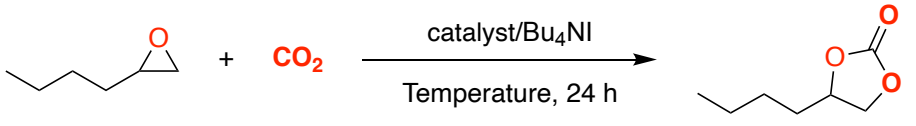


**1a** **1b**

| Entry | Catalyst | % Conversion[a] |
|---|---|---|
| 1 | **$In(NMIz)_2L^{Me}$** | 73 |
| 2 | **$In(DMAP)_2L^{Me}$** | 72 |
| 3[b] | **$In(NMIz)_2L^{Me}$** | - |
| 4[c] | **NMIz** | 62 |
| 5[d] | **$In(NMIz)_2L^{Me}$** | >99 |
| 6[d] | **$In(DMAP)_2L^{Me}$** | 98 |
| 7[d] | ---- | 26 |

**Conditions**: 1,2-epoxyhexane (**1a**) (1.0 g, 9.98 mmol), catalyst (2.0 mol %), 24 h, 100 °C, $CO_2$ (2.63 g, 59.8 mmol, 6.0 equiv., approx. 1.5 MPa). [a]Conversion of **1a** determined by inspection of the $^1H$ NMR spectrum of the crude reaction mixture. [b]40 °C. [c]0.8 mol % NMIz, $Bu_4NI$ (2 mol %), 45 °C. [d] catalyst (0.4 mol %), $Bu_4NI$ (2 mol %), 24 h, 45 °C.

Since the indium complex was found to act as a Lewis acid catalyst, an investigation of the Lewis acidity of indium-containing species has been performed and is summarised in Table 5.3. The AN value was calculated using the Gutmann-Beckett method[116] to measure the Lewis acidity of each

synthesised indium compound by acquiring the observed chemical shift from the solution of triethylphosphine oxide ($Et_3PO$) and indium compounds in $CDCl_3$ using $^{31}P\{^1H\}$ NMR.

**Table 5.3** Gutmann-Beckett $^{31}P\{^1H\}$ NMR and calculated acceptor numbers (AN) of indium compounds in comparison with gallium congener of the same structure.

| Entry | Catalyst | δ / ppm[a] | AN[b] |
|---|---|---|---|
| 1 | **In(NMIz)$_2$L$^{Me}$** | 58.24 | 38.10 |
| 2 | **In(DMAP)$_2$L$^{Me}$** | 58.10 | 37.79 |
| 3[c] | GaL$^{Me}$ | 62.23 | 46.92 |

**Conditions**: Solution in $CDCl_3$, [a]Observed chemical shift of the 1:1 $Et_3PO$ ratio with indium compounds. [b]AN calculated using equation 6.1 of Chapter 6 of this thesis. [c]Obtained from reference 4.

As shown in Table 5.3, **In(NMIz)$_2$L$^{Me}$** and **In(DMAP)$_2$L$^{Me}$** have only a minor difference in the chemical shift of the $Et_3PO$ adduct, which is in line with the catalytic activities being somewhat similar (Table 5.2, Entries 5-6). The acceptor number (AN) of the indium compounds was lower than the corresponding **GaL$^{Me}$** complex, which agrees with the optimised conditions used in the cycloaddition reaction (Table 5.3, Entry 3). The unexpected broadening of the $Et_3PO$-**In(NMIz)$_2$L$^{Me}$** Lewis pair could indicate a rapid exchange of $Et_3PO$, which Mosquera/Hamilton/Whiteoak and co-workers also reported for the **GaL$^{Me}$** catalyst (Figure 5.5).[155]

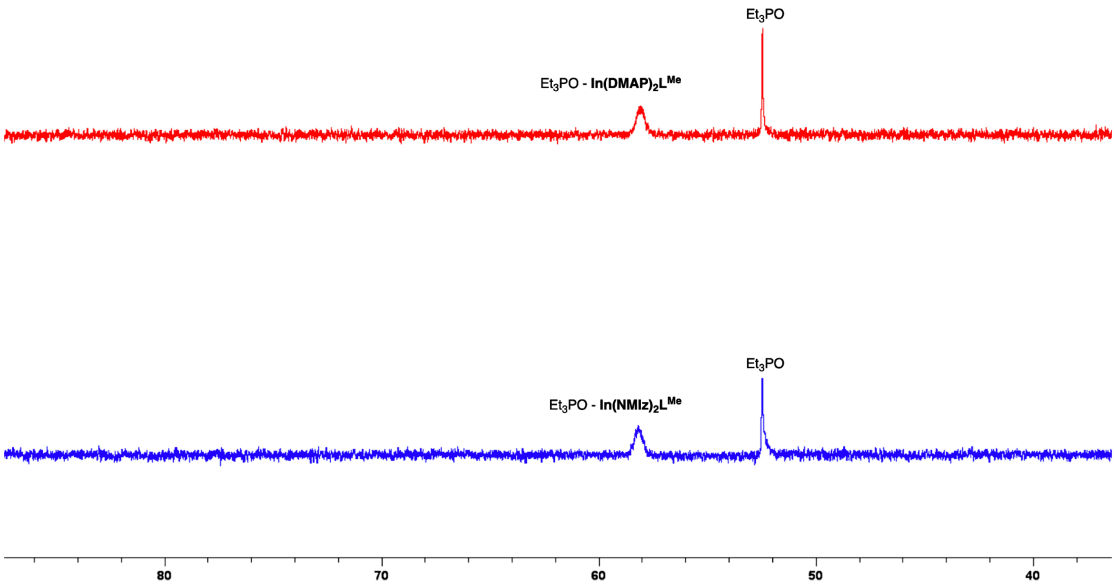


**Figure 5.5** $^{31}P\{^{1}H\}$ spectra (298 K) of indium compounds showing the chemical shift of the $Et_3PO$ and the Lewis acid pair for the measurement of the AN using the Gutmann-Beckett method ($Et_3PO$, $CDCl_3$).

The proposed reaction mechanism for the cycloaddition of $CO_2$ with 1,2-epoxyhexane is similar to cyclic carbonate formation using **GaL$^{Me}$** catalyst (Scheme 5.3). Since the process undergoes a Lewis acid catalysis type of interaction, the initial coordination of the epoxide to the indium centre (Lewis acid) is followed by a Lewis base-mediated ring-opening step resulting from the nucleophilic iodide $Bu_4NI$ co-catalyst (Int. 1). However, the reaction could proceed without the presence of $Bu_4NI$ co-catalyst at a high temperature where the attached ligand (DMAP) can act as a co-catalyst in the reaction. Then $CO_2$ insertion occurs into the In-O bond (Int. 2) and closes the ring, releasing the co-catalyst and catalyst (Int. 3), forming a cyclic carbonate product **1b**. The ring-opening of the epoxide occurs at the least hindered carbon atom, as shown in the mechanism.

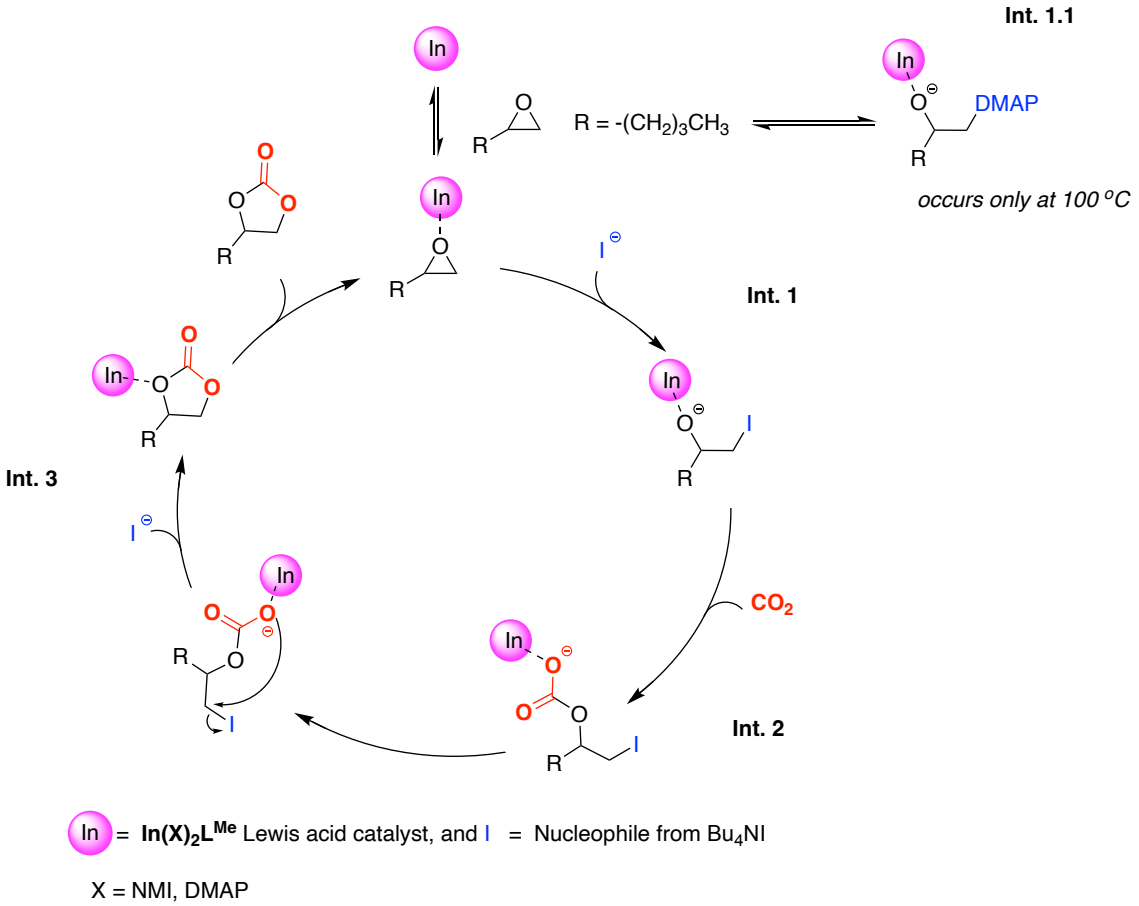


**Scheme 5.4** The proposed general reaction mechanism for the formation of compound **1b** from a coupling reaction between 1,2-epoxyhexane and $CO_2$ catalysed by **In(NMIz)$_2$L$^{Me}$** and **In(DMAP)$_2$L$^{Me}$** where the ring-opening step occurs at the least hindered carbon atom (to form Int. 1).

### 5.2.5 Substrate scope for the $CO_2$ cycloaddition reaction

The indium complexes were found to be efficient catalysts for cyclic carbonate formation under mild conditions based on the above results. The optimised binary catalyst system reaction conditions were selected from Table 5.1 Entry 10 for the cycloaddition of $CO_2$ and epoxide for both terminal and internal substrates. The summary of all compounds obtained from this work was listed in Scheme 5.5. The results show a high conversion with terminal substrates with an average yield of 98 %. Epoxides bearing an alkyl substituent like 1,2-epoxyhexane (**1a**) and propylene oxide (**2a**) were readily converted into the desired products (**1b** and **2b**, respectively) with an excellent yield. The epoxides with bulky *tert*-butyl

substituents **6a** resulted in a high conversion rate of 95 %, where the desired product (**6b**) could potentially produce a lower yield because of steric effects. The epoxide bearing an alkyl halide substituent (**3a**) also reacted to $CO_2$ with a complete conversion rate to give the corresponding cyclic carbonate **3b**. Furthermore, cyclic carbonates functionalised with alkenes (**7b**), alcohols (**8b**), alkynes (**10b**), ethers (**4b**, **10b**), and aromatics (**5b**, **11b**) showed a decent and almost complete quantitative yields.

The challenging internal epoxides were converted into the corresponding cyclic carbonates (**9b**, **12b** and **13b**) with a reasonable yield of 70 %, 40 %, and 78 %, respectively, likely owing to steric effects. Whilst trace amount of cyclic carbonate product was observed from the four-membered oxirane, oxetane (**14a**).

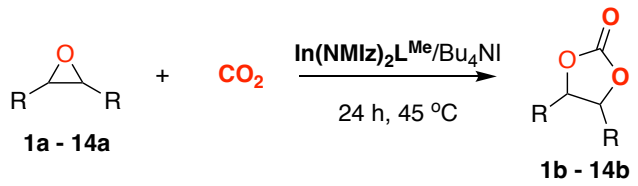


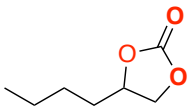

**1b**

>99 %

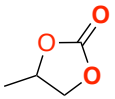

**2b**

>99 %

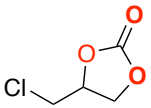


**3b**

>99 %

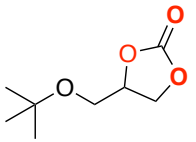

**4b**

>99 %

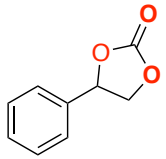

**5b**

96 %

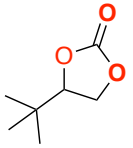

**6b**

95 %

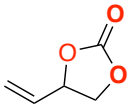

**7b**

96 %

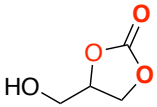


**8b**

>99 %

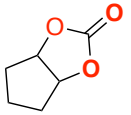

**9b**

70 %

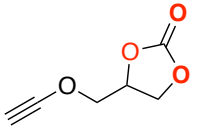

**10b**

>99 %

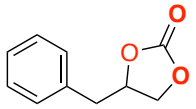

**11b**

99 %

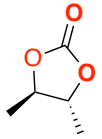

**12b**

40 %

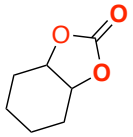

**13b**

78 %

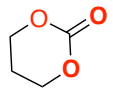

**14b**

trace

**Scheme 5.5** Cycloaddition of $CO_2$ with various epoxides using **In(NMIz)$_2$L$^{Me}$** catalyst and $Bu_4NI$ co-catalyst. **Conditions**: Epoxides(**1a-14a**) (1.0 g), 0.4 mol % catalyst, 2.0 mol % $Bu_4NI$, $CO_2$ (2.63 g, 59.8 mmol, 6.0 equiv., approx. 15 bar). Conversion of **1b-14b** determined by inspection of the $^1H$ NMR spectrum of the crude reaction mixture.

## 5.3 Conclusions and Outlook

In conclusion, the cycloaddition reaction of epoxide and $CO_2$ for synthesising cyclic carbonate was possible using an indium aminotrisphenolate compound as catalyst. This is the first example of indium aminotrisphenolate complex applied as a catalyst for this conversion. The catalyst system displayed high catalytic activity and was demonstrated to be more active than other reported indium compounds. The complex was highly stable either with DMAP or NMIz ligands. The synthesised indium complex as part of a binary catalyst system provides a wide substrate scope, including moderate to good conversions for internal epoxides under relatively mild reaction conditions. Conversion of epoxides when only the indium complex was used at high temperature without a co-catalyst was observed, presenting possibilities for future application. It appears that the NMIz and DMAP ligands could be displaced, providing other opportunities. Overall, these results show that indium has the potential to be used as a catalyst for cycloaddition of $CO_2$/epoxide. Furthermore, they should be further studied for their use as catalysts for the copolymerisation of epoxides/$CO_2$ since indium has been reported to promote this reaction.

# Chapter 6

Experimental

## 6.1 Introduction

### 6.1.1 General conditions

Unless otherwise noted, all reactions and manipulations were performed under inert conditions using standard Schlenk line techniques under a dry nitrogen atmosphere. A MBraun inert atmosphere glove box with an integrated purifier unit was used. Before use, glassware and cannulas were oven-dried for at least 24 h at 110 °C prior to use.

### 6.1.2 Solvents

All solvents used for air/moisture sensitive experiments were purchased (Fisher Scientific) anhydrous, over molecular sieves, packaged under argon in resealable ChemSeal™ bottles and used without further purification. All NMR solvents used in the experiment were used directly as purchased and without further purification.

### 6.1.3 General Reagents

All reagents were purchased from various suppliers (Merck, Fisher Scientific and Fluorochem) unless otherwise stated and were used as received. KH dispersed in mineral oil was purchased from Merck and purified through three cycles of washing with hexane to remove the mineral oil and thereafter stored in the glovebox. Carbon dioxide gas was purchased from BOC Ltd., which was converted to solid form using a dry ice maker at Sheffield Hallam University.

### 6.1.4 Analytical Instrumentation

$^{1}$H NMR (400 MHz, 298K), $^{13}$C{$^{1}$H} NMR (100 MHz, 298K), $^{19}$F{$^{1}$H} NMR (376 MHz, 298K), $^{31}$P{$^{1}$H} NMR (162 MHz, 298K) and 2D NMR were recorded using

Bruker AV-400 Nuclear Magnetic Resonance (NMR) spectrometer with chemical shifts reported as ppm and referenced to the residual deuterated solvent signal. Infrared spectroscopy data were recorded on a Bruker ALPHA Fourier Transform-Infrared Spectrometer (FT-IR). High-Resolution Mass Spectra (HRMS) were recorded using a XEVO G2-Xs QTof Mass Spectrometer in ASAP+ mode unless otherwise stated. UV-Vis spectra were obtained using a Thermo Scientific Genesys 10s Spectrophotometer. Crystallographic data were collected by Professor Simon J. Coles and Dr Peter N. Horton at the Engineering and Physical Sciences Research Council (EPSRC) National Crystallography Service (NCS) at the University of Southampton for the structures reported in **Chapter 2**, whereas the structures reported in **Chapters 4** and **5** data were collected by Dr Lucía Álvarez-Miguel at the Universidad de Alcalá, Madrid, Spain.

#### 6.1.4.1 X-ray crystallography

All compounds suitable for single X-ray diffraction analysis were prepared through recrystallisation of the sample by vapour diffusion of pentane into the sample solution in chloroform for up to three weeks unless otherwise stated. Structural determinations of crystals acquired from **Chapter 2** were performed at NCS Southampton, where crystals suitable for the analysis were chosen and mounted on a MITIGEN holder in perfluoroether oil on a Rigaku FRE+ or 007HF equipped with Varimax confocal mirrors and an AFC12 or AFC11 goniometer, and a diffractometer detector HyPix 6000. Crystal was held at a steady T = 100(2) K during data collection. The structure was solved with the ShelXT 2018/2 solution program[232] using dual methods and Olex2 as the graphical interface. The model was refined with the ShelXL 2018/3 program[233] using full-matrix least-squares minimisation on $F^2$. All non-hydrogen atoms were refined anisotropically.

Hydrogen atom positions were calculated geometrically and refined using the riding model.

Following the analysis done at the Universidad de Alcalá, Madrid, Spain. An Oxford Diffraction Supernova diffractometer, equipped with an Atlas CCD area detector and a four-circle kappa goniometer, were used to collect the diffraction data of the crystals. The Mo source with multilayer optics was then used for data collection. Further analysis on the sample such as empirical absorption correction, data integration, and scaling were performed using the CrysAlis Program package.[234] The crystal structures were elucidated using direct methods and refined by Full-Matrix-Least-Squares against F2 with SHELX[235,236] under OLEX2.[237] Full-matrix least-squares refinements were carried out by minimizing $\Sigma_w(Fo_2 - Fc_2)^2$ with the SHELXL weighting scheme and stopped at shift/err < 0.001. The hydrogen atoms were placed at idealized positions and refined using the riding model whilst non-hydrogen atoms were refined anisotropically. The final residual electron density maps showed no remarkable features. Graphics were made with OLEX2 and MERCURY.[238,239]

### 6.1.5 Synthesis of aminotrisphenolate ligand

The starting ligands were prepared according to the reported literature with minor modifications.[240]

**Tris(2-hydroxy-3,5-dimethylbenzyl)amine ($H_3L^{Me}$)**

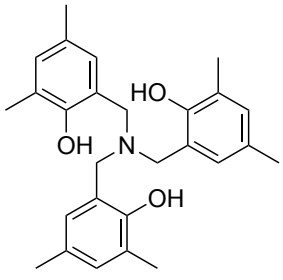


A mixture of 2,4-dimethylphenol (15.1 g, 124 mmol), hexamethylenetetramine, HMTA (3.9 g, 27.6 mmol) and *p*-toluenesulfonic acid monohydrate, $TsOH \cdot H_2O$ (0.1 g, 0.53 mmol) was refluxed at 110 °C for 24 h. Then a further 4.5 g of 2,4-dimethylphenol (0.037 mmol) was added to the reaction mixture and

was left stirring at 110 °C for another 48 h. The mixture solidified and was allowed to cool down to room temperature, and 30 mL of MeOH was added. The solution was sonicated until a loose yellow solid separated from the solid. The mixture was filtered off, washed with cold MeOH, and recrystallised from acetone. The resulting crystals were dried *in vacuo* to give a pale-yellow solid (10.4 g, 24.8 mmol, 90 %). **$^{1}$H NMR (400 MHz, $CDCl_3$, 298 K, ppm)** δ: 6.85 (d, 3H, *J* = 2.0 Hz), 6.72 (d, 3H, *J* = 2.0 Hz), 6.37 (s, 3H, OH), 3.62 (s, 6H), 2.21 (s, 9H), 2.18 (s, 9H). **$^{13}$C{$^{1}$H} NMR (100 MHz, $CDCl_3$, 298 K, ppm)** δ: 151.1, 131.4, 129.2, 128.9, 124.6, 121.8, 56.5, 20.45, 15.98 ppm. **HRMS (ASAP, m/z)** calculated for $[C_{27}H_{33}NO_3+H]^+$: 420.2539; found: 420.2585.

**Tris(3,5-dichloro-2-hydroxybenzyl)amine($H_3L^{Cl}$)**

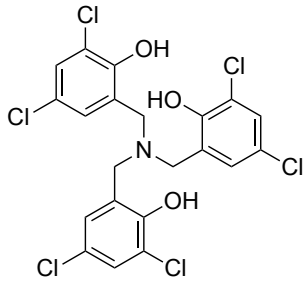


This compound was prepared from 2,4-dichlorophenol (20.2 g, 124 mmol), hexamethylene-tetramine, HMTA (3.9 g, 27.6 mmol) and *p*-toluenesulfonic acid monohydrate, $TsOH \cdot H_2O$ (0.1 g, 0.53 mmol), in a manner analogous to **$H_3L^{Me}$**. The obtained compound was dried in vacuo to give a white powder (10.32 g, 19.04 mmol, 69 %). **$^{1}$H NMR (400 MHz, $CDCl_3$, 298 K, ppm)** δ: 7.23 (d, 3H, *J* = 2.47 Hz), 7.02 (d, 3H, *J* = 2.47 Hz), 3.72 (s, 6H). **$^{13}$C{$^{1}$H} NMR (100 MHz, $CDCl_3$, 298 K, ppm)** δ: 149.8, 129.1, 128.6, 124.8, 124.7, 121.1, 55.35 ppm. **HRMS (ASAP, m/z)** calculated for $[C_{21}H_{15}Cl_6NO_3+H]^+$: 539.9261; found: 541.9286.

### 6.1.6 General procedure for the catalytic cycloaddition of $CO_2$ and epoxides under solvent-free conditions

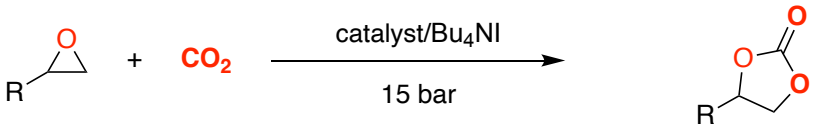


**Scheme 6.1** General procedure for the catalytic reaction of $CO_2$ cycloaddition to epoxides under solvent-free conditions.

All cycloaddition reactions were conducted using a 50 mL stainless-steel material pressure reactor purchased from ASYNT equipped with a pressure relief valve, gauge, a 50 mL internal volume, PTFE vessel and a thermowell. The reactor was placed in a DrySyn base and was pre-heated to a specific temperature using a hotplate fitted with a temperature controller. The PTFE vessel was removed from the reactor and was charged with the desired amount of catalyst, co-catalyst and substrate. After adding all the compounds with a cylindrical stir bar, the PTFE vessel was placed back in the reactor. Freshly prepared dry ice (2.63 g, 59.8 mmol, 6.0 equiv., ~15 bar final pressure) was added to the vessel, and the pressure reactor was quickly sealed. The reactor was then placed in the pre-heated adaptor and was left stirring for 24 h. Afterwards, the reactor was allowed to cool and was placed in an ice bath. Once cooled down, the reactor was removed from the ice bath, and $CO_2$ gas was slowly released until ambient pressure was reached. An aliquot of the crude was collected and dissolved in deuterated solvent. The percentage yield of each reaction was determined based on the $^1$H NMR spectrum of the crude product with mesitylene as the internal standard. This procedure was repeated for all cyclic carbonates synthesised during the optimisation and substrate scope. The crude mixture was purified using a flash column chromatography eluting with gradient 70:30 hexane/ethyl acetate, and the product was further characterised by NMR and IR, which were

consistent with those reported in the literature and in good agreement with the assigned structures.[54,101]

### 6.1.7 Characterisation of cyclocarbonate products

**4-butyl-1,3-dioxolan-2-one (1b)**[101]

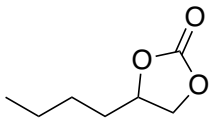

Colourless oil. **$^{1}$H NMR (400 MHz, $CDCl_3$, 298 K, ppm)** δ: 4.71-4.64 (qd, 1H, *J* = 7.48, 5.44 Hz), 4.50 (dd, 1H, *J* = 8.44, 7.82 Hz), 4.04 (dd, 1H, *J* = 8.39, 7.21 Hz), 1.82-1.72 (m, 1H), 1.66 (ddt, 1H, *J* = 14.64, 10.79, 4.58 Hz), 1.50-1.37 (m, 2H), 1.39-1.28 (m, 2H), 0.89 (t, 3H, *J* = 7.08 Hz) **$^{13}$C{$^{1}$H} NMR (125 MHz, $CDCl_3$, 298 K, ppm)** δ:155.15, 69.43, 33.53, 26.42, 22.24, 13.78. **IR ($\nu_{CO}$)** 1784 cm$^{-1}$.

**4-methyl-1,3-dioxolan-2-one (2b)**[101]

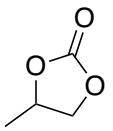

Pale yellow oil. **$^{1}$H NMR (400 MHz, $CDCl_3$, 298 K, ppm)** δ: 4.87-4.79 (m, 1H), 4.53 (dd, 1H, *J* = 8.39, 7.71 Hz), 3.99 (dd, 1H, *J* = 8.41, 7.22 Hz), 1.45 (d, 3H, *J* = 6.26 Hz). **$^{13}$C{$^{1}$H} NMR (125 MHz, $CDCl_3$, 298 K, ppm)** δ: 155.10, 73.61, 70.69, 19.39. **IR ($\nu_{CO}$)** 1780 cm$^{-1}$.

**4-(chloromethyl)-1,3-dioxolan-2-one (3b)**[101]

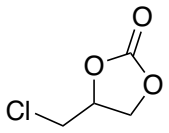

Pale yellow oil. **$^{1}$H NMR (400 MHz, $CDCl_3$, 298 K, ppm)** δ: 4.98 (dtd, 1H, *J* = 8.13, 5.33, 3.77 Hz), 4.57 (dd, 1H, *J* = 8.92, 8.30 Hz), 4.38 (dd, 1H, *J* = 8.87, 5.71 Hz), 3.81-3.68 (m, 2H). **$^{13}$C{$^{1}$H} NMR (125 MHz, $CDCl_3$, 298 K, ppm)** δ: 154.33, 74.37, 66.99, 43.87. **IR ($\nu_{CO}$)** 1778 cm$^{-1}$.

**4-(tert-butoxymethyl)-1,3-dioxolan-2-one (4b)**[176]

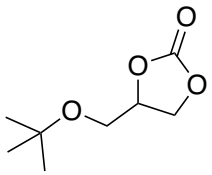

Pale yellow oil. **$^1$H NMR (400 MHz, $CDCl_3$, 298 K, ppm)** δ: 4.79-4.73 (m, 1H), 4.46 (t, 1H, *J* = 8.26 Hz), 4.36 (dd, 1H, *J* = 8.24, 5.80 Hz), 3.60 (dd, 1H, *J* = 10.38, 4.38 Hz), 3.50 (dd, 1H, *J* = 10.42, 3.54 Hz), 1.17 (s, 9H). **$^{13}$C{$^1$H} NMR (125 MHz, $CDCl_3$, 298 K, ppm)** δ: 155.22, 75.23, 73.86, 66.55, 61.27, 27.28. **IR ($\nu_{CO}$)** 1785 cm$^{-1}$.

**4-phenyl-1,3-dioxolan-2-one (5b)**[101]

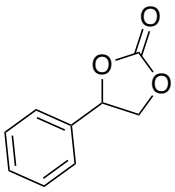

Pale yellow oil. **$^1$H NMR (400 MHz, $CDCl_3$, 298 K, ppm)** δ: 7.45-7.34(m, 5H), 5.67 (t, 1H, *J* = 8.00 Hz), 4.79 (dd, 1H, *J* = 8.63, 8.20 Hz), 4.32 (dd, 1H, *J* = 8.60, 7.85 Hz). **$^{13}$C{$^1$H} NMR (125 MHz, $CDCl_3$, 298 K, ppm)** δ: 154.94, 135.84, 129.73,129.24, 125.94, 78.05, 71.22. **IR ($\nu_{CO}$)** 1781 cm$^{-1}$.

**4-(tert-butyl)-1,3-dioxolan-2-one (6b)**[101]

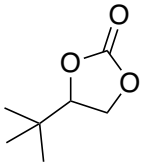

Colourless oil. **$^1$H NMR (400 MHz, $CDCl_3$, 298 K, ppm)** δ: 4.42-4.36 (m, 2H), 4.25-4.19 (m, 1H), 0.96 (s, 9H). **$^{13}$C{$^1$H} NMR (125 MHz, $CDCl_3$, 298 K, ppm)** δ: 155.22, 83.72, 65.66, 33.42, 24.13. **IR ($\nu_{CO}$)** 1788 cm$^{-1}$.

**4-vinyl-1,3-dioxolan-2-one (7b)**[101]

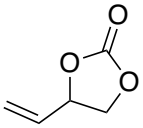

Yellow oil. **$^1$H NMR (400 MHz, $CDCl_3$, 298 K, ppm)** δ: 5.92-5.83 (m, 1H), 5.50-5.40 (m, 2H), 5.11 (q, 1H, *J* = 7.50 Hz), 4.58 (t, 1H, *J* = 8.30 Hz), 4.13 (t, 1H, *J* = 8.05 Hz). **$^{13}$C{$^1$H} NMR (125 MHz, $CDCl_3$, 298 K, ppm)** δ: 154.84, 132.18, 121.27, 77.39, 69.12. **IR ($\nu_{CO}$)** 1780 cm$^{-1}$.

**4-(hydroxymethyl)-1,3-dioxolan-2-one (8b)**[101]

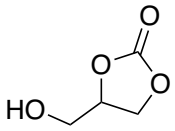

Pale yellow oil. **$^1$H NMR (400 MHz, DMSO- $d_6$, 298 K, ppm)** δ: 5.27 (t, 1H, *J* = 5.50 Hz), 4.82-4.77 (m, 1H), 4.50 (t, 1H, *J* = 8.34 Hz), 4.29 (dd, 1H, *J* = 8.14, 5.82 Hz), 3.67 (ddd, 1H, *J* = 12.65, 5.32, 2.79 Hz), 3.51 (ddd, 1H, *J* = 12.64, 5.52, 3.36 Hz). **$^{13}$C{$^1$H} NMR (125 MHz, DMSO-$d_6$, 298 K, ppm)** δ: 155.65, 77.48, 66.31, 61.04. **IR ($\nu_{CO}$)** 1762 cm$^{-1}$.

**Tetrahydro-4H-cyclopenta[d][1,3]dioxol-2-one (9b)**[176]

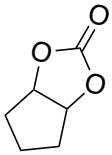

Colourless oil. **$^1$H NMR (400 MHz, $CDCl_3$, 298 K, ppm)** δ: 5.09-5.07 (m, 2H), 2.13-2.08 (m, 2H), 1.80-1.62 (m, 4H). **$^{13}$C{$^1$H} NMR (125 MHz, $CDCl_3$, 298 K, ppm)** δ: 155.49, 81.87, 33.15, 21.55. **IR ($\nu_{CO}$)** 1780 cm$^{-1}$.

**4-((ethynyloxy)methyl)-1,3-dioxolan-2-one (10b)**[241]

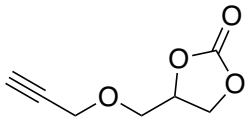

Yellow oil. **$^1$H NMR (400 MHz, $CDCl_3$, 298 K, ppm)** δ: 4.85 (tdd, 1H, *J* = 8.42, 6.03, 3.77 Hz), 4.50 (t, 1H, *J* = 8.42 Hz), 4.38 (dd, 1H, *J* = 8.42, 6.04 Hz), 4.21 (qd, 2H, *J* = 15.15, 13.58 Hz), 3.74 (qd, 2H, *J* = 13.32, 10.81 Hz), 2.48 (t, 1H, *J* = 2.38 Hz). **$^{13}$C{$^1$H} NMR (125 MHz, $CDCl_3$, 298 K, ppm)** δ: 154.97, 78.60, 75.64, 74.85, 68.46, 66.20, 58.79. **IR ($\nu_{CO}$)** 1781 cm$^{-1}$.

**4-benzyl-1,3-dioxolan-2-one (11b)**[101]

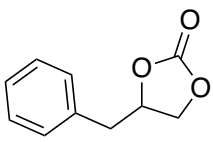

Colourless oil. **$^1$H NMR (400 MHz, $CDCl_3$, 298 K, ppm)** δ: 7.32-7.17 (m, 5H), 4.92-4.85 (m, 1H), 4.39 (dd, 1H, *J* = 8.59, 7.89 Hz), 4.11 (dd, 1H, *J* = 8.63, 6.89 Hz), 3.08 (dd, 1H, *J* = 14.24, 6.42 Hz), 2.95

(dd, 1H, *J* = 14.23, 6.35 Hz). **$^{13}C\{^{1}H\}$ NMR (125 MHz, $CDCl_3$, 298 K, ppm)** δ: 154.93, 134.08, 129.41, 128.97, 127.53, 76.95, 68.56, 39.52. **IR ($\nu_{CO}$)**1781 $cm^{-1}$.

**(4R,5R)-4,5-dimethyl-1,3-dioxolan-2-one (12b)**[101]

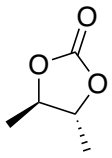

White solid. **$^{1}H$ NMR (400 MHz, $CDCl_3$, 298 K, ppm)** δ: 4.34-4.27 (m, 2H), 1.43-1.41 (m, 6H). **$^{13}C\{^{1}H\}$ NMR (125 MHz, $CDCl_3$, 298 K, ppm)** δ: 154.50, 79.89, 18.35. **IR ($\nu_{CO}$)** 1782 $cm^{-1}$.

**Hexahydrobenzo[d][1,3]dioxol-2-one (13b)**[101]

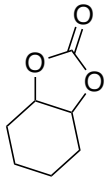

Yellow oil. **$^{1}H$ NMR (400 MHz, $CDCl_3$, 298 K, ppm)** δ: 4.66-4.63 (m, 2H), 1.87-1.84 (m, 4H), 1.61-1.52 (m, 2H), 1.42-1.33 (m, 2H). **$^{13}C\{^{1}H\}$ NMR (125 MHz, $CDCl_3$, 298 K, ppm)** δ: 155.35, 75.73, 26.75, 19.15. **IR ($\nu_{CO}$)** 1784 $cm^{-1}$.

**1,3-dioxan-2-one (14b)**[101]

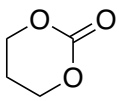

White solid. **$^{1}H$ NMR (400 MHz, $CDCl_3$, 298 K, ppm)** δ: 4.42 (t, 4H, *J* = 5.71 Hz), 2.14-2.08 (m, 2H). **$^{13}C\{^{1}H\}$ NMR (125 MHz, $CDCl_3$, 298 K, ppm)** δ: 148.51, 67.96, 27.24. **IR ($\nu_{CO}$)** 1788 $cm^{-1}$.

### 6.2.1 Experimental Details for Chapter 2ynthesis of boron-containing aminotrisphenolate catalyst

**Synthesis of compound A**

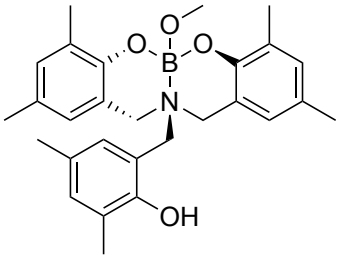

To a stirred solution of **$H_3L^{Me}$** (500 mg, 1.19 mmol) in toluene (15 mL) was added trimethyl borate (124 mg, 1.19 mmol) dropwise at −78 °C. The reaction mixture was allowed to warm up to room temperature before being heated at reflux for 2 h. The reaction mixture was allowed to cool down and solvent was removed under vacuum. The crude product was sequentially washed with hexane and diethyl ether. The obtained compound was dried in vacuo resulting **A** as a white powder (471 mg, 1.03 mmol, 86 %). Crystals suitable for X-ray crystallography were grown by slow diffusion of pentane into a concentrated chloroform solution of the final product. **$^1$H N$^1$MR (400 MHz, $CDCl_3$, 298 K, ppm)** δ: 8.57 (s, 1H), 6.91 (s, 1H), 6.85 (s, 2H), 6.66 (s, 1H), 6.53 (s, 2H), 4.22 (s, 2H), 3.98 (m, 4H), 3.46 (s, 3H), 2.22-2.16 (m, 18H). **$^{13}$C{$^1$H} NMR (100 MHz, $CDCl_3$, 298 K, ppm)** δ: 153.21, 149.08, 133.03, 131.69, 130.90, 128.33, 127.89, 127.56, 126.45, 124.45, 116.88, 115.98, 57.14, 56.46, 49.86, 20.42, 20.24, 16.45, 16.00. **$^{11}$B NMR (128 MHz, $CDCl_3$, 298 K, ppm)** δ: 2.49. **HRMS (ESI+, m/z, MeOH)** calculated for $[C_{28}H_{34}BNO_4+Na]^+$: 482.2479; found: 482.2477. **IR (298 K, cm$^{-1}$)** 2917, 1482, 1444, 1246, 1216, 1158, 1096, 1054, 1028, 858, 795, 757, 725.

**Synthesis of compound B**

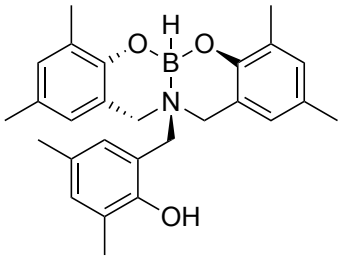

To a stirred solution of **$H_3L^{Me}$** (500 mg, 1.19 mmol) in dichloromethane (15 mL) was added $BH_3$.THF (1.0 M in tetrahydrofuran, 1.19 mL, 1.19 mmol) dropwise at −78 °C. The solution was allowed to warm to room temperature and was left stirring for 3 h. The solvent was removed under vacuum afterwards, and the crude product was sequentially washed with hexane and diethyl ether. The obtained compound was dried in vacuo resulting **B** as a white powder (429 mg, 1.00 mmol, 84 %). **$^1$H NMR (400 MHz, $CDCl_3$, 298 K, ppm)** δ: 7.42 (s, 1H), 6.98 (s, 1H), 6.90 (s, 2H), 6.77 (s, 1H), 6.58 (s, 2H), 4.15 (d, 2H, *J* = 14.6 Hz), 4.04 (d, 2H, *J* = 14.6 Hz), 4.03 (s, 2H), 2.24-2.21 (m, 18H). **$^{13}$C{$^1$H} NMR (100 MHz, $CDCl_3$, 298 K, ppm)** δ: 153.12, 148.26, 133.28, 132.05, 131.12, 128.82, 128.62, 128.11, 126.64, 124.90, 115.93, 115.85, 55.55, 54.57, 20.47, 20.39, 16.52, 16.24. **$^{11}$B NMR (128 MHz, $CDCl_3$, 298 K, ppm)** δ: 2.40, 1.80. **HRMS (ESI+, m/z, MeOH)** calculated for $[C_{27}H_{32}BNO_3+Na]^+$: 452.2373; found: 452.2361. **IR (298 K, cm$^{-1}$)** 3265, 2917, 2424, 1481, 1231, 1136, 1012, 857, 780, 726.

**Synthesis of compound C**

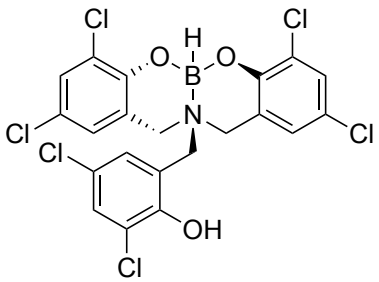

To a stirred solution of **$H_3L^{Cl}$** (500 mg, 0.92 mmol) in dichloromethane (15 mL) was added $BH_3$.THF (1.0 M in tetrahydrofuran, 0.92 mL, 0.92 mmol) dropwise at −78 °C. The solution was allowed to warm to room temperature and was left stirring for 3 h. The solvent was removed under vacuum afterwards, and the crude product was sequentially washed with hexane and diethyl ether. The obtained compound was dried in vacuo resulting **C** as a white

powder (402 mg, 0.73 mmol, 79 %). Crystals suitable for X-ray crystallography were grown by slow diffusion of pentane into a concentrated chloroform solution of the final product. **$^{1}$H NMR (400 MHz, $CDCl_3$, 298 K, ppm)** δ: 7.49 (d, 1H, *J* = 2.4 Hz), 7.33 (d, 2H, *J* = 2.4 Hz), 7.02 (d, 1H, *J* = 2.4 Hz), 6.82 (d, 2H, *J* = 2.4 Hz), 6.05 (br s, 1H), 4.18 (s, 2H), 4.15 (d, 2H, *J* = 15.3 Hz), 3.88 (d, 2H, *J* = 15.3 Hz). **$^{13}$C{$^{1}$H} NMR (100 MHz, $CDCl_3$, 298 K, ppm)** δ: 150.11, 147.44, 132.82, 130.82, 129.94, 126.00, 125.40, 124.91, 124.40, 122.02, 118.33, 117.41, 52.89, 52.78. **$^{11}$B NMR (128 MHz, $CDCl_3$, 298 K, ppm)** δ: 3.08. **HRMS (ESI+, m/z, MeOH)** calculated for $[C_{21}H_{14}BCl_6NO_3+Na]^+$: 573.9066; found: 573.9092. **IR (298 K, cm$^{-1}$)** 3494, 2918, 2436, 2375, 1462, 1362, 1114, 1005, 855. 753.

**Synthesis of compound D**

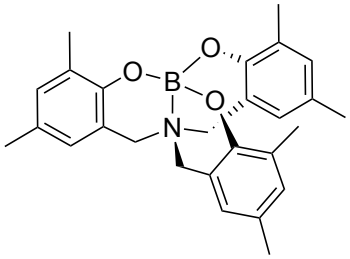


To a stirred solution of **$H_3L^{Me}$** (500 mg, 1.19 mmol) in dichloromethane (15 mL) was added $BCl_3$ (1.0 M in dichloromethane, 1.19 mL, 1.19 mmol) dropwise at −78 °C. The solution was allowed to warm to room temperature and was left stirring for 24 h. The solvent was removed under vacuum afterwards, and the crude product was washed with hexane. The obtained compound was dried in vacuo resulting **D** as a white powder (371 mg, 0.87 mmol, 73 %). **$^{1}$H NMR (400 MHz, $CDCl_3$, 298 K, ppm)** δ: 6.91 (d, 3H, *J* = 1.4 Hz), 6.54 (d, 3H, *J* = 1.4 Hz), 4.12 (br s, 6H), 2.22 (s, 9H), 2.21 (s, 9H). **$^{13}$C{$^{1}$H} NMR (100 MHz, $CDCl_3$, 298 K, ppm)** δ: 148.24, 131.46, 128.32, 128.25, 124.42, 114.81, 56.31, 20.43, 16.29. **$^{11}$B NMR (128 MHz, $CDCl_3$, 298 K, ppm)** δ: 1.80. **HRMS (ESI+, m/z, MeOH)** calculated for $[C_{27}H_{30}BNO_3+Na]^+$: 450.2216; found:

450.2201. **IR (298 K, cm$^{-1}$)** 2911, 1483, 1243, 1108, 855, 811, 728. This data is in agreement with the reported literature.[161]

**Synthesis of compound A'**

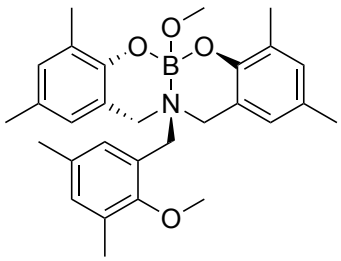

To a solution of **A** (200 mg, 0.44 mmol) in acetonitrile (10 mL) was added potassium carbonate (120 mg, 0.87 mmol) and methyl iodide (247 mg, 1.74 mmol) dropwise and was stirred overnight at room temperature. After this time, the reaction was filtered through celite® and the solvent removed. The crude product was washed with hexane and dried in vacuo resulting **A'** as a white powder (189 mg, 0.40 mmol, 92 %). **$^{1}$H NMR (400 MHz, $CDCl_3$, 298 K, ppm)** δ: 7.07 (d, 2H, *J* = 1.2 Hz), 6.89 (s, 1H), 6.73 (d, 2H, *J* = 1.2 Hz), 6.52 (s, 1H), 4.20 (s, 2H), 4.11 (d, 2H, *J* = 14.6 Hz), 3.69 (d, 2H, *J* = 14.6 Hz), 3.55 (s, 3H), 3.47 (s, 3H), 2.32 (s, 3H), 2.26 (s, 9H), 2.21 (s, 6H). **$^{13}$C{$^{1}$H} NMR (100 MHz, $CDCl_3$, 298 K, ppm)** δ: 156.74, 149.57, 133.66, 133.30, 132.68, 131.66, 130.69, 130.58, 127.65, 127.41, 124.91, 122.60, 116.50, 60.68, 53.29, 50.32, 20.63, 20.46, 16.35, 16.18. **$^{11}$B NMR (128 MHz, $CDCl_3$, 298 K, ppm)** δ: 2.72. **HRMS (ESI+, m/z, MeOH)** calculated for $[C_{29}H_{36}BNO_4+Na]^+$: 496.2635; found: 496.2631. **IR (298 K, cm$^{-1}$)** 2932, 2824, 1483, 1441, 1248, 1225, 1130, 1050, 1009, 863, 814, 728.

## 6.3 Experimental Details for Chapter 3

### 6.3.1 Synthesis of aryl borate catalyst

**Tris(4-methoxyphenyl)borate (E)**

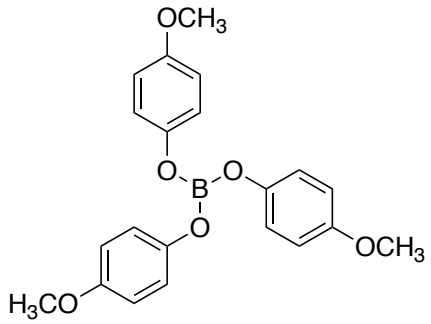

A solution of $BCl_3$ (1.0 M in hexane, 4.85 mL, 4.85 mmol) in dichloromethane (30 mL) was cooled down to –60 °C. In a separate Schlenk tube, a solution of 4-methoxyphenol (1.81 g, 14.55 mmol) in dichloromethane (20 mL) was prepared and was transferred dropwise to the $BCl_3$ solution using a cannula. The reaction mixture was maintained to –60 °C for 4 h whilst stirring and allowed to warm up at room temperature for another 30 min. After the reaction, the solvent was removed under vacuum, and the crude product was cooled down to –35 °C, followed by slow titration with cold pentane. The obtained compound was dried in vacuo to give **E** a solid white product and was stored in the glove box. (1.66 g, 4.37 mmol, 90 %). **$^1$H NMR (400 MHz, $CDCl_3$, 298 K, ppm)** δ: 7.04 (dd, 6H, *J* = 6.74, 2.32 Hz), 6.83 (dd, 6H, *J* = 6.76, 2.30 Hz), 3.87 (s, 9H). **$^{13}$C{$^1$H} NMR (100 MHz, $CDCl_3$, 298 K, ppm)** δ: 155.52, 146.73, 120.80, 114.27, 55.61. **HRMS (ASAP, m/z)** calculated for [$C_{21}H_{21}BO_6$]: 380.1431; found: 380.1482.

**Tris(4-methylphenyl)borate (F)**

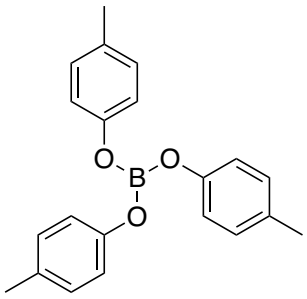

The compound was prepared using the same procedure described for compound **E** except *p*-cresol (1.57 g, 14.55 mmol) was used. **Compound F** was obtained as a white powder (1.47 g, 4.41 mmol, 91 %). **$^1$H NMR (400 MHz, $CDCl_3$, 298 K,**

**ppm)** δ: 7.10 (dd, 6H, *J* = 5.97, 2.20 Hz), 7.00 (dd, 6H, *J* = 6.47, 2.04 Hz), 2.31 (s, 9H). **$^{13}C\{^{1}H\}$ NMR (100 MHz, $CDCl_3$, 298 K, ppm)** δ: 150.76, 132.76, 129.71, 119.93, 20.74. **HRMS (ASAP, m/z)** calculated for [$C_{21}H_{21}BO_3$]: 332.1584; found: 332.1605.

**Tris(4-chlorophenyl)borate (G)**

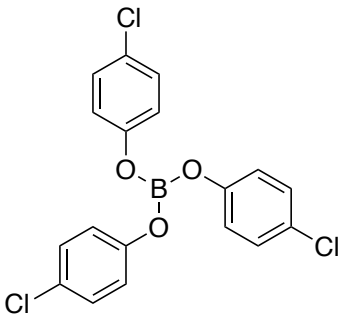


The compound was prepared using the same procedure described for compound **E** except 4-Chlorophenol (1.87 g, 14.55 mmol) was used. **Compound G** was obtained as a white solid product (1.55 g, 3.93 mmol, 81 %). **$^{1}H$ NMR (400 MHz, $CDCl_3$, 298 K, ppm)** δ: 7.28 (dd, 6H, *J* = 6.71, 2.18 Hz), 7.04 (dd, 6H, *J* = 6.72, 2.18 Hz). **$^{13}C\{^{1}H\}$ NMR (100 MHz, $CDCl_3$, 298 K, ppm)** δ: 151.09, 129.40, 129.02, 121.44. **HRMS (ASAP, m/z)** calculated for [$C_{18}H_{12}BCl_3O_3$]: 391.9945; found: 391.9983.

**Tris(4-fluorophenyl)borate (H)**

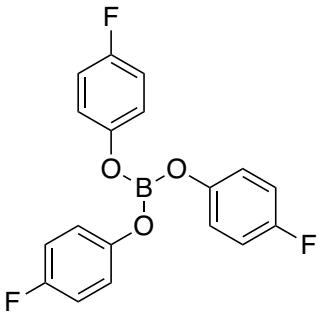


The compound was prepared using the same procedure described for compound **E** except 4-Fluorophenol (1.63 g, 14.55 mmol) was used. **Compound H** was obtained as a yellow powder (1.37 g, 3.98 mmol, 82 %). **$^{1}H$ NMR (400 MHz, $CDCl_3$, 298 K, ppm)** δ: 7.08-7.02 (m, 6H), 7.01-6.97 (m, 6H). **$^{13}C\{^{1}H\}$ NMR (100 MHz, $CDCl_3$, 298 K, ppm)** δ: 160.16, 157.75, 148.61 121.24, 121.16, 115.73. **$^{19}F\{^{1}H\}$ NMR (376 MHz, 298K, ppm)** δ: −120.03. **HRMS (ASAP, m/z)**

calculated for [$C_{18}H_{12}BF_3O_3$]: 344.0832; found: 344.0844.

**Tris(4-(trifluoromethyl)phenyl)borate (I)**

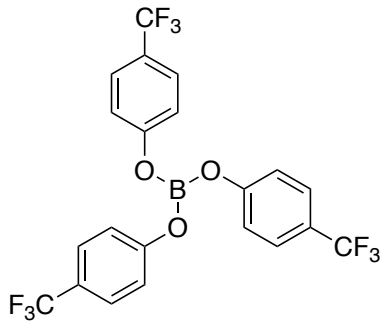

The compound was prepared using the same procedure described for compound **E** except 4-(trifluoromethyl)phenol (2.36 g, 14.55 mmol) was used. **Compound I** was obtained as a pale-yellow powder (2.11 g, 4.27 mmol, 88 %). **$^1$H NMR (400 MHz, $CDCl_3$, 298 K, ppm)** $\delta$: 7.62 (d, 6H, *J* = 8.53 Hz), 7.24 (d, 6H, *J* = 8.53 Hz). **$^{13}$C{$^1$H} NMR (100 MHz, $CDCl_3$, 298 K, ppm)** $\delta$: 154.85, 126.96, 126.93, 120.50. **$^{19}$F{$^1$H} NMR (376 MHz, 298K, ppm)** $\delta$: –61.97. **HRMS (ASAP, m/z)** calculated for [$C_{21}H_{12}BF_9O_3$]: 494.0736; found: 494.0840.

### 6.3.2 General procedure on measuring the Lewis acidity *via* Gutmann Beckett method

This procedure was carried out under an inert atmosphere using the glove box. Dried $CDCl_3$ solvent was purchased and was used directly inside the glove box. A stock solution of 20 mM triethylphosphine oxide ($Et_3PO$) in $CDCl_3$ and 20 mM of each boron aryl compound in $CDCl_3$ were prepared. An aliquot of 0.5 mL boron solution was charged to the NMR tube, and 0.4 mL of $Et_3PO$ solution was added to the tube. A capillary tube with one closed end was filled with $Et_3PO$ solution using a syringe and sealed with Teflon tape. Subsequently, the capillary tube was inserted into the NMR tube containing the mixture. The NMR tube was tightly sealed, and $^{31}$P{$^1$H} NMR was recorded, and the Acceptor Number (AN) calculated using the equation:

$$\mathrm{AN} = 2.21\,(\delta_{\mathrm{sample}} - 41.0) \qquad \textbf{Equation 6.1}$$

## 6.4 Experimental Details for Chapter 4

### 6.4.1 Synthesis of gallium-containing aminotrisphenolate catalyst

**Synthesis of $GaL^{Me}$**

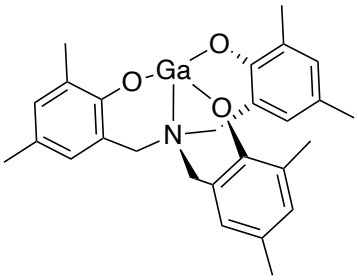


A 100 mL-round bottom flask was charged with **$H_3L^{Me}$** (500 mg, 1.19 mmol), $Ga(OEt)_3$ (307 mg, 1.50 mmol) and toluene (20 mL). The mixture was heated at 110 °C and was left stirring overnight. The flask was allowed to cool down to room temperature, filtered through celite®, and the solvent removed under vacuum. The resulting solid was then washed with hexane (2 × 15 mL) and dried under vacuum to provide **$GaL^{Me}$** as a white powder (592 mg, 81 %). **$^1$H NMR (400 MHz, $CDCl_3$, 298 K, ppm)** δ: 6.90 (s, 3H), 6.61 (s, 3H), 3.71 (br s, 6H), 2.22 (s, 9H), 2.18 (s, 9H). **$^{13}C\{^1H\}$ NMR (100 MHz, $CDCl_3$, 298 K, ppm)** δ: 155.46, 132.20, 129.05, 128.17, 127.29, 119.84, 58.77, 20.36, 16.65. **HRMS (ASAP, m/z)** calculated for $[C_{27}H_{30}GaNO_3+H]^+$: 486.1560; found: 486.1556. The NMR spectra are consistent with those reported in the literature.[196]

**Synthesis of $GaL^{Cl}$.EtOH**

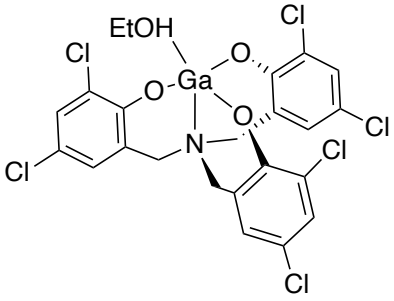


The compound was prepared using the same procedure described for **$GaL^{Me}$** except that **$H_3L^{Cl}$** (607 mg, 1.12 mmol) and $Ga(OEt)_3$ (229 mg, 1.12 mmol) were used. **$GaL^{Cl}$.EtOH** was obtained as a white powder (650 mg, 89 %). The NMR spectra are consistent with those reported in the literature. [196]

### 6.4.2 Synthesis of Aziridine Substrates

**1-isopropyl-2-phenylaziridine (15a)**

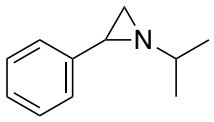

[Step 1] A mixture of styrene oxide (3.6 g, 30 mmol, 3.44 mL) and isopropylamine (1.77 g, 30 mmol, 2.46 mL) was stirred at room temperature under a nitrogen atmosphere. LiBr (130 mg, 5 mol %) was added to the mixture and was left stirring overnight. Once the reaction was completed, which turned to solid, the mixture was diluted with water (20 mL) and extracted with diethyl ether (2 x 20 mL). The combined ethereal extracts were dried with $Mg_2SO_4$ and were concentrated under vacuum to afford the amino alcohol [2-(isopropylamino)-2-phenylethan-1-ol] (5.11 g, 28.5 mmol, 95 %). This product was used in Step 2 without further purification.

[Step 2] (note: it is essential to carry out this procedure under an inert atmosphere) A solution of triphenylphosphine (5.25 g, 20 mmol) in acetonitrile (10 mL) was prepared and placed in an ice bath. An ice-cold solution of bromine (3.20 g, 20 mmol, 1.02 mL) in acetonitrile (10 mL) was added dropwise followed by amino alcohol [2-(isopropylamino)-2-phenylethan-1-ol] (3.59 g, 20 mmol). An ice-cold solution of triethylamine (6.07 g, 60 mmol, 8.35 mL) in acetonitrile (30 mL) was added slowly to the mixture and was left to stir for 1 h at room temperature. The resulting solid, triethylamine hydrobromide/triphenylphosphine oxide, was filtered off, and the filtrate was concentrated under a vacuum. The residue was treated with hexane (5 x 10 mL; upon the final treatment, the viscous reaction residue turned solid), and the accumulated solutions were combined and concentrated to 10 mL. Remaining triphenylphosphine oxide was removed through filtration of the remaining solution, and the solvent was evaporated to provide **15a** as a colourless oil (2.90 g, 18.0 mmol, 90 %). **$^1$H NMR (400 MHz, $CDCl_3$, 298 K, ppm)** $\delta$: 7.30-7.18 (m, 5H), 2.33 (dd, 1H, J = 6.55, 3.32 Hz), 1.88

(d, 1H, J = 3.28 Hz), 1.66-1.58 (m, 2H), 1.17 (d, 6H, J = 6.28 Hz). **$^{13}C\{^{1}H\}$ NMR (100 MHz, $CDCl_3$, 298 K, ppm)** δ: 140.55, 128.24, 126.75, 126.43, 61.89, 40.88, 36.59, 22.38, 21.82. **HRMS (ASAP, m/z)** calculated for $[C_{11}H_{15}N+H]^+$: 162.1283; found: 162.1244.

**2-phenyl-1-propylaziridine (16a)**

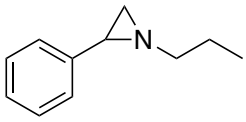

The compound was prepared using the same procedure described for **15a** except propylamine (1.77 g, 30 mmol, 2.46 mL) and styrene oxide (3.6 g, 30 mmol, 3.44 mL) were used. **Compound 16a** was obtained as a white crystalline solid. (2.93 g, 18.2 mmol, 91 %). **$^{1}H$ NMR (400 MHz, $CDCl_3$, 298 K, ppm)** δ: 7.33-7.21 (m, 5H), 2.51 (dt, 1H, J = 11.51, 7.27 Hz), 2.34-2.28 (m, 2H), 1.92 (d, 1H, J = 3.39 Hz), 1.67 (dd, 3H, J = 14.76, 7.20 Hz), 0.98 (t, 3H, J = 7.43 Hz) **$^{13}C\{^{1}H\}$ NMR (100 MHz, $CDCl_3$, 298 K, ppm)** δ: 140.53, 128.27, 126.76, 126.18, 63.61, 41.24, 37.72, 23.05, 12.01. **HRMS (ASAP, m/z)** calculated for $[C_{11}H_{15}N+H]^+$: 162.1283; found: 162.1277.

**1-phenethyl-2-phenylaziridine (17a)**

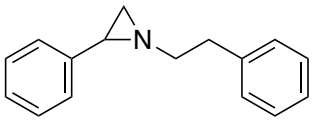

The compound was prepared using the same procedure described for **15a** except phenethylamine (3.64 g, 30 mmol, 3.78 mL) and styrene oxide (3.6 g, 30 mmol, 3.44 mL) were used. **Compound 17a** was obtained as a yellow oil (3.98 g, 17.8 mmol, 89 %). **$^{1}H$ NMR (400 MHz, $CDCl_3$, 298 K, ppm)** δ: 7.32-7.19 (m, 10H), 2.94 (t, 2H, J = 7.60 Hz), 2.76 (dt, 1H, J = 11.50, 7.61 Hz), 2.64-2.57 (m, 1H), 2.30 (dd, 1H, J = 6.54, 3.36 Hz), 1.92 (d, 1H, J = 3.35 Hz), 1.66 (t, 1H, J = 6.29 Hz). **$^{13}C\{^{1}H\}$**

**NMR (100 MHz, $CDCl_3$, 298 K, ppm)** δ: 140.26, 140.00, 128.84, 128.36, 128.25, 126.85, 126.17, 126.08, 63.39, 41.41, 37.90, 36.43. **HRMS (ASAP, m/z)** calculated for $[C_{16}H_{17}N+H]^+$: 224.1439; found: 224.1443.

**7-phenyl-7-azabicyclo[4.1.0]heptane (18a)**

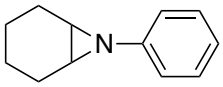

The compound was prepared using the same procedure described for **15a** except aniline (2.79 g, 30 mmol, 2.74 mL) and cyclohexene oxide (2.94 g, 30 mmol, 3.04 mL) were used. **Compound 18a** was obtained as a colourless oil (2.71 g, 15.6 mmol, 78 %). **$^1$H NMR (400 MHz, $CDCl_3$, 298 K, ppm)** δ: 7.02 (t, 1H, J = 7.76 Hz), 6.84 (d, 2H, J = 8.79 Hz), 6.76 (t, 2H, J = 6.09 Hz), 2.22 (d, 2H, J = 4.00 Hz), 1.99-1.95 (m, 2H), 1.82-1.77 (m, 2H), 1.43-1.38 (m, 2H), 1.25-1.07 (m, 2H). **$^{13}$C{$^1$H} NMR (100 MHz, $CDCl_3$, 298 K, ppm)** δ: 155.68, 129.35, 122.2050, 120.41, 39.01, 25.06, 20.28. **HRMS (ASAP, m/z)** calculated for $[C_{12}H_{15}N+H]^+$: 174.1283; found: 174.1245.

**1-isobutyl-2-phenylaziridine (19a)**

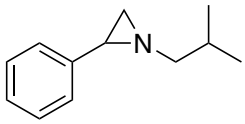

The compound was prepared using the same procedure described for **15a** except isobutylamine (2.19 g, 30 mmol 2.98 mL) and styrene oxide (3.6 g, 30 mmol, 3.44 mL) were used. **Compound 19a** was obtained as a white crystalline solid. (3.15 g, 18.0 mmol, 90 %). **$^1$H NMR (400 MHz, $CDCl_3$, 298 K, ppm)** δ: 7.31-7.19 (m, 5H), 2.45 (dd, 1H, J = 11.56, 7.12 Hz), 2.29 (dd, 1H, J = 6.48, 3.28 Hz), 2.7 (dd, 1H, J = 11.57, 6.50 Hz), 1.93-1.87 (m, 2H), 1.66 (d, 1H, J = 6.56 Hz), 0.97 (dd, 6H, J = 15.53, 6.68 Hz) **$^{13}$C{$^1$H} NMR (100 MHz, $CDCl_3$, 298 K, ppm)** δ: 140.62, 128.25,

126.71, 126.16, 69.72, 41.51, 37.84, 29.27, 20.99, 20.95. **HRMS (ASAP, m/z)** calculated for $[C_{12}H_{17}N+H]^+$: 176.1439; found: 176.1442.

**1-(4-methoxybenzyl)-2-phenylaziridine (20a)**

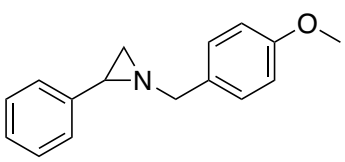

The compound was prepared using the same procedure described for **15a** except 4-methoxylbenzylamine (4.12 g, 30 mmol, 3.92 mL) and styrene oxide (3.6 g, 30 mmol, 3.44 mL) were used. **Compound 20a** was obtained as a colourless oil (4.21 g, 17.6 mmol, 88 %). **$^1$H NMR (400 MHz, $CDCl_3$, 298 K, ppm)** δ: 7.35-7.26 (m, 7H), 6.88 (dd, 2H, J = 6.61, 2.10 Hz), 3.83 (s, 3H), 3.61 (q, 2H, J = 14.24 Hz), 2.52 (dd, 1H, J = 6.51, 3.37Hz), 1.99 (d, 1H, J = 3.34 Hz), 1.86 (d, 1H, J = 6.54 Hz). **$^{13}$C{$^1$H} NMR (100 MHz, $CDCl_3$, 298 K, ppm)** δ: 158.66, 140.19, 131.23, 129.10, 128.28, 126.85, 126.27, 113.77, 64.20, 55.27, 41.39, 37.81. **HRMS (ASAP, m/z)** calculated for $[C_{16}H_{17}NO+H]^+$: 240.1388; found: 240.1201.

**1-cyclohexyl-2-phenylaziridine (21a)**

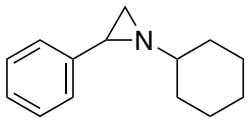

The compound was prepared using the same procedure described for **15a** except cyclohexylamine (2.98 g, 30 mmol, 3.44 mL) and styrene oxide (3.6 g, 30 mmol, 3.44 mL) were used. Compound **21a** was obtained as a colourless oil (3.51 g, 17.4 mmol, 87 %). **$^1$H NMR (400 MHz, $CDCl_3$, 298 K, ppm)** δ: δ: 7.30-7.18 (m, 5H), 2.35 (dd, 1H, J = 6.58, 3.36 Hz), 1.89-1.17 (m, 13H). **$^{13}$C{$^1$H} NMR (100 MHz, $CDCl_3$, 298 K, ppm)** δ: 140.71, 128.22, 126.70, 126.47, 69.76, 40.16, 35.92, 33.00, 32.32, 26.17, 24.91, 24.87. **HRMS (ASAP, m/z)** calculated for $[C_{14}H_{19}N+H]^+$: 202.1596; found: 202.1474.

**1-hexyl-2-phenylaziridine (22a)**

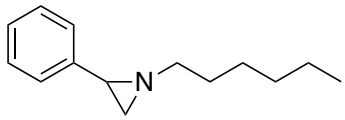

The compound was prepared using the same procedure described for **15a** except hexylamine (3.04 g, 30 mmol, 3.96 mL) and styrene oxide (3.6 g, 30 mmol, 3.44 mL) were used. Compound **22a** was obtained as a colourless oil (3.74 g, 18.4 mmol, 92 %). **$^{1}$H NMR (400 MHz, $CDCl_3$, 298 K, ppm)** δ: 7.31-7.20 (m, 5H), 2.48 (dt, 1H, J = 14.81, 5.75 Hz), 2.36-2.28 (m, 2H), 1.89 (t, 1H, J = 3.45 Hz), 1.66-1.58 (m, 3H), 1.38-1.25 (m, 6H), 0.88 (t, 3H, J = 6.94 Hz). **$^{13}$C{$^{1}$H} NMR (100 MHz, $CDCl_3$, 298 K, ppm)** δ: 140.54, 128.26, 126.75, 126.18, 61.92, 41.27, 37.78, 31.84, 29.80, 27.14, 22.61, 14.06. **HRMS (ASAP, m/z)** calculated for $[C_{14}H_{21}N+H]^+$: 204.1752; found: 204.1772.

**1-(4-chlorophenyl)-2-phenylaziridine (23a)**

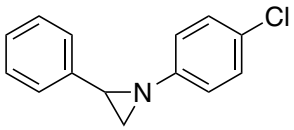

The compound was prepared using the same procedure described for **15a** except 4-chloroaniline (3.83 g, 30 mmol, 2.68 mL) and styrene oxide (3.6 g, 30 mmol, 3.44 mL) were used. **Compound 24a** was obtained as a colourless oil (3.68 g, 16.0 mmol, 80 %). **$^{1}$H NMR (400 MHz, $CDCl_3$, 298 K, ppm)** 7.37-7.30 (m, 5H), 7.21 (dd, 2H, J = 6.64, 2.12 Hz), 6.98 (dd, 2H, J = 6.65, 2.12 Hz), 3.08 (dd, 1H, J = 6.44, 3.39 Hz), 2.43 (dddd, 2H, J = 4.93, 7.02, 1.07 Hz). **$^{13}$C{$^{1}$H} NMR (100 MHz, $CDCl_3$, 298 K, ppm)** δ: 153.13, 138.92, 128.99, 128.53, 127.50, 126.16, 121.85, 41.84, 37.77. **HRMS (ASAP, m/z)** calculated for $[C_{14}H_{12}ClN+H]^+$: 230.0737; found: 230.0612.

**1,2-diphenylaziridine (24a)**

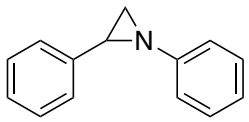

The compound was prepared using the same procedure described for **15a** except aniline (2.79 g, 30 mmol, 2.74 mL) and styrene oxide (3.6 g, 30 mmol, 3.44 mL) were used. **Compound 25a** was obtained as a colourless oil (3.32 g, 17.0 mmol, 85 %). **$^{1}$H NMR (400 MHz, $CDCl_3$, 298 K, ppm)** δ: 7.43-7.39 (m, 4H), 7.37-7.26 (m, 3H), 7.11 (d, 2H, J = 8.07 Hz), 7.04 (t, 1H, J = 7.33 Hz), 3.14 (dd, 1H, J = 6.36, 3.29 Hz), 2.50 (d, 1H, J = 6.44 Hz), 2.44 (d, 1H, J = 3.25 Hz). **$^{13}$C{$^{1}$H} NMR (100 MHz, $CDCl_3$, 298 K, ppm)** δ: 154.57, 139.46, 129.07, 128.51, 127.36, 126.23, 122.57, 120.60, 41.60, 37.63. **HRMS (ASAP, m/z)** calculated for $[C_{14}H_{13}N+H]^+$: 196.1126; found: 196.1138.

**1-(4-ethoxyphenyl)-2-phenylaziridine (25a)**

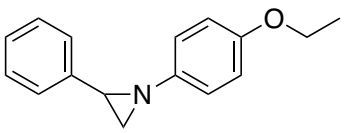

The compound was prepared using the same procedure described for **15a** except 4-ethoxyaniline (4.12 g, 30 mmol, 3.86 mL) and styrene oxide (3.6 g, 30 mmol, 3.44 mL) were used. **Compound 23a** was obtained as a colourless oil (3.92 g, 16.4 mmol, 82 %). **$^{1}$H NMR (400 MHz, $CDCl_3$, 298 K, ppm)** δ: 7.39-7.26 (m, 5H), 6.98 (dd, 2H, J = 6.68, 2.24 Hz), 6.80 (dd, 2H, J = 6.67, 2.24 Hz), 3.99 (q, 2H, J = 6.98 Hz), 3.03 (dd, 1H, J = 6.48, 3.37 Hz), 2.41 (dd, 1H, J = 6.48, 1.10 Hz), 2.37 (dd, 1H, J = 3.38, 1.11 Hz), 1.39 (t, 3H, J = 6.99 Hz) . **$^{13}$C{$^{1}$H} NMR (100 MHz, $CDCl_3$, 298 K, ppm)** δ: 154.57, 147.81, 139.57, 128.45, 127.25, 126.19, 121.31, 115.00, 63.78, 41.89, 37.82, 14.94. **HRMS (ASAP, m/z)** calculated for $[C_{16}H_{17}NO+H]^+$: 240.1388; found: 240.1222.

**2-(4-chlorophenyl)-1-phenylaziridine (26a)**

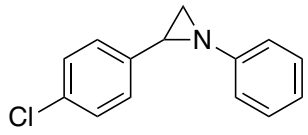

The compound was prepared using the same procedure described for **15a** except aniline (2.80 g, 30 mmol, 2.74 mL) and 4-chlorostyrene oxide (4.64 g, 30 mmol, 3.62 mL) were used. **Compound 26a** was obtained as a colourless oil (3.32 g, 17.0 mmol, 85 %). **$^1$H NMR (400 MHz, $CDCl_3$, 298 K, ppm)** δ: δ: 7.30-7.18 (m, 6H), 6.98-6.92 (m, 3H), 3.01 (dd, 1H, J = 6.41, 3.29 Hz), 2.41 (dd, 1H, J = 6.41, 1.12 Hz), 2.29 (dd, 1H, J = 3.27, 1.16 Hz). **$^{13}$C{$^1$H} NMR (100 MHz, $CDCl_3$, 298 K, ppm)** δ: 154.21, 138.05, 133.05, 129.12, 128.63, 127.56, 122.73, 120.51, 40.93, 37.75. **HRMS (ASAP, m/z)** calculated for $[C_{14}H_{12}ClN+H]^+$: 230.0737; found: 230.0733.

### 6.4.3 General procedure for carboxylation of aziridine with $CO_2$

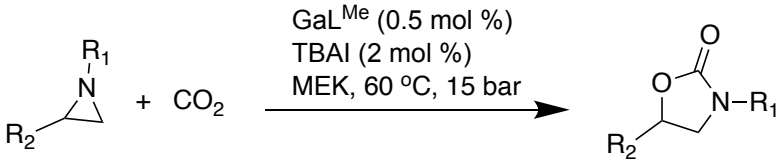


**Scheme 6.2** General procedure for the carboxylation of aziridine with $CO_2$.

A 50 mL high-pressure reactor equipped with a magnetic stir bar was charged with isopropyl-2-phenylaziridine (**15a**) (1.0 g, 6.2 mmol), **GaL$^{Me}$** catalyst (15.1 mg, 0.031 mmol), $Bu_4NI$ (45.8 mg, 0.1240 mmol) and MEK (1.0 mL). Then solid $CO_2$ (~2.5 g) was added immediately upon closing the reactor and was left stirring at 60°C for 24 h. After the reaction, the reactor was allowed to cool down in an ice bath, and the pressure was slowly decreased to ambient pressure. An aliquot of the resultant mixture was then collected and dissolved in $CDCl_3$. The percent conversion of the sample was based on the NMR yield taken from the $^1H$ NMR

spectrum of the crude sample mixture using mesitylene as an internal standard. The crude mixture was purified using a flash column chromatography eluting with gradient 70:30 hexane/ethyl acetate, and the product was further characterised by NMR, FT-IR and HRMS, which were consistent with those reported in the literature and in good agreement with the assigned structures.

**3-isopropyl-5-phenyloxazolidin-2-one (15b)**[242]

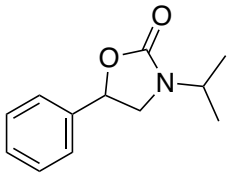

Colourless oil. **$^{1}$H NMR (400 MHz, $CDCl_3$, 298 K, ppm)** δ: 7.41-7.34 (m, 5H), 5.48 (t, 1H, J = 8.12 Hz), 4.19 (qui, 1H, J = 6.77 Hz), 3.86 (t, 1H, J = 8.70 Hz), 3.37 (dd, 1H, J = 8.55, 7.52 Hz), 1.22 (d, 3H, J = 6.79 Hz), 1.16 (d, 3H, J = 6.75 Hz). **$^{13}$C{$^{1}$H} NMR (100 MHz, $CDCl_3$, 298 K, ppm)** δ: 157.15, 139.00, 128.91, 128.76, 125.48, 74.52, 47.40, 44.90, 20.06, 19.58. **HRMS (ASAP, m/z)** calculated for $[C_{12}H_{15}NO_2+H]^+$: 206.1181; found: 206.1139. **FT-IR ($\nu_{CO}$)** 1738 cm$^{-1}$.

**5-phenyl-3-propyloxazolidin-2-one (16b)**[242]

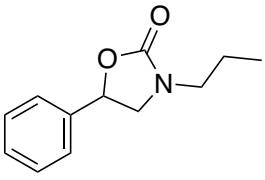

Colourless oil. **$^{1}$H NMR (400 MHz, $CDCl_3$, 298 K, ppm)** δ: 7.40-7.34 (m, 5H), 5.49 (dd, 1H, J = 8.53, 7.67 Hz), 3.91 (t, 1H, J = 8.74 Hz), 3.43 (dd, 1H, J = 8.65, 7.42 Hz), 3.34-3.20 (m, 2H), 1.59 (dd, 2H, J = 7.36 Hz), 0.94 (t, 3H, J = 7.40 Hz). **$^{13}$C{$^{1}$H} NMR (100 MHz, $CDCl_3$, 298 K, ppm)** δ: 158.01, 138.91, 128.92, 128.78, 125.50, 74.32, 52.18, 45.83, 20.68, 11.10. **HRMS (ASAP, m/z)** calculated for $[C_{12}H_{15}NO_2+H]^+$: 206.1181; found: 206.1142. **IR ($\nu_{CO}$)** 1745 cm$^{-1}$.

**3-phenethyl-5-phenyloxazolidin-2-one (17b)**[243]

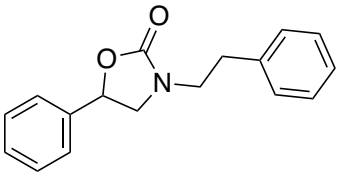

Colourless oil. **$^{1}$H NMR (400 MHz, $CDCl_3$, 298 K, ppm)** δ: 7.28-7.11 (m, 10H), 5.30 (dd, 1H, J = 8.74, 7.32 Hz), 3.65 (t, 1H, J = 8.73 Hz), 3.48 (t, 2H, J = 7.13 Hz), 3.21 (dd, 1H, J = 8.57, 7.27 Hz), 2.81 (td, 2H, J = 7.22, 2.64 Hz). **$^{13}$C{$^{1}$H} NMR (100 MHz, $CDCl_3$, 298 K, ppm)** δ: 157.79, 138.72, 138.22, 128.85, 128.79, 128.72, 126.69, 125.59, 74.38, 52.67, 45.44, 34.01. **HRMS (ASAP, m/z)** calculated for $[C_{17}H_{17}NO_2+H]^+$: 268.1338; found: 268.1333. **IR ($\nu_{CO}$)** 1740 cm$^{-1}$.

**3-phenylhexahydrobenzo[d]oxazol-2(3H)-one (18b)**[244]

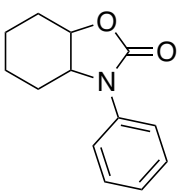

Colourless oil. **$^{1}$H NMR (400 MHz, $CDCl_3$, 298 K, ppm)** δ: 7.41-7.38 (m, 2H), 7.23-7.16 (m, 3H), 4.09-4.00 (m, 1H), 3.63-3.57 (m, 1H), 2.37-2.28 (m, 2H), 2.02-1.92 (m, 2H), 1.81-1.42 (m, 4H). **$^{13}$C{$^{1}$H} NMR (100 MHz, $CDCl_3$, 298 K, ppm)** δ: 155.52, 137.07, 129.02, 125.39, 122.05, 81.30, 63.84, 28.73, 28.34, 23.46, 23.29. **HRMS (ASAP, m/z)** calculated for $[C_{12}H_{15}NO_2$ +H]$^+$: 218.1181; found: 218.1711. **IR ($\nu_{CO}$)** 1745 cm$^{-1}$.

**3-isobutyl-5-phenyloxazolidin-2-one (19b)**[242]

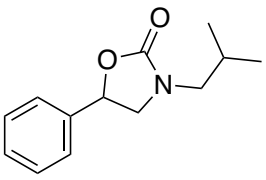

White solid. **$^{1}$H NMR (400 MHz, $CDCl_3$, 298 K, ppm)** δ: 7.41-7.35 (m, 5H), 5.49 (dd, 1H, J = 8.58, 7.60 Hz), 3.92 (t, 1H, J = 8.77 Hz), 3.43 (dd, 1H, J = 8.81, 7.30 Hz), 3.17-3.04 (m, 2H), 1.88 (qui, 1H, J = 6.94 Hz), 0.93 (t, 6H, J = 6.78, 6.58 Hz). **$^{13}$C{$^{1}$H} NMR (100 MHz, $CDCl_3$, 298 K, ppm)** δ: 158.25, 138.94, 128.92, 128.78, 125.48, 74.31, 52.86, 51.81, 26.87, 19.93, 19.90. **HRMS (ASAP, m/z)** calculated for $[C_{13}H_{17}NO_2+H]^+$: 220.1338; found: 220.1346. **IR ($\nu_{CO}$)** 1735 cm$^{-1}$.

**3-(4-methoxybenzyl)-5-phenyloxazolidin-2-one (20b)**

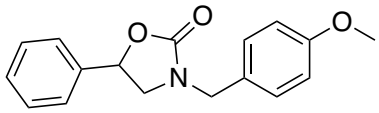

Pale yellow oil. **$^1$H NMR (400 MHz, $CDCl_3$, 298 K, ppm)** δ: 7.37-7.33 (m, 3H), 7.31-7.26 (m, 2H), 7.22 (d, 2H, J = 8.43 Hz), 6.87 (d, 2H, J = 8.42 Hz), 5.45 (t, 1H, J = 8.14 Hz), 4.48 (d, 1H, J = 14.68 Hz), 4.35 (d, 1H, J = 14.68 Hz), 3.80 (s, 3H), 3.76-3.72 (m, 1H), 3.28 (t, 1H, J = 8.17 Hz). **$^{13}$C{$^1$H} NMR (100 MHz, $CDCl_3$, 298 K, ppm)** δ: 159.41, 138.64, 129.59, 128.88, 128.79, 127.65, 125.53, 114.22, 74.52, 55.31, 51.43, 47.83. **HRMS (ASAP, m/z)** calculated for $[C_{17}H_{17}NO_2+H]^+$: 284.1287; found: 284.1293. **IR ($\nu_{CO}$)** 1747 cm$^{-1}$.

**3-cyclohexyl-5-phenyloxazolidin-2-one (21b)**[242]

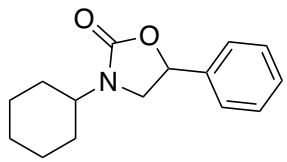

White crystals. **$^1$H NMR (400 MHz, $CDCl_3$, 298 K, ppm)** δ: 7.41-7.31 (m, 5H), 5.47 (t, 1H, J = 8.08 Hz), 3.88 (t, 1H, J = 8.73 Hz), 3.78-3.72 (m, 1H), 3.39 (t, 1H, J = 8.02 Hz), 1.87-1.00 (m, 10H). **$^{13}$C{$^1$H} NMR (100 MHz, $CDCl_3$, 298 K, ppm)** δ: 157.24, 139.07, 128.89, 128.73, 125.49, 74.59, 52.57, 48.33, 30.58, 30.11, 25.38, 25.32, 25.29. **HRMS (ASAP, m/z)** calculated for $[C_{15}H_{19}NO_2+H]^+$: 246.1494; found: 246.1494. **IR ($\nu_{CO}$)** 1737 cm$^{-1}$.

**3-hexyl-5-phenyloxazolidin-2-one (22b)**[194]

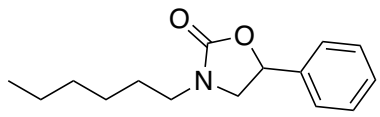

Colourless oil. **$^1$H NMR (400 MHz, $CDCl_3$, 298 K, ppm)** δ: 7.40-7.33 (m, 5H), 5.48 (t, 1H, J = 8.09 Hz), 3.91 (t, 1H, J = 8.73 Hz), 3.42 (dd, 1H, J = 8.65, 7.42 Hz), 3.36-3.22 (m, 2H), 1.58-1.50 (m, 2H), 1.30-1.29 (m, 6H), 0.87 (t, 3H, J = 6.73 Hz). **$^{13}$C{$^1$H} NMR (100 MHz, $CDCl_3$, 298 K, ppm)** δ: 157.93, 138.93, 128.90, 128.77, 125.50, 74.31,

52.17, 44.21, 31.41, 27.32, 26.28, 22.53, 14.00. **HRMS (ASAP, m/z)** calculated for $[C_{15}H_{21}NO_2+H]^+$: 248.1651; found: 248.1613. **IR ($\nu_{CO}$)** 1743 $cm^{-1}$.

**3-(4-ethoxyphenyl)-5-phenyloxazolidin-2-one (23b)**

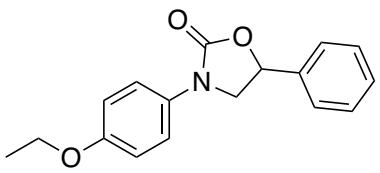

Pale yellow oil. **$^1$H NMR (400 MHz, $CDCl_3$, 298 K, ppm)** δ: 7.44-7.42 (m, 7H), 6.91-6.89 (m, 2H), 5.62 (dd, 1H, J = 8.64, 7.60 Hz), 4.33 (t, 1H, J = 8.80 Hz), 4.01 (q, 2H, J = 6.99 Hz), 3.93-3.90 (m, 1H), 1.42-1.40 (m, 3H). **$^{13}$C{$^1$H} NMR (100 MHz, $CDCl_3$, 298 K, ppm)** δ: 155.66, 154.69, 137.51, 131.24, 129.02, 128.97, 125.74, 120.40, 114.46, 74.10, 63.73, 53.63, 14.96. **HRMS (ASAP, m/z)** calculated for $[C_{17}H_{17}NO_3+H]^+$: 284.1287; found: 284.1306. **IR ($\nu_{CO}$)** 1713 $cm^{-1}$.

**3-(4-chlorophenyl)-5-phenyloxazolidin-2-one (24b)**

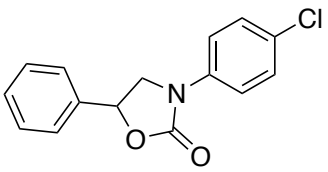

Colourless oil. **$^1$H NMR (400 MHz, $CDCl_3$, 298 K, ppm)** δ: 7.55-7.53 (m, 2H), 7.46-7.41 (m, 5H), 7.31-7.28 (m, 2H), 5.60 (t, 1H, J = 6.97 Hz), 4.34 (dd, 1H, J = 8.88, 5.10 Hz), 3.88 (dd, 2H, J = 8.53, 7.78 Hz). **$^{13}$C{$^1$H} NMR (125 MHz, $CDCl_3$, 298 K, ppm)** δ: 154.42, 138.19, 136.85, 129.24, 129.18, 129.08, 129.00, 125.49, 119.12, 74.64, 51.75. **HRMS (ASAP, m/z)** calculated for $[C_{15}H_{12}ClNO_2+H]^+$: 274.0635; found: 274.0677. **IR ($\nu_{CO}$)** 1710 $cm^{-1}$.

**3,5-diphenyloxazolidin-2-one (25b)**[192]

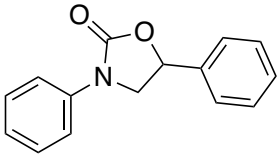

Colourless oil. **$^1$H NMR (400 MHz, $CDCl_3$, 298 K, ppm)** δ: 7.54-7.50 (m, 2H), 7.37-7.28 (m, 7H), 7.14-7.10 (m, 1H), 5.61 (dd, 1H, J = 8.62, 7.58 Hz), 4.35 (dt, 1H, J = 12.38, 8.83 Hz ), 3.92 (ddd, 1H, J = 15.30, 8.90, 7.53 Hz). **$^{13}$C{$^1$H} NMR (125 MHz,**

**$CDCl_3$, 298 K, ppm)** δ: 154.70, 138.14, 138.12, 129.10, 129.04, 125.69, 124.17, 118.29, 74.06, 52.70. **HRMS (ASAP, m/z)** calculated for $[C_{15}H_{13}NO_2+H]^+$: 240.1025; found: 240.1005. **IR ($\nu_{CO}$)** 1752 $cm^{-1}$.

**3-tosyloxazolidin-2-one (27b)**

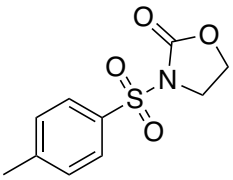

White crystals. **$^1$H NMR (400 MHz, $CDCl_3$, 298 K, ppm)** δ: 7.94 (d, 2H, J = 7.99 Hz), 7.37 (d, 2H, J = 8.04 Hz), 4.36 (t, 2H, J = 7.74 Hz), 4.05 (t, 2H, J = 7.74 Hz), 2.45 (s, 3H). **$^{13}$C{$^1$H} NMR (100 MHz, $CDCl_3$, 298 K, ppm)** δ: 152.04, 145.86, 133.79, 129.94, 128.34, 62.26, 44.61, 21.75. **HRMS (ASAP, m/z)** calculated for $[C_{10}H_{11}NO_4S+H]^+$: 242.0487; found: 242.0497. **IR ($\nu_{CO}$)** 1762 $cm^{-1}$.

**(5S)-5-(hydroxymethyl)-3-((R)-1-phenylethyl)-3l4-oxazolidin-2-one (28b)**

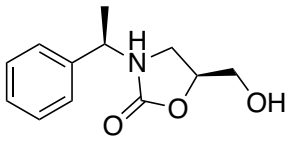

White crystals. **$^1$H NMR (400 MHz, $CDCl_3$, 298 K, ppm)** δ: 7.36-7.29 (m, 5H), 5.22 (q, 1H, J = 7.10 Hz), 4.62-4.56 (m, 1H), 3.77-3.71 (m, 1H), 3.57-3.50 (m, 2H), 3.03 (dd, 1H, J = 8.57, 6.54 Hz), 1.94 (t, 1H, J = 6.65 Hz), 1.59 (t, 3H, J = 3.55 Hz). **$^{13}$C{$^1$H} NMR (100 MHz, $CDCl_3$, 298 K, ppm)** δ: 157.35, 139.33, 128.73, 127.88, 126.91, 73.54, 63.28, 51.50, 41.50, 16.61. **HRMS (ASAP, m/z)** calculated for $[C_{12}H_{16}NO_3+H]^+$: 222.1130; found: 222.1104. **IR ($\nu_{CO}$)** 1700 $cm^{-1}$.

**1,4-bis(4-chlorophenyl)-2,5-diphenylpiperazine (29)**

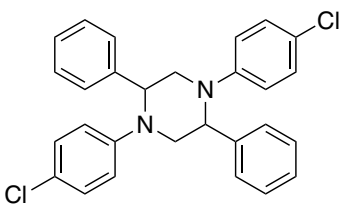

White crystals. **$^1$H NMR (400 MHz, $CDCl_3$, 298 K, ppm)** δ: 7.35 (d, 4H, J = 7.09 Hz), 7.27-7.23 (m, 4H), 7.20-7.16 (m, 2H), 6.97 (dd, 4H, J = 6.88, 2.18 Hz),

6.57 (dd, 4H, J = 6.88, 2.19 Hz), 4.70 (q, 2H, J = 3.92 Hz), 3.98 (dd, 2H, J = 12.94, 3.90 Hz), 3.62 (dd, 2H, J = 12.92, 7.97 Hz). **$^{13}C\{^{1}H\}$ NMR (100 MHz, $CDCl_3$, 298 K, ppm)** δ: 148.19, 141.04, 128.70, 128.60, 127.54, 126.78, 124.15, 117.85, 62.86, 55.41. **HRMS (ASAP, m/z)** calculated for $[C_{28}H_{24}Cl_2N_2+H]^+$: 459.1395; found: 459.1443.

**1,2,4,5-tetraphenylpiperazine (30)**

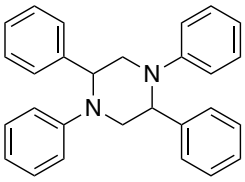

White crystals. **$^{1}H$ NMR (400 MHz, $CDCl_3$, 298 K, ppm)** δ: 7.43-7.40 (m, 4H), 7.39-7.35 (m, 4H), 7.28 (t, 2H, J = 8.37 Hz), 7.16 (dd, 4H, J = 8.80, 7.28 Hz), 6.77-6.68 (m, 6H), 4.88 (dd, 2H, J = 10.41, 5.25 Hz), 4.21 (dd, 2H, J = 14.73, 5.26 Hz), 3.80 (dd, 2H, J = 14.74, 10.45 Hz). **$^{13}C\{^{1}H\}$ NMR (100 MHz, $CDCl_3$, 298 K, ppm)** δ: 148.60, 141.24, 129.24, 128.95, 127.46, 126.12, 117.70, 113.57, 61.14, 49.64. **HRMS (ASAP, m/z)** calculated for $[C_{28}H_{26}N_2+H]^+$: 391.2174; found: 391.2234.

**1,4-bis(4-ethoxyphenyl)-2,5-diphenylpiperazine (31)**

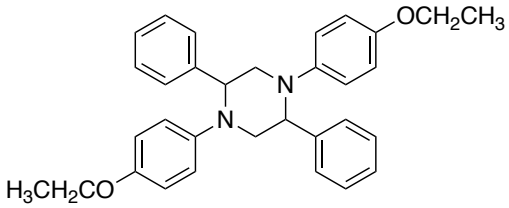

White crystals. **$^{1}H$ NMR (400 MHz, $CDCl_3$, 298 K, ppm)** δ: 7.54 (d, 4H, J = 7.13 Hz), 7.31-7.27 (m, 4H), 7.24-7.20 (m, 2H), 6.80-6.71 (m, 8H), 4.70 (dd, 2H, J = 7.86, 4.58 Hz), 3.91 (q, 4H, J = 6.99 Hz), 3.75-3.63 (m, 4H), 1.34 (t, 6H, J = 6.99 Hz). **$^{13}C\{^{1}H\}$ NMR (100 MHz, $CDCl_3$, 298 K, ppm)** δ: 152.56, 143.81, 141.19, 128.40, 127.41, 127.09, 118.50, 115.15, 63.74, 61.70, 53.61, 14.96. **HRMS (ASAP, m/z)** calculated for $[C_{32}H_{34}N_2O_2+H]^+$: 479.2699; found: 479.2765 .

**2,5-bis(4-chlorophenyl)-1,4-diphenyl-1l4-piperazine (32)**

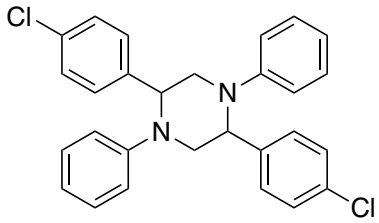

White crystals. **$^{1}$H NMR (400 MHz, $CDCl_3$, 298 K, ppm)** δ: 7.57-7.52 (m, 2H, J = 7.09 Hz), 7.49-7.43 (m, 4H), 7.34-7.31 (m, 4H), 7.20-7.14 (m, 4H), 7.10-7.06 (m, 4H), 4.82 (dd, 2H, J = 9.86, 5.04 Hz), 4.08 (dd, 2H, J = 14.43, 5.00 Hz), 3.72 (dd, 2H, J = 14.46, 9.87 Hz). **$^{13}$C{$^{1}$H} NMR (100 MHz, $CDCl_3$, 298 K, ppm)** δ: 149.57, 140.00, 129.30, 129.13, 128.70, 127.75, 120.24, 117.84, 62.32, 56.75. **HRMS (ASAP, m/z)** calculated for $[C_{28}H_{24}Cl_2N_2+H]^+$: 459.1395; found: 459.1397.

### 6.4.4 Synthesis of functionalised cellulose

#### 6.4.4.1 Synthesis of epoxide functionalised cellulose (33)

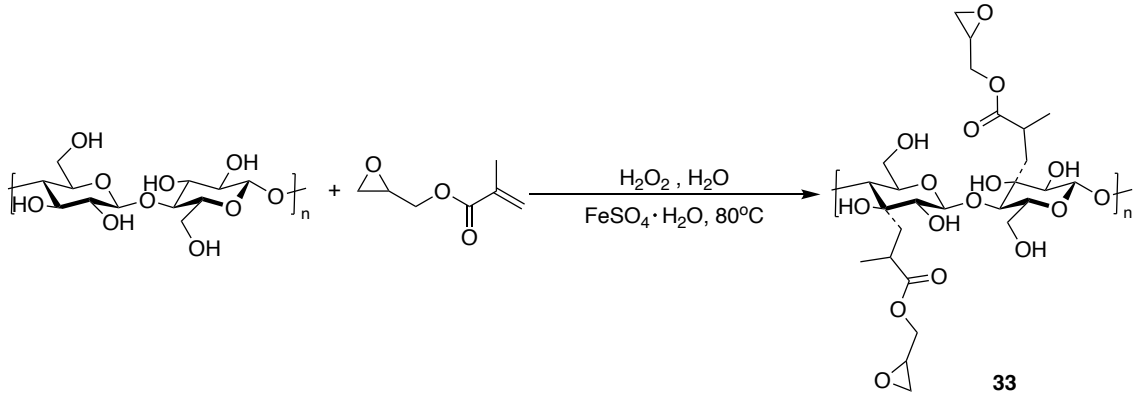


33

A 500 mL three-neck round bottom flask with a stirrer was added with 300 mL of water and heated to 80 °C. Afterwards, 6 g of cellulose fibres were added and allowed to swell for an hour while maintaining the temperature. Using an inlet funnel, a freshly prepared stock solution of 0.15 M $FeSO_4.7H_2O$ (8 mL) was added dropwise to the flask and followed by the dropwise addition of 30% $H_2O_2$ solution (50 mL) and was left stirring for 30 minutes. Then, 12 mL of glycidyl methacrylate (GMA) was added and was left stirring for 30 minutes. Subsequently, the flask was allowed to cool down, and the fibre was filtered and

washed with acetone. The residue was further washed with acetone using Soxhlet extraction for 24 h. The white cellulose solid was dried under vacuum and the FT-IR spectrum obtained. **IR ($\nu_{CO}$)** 1723 cm$^{-1}$.

#### 6.4.4.2 Synthesis of cyclic carbonate functionalised cellulose (34)

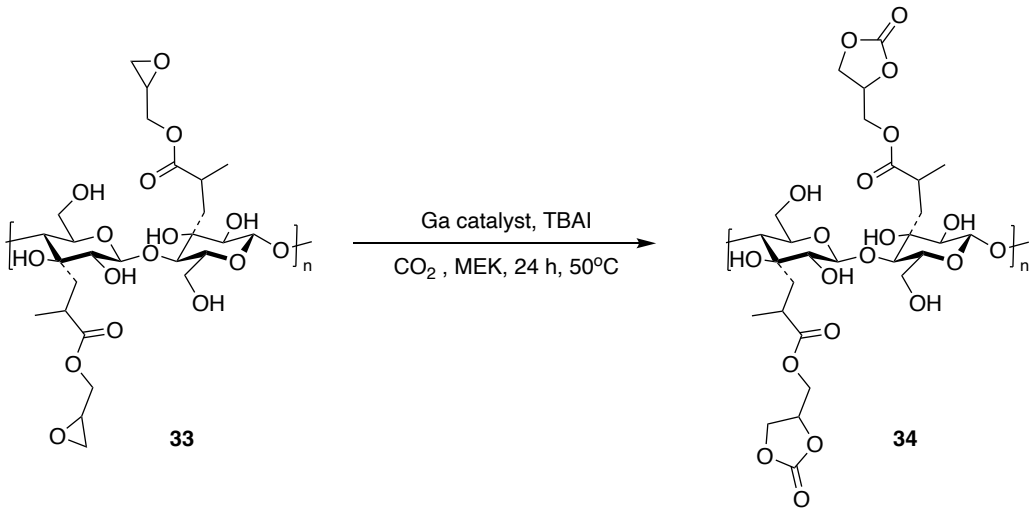


33 34

A 50 mL pressure reactor equipped with a stirrer was charged with Ga catalyst (5.0 mg), $Bu_4NI$ (184 mg), epoxide functionalised cellulose (1.0 g), and MEK (5 mL) solvent. A freshly prepared dry ice (2.90 g) was introduced, and the reactor was sealed immediately and was left stirring for 24 h at 50 °C. Afterwards, the reactor was allowed to cool down, and the pressure was slowly released. The product was then removed from the reaction chamber and was filtered using Buchner filtration and washed with acetone. The solvent was removed using a vacuum, and the product was analysed using FT-IR. **IR ($\nu_{CO}$, cm$^{-1}$)** 1790, 1720.

### 6.4.5 General procedure for antimicrobial assay of cyclic carbonate functionalised cellulose

**Bacteria**

*Staphylococcus aureus* SH 1000 and *Escherichia coli* JM 109 were obtained from an antimicrobial laboratory-acquired from Dr. Sarah Forbe's group at Sheffield Hallam University, Sheffield, United Kingdom.

**Chemical reagents and growth media**

Bacteriological growth media were purchased from Oxoid Ltd. Unless otherwise stated, all other chemical reagents were purchased from Merck (Dorset, United Kingdom). Bacterial growth media were sterilised at 121 °C and 15 psi for approximately 30 min prior to use.

**Sample disc-diffusion method**

Disc diffusion method was executed according to the British Society for Antimicrobial Chemotherapy (BSAC) standardised disc susceptibility testing method with minor modification.[216] Bacteria were cultured on Mueller Hinton Agar (MHA) and Broth. All bacteria were incubated aerobically at 37°C for 18 h unless stated otherwise.

**Inoculum preparation (Setting up an overnight culture)**

A single colony of bacteria was taken off from the streak of each bacterium plate and was placed in a sterile universal tube with 5 mL Mueller Hinton Broth (MHB) using an inoculation loop. The broth was incubated overnight with shaking (100-200 rpm) at 37°C. Following incubation, a spectrophotometer was set to 600 nm with 1 mL of fresh MHB as blank. The absorbance of the prepared inoculum was measured and was diluted based on the dilution factor from the equation:

$$\boldsymbol{Dilution\ factor} = \frac{\boldsymbol{OD_{measured}}}{\boldsymbol{OD_{600}}} \qquad \textbf{Equation 6.2}$$

where $OD_{600}$ is $0.008$.

**Inoculation of MHA plate**

Three biological replicates were prepared for each organism. From the standardised inoculum, 100 µL was taken and placed in the MHA plate. The

inoculum was spread evenly to the entire surface of the plate using an L-shaped spreader. The plate was left to dry, and the sample disc was placed on the surface of the plate. Before adding the sample disc, the spatula used to place the disc to the plate was sterilised in each disc placed in the plate. The plate was then incubated overnight, and the inhibition zone was measured using a ruler.

## 6.5 Experimental Details for Chapter 5

### 6.5.1 Synthesis of Indium-containing aminotrisphenolate catalyst

**Compound $InL^{Me}(MeIm)_2$**

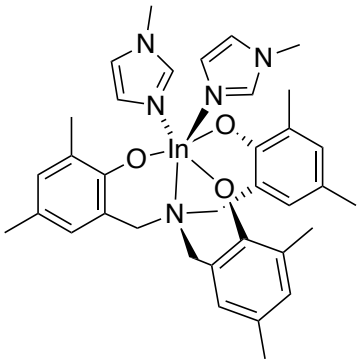


Using a 100 mL Schlenk tube, lithium methoxide solution (4.76 mL, 1.0 M in MeOH) was added dropwise to a solution of **$H_3L^{Me}$** (500 mg, 1.19 mmol) in methanol at -78 °C and was left stirring for 1 h under inert conditions. After an hour, $InCl_3$ (263 mg, 1.19 mmol), dissolved in 30 mL MeOH, was added to the trilithium salt of **$H_3L^{Me}$**, resulting in a clear yellowish solution. An excess of 1-methylimidazole (1 mL, 12.55 mmol) was added to the solution, at which point a white precipitate formed. The reaction was left stirring overnight at room temperature. The white precipitate was collected and was recrystallised from THF/hexane resulting in white crystals (712 mg, 1.02 mmol, 86 %). **$^1$H NMR (400 MHz, $CDCl_3$, 298 K, ppm)** $\delta$: 7.93 (br s, 2H), 7.36 (br s, 2H), 6.91 (s, 2H), 6.72 (s, 3H), 6.50 (s, 3H), 3.72 (s, 12H), 2.11 (s, 9H), 2.07 (s, 9H). **$^{13}$C{$^1$H} NMR (100 MHz, $CDCl_3$, 298 K, ppm)** $\delta$: 160.45, 138.86, 131.12, 129.33, 129.05, 127.53, 123.95, 121.28, 120.40, 61.30, 34.01, 20.33, 17.00. **HRMS (ASAP, m/z)** calculated for 2[($C_{35}H_{42}InN_5O_3$)-($C_8H_{12}N_4$)]+$H^+$: 1063.2607; found: 1063.2592.

**Compound $InL^{Me}(DMAP)_2$**

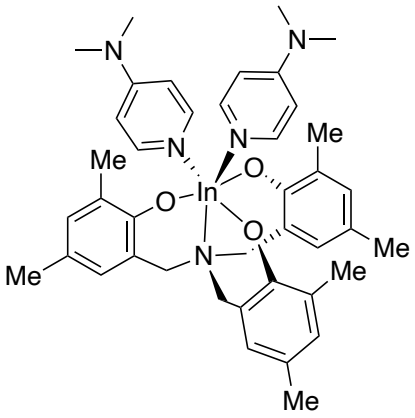

The compound was prepared using the same procedure described for **$InL^{Me}(MeIm)_2$** except in excess of **DMAP** was used**. $InL^{Me}(DMAP)_2$** was obtained as a white powder (812 mg, 1.05 mmol, 88 %). **$^1$H NMR (400 MHz, $CDCl_3$, 298 K, ppm)** $\delta$: 8.60 (br s, 4H), 6.75 (s, 3H), 6.53 (br s, 7H), 3.71 (br, 6H), 3.05 (s, 12H), 2.13 (s, 9H), 2.09 (s, 9H). **$^{13}C\{^1H\}$ NMR (100 MHz, $CDCl_3$, 298 K, ppm)** $\delta$: 160.15, 131.24, 129.28, 127.80, 124.26, 121.26, 106.57, 61.06, 39.17, 20.35, 16.98. **HRMS (ASAP, m/z)** calculated for $2[(C_{41}H_{50}InN_5O_3)-(C_{14}H_{20}N_4)]+H^+$: 1063.2607; found: 1063.2587.

# Chapter 7

General Discussions, Conclusions and Future Work

## 7.1 General Discussions

The group 13 elements of the periodic table are powerful Lewis acids and, in this context, prior to this work, aluminium compounds had been found to be some of the most efficient catalysts for the synthesis of cyclic carbonates. Kleij and co-workers first discovered an aluminium aminotrisphenolate catalyst to have high activity in converting carbon dioxide into cyclic carbonates in 2013.

This thesis aimed to develop novel group 13 catalysts to convert $CO_2$ into valuable products such as cyclic carbonates and oxazolidinones. In chapter 2, the synthesis of metal catalysts was challenging due to the sensitive characteristics of starting materials, resulting in incomplete coordination of the ligand on the metal in some cases.

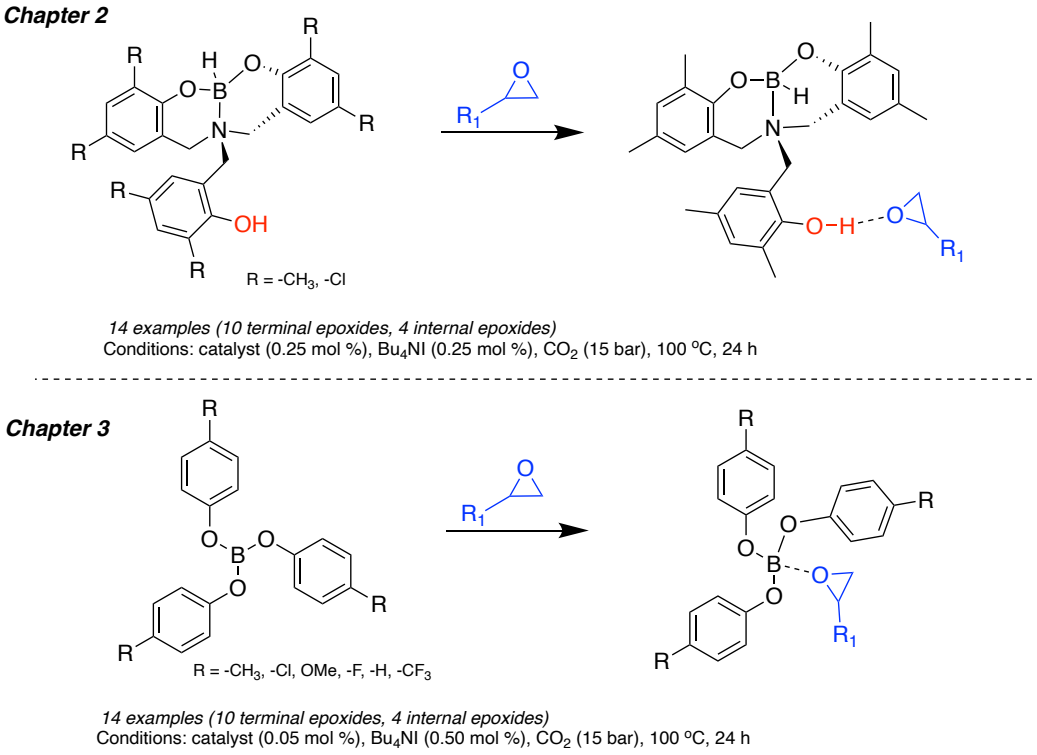


This unanticipated result presented another opportunity wherein the incomplete coordination of a ligand does not inhibit the catalytic properties of the complex.

Instead, the compound could still convert $CO_2$ and epoxide into cyclic carbonates through hydrogen-bonding interaction from the uncoordinated phenol ring of the ligand. In a related study, chapter 3 focused on the preparation of a series of borate compounds and they were found to be active as catalysts for the cycloaddition reaction, but this time, operating through Lewis acid catalysis.

With the discovery in 2021 that gallium aminotrisphenolate as a more efficient catalyst than its aluminium congener,[196] the same gallium compound has been used to successfully synthesised oxazolidinone products (**15b-22b, 27b-28b**), results which are reported in chapter 4. Oxazolidinones are of significant interest due to them being a scaffold in many compounds which display antibacterial activity. It has been possible to develop a catalyst system presenting high conversions of aziridines and $CO_2$ to oxazolidinone under mild conditions. An unexpected product was also synthesized from an aziridine bearing two aromatic substituents, where a facile and high-yielding access to piperazines (**29-32**), dimeric coupling products of aziridine substrates, was achieved. The same gallium catalyst successfully converted epoxide-functionalised cellulose into cyclic carbonate-functionalised cellulose (**34**). The resulting functionalized cellulose compound was tested for antibacterial application against *S. aureus* and *E. coli* microorganisms and showed a high zone of inhibition against *S. aureus* but minor effect on *E. coli*. The reaction between episulfide and $CO_2$, catalysed by the gallium complex produced an intractable white solid which proved difficult to characterise and which is possibly polymeric.

***Chapter 4***

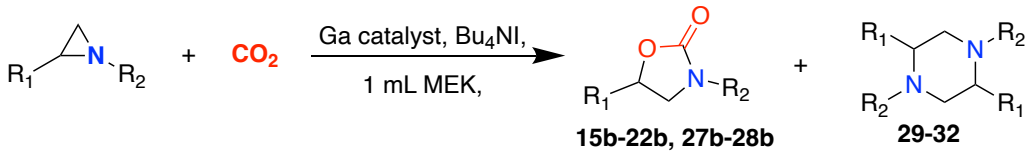


*14 examples (9 terminal aziridine, 5 internal aziridine)*
Conditions: catalyst (0.5 mol %), $Bu_4NI$ (2.0 mol %), $CO_2$ (15 bar), 60 °C, 24 h

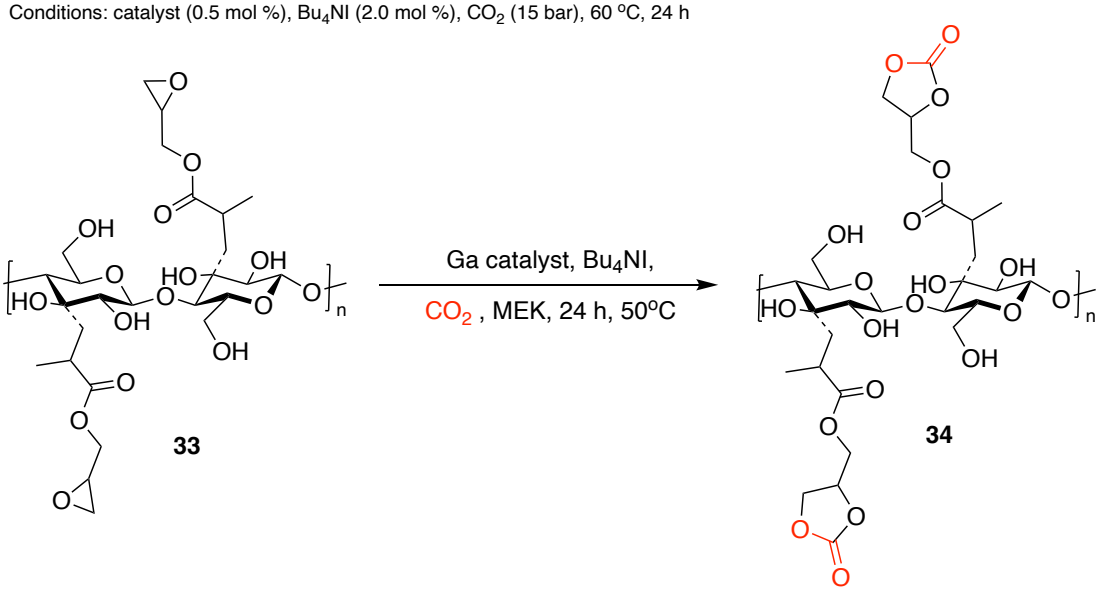


Another element from group 13, indium, was also investigated for its potential to be a catalyst or the reaction between $CO_2$ and epoxides. The indium aminotrisphenolate compound that was synthesised showed relatively good efficiency, but its activity was significantly lower than the gallium compounds.

***Chapter 5***

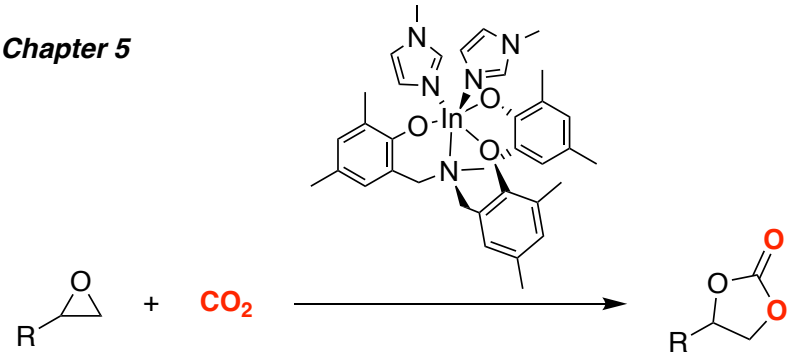


*14 examples (10 terminal epoxides, 4 internal epoxides)*
Conditions: catalyst (0.04 mol %), $Bu_4NI$ (2.0 mol %), $CO_2$ (15 bar), 45 °C, 24 h

## 7.2 Conclusion

This research synthesised metal complexes from group 13 elements as catalysts for the utilisation of $CO_2$, which includes the production of cyclic carbonates and oxazolidinone. Metal catalysts synthesized, have included boron, gallium and indium, supported by an aminotrisphenolate ligand. The analogous aluminium catalyst was already known as a powerful catalyst for cyclic carbonate production. The use of the gallium complex to convert aziridines and $CO_2$ into oxazolidinone under mild conditions was achieved successfully. However, bulky substrates produced the unexpected piperazine formed from dimerization of the substrate. The gallium catalyst has also been used for the reaction between epoxide functionalised cellulose and $CO_2$ and the resulting material was tested for its antibacterial properties. The antibacterial analysis was performed using a modified disc diffusion method using two different microorganisms which showed a large zone of inhibition against *S. aureus* but much lower against *E.coli*.

## 7.3 Future work

The synthesis of boron aminotrisphenolate compounds with incomplete ligand coordination of the ligand was not expected at the start of this study. Further, these complexes cannot engage in Lewis acid catalysis as was hoped. This is likely due to the presence of a nitrogen atom that completely fills the p-orbital. In this context, it would be interesting to prepare a ligand that replaces the nitrogen atom with *C-H* so no electrons are transferred to the p-orbital leaving it vacant and as a result providing the potential for a novel strong Lewis acid catalyst.

In this work dry ice was used as $CO_2$ source. Since dry ice is more manageable than gaseous $CO_2$, another factor is to investigate the optimal

amount of $CO_2$ required for the production of cyclic carbonate compounds. The gallium catalyst synthesis for converting aziridine and $CO_2$ into oxazolidinone was successful, which also produced another product called piperazine. The by-product produced was unusual, and it would be interesting to further optimize these conditions. Moreover, further antibacterial analysis of the cyclic carbonate functionalised cellulose against a different variety of microorganisms should be performed. Finally, the indium aminotrisphenolate compound should be further investigated for the production of copolymerisation of epoxides/$CO_2$ whereby recently indium-containing catalysts have been reported to promote this type of reaction.

## References


1 C. J. Whiteoak, N. Kielland, V. Laserna, E. Escudero-Adán C., E. Martin and A. W. Kleij, *J. Am. Chem. Soc.,* 2013, **135**, 1228-1231.

2 Q. Liu, L. Wu, R. Jackstell and M. Beller, *Nat. Commun.,* 2015, **6**, 1-7.

3 M. Cain, J. Lynch, M. R. Allen, J. S. Fuglestvedt, D. J. Frame and A. H. Macey, *Npj Clim. Atmos. Sci.,* 2019, **2**, 1-7.

4 Trends in Atmospheric Carbon Dioxide, https://gml.noaa.gov/ccgg/trends/global.html,(accessed May 2022).

5 Our World in Data, https://ourworldindata.org/co2-and-other-greenhouse-gas-emissions, (accessed May 2022).

6 C. Maeda, Y. Miyazaki, T. Ema, *Catal. Sci. Technol.,* 2014, **4**,1482-1497.

7 Trends in Atmospheric Carbon dioxide: $CO_2$ Emissions, https://gml.noaa.gov/ccgg/trends/ff.html, (accessed June 2022).

8 C. Martín, G. Fiorani and A. W. Kleij, *ACS Catal.,* 2015, **5**, 1353-1370.

9 A. Álvarez, M. Borges, J. J. Corral-Pérez, J. G. Olcina, L. Hu, D. Cornu, R. Huang, D. Stoian and A. Urakawa, *ChemPhysChem.,* 2017, **18**, 3135-3141.

10 Y. Shen, W. Duan and M. Shi, *Eur. J. Org. Chem.,* 2004, **2004**, 3080-3089.

11 A. K. Srivastava, *Int. J. Quantum Chem.,* 2018, **119**, 1642-1649.

12 J. L. Wadham, J. R. Hawkings, L. Tarasov, L. J. Gregoire, R. G. M. Spencer, M. Gutjahr, A. Ridgwell and K. E. Kohfeld, *Nat. Commun.,* 2019, **10**, 1-17.

13 P. Lanzafame, S. Abate, C. Ampelli, C. Genovese, R. Passalacqua, G. Centi and S. Perathoner, *ChemSusChem.,* 2017, **10**, 4409-4419.

14 S. Moret, P. J. Dyson and G. Laurenczy, *Nat. Commun.,* 2014, **5**, 1-7.

15 V. Caló, A. Nacci, A. Monopoli and A. Fanizzi, *Org. Lett.,* 2002, **4**, 2561-2563.

16 J. Cornil, L. Gonnard, A. Guérinot, S. Reymond and J. Cossy, *Eur. J. Org. Chem.,* 2014, **2014**, 4958-4962.

17 V. Laserna, W. Guo and A. W. Kleij, *Adv. Synth. Catal.,* 2015, **342**, 2849-2854.

18 C. Sun, J. Liu, Y. Gong, D. P. Wilkinson and J. Zhang, *Nano Energy,* 2017, **33**, 363-386.

19 S. Caron, R. W. Dugger, S. G. Ruggeri, J. A. Ragan and D. H. B. Ripin, *Chem Rev.,* 2006, **106**, 2943-2989.

20 M. Fleischer, H. Blattmann and R. Mülhaupt, *Green Chem.,* 2013, **15**, 934-942.

21 M. Pagliaro, A. Fidalgo, L. Palmisano, L. Ilharco, F. Parrino and R. Ciriminna, *ACS Omega,* 2018, **3**, 4884-4890.

22 J. Feng, R. Zhuo and X. Zhang, *Prog. Polym. Sci.,* 2011, **37**, 211-236.

23 A. J. Kamphuis, F. Picchioni and P. P. Pescarmona, *Green Chem.,* 2019, **21**, 406-448.

24 X. Lu and D. J. Darensbourg, *Chem. Soc. Rev.,* 2012, **41**, 1462-1484.

25 A. Decortes, A. M. Castilla and A. W. Kleij, *Angew. Chem. Int. Ed.,* 2010, **49**, 9822-9837.

26 S. Gaillard, C. S. J. Cazin and S. P. Nolan, *Acc. Chem. Res.,* 2012, **45**, 778-787.

27 M. Nolan and M. Fronzi, *Catal. Today,* 2019, **326**, 68-74.

28 M. R. Kember, A. Buchard and C. K. Williams, *Chem. Commun.,* 2010, **47**, 141-163.

29 P. P. Pescarmona and M. Taherimehr, *Catal. Sci. Technol.,* 2012, **2**, 2169-2187.

30 D. J. Diekema and R. N. Jones, *Lancet,* 2001, **358**, 1975-1982.

31 C. Foti, A. Piperno, A. Scala and O. Giuffrè, *Molecules,* 2021, **26**, 1-13.

32 M. Feller, E. Ben-Ari, Y. Diskin-Posner and D. Milstein, *J. Coord. Chem.,* 2018, **71**, 1679-1689.

33 L. Zhao, J. Chen, W. Li and A. Lu, *J. $CO_2$ Util.,* 2019, **29**, 172-178.

34 G. Trott, P. K. Saini and C. K. Williams, *Philos. Trans. R. Soc.,* 2016, **374**, 1-19.

35 S. Klaus, M. W. Lehenmeier, C. E. Anderson and B. Rieger, *Coord. Chem. Rev.,* 2011, **255**, 1460-1479.

36 G. A. Olah, A. Goeppert and G. K. S. Prakash, *J. Org. Chem.,* 2009, **74**, 487-498.

37 A. R. da Silva, D. A. Dos Santos, M. W. Paixão and A. G. Corrêa, *Molecules,* 2019, **24**, 1-23.

38 N. Havare and D. A. Plattner, *Helv. Chim. Acta.,* 2009, **92**, 623-628.

39 I. V. Khavrutskii, D. G. Musaev and K. Morokuma, *Proc. Natl. Acad. Sci. U. S. A.,* 2004, **101**, 5743-5748.

40 J. D. Neighbors, N. R. Mente, K. D. Boss, D. W. Zehnder and D. F. Wiemer, *Tetrahedron Lett.,* 2008, **49**, 516-519.

41 L. Rosi, M. Bartoli, A. Undri, M. Frediani and P. Frediani, *J. Mol. Catal. A Chem.,* 2015, **408**, 278-286.

42 Q. Tian, Y. C. Yuan, M. Z. Rong and M. Q. Zhang, *J. Mater. Chem.,* 2009, **19**, 1289-1296.

43 J. Chen, Z. Liu, J. Jiang, X. Nie, Y. Zhou and R. E. Murray, *RSC Adv.,* 2015, **5**, 56171-56180.

44 I. Cerkez, H. B. Kocer, S. D. Worley, R. M. Broughton and T. S. Huang, *Langmuir,* 2011, **27**, 4091-4097.

45 P. H. Cui, N. Petrovic and M. Murray, *Br J Pharmacol,* 2011, **162**, 1143-1155.

46 C. Lim, A. M. Holder, J. T. Hynes and C. B. Musgrave, *Inorg. Chem.,* 2013, **52**, 10062-10066.

47 X. Lu, W. Ren and G. Wu, *Acc. Chem. Res.,* 2012, **45**, 1721-1735.

48 G. Fiorani, W. Guo and A. W. Kleij, *Green Chem.,* 2015, **17**, 1375-1389.

49 C. J. Whiteoak, G. Salassa and A. W. Kleij, *Chem. Soc. Rev.,* 2012, **41**, 622-631.

50 C. J. Whiteoak, A. Nova, F. Maseras and A. W. Kleij, *ChemSusChem,* 2012, **5**, 2032-2038.

51 C. J. Whiteoak, A. H. Henseler, C. Ayats, A. W. Kleij and M. A. Pericàs, *Green Chem.,* 2014, **16**, 1552-1559.

52 X. Wu, C. Chen, Z. Guo, M. North and A. C. Whitwood, *ACS Catal.,* 2019, **9**, 1895-1906.

53 L. Martínez-Rodríguez, J. Otalora Garmilla and A. W. Kleij, *ChemSusChem,* 2016, **9**, 749-755.

54 A. Decortes, A. M. Castilla and A. W. Kleij, *Angew. Chem. Int. Ed.,* 2010, **49**, 9822-9837.

55 D. J. Kim, Y. Hong, S. H. Kim, K. M. Lee, S. Mun, S. Yoon, J. Lee, Y. Do and Y. Kim, *Inorg. Chim. Acta,* 2011, **378**, 311-314.

56 C. Maeda, Y. Miyazaki and T. Ema, *Catal. Sci. Technol.,* 2014, **4**, 1482-1497.

57 A. Kilic, F. Alcay, M. Aydemir, M. Durgun, A. Keles and A. Baysal, *Spectrochim Acta A.,* 2015, **142**, 62-72.

58 M. Alves, B. Grignard, R. Mereau, C. Jerome, T. Tassaing and C. Detrembleur, *Catal. Sci. Technol.,* 2017, **7**, 2651-2684.

59 S. Liu, N. Suematsu, K. Maruoka and S. Shirakawa, *Green Chem.,* 2016, **18**, 4611-4615.

60 M. North and C. Young, *Catal. Sci. Technol.,* 2011, **1**, 93-99.

61 M. Alvaro, C. Baleizao, D. Das, E. Carbonell and H. García, *J. Catal.,* 2004, **228**, 254-258.

62 S. M. Sadeghzadeh, *Green Chem.,* 2015, **17**, 3059-3066.

63 J. W. Comerford, I. D. V. Ingram, M. North and X. Wu, *Green Chem.,* 2015, **17**, 1966-1987.

64 B. Dutta, J. Sofack-Kreutzer, A. A. Ghani, V. D'Elia, J. D. A. Pelletier, M. Cokoja, F. E. Kühn and J. Basset, *Catal. Sci. Technol.,* 2014, **4**, 1534-1538.

65 C. J. Whiteoak, N. Kielland, V. Laserna, F. Castro-Gómez, E. Martin, E. C. Escudero-Adán, C. Bo and A. W. Kleij, *Chem. Eur. J.,* 2014, **20**, 2264-2275.

66 D. R. Moore, M. Cheng, E. B. Lobkovsky and G. W. Coates, *J. Am. Chem. Soc.,* 2003, **125**, 11911-11924.

67 C. R. Shugrue and S. J. Miller, *Chem. Rev.,* 2017, **117**, 11894-11951.

68 Tomáš Weidlich and Barbora Kamenická, *Catalysts,* 2022, **12**, 298.

69 K. M. Diemoz and A. K. Franz, *J. Org. Chem.,* 2019, **84**, 1126-1138.

70 V. Ji Ram, A. Sethi, M. Nath and R. Pratap, *Chemistry of Heterocycles*, ed. V., Elsevier, 2019,19-92.

71 H. H. Peter, H. Dziuba-Traber and D. Boerner, *Eur. J. Cancer Clin. Oncol.,* 1984, **20**, 353-359.

72 W. T. Bradner, *Cancer Treat. Rev.,* 2001, **27**, 35-50.

73 D. E. Holst, D. J. Wang, M. J. Kim, I. A. Guzei and Z. K. Wickens, *Nature,* 2021, **596**, 74-79.

74 B. Bozdogan and P. C. Appelbaum, *Int. J. Antimicrob. Agents,* 2004, **23**, 113-119.

75 S. Donadio, S. Maffioli, P. Monciardini, M. Sosio and D. Jabes, *J. Antibiot.,* 2010, **63**, 423-430.

76 T. F. Durand-Reville, A. A. Miller, J. P. O'Donnell, X. Wu, M. A. Sylvester, S. Guler, R. Iyer, A. B. Shapiro, N. M. Carter, C. Velez-Vega, S. H. Moussa, S. M. McLeod, A. Chen, A. M. Tanudra, J. Zhang, J. Comita-Prevoir, J. A. Romero, H. Huynh, A. D. Ferguson, P. S. Horanyi, S. J. Mayclin, H. S. Heine, G. L. Drusano, J. E. Cummings, R. A. Slayden and R. A. Tommasi, *Nature,* 2021, **597**, 698-702.

77 X. Yang, R. Guo, B. Xie, Q. Lai, J. Xu, N. Hu, L. Wan, M. Dai and B. Zhang, *J Orthop. Surg. Res.,* 2021, **16**, 1-8.

78 M. Wang, H. Wei, Y. Zhao, L. Shang, L. Di, C. Lyu and J. Liu, *Bosn. J. Basic Med. Sci.,* 2019, **19**, 86-93.

79 A. C. Singer, H. Shaw, V. Rhodes and A. Hart, *Front Microbiol.,* 2016, **7**, 1-22.

80 C. Nathan and O. Cars, *N. Engl. J. Med.,* 2014, **371**, 1761-1763.

81 B. Aslam, W. Wang, M. I. Arshad, M. Khurshid, S. Muzammil, M. H. Rasool, M. A. Nisar, R. F. Alvi, M. A. Aslam, M. U. Qamar, M. K. F. Salamat and Z. Baloch, *Infect Drug Resist.,* 2018, **11**, 1645-1658.

82 P. W. Ament, N. Jamshed and J. P. Horne, *Am. Fam. Physician,* 2002, **65**, 663-670.

83 K. S. Kokilambigai, K. S. Lakshmi, A. Sai Susmitha, R. Seetharaman and J. Kavitha, *Crit. Rev. Anal. Chem.,* 2020, **50**, 179-188.

84 J. F. Barrett, *Curr. Opin. Investig. Drugs,* 2000, **1**, 181-187.

85 G. G. Zhanel, R. Love, H. Adam, A. Golden, S. Zelenitsky, F. Schweizer, B. Gorityala, P. R. S. Lagacé-Wiens, E. Rubinstein, A. Walkty, A. S. Gin, M. Gilmour, D. J. Hoban, J. P. Lynch and J. A. Karlowsky, *Drugs,* 2015, **75**, 253-270.

86 D. Ben-Ishai, *J. Am. Chem. Soc.,* 1956, **78**, 4962-4965.

87 S. Pulla, V. Unnikrishnan, P. Ramidi, S. Z. Sullivan, A. Ghosh, J. L. Dallas and P. Munshi, *J. Mol. Catal. A Chem.,* 2011, **338**, 33-43.

88 M. Zhou, X. Zheng, Y. Wang, D. Yuan and Y. Yao, *ChemCatChem,* 2019, **11**, 5783-5787.

89 T. Baronsky, C. Beattie, R. W. Harrington, R. Irfan, M. North, J. G. Osende and C. Young, *ACS Catal.,* 2013, **3**, 790-797.

90 D. R. Varma and I. Guest, *J. Toxicol. Environ. Health.,* 1993, **40**, 513-529.

91 H. Kawanami and Y. Ikushima, *Tetrahedron Lett.,* 2002, **43**, 3841-3844.

92 N. Srivastav, R. Singh, V. Kaur, J. ö Wagler and E. Kroke, *Inorg. Chim. Acta,* 2017, **463**, 54-60.

93 C. Hu, X. Chen, M. Niu, Q. Zhang, R. Duan, X. Pang, *Macromolecules,* 2022, **2**, 652-657.

94 J. Rintjema, R. Epping, G. Fiorani, E. Martín, E. C. Escudero-Adán and A. W. Kleij, *Angew. Chem. Int. Ed.,* 2016, **55**, 3972-3976.

95 M. Taherimehr, S. Al-Amsyar, C. J. Whiteoak, A. W. Kleij and P. P. Pescarmona, *Green Chem.,* 2013, **15**, 3083-3090.

96 T. Ema, Y. Miyazaki, S. Koyama, Y. Yano and T. Sakai, *Chem. Commun.,* 2012, **48**, 4489-4491.

97 C. J. Whiteoak, C. J. Whiteoak, E. Martin, M. M. Belmonte, J. Benet-Buchholz and A. W. Kleij, *Adv. Synth. Catal.,* 2012, **354**, 469-476.

98 A. Decortes, R. M. Haak, C. Martín, M. M. Belmonte, E. Martin, J. Benet-Buchholz and A. W. Kleij, *Macromolecules,* 2015, **48**, 8197-8207.

99 C. J. Whiteoak, N. Kielland, V. Laserna, E. Escudero-Adán C., E. Martin and A. W. Kleij, *J. Am. Chem. Soc.,* 2013, **135**, 1228-1231.

100 P. Ramidi, N. Gerasimchuk, Y. Gartia, C. M. Felton and A. Ghosh, *Dalton Trans.,* 2013, **42**, 13151-13160.

101 C. R. Shugrue and S. J. Miller, *Chem. Rev.,* 2017, **117**, 11894-11951.

102 L. Ji, S. Griesbeck and T. B. Marder, *Chem. Sci.,* 2017, **8**, 846-863.

103 P. Eisenberger and C. M. Crudden, *Dalton Trans.,* 2017, **46**, 4874-4887.

104 Z. Xue, X. Zhao, J. Wang and T. Mu, *Chem. Asian J.,* 2017, **12**, 2271-2277.

105 N. Kihara, N. Hara and T. Endo, *J. Org. Chem.,* 1993, **58**, 6198-6202.

106 A. Kilic, E. Yasar and E. Aytar, *Sustain. Energ. Fuels,* 2019, **3**, 1066-1077.

107 E. Aytar and T. B. Marder, *Sustain. Energ. Fuels,* 2018, **9**, 1021-1027.

108 D. Bai, G. Nian, G. Wang and Z. Wang, *Appl. Organomet. Chem.,* 2013, **27**, 184-187.

109 K. A. Andrea and F. M. Kerton, *ACS Catal.,* 2019, **9**, 1799-1809.

110 A. G. Massey and A. J. Park, *J. Organomet. Chem.,* 1966, **5**, 218-225.

111 M. Jakubczyk, A. Adamczyk-Woźniak and A. Sporzyński, *Rybachenko,* 2011, 53-68.

112 D. J. Darensbourg, J. R. Wildeson, J. C. Yarbrough and J. H. Reibenspies, *J. Am. Chem. Soc.,* 2000, **122**, 12487-12496.

113 G. W. Coates and D. R. Moore, *Angew. Chem. Int. Ed.,* 2004, **43**, 6618-6639.

114 G. Wu, P. Xu, X. Lu, Y. Zu, S. Wei, W. Ren and D. J. Darensbourg, *Macromolecules,* 2013, **46**, 2128-2133.

115 D. Zhang, S. K. Boopathi, N. Hadjichristidis, Y. Gnanou and X. Feng, *J. Am. Chem. Soc.,* 2016, **138**, 11117-11120.

116 L. Zhao, J. Chen, W. Li and A. Lu, *J. $CO_2$ Util.,* 2019, **29**, 172-178.

117 J. Wang and Y. Zhang, *ACS Catal.,* 2016, **6**, 4871-4876.

118 G. Yang, Y. Zhang, R. Xie and G. Wu, *J. Am. Chem. Soc.,* 2020, **142**, 12245-12255.

119 S. Dagorne, M. Normand, E. Kirillov and J. Carpentier, *Coord. Chem. Rev.,* 2013, **257**, 1869-1886.

120 J. Beament, M. F. Mahon, A. Buchard and M. D. Jones, *N. J. Chem.,* 2017, **41**, 2198-2203.

121 A. Pietrangelo, M. A. Hillmyer and W. B. Tolman, *Chem. Commun.,* 2009, 2736-2737.

122 S. Ghosh, R. R. Gowda, R. Jagan and D. Chakraborty, *Dalton Trans.,* 2015, **44**, 10410-10422.

123 A. Thevenon, A. Cyriac, D. Myers, A. J. P. White, C. B. Durr and C. K. Williams, *J. Am. Chem. Soc.,* 2018, **140**, 6893.

124 D. J. Darensbourg and D. R. Billodeaux, *C. R. Chim.,* 2004, **7**, 755-761.

125 M. Tschan, J. Guo, S. Raman, E. Brulé, T. Roisnel, M. Rager, R. Legay, G. Durieux, B. Rigaud and C. Thomas, *Dalton Trans.,* 2014, **43**, 4550-4564.

126 R. M. Clarke and T. Storr, *Dalton Trans.,* 2014, **43**, 9380-9391.

127 M. Aresta and A. Dibenedetto, *Dalton Trans.,* 2007, 2975-2992.

128 W. Marckwald and F. Struwe, *Ber. Dtsch. Chem. Ges.,* 1922, **55**, 457-463.

129 T. F. Cummings and J. R. Shelton, *J. Org. Chem.,* 1960, 25, 419-423.

130 G. L. Och and H. Thomasson, *Geol. Fören. Stockh. Förh.,* 1923, **45**, 379-385.

131 T. R. Dargaville, P. J. De Bruyn, A. S. C. Lim, M. G. Looney, A. C. Potter, D. H. Solomon and X. Zhang, *J. Polym. Sci., Part A: Polym. Chem.,* 1997, **35**, 1389-1398.

132 S. Sopeña, E. Martin, E. Escudero-Adán C. and A. W. Kleij, *ACS Catal.,* 2017, **7**, 3532-3539.

133 N. Zanda, A. Sobolewska, E. Alza, A. W. Kleij and M. Pericàs A., *ACS Sustain. Chem. Eng.,* 2021, **9**, 4391-4397.

134 L. Guo, K. J. Lamb and M. North, *Green Chem.,* 2021, **23**, 77-118.

135 V. Aomchad, À Cristòfol, F. Della Monica, B. Limburg, V. D'Elia and A. W. Kleij, *Green Chem.,* 2021, **23**, 177-1113.

136 C. Martín, A. Pizzolante, E. C. Escudero-Adán and A. W. Kleij, *Eur. J. Inorg. Chem.,* 2018, **2018**, 1921-1927.

137 A. Lehtonen and R. Sillanpää, *Polyhedron,* 2007, **26**, 5293-5300.

138 A. Lehtonen and V. G. Kessler, *Inorg. Chem. Commun.,* 2004, **7**, 691-693.

139 C. Martín, C. J. Whiteoak, E. Martin, E. Escudero-Adán C., J. R. Galán-Mascarós and A. W. Kleij, *Inorg. Chem.,* 2014, **53**, 11675-11681.

140 M. G. Davidson, C. L. Doherty, A. L. Johnson and M. F. Mahon, *Chem. Commun.,* 2003, 1832-1833.

141 S. Groysman, S. Segal, M. Shamis, I. Goldberg, M. Kol, Z. Goldschmidt and E. Hayut-Salant, *Dalton Trans.,* 2002, 3425-3426.

142 S. Groysman, I. Goldberg, Z. Goldschmidt and M. Kol, *Inorg. Chem.,* 2005, **44**, 5073-5080.

143 T. Omiya, S. Natta, K. Wised, K. Tsutsumi and K. Nomura, *Polyhedron,* 2017, **125**, 9-17.

144 Y. Kim and J. G. Verkade, *Organometallics,* 2002, **21**, 2395-2399.

145 P. M. Gurubasavaraj and K. Nomura, *Inorg. Chem.,* 2009, **48**, 9491-9500.

146 Y. Takii, P. M. Gurubasavaraj, S. Katao and K. Nomura, *Organometallics,* 2012, **31**, 8237-8248.

147 J. G. Verkade S. Katao and K. Nomura, *Inorg. Chem.,* 2010, **21**, 237-248.

148 L. E. Turner, M. G. Davidson, M. D. Jones, H. Ott, V. S. Schulz and P. J. Wilson, *Inorg. Chem.,* 2006, **45**, 6123-6125.

149 A. Chandrasekaran, R. O. Day and R. R. Holmes, *Inorg. Chem.,* 2000, **39**, 5683-5689.

150 L. Álvarez-Miguel, J. D. Burgoa, M. E. G. Mosquera, A. Hamilton and C. J. Whiteoak, 2021, **13**, 4099-4110.

151 Y. Kim and J. G. Verkade, *Inorg. Chem.,* 2003, **42**, 4804-4806.

152 A. J. Chumura, M. G. Davidson, C. J. Frankis, M. D. Jones and M. D. Lunn, Chem. Commun., 2008, 1293-1295.

153 A. Lehtonen and R. Sillanpää, *Organometallics,* 2005, **24**, 2795-2800.

154 A. J. Chmura, A. J. Chmura, C. J. Chuck, M. G. Davidson, M. D. Jones, M. D. Lunn, S. D. Bull and M. F. Mahon, *Angew. Chem.,* 2007, **119**, 2330-2333.

155 J. Guo, P. Haquette, J. Martin, K. Salim and C. M. Thomas, *Angew. Chem. Int. Ed.,* 2013, **52**, 13584-13587.

156 D. J. Kim, Y. Hong, S. H. Kim, K. M. Lee, S. Mun, S. Yoon, J. Lee, Y. Do and Y. Kim, *Inorg. Chim. Acta.,* 2011, **378**, 311-314.

157 M. Yasuda, S. Yoshioka, S. Yamasaki, T. Somyo, K. Chiba and A. Baba, *Org. Lett.,* 2006, **8**, 761-770.

158 D. G. Lonnon, D. C. Craig and S. B. Colbran, *Dalton Trans.,* 2006, 3785-3797.

159 H. Braunschweig, C. Kollann and D. Rais, *Angew. Chem. Int. Ed.,* 2006, **45**, 5254-5274.

160 F. Jakle, *Coord. Chem. Rev.,* 2006, **250**, 1107-1121.

161 C. A. Brown and S. Krishnamurthy, *J. Org. Chem.,* 1978, **43**, 2731-2732.

162 H. Wang, L. Wu, Z. Lin and Z. Xie, *Angew. Chem. Int. Ed Engl.,* 2018, **57**, 8708-8713.

163 V. Nori, F. Pesciaioli, A. Sinibaldi, G. Giorgianni and A. Carlone, *Catalysts,* 2021, **12**, 1-27.

164 C. Maeda, Y. Miyazaki and T. Ema, *Catal. Sci. Technol.,* 2014, **4**, 1482-1497.

165 J. T. Grant, W. P. McDermott, J. M. Venegas, S. P. Burt, J. Micka, S. P. Phivilay, C. A. Carrero and I. Hermans, *ChemCatChem,* 2017, **9**, 3623-3626.

166 W. E. Piers, S. C. Bourke and K. D. Conroy, *Angew. Chem. Int. Ed.,* 2005, **44**, 5016-5036.

167 F. Meng, K. P. McGrath and A. H. Hoveyda, *Nature,* 2014, **513**, 367-374.

168 S. Namirembe and J. P. Morken, *Chem. Soc. Rev.,* 2019, **48**, 3464-3474.

169 Z. Jiang, B. Wang and Z. Shi, *Chin. J. Chem.,* 2018, **36**, 950-954.

170 G. Chai, Y. Qiao, P. Zhang, R. Guo, J. Wang and J. Chang, *Org. Lett.,* 2020, **22**, 8023-8027.

171 D. Wu, L. Kong, Y. Li, R. Ganguly and R. Kinjo, *Nat. Commun.,* 2015, **6**, 1-6.

172 Y. Zhang, G. Yang, R. Xie, L. Yang, B. Li and G. Wu, *Angew. Chem. Int. Ed.,* 2020, **59**, 23291-23298.

173 M. Shekarriz, B. Ghanbari, S. Taghipoor, A. A. Khalili, F. Hajialiakbari, M. Adibi and M. Soleymani, *Asian J. Chem.,* 2010, **22**, 3646-3652.

174 M. Pineschi, F. Bertolini, P. Crotti and F. Macchia, *Org. Lett.,* 2006, **8**, 2627-2630.

175 L. Ji, S. Griesbeck and T. B. Marder, *Chem. Sci.,* 2017, **8**, 846-863.

176 T. Taniguchi, *Chem. Eur. J.,* 2022, **28**, 1-8.

177 J. Rintjema, R. Epping, G. Fiorani, E. Martín, E. Escudero-Adán C. and A. W. Kleij, *Angew. Chem. Int. Ed.,* 2016, **55**, 3972-3976.

178 S. Li, W. Wang, S. Lei and J. Cui, *ChemistrySelect,* 2021, **6**, 7732-7735.

179 S. Manzoor and N. Hoda, *Eur. J. Med. Chem.,* 2020, **206**, 112787.

180 G. I. Makarov and R. V. Reshetnikova, *J. Mol. Graph. Model.,* 2021, **105**, 1-6.

181 W. J. Close, *J. Am. Chem. Soc.,* 1951, **73**, 95-98.

182 K. Chinnam Naidu, G. Ravi Babu, L. Gangaiah, K. Mukkanti and G. Madhusudhan, *Tetrahedron Lett.,* 2010, **51**, 1226-1229.

183 M. Costa, G. P. Chiusoli and M. Rizzardi, *Chem. Commun.,* 1996, 1699-1700.

184 M. Shi and Y. Shen, *J. Org. Chem.,* 2002, **67**, 16-21.

185 N. D. Ca', B. Gabriele, G. Ruffolo, L. Veltri, T. Zanetta and M. Costa, *Adv. Synth. Catal.,* 2011, **353**, 133-146.

186 Y. Kayaki, M. Yamamoto, T. Suzuki and T. Ikariya, *Green Chem.,* 2006, **8**, 1019-1021.

187 A. Sudo, Y. Morioka, F. Sanda and T. Endo, *Tetrahedron Lett.,* 2004, **45**, 1363-1365.

188 Y. Du, Y. Wu, A. Liu and L. He, *J. Org. Chem.,* 2008, **73**, 4709-4712.

189 H. Jiang, J. Ye, C. Qi and L. Huang, *Tetrahedron Lett.,* 2010, **51**, 928-932.

190 A. W. Miller and S. T. Nguyen, *Org. Lett.,* 2004, **6**, 2301-2304.

191 M. Sengoden, M. North and A. C. Whitwood, *ChemSusChem,* 2019, **12**, 3296-3303.

192 L. Álvarez-Miguel, J. D. Burgoa, M. E. G. Mosquera, A. Hamilton and C. J. Whiteoak, 2021, **13**, 4099-4110.

193 E. Vismara, L. Melone, G. Gastaldi, C. Cosentino and G. Torri, *J. Hazard. Mater.,* 2009, **170**, 798-808.

194 A. K. Chakraborti, S. Rudrawar and A. Kondaskar, *Eur. J. Org. Chem.,* 2004, **2004**, 3597-3600.

195 W. Ren, Y. Liu and X. Lu, *J. Org. Chem.,* 2014, **79**, 9771-9777.

196 H. Suzuki and H. Tani, *Chem. Lett.,* 1984, **13**, 2129-2130.

197 J. Huang, W. Xu, H. Xie and S. Li, *J. Org. Chem.,* 2012, **77**, 7506-7511.

198 W. Cunico, C. R. B. Gomes, M. Moreth, D. P. Manhanini, I. H. Figueiredo, C. Penido, M. G. M. O. Henriques, F. P. Varotti and A. U. Krettli, *Eur. J. Med. Chem.,* 2009, **44**, 1363-1368.

199 J. Szejtli, *Starch - Stärke,* 2003, **55**, 191-196.

200 T. Hirotsu, *Thin Solid Films,* 2006, **506-507**, 173-175.

201 T. Kondo, H. Kubota and R. Katakai, *J. Appl. Polym. Sci.,* 1999, **74**, 2462-2469.

202 P. R. S. Reddy, G. Agathian and A. Kumar, *Radiat. Phys. Chem.,* 2005, **72**, 511-516.

203 T. S. Anirudhan, S. Jalajamony and L. Divya, *Ind. Eng. Chem. Res.,* 2009, **48**, 2118-2124.

204 United States Patent, Free-radical functionalized polysaccharides, https://patentimages.storage.googleapis.com/91/bc/39/75082706f4f267/US7754878.pdf, (accessed June 2022).

205 S. Coseri, G. Biliuta, B. C. Simionescu, *Polym. Chem.,* 2018, **9**, 961-967.

206 E. F. Palermo, K. Lienkamp, E. R. Gillies and P. J. Ragogna, *Angew. Chem. Int. Ed.,* 2019, **58**, 3690-3693.

207 T. P. M. Sunthar, F. Boschetto, H. N. Doan, T. Honma, K. Kinashi, T. Adachi, E. Marin, W. Zhu and G. Pezzotti, *Antibiotics,* 2021, **10**, 1-16.

208 T. M. Mututuvari, A. L. Harkins and C. D. Tran, *J. Biomed. Mater. Res. A.,* 2013, **101**, 3266-3277.

209 O. Hauenstein, M. Reiter, S. Agarwal, B. Rieger and A. Greiner, *Green Chem.,* 2016, **18**, 760-770.

210 O. Hauenstein, M. M. Rahman, M. Elsayed, R. Krause-Rehberg, S. Agarwal, V. Abetz and A. Greiner, *Adv. Mater. Technol.,* 2017, **2**, 1-26.

211 O. Hauenstein, S. Agarwal and A. Greiner, *Nat. Commun.,* 2016, **7**, 1-7.

212 Y. Shai, *Biochim. Biophys. Acta – Biomembr.,* 1999, **1462**, 55-70.

213 E. F. Palermo, K. Lienkamp, E. R. Gillies and P. J. Ragogna, *Angew. Chem. Int. Ed.,* 2019, **58**, 3690-3693.

214 N. W. Schmidt and G. C. L. Wong, *Curr. Opin. Solid State Mater. Sci.,* 2013, **17**, 151-163.

215 E. Vismara, G. Bertolini, C. Bongio, N. Massironi, M. Zarattini, D. Nanni, C. Cosentino and G. Torri, *Nanomaterials (Basel, Switzerland),* 2021, **11**, 1-26.

216 BSAC Methods for Antimicrobial Susceptibility Testing, https://bsac.org.uk/wp-content/uploads/2012/02/BSAC-disc-susceptibility-testing-method-Jan-2015.pdf, (accessed February 2022)

217 International Patent, Method for the preparation of a monothiocarbonate compound, https://patentimages.storage.googleapis.com/d0/f7/60/6e7232da7c86ad/WO2019034468A1.pdf, (accessed February 2022).

218 M. Luo, X. -. Zhang and D. J. Darensbourg, *Catal. Sci. Tech.,* 2016, **6**, 188-192.

219 J. Yang, H. Wu, Y. Li, X. Zhang and D. J. Darensbourg, *Angew. Chem. Int. Ed Engl.,* 2017, **56**, 5774-5779.

220 M. Luo, X. Zhang and D. J. Darensbourg, *Acc. Chem. Res.,* 2016, **49**, 2209-2219.

221 N. M. Bingham, Z. Abousalman-Rezvani, K. Collins, P. J. Roth, *Polym. Chem.*, 2022, **13**, 2880-2901.

222 S. Dagorne and R. Wehmschulte, *ChemCatChem,* 2018, **10**, 2509-2520.

223 R. J. Motekaitis, A. E. Martell, S. A. Koch, Hwang, D. A. Quarless and M. J. Welch, *Inorg. Chem.,* 1998, **37**, 5902-5911.

224 I. Shibata, I. Mitani, A. Imakuni and A. Baba, *Tetrahedron Lett.,* 2011, **52**, 721-723.

225 B. Michelet, J. Colard-Itté, G. Thiery, R. Guillot, C. Bour and V. Gandon, *Chem. Commun. (Camb).,* 2015, **51**, 7401-7404.

226 K. A. Andrea, A. R. Beckett, G. G. Briand, S. A. Martell, J. Masuda, K. M. Morrison and E. M. T. Yammine, *J. Organomet. Chem.,* 2020, **919**, 1-9.

227 H. A. Baalbaki, H. Roshandel, J. E. Hein and P. Mehrkhodavandi, *Catal. Sci. Technol.,* 2021, **11**, 2119-2129.

228 M. Assis, N. G. Macedo, T. R. Machado, M. M. Ferrer, A. F. Gouveia, E. Cordoncillo, R. Torres-Mendieta, H. Beltrán-Mir, G. Mínguez-Vega, E. R. Leite, J. R. Sambrano, J. Andrés and E. Longo, *Part. Part. Syst. Charact.,* 2018, **35**, 21745-21753.

229 T. Jiang, T. Zou, G. Wang, B. Wang and Z. Chen, *Energy Rep.,* 2022, **8**, 5668-5677.

230 Z. Bitar, A. Fecant, E. Trela-Baudot, S. Chardon-Noblat and D. Pasquier, *Appl. Catal. B, Environ.,* 2016, **189**, 172-180.

231 G. M. Sheldrick, *Acta Crystallogr. C. Struct. Chem.,* 2015, **71**, 3-8.

232 O. V. Dolomanov, L. J. Bourhis, R. J. Gildea, J. A. K. Howard and H. Puschmann, *J. Appl. Crystal.,* 2009, **42**, 339-341.

233 G. M. Sheldrick, *J. Appl. Crystal.,* 2015, **8**, 13-18.

234 Diffraction RO Rigaku Oxford Diffraction, CrysAlisPro Software System v. 1.171.37.35, 2014.

235 G. M. Sheldrick, *Acta Cryst. A.,* 2008, **64**, 112-122.

236 J. Lubben, C. M. Wandtke, C. B. Hubschle, M. Ruf, G. M. Sheldrick, B. Dittrich., *Acta Crystallogr. A.,* 2019, **75**, 50-62.

237 O. V. Dolomanov, L. J. Bourhis, R. J. Gildea, J. A. K. Howard and H. Puschmann, *J. Appl. Cryst.,* 2009, **42**, 339-341.

238 I. J. Bruno, J. C. Cole, P. R. Edgington, M. Kessler, C. F. Macrae, P. McCabe, J. Pearson and R. Taylor, *Acta Crystallogr. B.,* 2002, **58**, 389-397.

239 P. R. Edgington, P. McCabe, C. F. Macrae, E. Pidcock, G. P. Shields, R. Taylor, M. Towler and J. Van De Streek, *J. Appl. Cryst,* 2006, **39**, 453-457.

240 V. Laserna, E. Martin, E. C. Escudero-Adán and A. W. Kleij, *ACS Catal.,* 2017, **7**, 5478-5482.

241 J. Martínez, J. Fernández-Baeza, L. F. Sánchez-Barba, J. A. Castro-Osma, A. Lara-Sánchez and A. Otero, *ChemSusChem,* 2017, **10**, 2886-2890.

242 Z. Yang, Y. Li, Y. Wei and L. He, *Green Chem.,* 2011, **13**, 2351-2353.

243 M. M. Vaidergorn, Z. A. Carneiro, C. D. Lopes, S. de Albuquerque, F. C. C. Reis, S. Nikolaou, J. F. R. e. Mello, G. L. Genesi, G. H. G. Trossini, A. Ganesan and F. S. Emery, *Eur. J. Med. Chem.,* 2018, **157**, 657-664.

244 E. H. M. Elageed, B. Chen, B. Wang, Y. Zhang, S. Wu, X. Liu and G. Gao, *Eur. J. Org. Chem.,* 2016, **2016**, 3650-3656.